Year : 2021

Postnatal development of the monkey entorhinal cortex: insights into normal memory development in humans

Piguet Oiivia

Piguet Oiivia, 2021, Postnatal development of the monkey entorhinal cortex: insights into normal memory development in humans

Originally published at : Thesis, University of Lausanne

Posted at the University of Lausanne Open Archive http://serval.unil.ch
Document URN : urn:nbn:ch:serval-BIB_C19E913534FE1

UNIL | Université de Lausanne

Faculté des Sciences Sociales et Politiques
Institut de psychologie

Postnatal development of the monkey entorhinal cortex: insights into normal memory development in humans

Thèse de Doctorat

présentée à la

Faculté des Sciences sociales et politiques
de l'Université de Lausanne

par

Olivia PIGUET

pour l'obtention du grade de
Docteure en Neurosciences

Jury

Prof. Pierre Lavenex, Directeur de thèse
Dr Irmgard Amrein, Experte
Prof. James Chrobak, Expert
Prof. Nicolas Toni, Expert

Lausanne
(2021)

Programme doctoral interuniversitaire en Neurosciences des Universités de Lausanne et Genève

LEMANIC NEURO SCIENCE DOCTORAL SCHOOL

UNIL | Université de Lausanne

UNIVERSITÉ DE GENÈVE

UNIL | Université de Lausanne
Faculté des sciences sociales et politiques

UNIVERSITÉ DE GENÈVE

LEMANIC NEURO SCIENCE DOCTORAL SCHOOL

IMPRIMATUR

Le Décanat de la Faculté des sciences sociales et politiques de l'Université de Lausanne, au nom du Conseil et sur proposition d'un jury formé des professeurs

- Pierre LAVENEX, Directeur de thèse, Professeur à l'Université de Lausanne
- Nicolas TONI, Professeur à l'Université de Lausanne
- Irmgard AMREIN, Research Associate à l'Université de Zürich
- James CHROBAK, Professeur à l'Université du Connecticut

autorise, sans se prononcer sur les opinions de la candidate, l'impression de la thèse de Madame Olivia PIGUET, intitulée:

« Postnatal development of the monkey entorhinal cortex: insights into normal memory development in humans. »

Nicky LE FEUVRE
Doyenne

Lausanne, le 11 novembre 2021

Résumé

Il est aujourd'hui établi que la formation hippocampique, dont fait partie le cortex entorhinal, est essentiel pour le traitement de la mémoire épisodique. Plusieurs études menées ces dernières années ont confirmé l'hypothèse selon laquelle différentes régions de la formation hippocampique montrent des différences de profils temporels de leur développement structurel. Ces études, couplées à différentes recherches fonctionnelles sur la mémoire, suggèrent que la maturation différentielle de circuits hippocampiques distincts pourrait sous-tendre l'émergence de processus mnésiques spécifiques "dépendant de l'hippocampe", menant finalement à l'émergence de la mémoire épisodique. Le cortex entorhinal étant la principale structure de connexion pour l'interaction bidirectionnelle entre le néocortex et l'hippocampe, connaître son développement structurel postnatal est essentiel pour comprendre l'émergence et le development de la mémoire. Mon travail complète des études précédentes faites au sein de notre laboratoire et fournit les données quantitatives fondamentales sur la maturation structurelle postnatale normale du cortex entorhinal chez le singe. Afin de fournir des estimations de volumes, de nombre de neurones et de tailles de corps neuronaux, j'ai effectué des analyses stéréologiques dans les différentes couches et subdivisions du cortex entorhinal chez le singe, de la naissance à l'âge adulte. Mes analyses ont révélé une maturation différentielle des subdivisions et couches du cortex entorhinal. La dernière partie de ce manuscrit est donc dédiée à la manière dont ces résultats contribuent à notre compréhension du développement normal de la mémoire chez l'humain. Ce travail supporte la théorie selon laquelle différents circuits hippocampiques ont des profils développementaux distincts, qui pourraient soutenir l'émergence de différent processus mnésique dépendant de l'hippocampe.

Abstract

It is now well established that the hippocampal formation, including the entorhinal cortex, is essential for the processing of episodic memory. Experimental data gathered in the last few years have confirmed the hypothesis that distinct regions of the hippocampal formation exhibit different time courses of structural development. Together with functional studies of memory, these findings suggest how the differential maturation of distinct hippocampal circuits might underlie the emergence of specific "hippocampus-dependent" memory processes, ultimately leading to the emergence of episodic memory. As the entorhinal cortex is the main getaway for bidirectional interaction between the neocortex and the hippocampus, a clear understanding of its structural postnatal development is essential to understand the emergence and development of these memory processes. My work completed previous studies from our laboratory by providing fundamental quantitative data on the normal structural maturation of the monkey entorhinal cortex during early postnatal life. In order to provide estimates of volumes, neuron numbers and neuronal soma sizes, I performed stereological analyses in the different layers and subdivisions of the monkey entorhinal cortex from birth to young adulthood. My results revealed a differential maturation of distinct subdivisions and layers of the entorhinal cortex. The final part of my dissertation discusses the contribution of my results to our understanding of normal memory development in humans. They support the theory that different hippocampal circuits exhibit distinct developmental profiles, which may subserve the emergence of different hippocampus-dependent memory processes.

Acknowledgements

The achievement of the present work would not have been possible without the help, work and support of many people that I would like to thank here.

First of all, I would like to express my deep gratitude to Professor Pierre Lavenex, who supported and guided me all along the project. In particular, I would like to thank him for all the very constructive advices, his availability and the trust he accorded me to carry this project to the end. Thank you very much.

I would address special thanks to Doctor Loïc Chareyron who was an amazing support at the beginning of my work. His availability and knowledge of stereological investigations has been essential to the realization of this work.

For the realization of a meticulous and long work like a thesis, sharing an office with great coworkers is undoubtedly a motivational help. I would therefore like to thank Giuliana, Mathilde and Emily for their friendship and all the great moment we had together.

For the intellectual and emotional support, special thanks are going to Doctor Pamela Banta Lavenex, who has always been here for me in good and more difficult moments of my work.

I also express my gratitude to Doctor Adeline Jabès who, with her previous investigations, opened the road to this work. In particular, I deeply thank her for the preparation of all the beautiful brain slices I used in my research.

None of my educational achievement would have been possible without the amazing support of my family, and especially of my parents, Elisabeth and Christophe, which have always been here for me and I know will always be. Thank you very much. I love both of you infinitely.

Finally, last but not least, I would like to deeply thank my husband Simon, who has always been an unwavering support through every step of my work and my life since we met. I would like to dedicate this work to him and to our sons, Gaël and Lucas, that I love more than anything in the world.

1. General introduction

The aim of this work is to characterize the postnatal structural development of the primate entorhinal cortex in order to better understand the neuronal substrates underlying the emergence of episodic memory. I will therefore devote the first chapter of this general introduction to a brief presentation of episodic memory. The second chapter will describe the anatomical features of the entorhinal cortex in order to highlight its multiple extrinsic and intrinsic connections and provide a preview of how the entorhinal cortex could contribute to the emergence of specific hippocampus-dependent memory processes. Finally, in the last chapter, I will present a summary of the current knowledge about the functional processes carried out by the entorhinal cortex.

1.1 Memory and the medial temporal lobe

The description of patient H.M. and nine other patients by Scoville and Milner marks the beginning of an intensive investigation of the role of the hippocampal formation in memory processes (Scoville & Milner, 1957). Suffering from severe epilepsy, H.M. underwent an extensive neurosurgery involving the bilateral removal of a major portion of his medial temporal lobe. After surgery, H.M. showed no obvious physiological or behavioural changes except for a very grave, recent memory loss, so severe as to prevent H.M. from remembering the locations of the rooms in which he lived, the names of his close associates, or even the way to the bathroom (Scoville, 1954). In contrast, old memories from his childhood seemed relatively intact (Milner, Squire, & Kandel, 1998). The impairment of H.M.'s recent memory, in absence of any other intellectual loss, provided initial evidence of the implication of the medial temporal lobe in memory processes. However, most interestingly, H.M. was still capable of some specific memory exercises. For example, he was able to hold immediate impressions in his mind, but as soon as his attention was diverted, they were lost (Milner et al., 1998). Moreover, he was able to learn a mirror-drawing task with stable retention from day to day, without any consciousness of his improvements (Milner et al., 1998). In sum, H.M.'s memory impairment did not impact all his memory but appeared limited to specific memory processes: the ability to convert short-term memory into conscious, long-term

autobiographical memory. This selective loss demonstrated that memory was not a unitary process, but that there were different kinds of memories subserved by different neurological substrates and that the formation of declarative memory depended on the integrity of the medial temporal lobe, including the hippocampal formation (Squire, 1992).

Declarative memory can be described as the capacity to remember facts and events consciously (Bartsch & Butler, 2013; Bird & Burgess, 2008; Milner et al., 1998). Declarative memory is further subdivided into two specific components: episodic memory and semantic memory (Tulving, 2002). Semantic memory comprises general knowledge and facts about the world in absence of a specific context (for example knowing that New York is a city located in the United States). Episodic memory can be described as the memory of our personal life experience. For example, knowing "how I spent my last vacation" or "what I did for my last birthday" is comprised in episodic memory. Episodic memory is absolutely central to building one's own identity. Episodic memory forms the record of my personal life and that is via episodic memory that I can remember my past, and therefore "Who I am". In sum, souvenirs of our own existence are built on our ability to form episodic memories. If we lose this ability tomorrow, we will be incapable, like H.M., of remembering who we are.

In order to study episodic memory, researchers have often considered its three fundamental components, the "what", "where" and "when" that necessarily compose an episode (Nyberg et al., 1996; Tulving, 2002). Episodic memory therefore does not simply refer to an event that happened in the past, but it is somehow reconstructed via the integration of its spatial and temporal components. When I remember my last vacation, I am able to tell that I spent three days with my friends (what) in Belgium (where) last spring (when). Among those components, the spatial (where) component of episodic memory, which is more specifically defined as allocentric spatial memory, has been investigated the most (Morris, 2007). Allocentric spatial memory consists in viewpoint-independent representations of the environment, in which spatial locations are coded in relation to different objects constituting the environment (O'Keef & Nadel, 1978). As a fundamental component of episodic memory, allocentric spatial memory has been shown to be dependent on the integrity of the hippocampal formation (Lavenex & Banta Lavenex, 2013), which will be at the centre of the next chapter.

1.2 Neuroanatomy

The hippocampal formation, which comprises, among other structures, the entorhinal cortex, has been shown to be critical for the formation of episodic memory. Therefore, in order to understand the neurobiological substrates participating in the emergence of memory processing, it is essential to have a general comprehension of the current knowledge about the anatomical organization of the hippocampal formation, including the entorhinal cortex. In the first section of this chapter, I describe the principal anatomical features of the hippocampal formation. As the focus of this work is specifically the entorhinal cortex, I will not expose in detail the connections of the different hippocampal subregions but will provide necessary descriptions in order to facilitate the comprehension of this work. The second section will be dedicated to the anatomy of the monkey entorhinal cortex, including its intrinsic and extrinsic connections. In a third section, I will provide a comparison of the anatomical features in the rat, monkey and human entorhinal cortex, as knowing the general similarities and differences between those three species is essential to extrapolate data acquired with animal models to the emergence of episodic memory in humans. Finally, the fourth and last section will summarize our current knowledge of the development of the hippocampus and entorhinal cortex.

1.2.1 Neuroanatomy of the hippocampal formation

The entorhinal cortex is part of a group of cortical regions located in the medial temporal lobe called the hippocampal formation. In addition to the entorhinal cortex, the hippocampal formation includes the dentate gyrus, the hippocampus, the subiculum, the presubiculum and the parasubiculum (Amaral & Lavenex, 2007). Ramón y Cajal and his student Lorente de Nó were the first to provide a detailed description of the hippocampal region at the beginning of the 20th century (Lorente de Nó, 1933, 1934; Ramón Y Cajal, 1909), and since then it has been the subject of intensive investigation especially because of its extraordinary configuration, and unique features (Boccara et al., 2015). A particular aspect of the hippocampal formation is that the passage of information through intrahippocampal circuits is largely unidirectional, as most regions do not have direct reciprocal connections (see detailed description below).

Intrinsic hippocampal circuits can therefore be considered to form a functional loop of information processing. Additionally, while the hippocampal formation appears to receive direct inputs from a relatively limited number of neocortical regions, each of these regions is a convergence zone that likely provides information from a much broader extent of the cortex (Lavenex & Amaral, 2000). In this way, the hippocampal formation is ultimately linked to much of the processing that takes place within the neocortex. Finally, its highly distributed three dimensional organization of intrinsic associational connections gives the hippocampal formation a unique advantage to integrate information (Amaral & Lavenex, 2007).

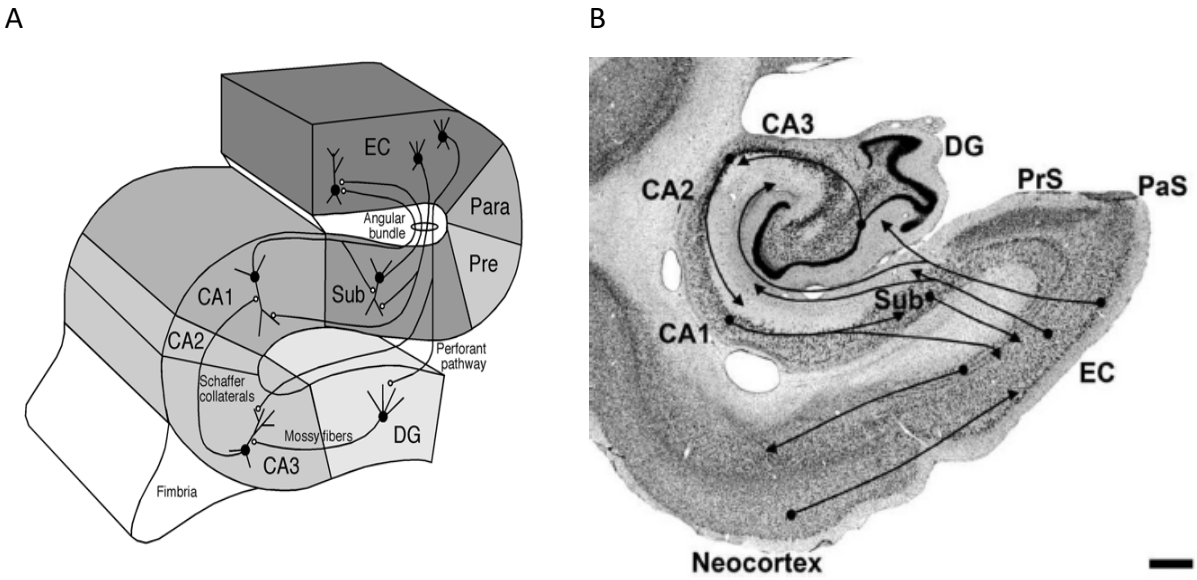

Figure 1: A. Schematic representation of the different pathways within the hippocampal formation (Reproduced from Amaral & Lavenex, 2007). **B.** Illustration of the main intrinsic hippocampal pathways, on a coronal section at mid rostro-caudal level of the rhesus monkey (*Macaca mulatta*) hippocampus. Scale bar = 1 mm (Reproduced from Lavenex & Banta Lavenex, 2013). EC: entorhinal cortex; DG: dentate gyrus; CA3, CA2, CA1: fields of the hippocampus proper; Sub: subiculum; Pre/PrS: presubiculum; Para/PaS: parasubiculum.

In this hippocampal circuit, the entorhinal cortex plays a critical role as it constitutes the main interface for bi-directional communication between the neocortex and the hippocampal formation. The hippocampal formation receives about two thirds of its neocortical input through the entorhinal cortex (Amaral & Lavenex, 2007). From the entorhinal cortex, cells located in layer II project to the dentate gyrus and CA3 through what is called the perforant pathway (Figure 1; (Lavenex & Amaral, 2000)). Parallelly, cells located in layer III of the

entorhinal cortex project to the subiculum and CA1 via the perforant and the alvear pathways (Amaral & Lavenex, 2007; Witter & Amaral, 1991). Then, the granule cells of the dentate gyrus project to CA3 via the mossy fibers (Kondo, Lavenex, & Amaral, 2008), and CA3 cells project further to CA1 via the Schaffer collaterals (Kondo, Lavenex, & Amaral, 2009), which in turn project to the subiculum. As the way of information processed through the hippocampal formation is unidirectional, it seems important to add that the dentate gyrus and CA3 do not project back to the superficial layers of the entorhinal cortex, CA3 does not project back to the dentate gyrus and CA1 does not project back to CA3 (Amaral & Lavenex, 2007; Witter & Amaral, 2021). Finally, to close the loop, CA1 and the subiculum project to the deep layers of the entorhinal cortex, that will relay the processed information back to the neocortex either directly (Munoz & Insausti, 2005) or via the perirhinal and parahippocampal cortices (Lavenex, Suzuki, & Amaral, 2002).

1.2.2 Neuroanatomy of the entorhinal cortex

As described above, the entorhinal cortex has a particularly important role in the hippocampal loop of memory processing, as it is the main entry point for sensory information to reach the hippocampus, as well as the main exit way for the information processed by the hippocampus toward cortical areas. More than just a relay for information to be processed, the entorhinal cortex is already a step of integration of information before it is transmitted to the hippocampus (Lavenex & Amaral, 2000). Additionally, the different subdivisions and layers of the entorhinal cortex are connected (extrinsically and intrinsically) to different brain regions and are thus implicated in different functional circuits. Having a global perspective of those regions and their connections is therefore critical in order to investigate the postnatal development of neuronal substrates supporting episodic memory.

In this subsection, I will first provide a brief description of the different subdivisions of the entorhinal cortex. I will then detail the connections of the entorhinal cortex with the hippocampal formation and the neocortex and finally, I will expose the main features of its intrinsic connections. I would like to specify that the following section will focus on studies in monkeys as it is the main subject of this thesis. The anatomical comparison of the rat, monkey and human entorhinal cortex will be considered in another section later in this chapter.

1.2.2.1 The monkey entorhinal cortex: subdivisions

Ramón Y Cajal (1901-1902) was the first to describe the entorhinal cortex, although he called it the “spheno-occipital ganglion”. The term entorhinal cortex, which literally means the cortex inside the rhinal (because of the proximity of the entorhinal cortex with the rhinal sulcus), was used for the first time by Brodmann (1909) who divided the area in two portions (a lateral area 28a and a medial area 28b) based on cytoarchitectonic characteristics (Boccara et al., 2015; Brodmann, 1909). Ramón Y Cajal’s student Lorente de Nó later subdivided the entorhinal cortex in a lateral, an intermediate, and a medial subdivision based on the projections to the hippocampal formation (Lorente de Nó, 1933).

In contrast to other hippocampal regions, the entorhinal cortex has a clear multilaminate appearance, which comprises six layers (Amaral, Insausti, & Cowan, 1987; Amaral & Lavenex, 2007). A particularity of the entorhinal cortex, compared to other cortical structures, is that there is no cell layer IV. In place of layer IV, we can observe a vacant layer called lamina dissecans. The layers are named along a superficial-to-deep axis. Layer I is the most superficial layer (close to the surface of the brain) and layer VI is the deepest layer of the cortex (close to the white matter).

The different subregions of the cynomolgus monkey (*Macaca fascicularis)* entorhinal cortex were originally defined by Amaral and colleagues (1987). They distinguished seven distinct subdivisions (Figure 4) and provided a description of their cytoarchitectonic organization in order to have precise and reliable criteria to discriminate those subdivisions and their layers: the olfactory subdivision (Eo), the rostral subdivision (Er), the lateral subdivision (El) (including the lateral rostral lr and the lateral caudal lc subdivisions), the intermediate subdivision (E_I), the caudal subdivision (E_C) and the caudal limiting subdivision (E_{CL}). Here are the descriptions of their localization.

Eo: The most rostral subdivision of the entorhinal cortex is named *the olfactory subdivision* according to the direct input that it receives from the olfactory bulb. Topographically, it adjoins medially first the piriform cortex and further the periamygdaloid cortex. Laterally, it is limited by area 35 of the perirhinal cortex at the rostral level and more caudally by the lateral subdivision of the entorhinal cortex. Note that the particularity of this subdivision is its lack of deep layers.

Er: *The rostral entorhinal cortex* is located in the rostral part of the entorhinal cortex and

is bounded medially by Eo and laterally by the lateral subdivision of the entorhinal cortex. Caudally, it adjoins the intermediate subdivision of the entorhinal cortex.

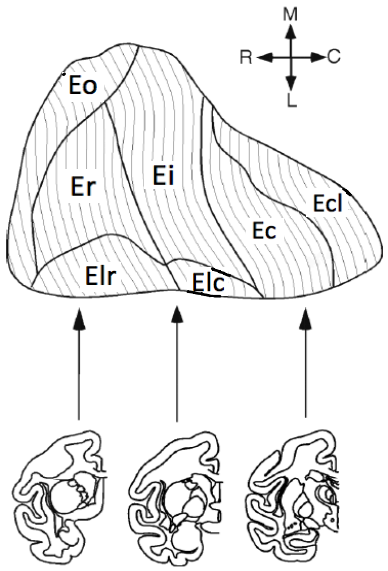

Figure 2 : Map of a *Macaca fascicularis* monkey entorhinal cortex and its seven subdivisions. Each thin line in the map represents a coronal section of the brain. Three rostrocaudal levels are illustrated below. Arrows in the top right corner indicate the general orientation of the map. Adapted from (Amaral et al., 1987).

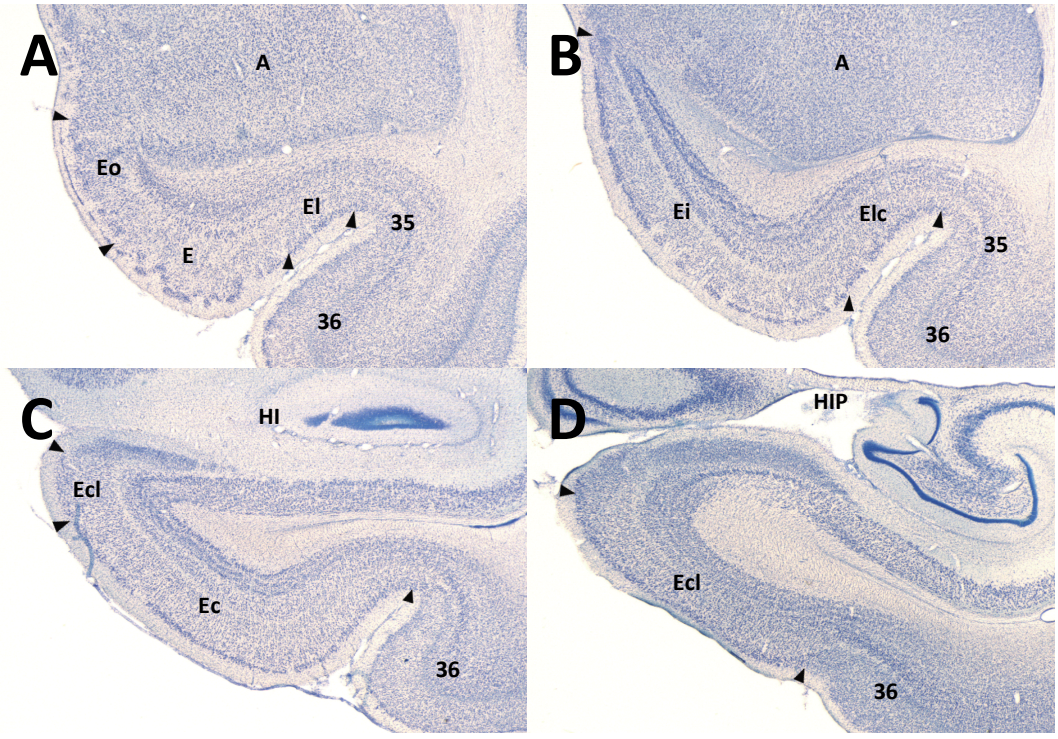

Figure 3: Low-magnification photomicrographs illustrating the main subdivisions of the rhesus monkey entorhinal cortex (*Macaca mulata)*, from rostral (A) to caudal (D). Scale bar = 1 mm. A: Amygdala; HIP: Hippocampus; Eo: The olfactory subdivision of the entorhinal cortex; Er: the rostral subdivision of the entorhinal cortex; Ei: the intermediate subdivision of the entorhinal cortex; Elr : the lateral rostral subdivision of the entorhinal cortex; Elc: the lateral caudal subdivision of the entorhinal cortex; Ec: the caudal subdivision of the entorhinal cortex; Ecl: the caudal limiting subdivision of the entorhinal cortex; 35 and 36: Brodmann's areas 35 and 36 of the perirhinal cortex.

Ei: *The intermediate subdivision* is approximately situated, on a rostrocaudal level, in the middle of the entorhinal cortex. Its lateral boundary is formed by the lateral subdivision of the entorhinal cortex and its medial boundary is constituted by Eo at first and then by the parasubiculum.

El: *The lateral entorhinal cortex* begins near the rostral pole of the entorhinal cortex and is separated in two distinct subdivisions: Elr and Elc. Medially, Elr borders Er and Elc borders Ei. Laterally, the rhinal sulcus forms the limit between E_L and the perirhinal cortex (mostly area 35 and at a caudal level Elc adjoins area 36).

Ec: *The caudal subdivision* is in the caudal part of the entorhinal cortex. It forms a medial boundary with the caudal limiting subdivision of the entorhinal cortex and a lateral boundary with area 36.

Ecl: *The caudal limiting subdivision* ends the entorhinal cortex caudally. It merges medially with the parasubiculum and laterally with area 36. Caudally, the parasubiculum and area TH will then take the place of the entorhinal cortex.

Among those subdivisions, Eo, Er and Elr can be considered as forming the rostral portion of the entorhinal cortex, while Elc, Ec and Ecl constitute the caudal portion. Finally, Ei, as suggested by its name, is an intermediate subdivision, which can be considered included in both rostral and caudal portions. Indeed, it shares some morphological characteristics, as well as extrinsic and intrinsic connections, with both the rostral and caudal portions of the entorhinal cortex (Chrobak & Amaral, 2007; Insausti, Amaral, & Cowan, 1987a).

The identification of the entorhinal subdivisions and layers is critical as they are connected to different hippocampal et neocortical regions and might contribute therefore to different neocortical-hippocampal functional circuits.

1.2.2.2 The monkey entorhinal cortex: extrinsic et intrinsic connections

The seven subdivisions of the monkey entorhinal cortex receive different cortical and subcortical inputs. The major source of neocortical inputs, about two-thirds of the total neocortical inputs, comes from the perirhinal and parahippocampal cortices (Insausti et al., 1987a; Suzuki & Amaral, 1994b). The projections of the perirhinal and parahippocampal cortices to the entorhinal cortex are distinct, but their target zones are partially overlapping. The perirhinal cortex projects to the rostral two-third of the entorhinal cortex, which corresponds to the subdivisions Eo, Er, Elr and Ei, while the parahippocampal cortex provides

inputs to the caudal two-third of the entorhinal cortex, which corresponds to the subdivisions Ei, Elc, Ec and Ecl (Suzuki & Amaral, 1994b). The reciprocity of the connections between the parahippocampal cortex and the entorhinal cortex is very important, while the degree of reciprocity between the perirhinal cortex and the entorhinal cortex depends on the mediolateral localization in the perirhinal cortex (Suzuki & Amaral, 1994b). The entorhinal cortex has a higher degree of reciprocity with the medial portions than the lateral portions of the perirhinal cortex (Suzuki & Amaral, 1994b).

In addition to the perirhinal and parahippocampal cortices, the entorhinal cortex also receives inputs from various cortical and subcortical regions (Insausti et al., 1987a; Insausti, Amaral, & Cowan, 1987b). The target areas of those projections are generally spatially restricted within the entorhinal cortex (Figure 4) (Insausti & Amaral, 2008). Rostral subdivisions (Eo, Er, Elr and Ei) receive direct projections from the amygdala, the lateral orbitofrontal cortex, the anterior cingulate cortex and the insular cortex, whereas caudal subdivisions (Ei, Ec and Ecl) are the targets of direct projections from the parietal cortex, the posterior cingulate cortex, the retrosplenial cortex and the superior temporal gyrus (Insausti & Amaral, 2008; Insausti et al., 1987a, 1987b; Kobayashi & Amaral, 2007). Additionally, intermediate levels of the entorhinal cortex receive projections from the upper bank of the superior temporal sulcus (Insausti & Amaral, 2008), and Eo receives direct projections from the olfactory bulb (Insausti et al., 1987a).

Because of its pattern of connections, the entorhinal cortex can be considered as the main gateway for bi-directional interaction between the neocortex and the hippocampal formation (Amaral & Lavenex, 2007; Lavenex, 2011, 2012). However, the entorhinal cortex is far from being just a relay to the hippocampus but constitutes an essential step in a hierarchy of associational networks participating in the integration of multimodal polysensory information within the medial temporal lobe memory system (Figure 5) (Lavenex & Amaral, 2000).

The perirhinal and parahippocampal cortices represent the first step of this hierarchical organization of associational networks. They receive a multitude of inputs from various unimodal and polymodal associational cortices (Suzuki & Amaral, 1994a) and the important intrinsic connections and the network of reciprocal, associational connections between them (Suzuki & Amaral, 1994b) potentially lead to substantial level of integration of information (Amaral & Lavenex, 2007).

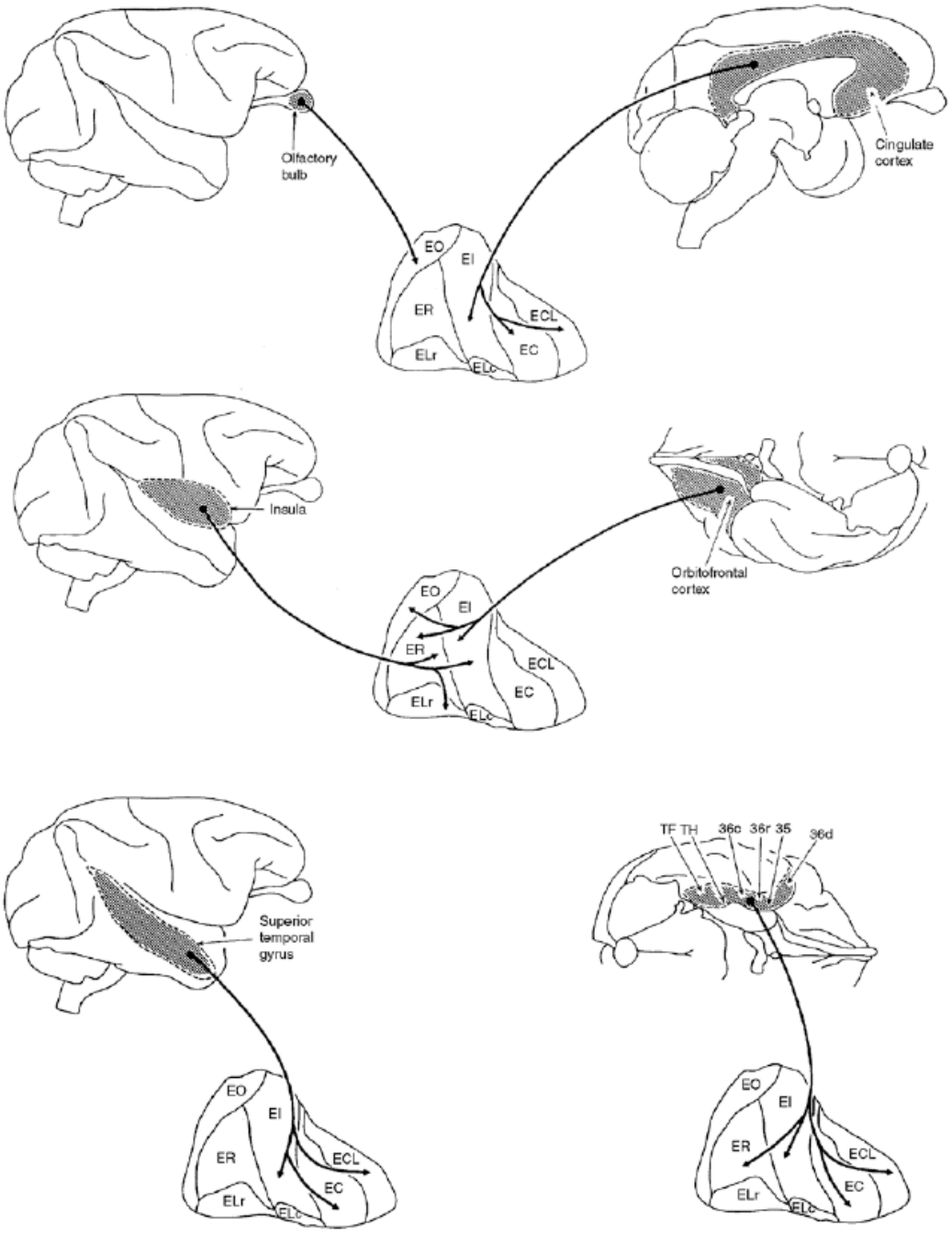

Figure 4 : Illustration of the major cortical inputs to the different subdivisions of the monkey entorhinal cortex ((Amaral & Lavenex, 2007) adapted from (Insausti et al., 1987a)).

Processed information is then transmitted to the entorhinal cortex which constitutes the second stage of this hierarchy of associational networks. Again, the high degree of intrinsic and associational connections within the entorhinal cortex (Chrobak & Amaral, 2007) increases further the level of integration of information before it is transmitted to the rest of

the hippocampal formation, via the perforant and alvear pathways (Lavenex & Amaral, 2000). The hippocampal formation can thus be considered as the final stage in a cascade of neocortical sensory processing (Amaral & Lavenex, 2007).

The progression of sensory information arriving from the neocortex through the perirhinal and parahippocampal cortices, the entorhinal cortex and hippocampal circuits leads to an increase of the level of integration, complexity, or abstraction at each stage of the process. Therefore, the entorhinal cortex is not only a relay for the information to be processed by the hippocampus, but rather participates actively in memory processing as it will be developed below with the description of functional studies (Lavenex & Amaral, 2000).

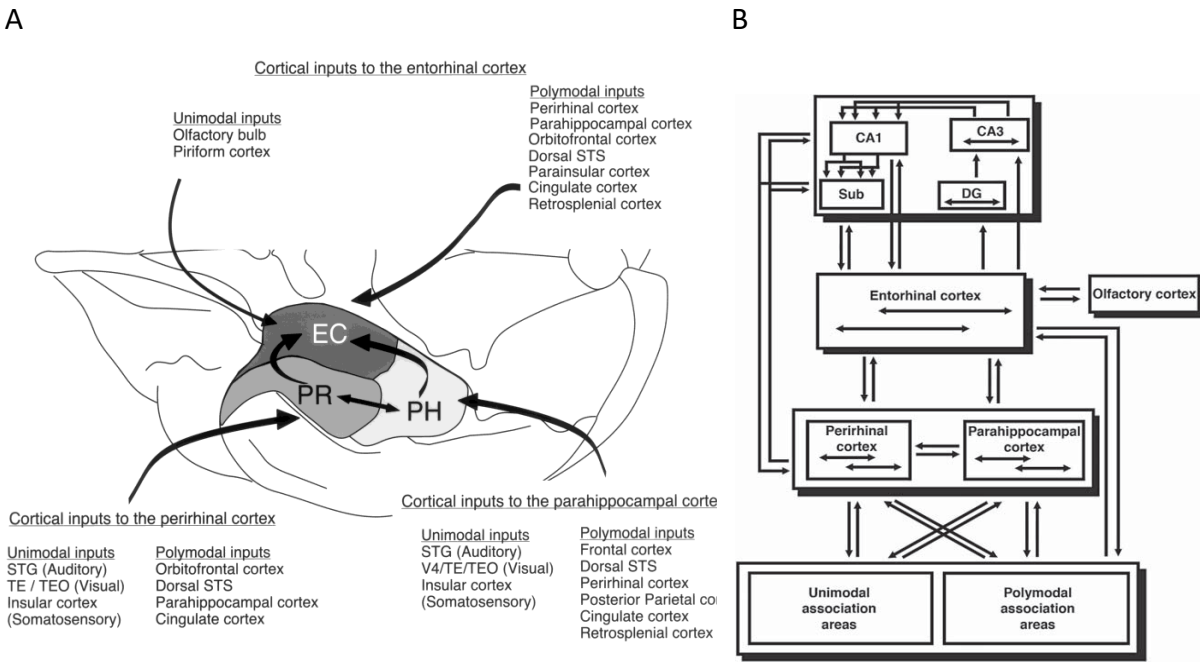

Figure 5: A. Schematic representation of the major connections of the entorhinal, perirhinal and parahippocampal cortices in the macaque monkey brain, from a ventral perspective. (Reproduced from Lavenex & Amaral, 2000) **B.** Schematic representation of the hierarchical organization of associational networks in the primate medial temporal lobe. DG: dentate gyrus; CA3, CA2, CA1: fields of the hippocampus proper; Sub: subiculum. (Reproduced from Lavenex & Amaral, 2000).

In addition to the differential connections of the entorhinal subdivisions, it is necessary to make a distinction between entorhinal layers, as they send and receive projections from different hippocampal areas. As mentioned above, superficial layers II and III are the origins of projections to the dentate gyrus and the hippocampus, while deep layers V and VI are the

targets of feedback projections from the hippocampus.

Entorhinal cortex layer II neurons project towards the dentate gyrus and CA3, through the perforant path, whereas entorhinal cortex layer III neurons project towards CA1 and the subiculum via the perforant and alvear pathways (Amaral & Lavenex, 2007; Witter & Amaral, 1991; Witter, Van Hoesen, & Amaral, 1989). More specifically, projections from the entorhinal cortex reach the outer two-third of the molecular layer of the dentate gyrus, the stratum lacunosum-moleculare of the hippocampus, and the molecular layer of the subiculum (Witter & Amaral, 1991; Witter et al., 1989). These projections reaching the dentate gyrus, hippocampus, and the subiculum are topographically organized. Neurons located in lateral portions of the entorhinal cortex project to caudal portions of the dentate gyrus and hippocampus. In contrast, neurons located in more medial portions of the entorhinal cortex project to rostral levels (Witter & Amaral, 1991; Witter et al., 1989). Additionally, the rostrocaudal location of the origin of these projections influences the location of termination in the dentate gyrus. While the rostral portion of the entorhinal cortex projects mostly to the outer portion of the molecular layer of the dentate gyrus, the caudal portion of the entorhinal cortex projects mostly to the middle molecular layer (Witter & Amaral, 1991). Rostral levels of the entorhinal cortex project toward the border of CA1 and the subiculum, whereas caudal levels of the entorhinal cortex project to more proximal portions of CA1, closer to CA2 and to more distal portions of the subiculum, closer to the presubiculum (Witter & Amaral, 1991).

Entorhinal cortex layer V and VI neurons receive feedback projections from CA1, the subiculum, presubiculum and parasubiculum, but not from the dentate gyrus and CA3 (Witter & Amaral, 2021). Additionally, layer III neurons of the entorhinal cortex, and some of layer I, II and V neurons, are the targets of a dense projection from the presubiculum and the parasubiculum. The projections from the hippocampus and subicular areas to the entorhinal cortex demonstrate a topographic organization that matches the topography of the projections from the entorhinal cortex to these areas (Figure 6; Witter & Amaral, 2021). Lateral portions of the entorhinal cortex receive projections from neurons located at caudal levels of CA1 and the subiculum, while medial portions of the entorhinal cortex receive projections from neurons located at more rostral levels. The topography of those efferent and afferent projections is particularly interesting, as it suggests that cells at different rostrocaudal levels would not be reached by the same type of information (Witter & Amaral, 2021).

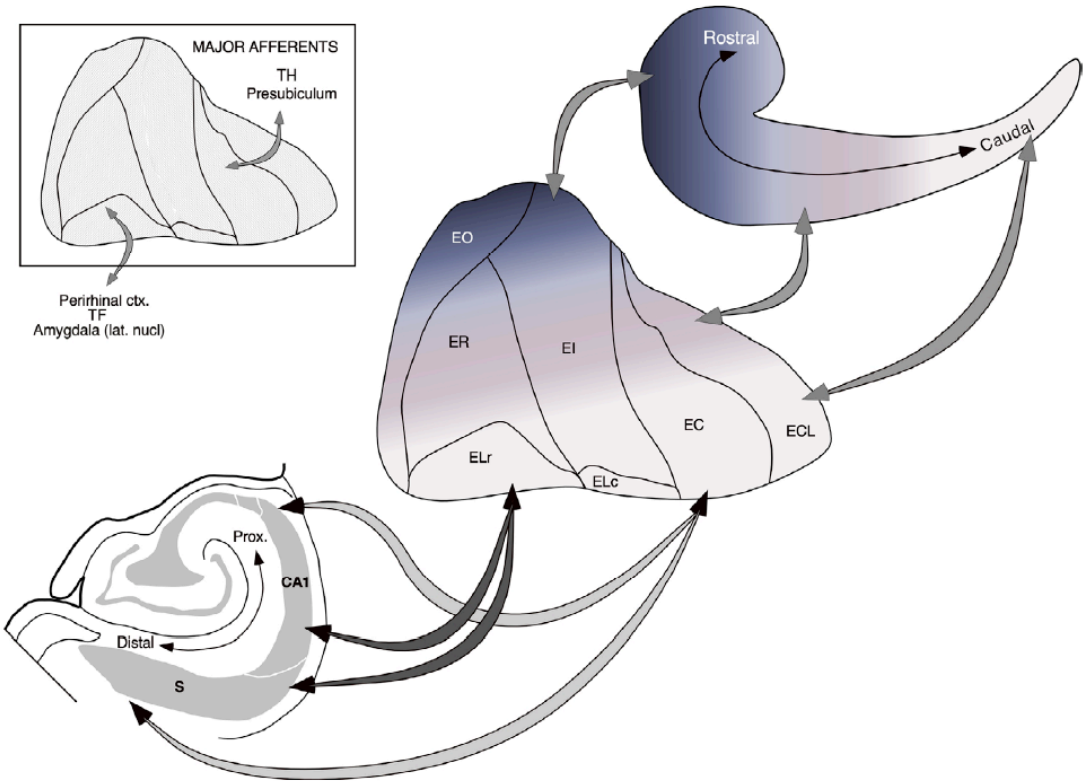

Figure 6 : Summary of the major topographical features of entorhinal inputs and outputs with hippocampal fields. (Reproduced from Witter & Amaral, 2021).

In addition to its afferent and efferent connections, the primate entorhinal cortex has an extensive system of associational connections that arises from both the deep and superficial layers (Chrobak & Amaral, 2007). At least two rostrocaudally oriented bands, a medial and a lateral one, as well as a third very medially located band including mainly Eo, have been identified, showing that the intrinsic connections of the entorhinal cortex are organized in bands oriented rostrocaudally (Chrobak & Amaral, 2007). However, in monkeys, those bands do not extent through the entire rostrocaudal length of the entorhinal cortex but have a maximum length of about one-third to one-half of the structure, suggesting some functional specialization between the rostral and caudal portions of the entorhinal cortex. Furthermore, anterograde tracer injections suggest that the caudal entorhinal cortex has more extensive associational connections than the rostral entorhinal cortex, as injections located at mid or caudal levels of the entorhinal cortex give rise to projections with a larger rostrocaudal extent than injections located in the rostral portion of the entorhinal cortex (Chrobak & Amaral, 2007). Finally, anterograde tracing and labelling studies indicate that deep

layers V and VI innervate the superficial layers of the entorhinal cortex (P. S. Buckmaster, Alonso, Canfield, & Amaral, 2004; Chrobak & Amaral, 2007). This point has important implications for the understanding of memory processing within the hippocampal formation. Indeed, as the superficial layers are the origins of projections to the hippocampus and the deep layers are the targets of projections back from the hippocampus, outputs from deep layers to superficial layers within the entorhinal cortex might regulate information reaching the hippocampus (Chrobak & Amaral, 2007).

In conclusion, the extensive extrinsic interconnections of the entorhinal with different brain regions and its important intrinsic neuronal network suggest a contribution of the entorhinal cortex to distinct neuronal circuits participating in the formation of episodic memory. Moreover, it suggests that the entorhinal cortex does not only make the connection between the neocortex and the hippocampal formation but participates actively in the integration of multimodal polysensory information within the medial temporal lobe and constitutes therefore a critical step in the hippocampal loop of memory processing.

1.2.3 Comparative anatomy of the rat, monkey and human entorhinal cortex

Animal models are used extensively to study the structure and functions of the human hippocampal formation, including the entorhinal cortex. Although animal models, especially rats, present obvious practical and ethical advantage in research, rats and monkeys are not humans and one should therefore be aware of the similarities and differences between those species before extrapolating the findings to humans (Lavenex, Banta Lavenex, & Favre, 2014). In the case of the entorhinal cortex, and the hippocampal formation in general, this point is particularly important as most of the functional studies are carried in rats. For this reason, I will compare, in this section, the available anatomical data in rats, monkeys and humans to demonstrate why knowing the anatomy of the monkey entorhinal cortex is essential in order to link fundamental research in rodents with memory processing in humans.

The hippocampal formation has a generally similar organization in mammals (Amaral & Lavenex, 2007; Insausti, 1993). The rhinal sulcus, which marks the border between the neocortex and the entorhinal cortex, and the hippocampal sulcus are common anatomical landmarks in many species to define the limit of the hippocampal formation, although the

rhinal sulcus is less noticeable in primates, especially in humans (Insausti, 1993). The particular layering of the entorhinal cortex, as it was described in a previous section, is also a common feature in many mammals. The entorhinal cortex usually comprises six layers with the same architectural principle: external and internal layers separated by a wide or narrow lamina dissecans (Insausti, 1993). However, the entorhinal cortex presents some differences from one species to another, and some distinctions should thus be presented.

The most evident difference concerns neuron numbers and the laminar organization. We observe an increase in number of cells at all levels of the entorhinal cortex, as well as clear differences in the organization of neurons (Insausti, 1993) from rats (West, Slomianka, & Gundersen, 1991) to humans (West & Slomianka, 1998), with an intermediate step in monkeys (Piguet, Chareyron, Banta Lavenex, Amaral, & Lavenex, 2018) (Figure 7). Additionally, the associational areas of the neocortex have stronger connection with the primate entorhinal cortex than with the rat (Amaral & Lavenex, 2007). Different, yet related subdivisions have also been identified in different species. In monkeys, as described in the previous section, the entorhinal cortex has been divided into seven subdivisions (Eo, Er, Elr, Elc, Ei, Ec and Ecl) (Amaral et al., 1987). However, based on some differences in the organization of the layers and their neuronal projections, different numbers of subdivisions have been identified in rats and humans.

In rats, the number of subdivisions considered varies between studies. In an attempt to divide the rat entorhinal cortex in a way that would make it comparable to the primate entorhinal cortex, Insausti and colleagues (1997) identified six subdivisions: Caudal entorhinal (CE), Medial entorhinal (ME), Ventral intermediate entorhinal (VIE), Dorsal intermediate entorhinal, (DIE), Dorsal Lateral entorhinal (DLE) , and Amygdalo-entorhinal transitional (AE) (Insausti, Herrero, & Witter, 1997). However, area AE, which was initially identified based on preliminary observations suggesting projections to the dentate gyrus, may today no longer be considered as a subdivision of the entorhinal cortex based on studies refuting these projections (Pitkanen, Pikkarainen, Nurminen, & Ylinen, 2000). The rat entorhinal cortex is therefore composed of five different subdivisions: CE and ME, which constitute the Medial entorhinal cortex (MEC), and VIE, DIE and DLE, which constitute the Lateral entorhinal cortex (LEC) (Boccara et al., 2015). Similar to the rat, five subdivisons corresponding to the description of Insausti et al. (1997) have been identified in the mouse based on cytoarchitectonic characteristics (van Groen, 2001). In the majority of functional studies,

however, the entorhinal cortex of rodents is subdivided into only two main areas, the medial entorhinal cortex (MEC), and the lateral entorhinal cortex (LEC), which correspond respectively to the caudal and rostral portions of the monkey entorhinal cortex (Amaral & Lavenex, 2007). Interestingly, a description by Gatome et al. (2009) proposed a cytoarchitectonic division in bats that shared characteristics with both rodents and primates. They described five subdivisions assembled in two global areas: MEA, which comprises Ecl and Ec, and LEA, which comprises Ei, Er and El (Gatome, Slomianka, Mwangi, Lipp, & Amrein, 2010).

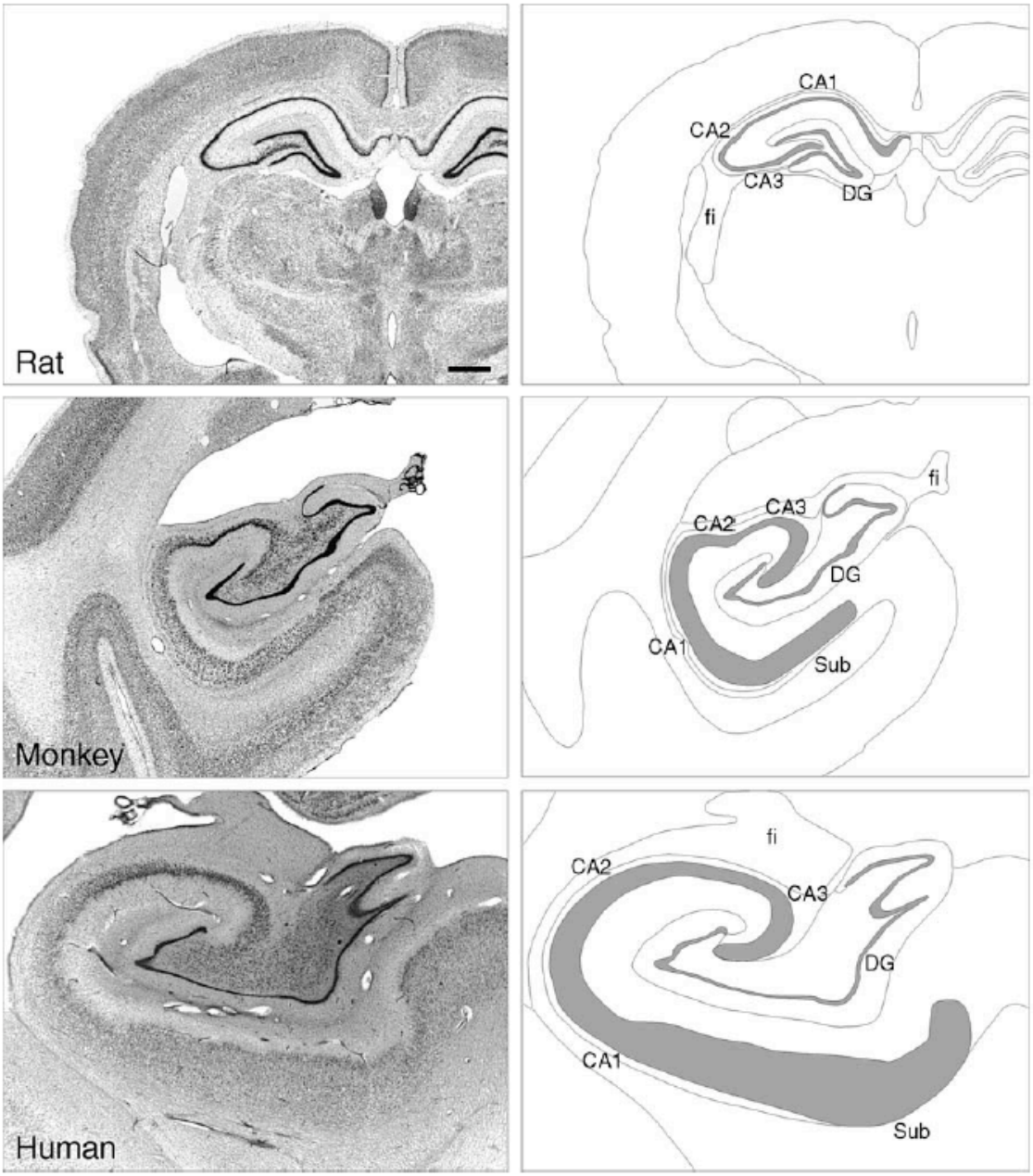

Figure 7: Nissl-stained sections and line drawings of the rat, monkey and human hippocampal formation. Scale bar = 1 mm. Reproduced from (Amaral & Lavenex, 2007)

One of the major distinctions between the entorhinal cortex of the rat and the entorhinal cortex of the monkey concerns their intrinsic associational connections. Although the intrinsic connections are organized in rostrocaudally oriented bands in both species, the rostrocaudal extent of the projections differs (Chrobak & Amaral, 2007; Dolorfo & Amaral, 1998a, 1998b). In the rat, the entorhinal projections cover the entire rostrocaudal extent of the entorhinal cortex (Dolorfo & Amaral, 1998a), while in the monkey, the projections extend for only one half or less of the rostrocaudal length of the entorhinal cortex (Chrobak & Amaral, 2007). Another important difference between the rat and monkey entorhinal cortex concerns the olfactory inputs. While the rat receives direct input from the olfactory bulb to the entire extent of the entorhinal cortex, the monkey receives olfactory inputs only in the olfactory subdivision Eo, which represents about 10% of the entire entorhinal cortex (Amaral & Lavenex, 2007; Insausti, Marcos, Arroyo-Jimenez, Blaizot, & Martinez-Marcos, 2002).

As for the rat, the number of subdivisions in the human entorhinal cortex has been subject to discussion. However, Insausti and colleagues (1995) performed a reliable cytoarchitectonic analysis of the human entorhinal cortex and identified different subdivisions that make it comparable to non-human primates. Their observations revealed eight distinct subdivisions: olfactory (Eo), lateral rostral (Elr), rostral (Er), medial intermediate (Emi), intermediate (Ei), lateral caudal (Elc), caudal (Ec), and caudal limiting (Ecl) (Insausti, Munoz-Lopez, Insausti, & Artacho-Perula, 2017; Insausti, Tunon, Sobreviela, Insausti, & Gonzalo, 1995). In general, they observed an organization very similar to monkeys, but the similarity varied depending on the subdivisions. The ones located in the rostral and medial portions of the entorhinal cortex had closer cytoarchitectonic features between the two species, than those located in lateral, intermediate and caudal portions, especially with respect to their lamination (Insausti et al., 1995). This point is consistent with observations that, in general, lateral and caudal portions of the entorhinal cortex express a higher development in non-human primates than in rodents, and in humans than in non-human primates (Insausti, 1993).

In addition to the similarity of its general organization, the entorhinal cortex shares a common topography of its projections to the dentate gyrus in rats, monkeys and humans (Figure 8) (Insausti, 1993; Witter, 2007). In all three species, the origin of the projections to the rest of the hippocampal formation is in the superficial layers of the entorhinal cortex. Moreover, the target zones of those projections in the hippocampus depend on the

mediolateral level of the origin of projection in the entorhinal cortex. Thus, the medial entorhinal cortex projects to the rostral hippocampus and, conversely, lateral and caudal entorhinal cortex project to the caudal hippocampus (Insausti, 1993).

In functional studies, the entorhinal cortex is classically divided into two major areas: the medial entorhinal cortex (MEA), or caudal entorhinal cortex in monkeys, and the lateral entorhinal cortex (LEA), or rostral entorhinal cortex in monkeys. Although this distinction is reductive, it has the major advantage to make the entorhinal cortex comparable between species. Indeed, if the rostrocaudal and mediolateral extents of the entorhinal cortex exhibit differences between species, it seems that a general organization is identifiable in many mammalian species: rostral and medial portions of the entorhinal cortex have less developed organization, while caudal and lateral portions have a more developed organization (Insausti, 1993).

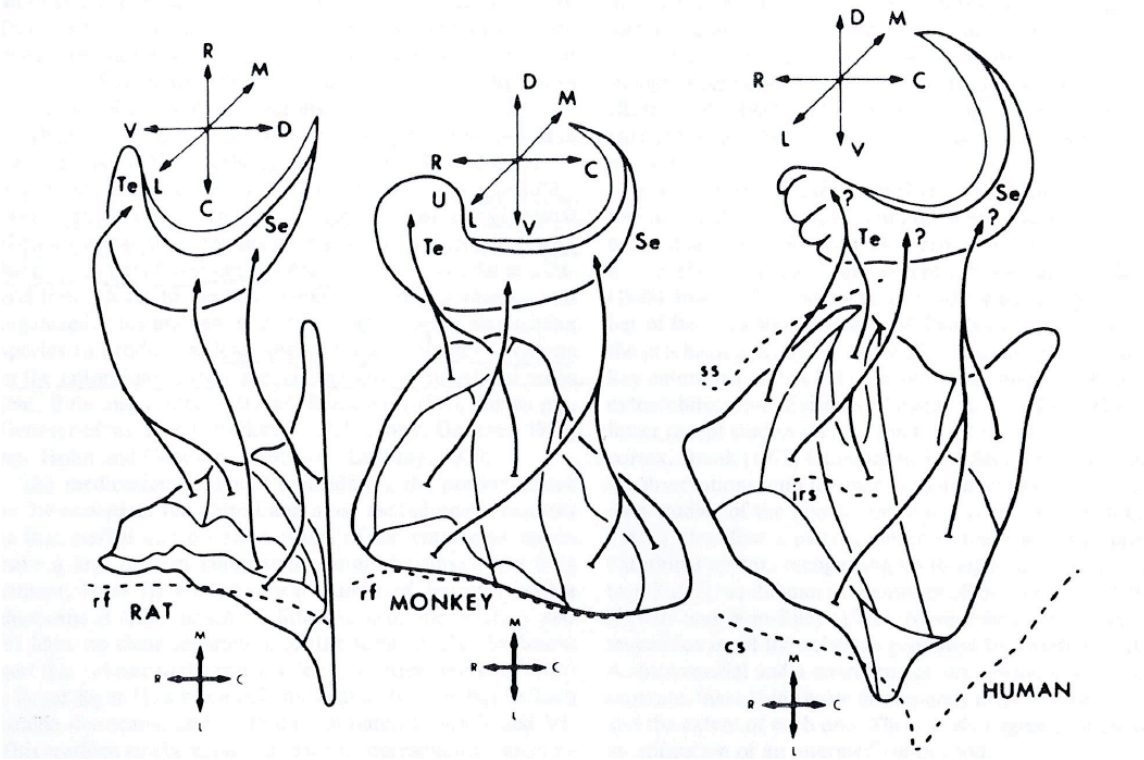

Figure 8 : Topography of projections from the entorhinal cortex to the rat, monkey and human dentate gyrus illustrating the similar organization between the three species (Insausti, 1993).

In conclusion, the overall organization and cytoarchitecture of the entorhinal cortex are similar in rats, monkeys and humans. However, there is a substantial increase in extrinsic and intrinsic connectivity in primates. In this comparative perspective, monkeys can be considered

as an important link between studies in rats and humans since their entorhinal cortex shares common characteristics with both species. Moreover, it is reasonable to think that brain structures and functions that are conserved between rat and monkeys are likely to be conserved in humans as well (Lavenex et al., 2014). Therefore, investigating the anatomy of the monkey entorhinal cortex is essential in order to link fundamental research in rodents with memory processes in humans.

1.2.4 The development of the hippocampal formation

This thesis is part of a larger project aimed to characterize the postnatal development of the primate hippocampal formation. Few years ago, two systematic, quantitative studies have been published by our laboratory on the early postnatal structural maturation of the dentate gyrus and the hippocampal formation in monkeys (Jabès, Lavenex, Amaral, & Lavenex, 2010, 2011). In the following section, I will summarize their findings, as they constitute the fundamental body of knowledge in the field, prior to my thesis. In addition, I will provide some information on what is currently known about the postnatal development of the human entorhinal cortex.

1.2.4.1 Development of the primate hippocampal formation

In a first study, Jabès and colleagues (2010) investigated the morphological changes of the monkey dentate gyrus from birth to adulthood (1-day-olds, 3-month-olds, 6-month-olds, 9-month-olds, 1-year-olds and adults). They first measured cell proliferation in the dentate gyrus using immunohistochemical detection of the protein Ki-67, an endogenous marker of cell division, and found a very high level of cell proliferation at birth, followed by an intermediate level until one year of age. Additionally, they used BrdU, an exogenous cell-division marker, in combination with NeuN, a neuron specific marker, and S100beta, a glia specific marker, to analyze the differentiation and survival of proliferating cells, four weeks after BrdU injection. The number of BrdU/NeuN positive cells and the number of BrdU/S100beta positive cells revealed a peak in the production of neurons and glial cells in the dentate gyrus within the first three postnatal months, followed by a sustained, intermediate level of production until at least one year of age. They also counted the number of Nissl-stained neurons to evaluate

the postnatal addition of neurons in the three layers of the dentate gyrus. Importantly, they found a large increase of neuron number in the granule cell layer between birth and three months of age, followed by a gradual increase until one year of age (Figure 9A). Their measurements also revealed that as much as 40% of the neurons present in the adult dentate gyrus were added postnatally. Their estimation of the volume of different layers further revealed significant increases from birth to beyond one year of age, which differed between layers (Figure 9B, C and D), suggesting distinct developmental profiles of those layers.

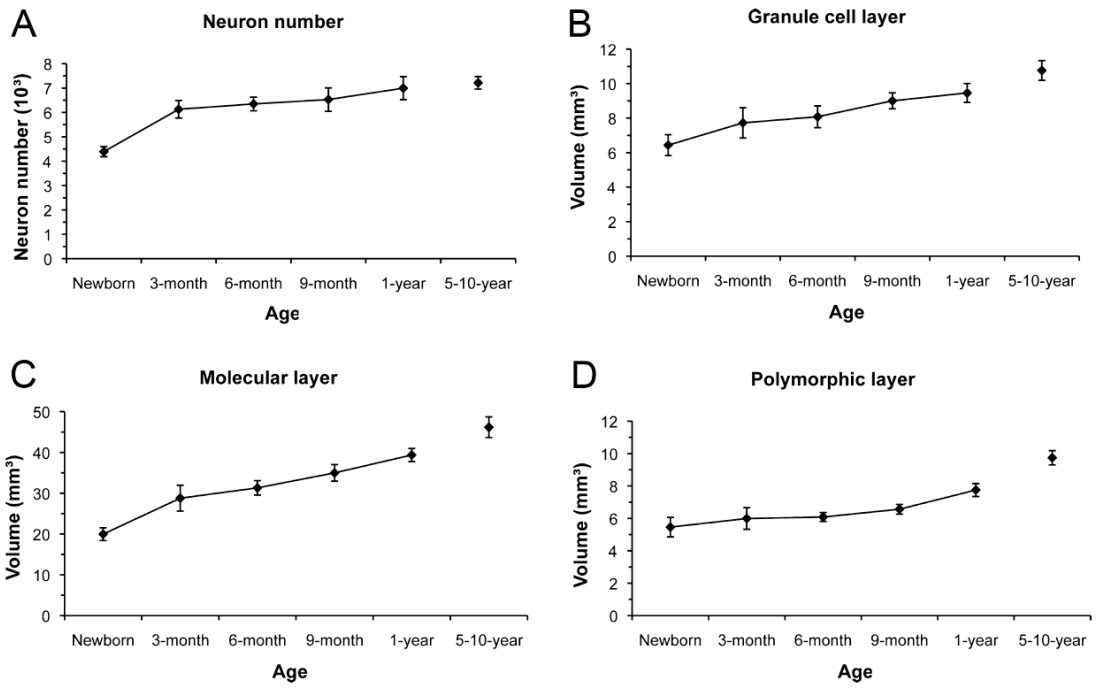

Figure 9: A: Number of neurons in the macaque monkey dentate gyrus at different ages from birth to adulthood. B-D: Volume of the different layers in the macaque monkey dentate gyrus from birth to adulthood. Reproduced from (Jabès et al., 2010).

In a second study, Jabès et al. (2011) published a quantitative analysis of the monkey hippocampal formation during early postnatal development. They estimated the number of Nissl-stained neurons, neuronal soma size and volumes of the different regions and layers of the hippocampal formation, at the exception of the entorhinal cortex. Their analysis revealed no difference in neuron number between different ages in any of these structures. However, their estimates of neuronal soma size showed a differential structural maturation within CA3

and the presubiculum (Table 1). Indeed, there was an increase in neuronal soma size in the proximal part of CA3 within the first three postnatal months, whereas there were no age-related differences in neuronal soma size in the distal part of CA3. These observations suggest that the distal portion of CA3, which receives direct projections from entorhinal cortex layer II neurons, might mature earlier than the proximal part of CA3, which receives projections from the dentate gyrus. Interestingly, in the presubiculum, which sends dense projections to layer III of the caudal part of the entorhinal cortex, they found that the average neuronal soma size was larger at birth than in adulthood.

	Birth	3 Months	6 Months	9 Months	1 Year	5–9 Years	Average
Dentate gyrus	578 ± 25	542 ± 37	536 ± 24	553 ± 24	503 ± 12	544 ± 46	543 ± 12
CA3 total	2,914 ± 159	3,004 ± 245	3,132 ± 206	3,432 ± 176	3,095 ± 82	3,516 ± 154	–
Proximal	2,255 ± 86	2,648 ± 227	3,014 ± 250	3,314 ± 130	2,892 ± 93	3,496 ± 188	–
Distal	3,295 ± 200	3,234 ± 260	3,193 ±192	3,503 ± 221	3,256 ± 80	3,532 ± 168	3,335 ± 76
CA2	2,673 ± 90	2,401 ± 248	2,750 ± 190	2,448 ± 389	2,573 ±294	2,465 ± 217	2,552 ± 96
CA1	2,129 ± 163	2,184 ± 207	2,684 ± 173	2,625 ± 383	2,565 ± 313	2,783 ± 282	2,495 ± 109
Subiculum	2,038 ± 92	1,890 ± 196	2,191 ± 153	2,121 ± 229	1,958 ± 243	1,861 ± 174	2,010 ± 72
Presubiculum	1,015 ± 55	1,070 ± 66	1,010 ± 29	1,072 ± 51	922 ± 28	754 ± 22	–
Parasubiculum	1,283 ± 56	1,255 ± 66	1,273 ± 39	1,305 ± 37	1,243 ± 44	1,249 ± 46	1,268 ± 18

Table 1: Soma size (μm^3 +- SEM) of principal neurons in the macaque monkey hippocampal formation. Reproduced from (Jabès et al., 2011).

As for neuronal soma size, the volumetric measurements of different regions and layers revealed a differential development of distinct regions and layers (Figure 10). In CA1, the volumes of stratum lacunosum moleculare, which receives projections from entorhinal cortex layer III neurons, revealed a relatively earlier development compared to strata oriens, pyramidale and radiatum, which receive projections from CA3 pyramidal neurons (Figure 10C). Finally, in the subiculum, the molecular layer, which receives projections from entorhinal cortex layer III neurons, exhibited an earlier development, as compared to the stratum pyramidale, which receives projections from CA1 pyramidal neurons.

To summarize, Jabès et al.'s results suggested a relatively late maturation of the dentate gyrus and CA3, as compared to CA1 and the subiculum, which continues beyond the first year of postnatal life. However, interestingly, the distal portion of CA3, which receives direct projections from entorhinal cortex layer II neurons, developed volumetrically earlier than the proximal portion. Similarly, in both CA1 and the subiculum, two regions that receive direct projections from entorhinal cortex layer III neurons, matured earlier than the rest of

the hippocampal structures. Knowing the maturation of the distinct layers of the entorhinal cortex seems therefore essential in order to better understand the structural neural correlates underlying the emergence of episodic memory.

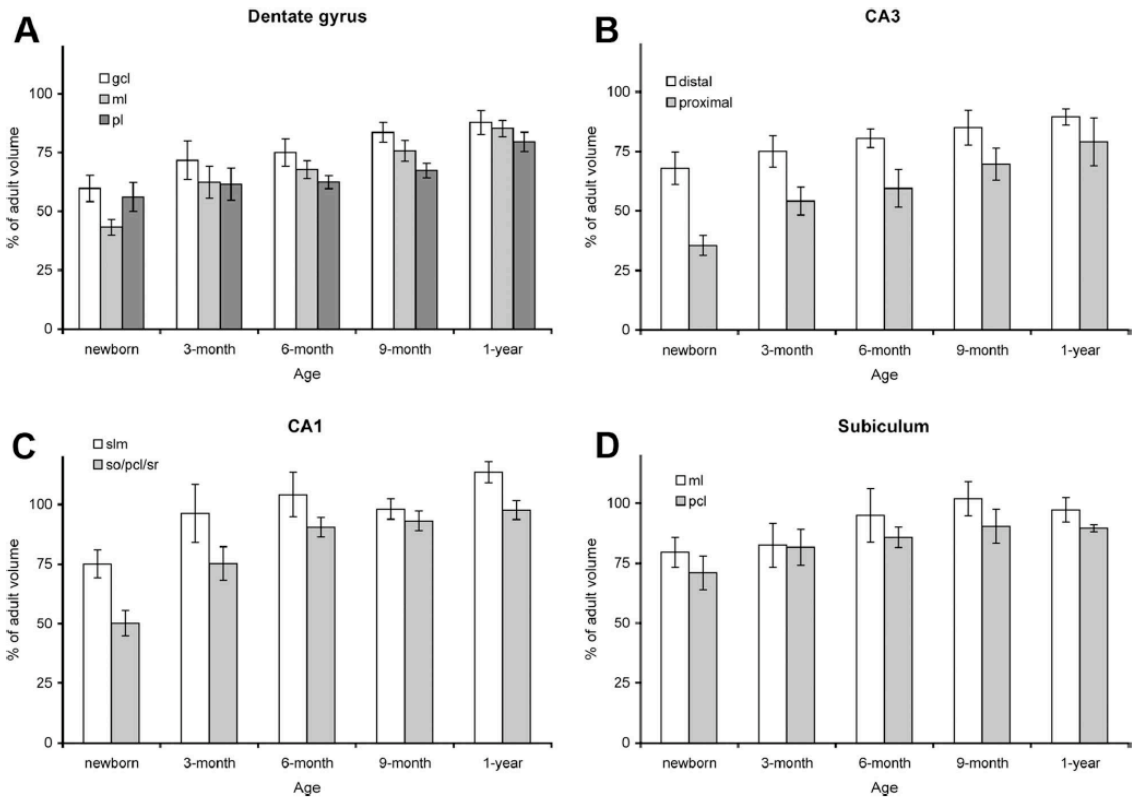

Figure 10: Percentage of adult volume in the different layers/regions of the macaque monkey dentate gyrus (A), CA3 field (B), CA1 field (C) and subiculum (D) at different postnatal ages. Slm: stratum lacunosum moleculare; so/pcl/sr: strata oriens, pyramidale and radiatum, which receives projections from CA3 pyramidal neurons; ml = molecular layer; pcl: stratum pyramidale. Reproduced from (Jabès et al., 2011)

In parallel to stereological studies, gene expression studies have been carried out in distinct regions of the rhesus monkey hippocampal formation during development (Favre, Banta Lavenex, & Lavenex, 2012a, 2012b; Lavenex & Banta Lavenex, 2013; Lavenex, Sugden, Davis, Gregg, & Lavenex, 2011). Lavenex et al. (2011) performed genome-wide microarray analysis of gene expression in five distinct regions of the hippocampal formation (entorhinal cortex, dentate gyrus, CA3, CA1 and subiculum) at four postnatal ages from birth to adulthood (1 day, 6 months, 1 year and 6-12 years of age) (Lavenex et al., 2011). They identified a large number of genes associated with glycolysis and glutamate metabolism in astrocytes that expressed

different expression levels in CA1 and CA3. In CA1, the expression of those genes decreased and reached adult-like level much earlier during postnatal development than what was observed in CA3 (Figure 11) (Favre et al., 2012b; Lavenex et al., 2011). Those observations are consistent with the stereological data suggesting a relatively earlier maturation of CA1 and a relatively later maturation of CA3 and provide further evidence of different profiles of maturation of different hippocampal circuits.

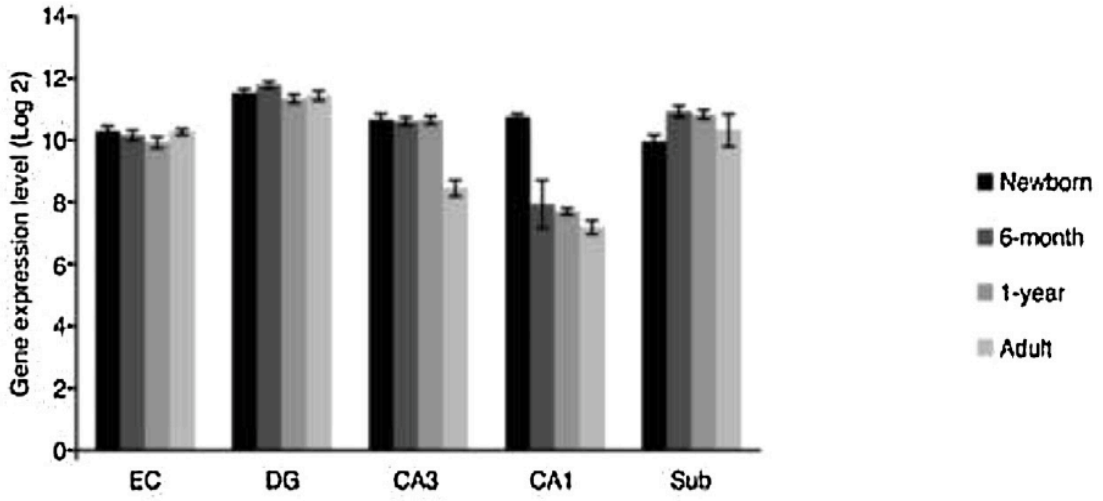

Figure 11: Expression levels of gene associated with glycolysis and glutamate metabolism in astrocytes at four postnatal ages in different subregions of the macaque monkey hippocampal formation. EC: entorhinal cortex; DG: dentate gyrus; CA3, CA1: fields of the hippocampus proper; Sub: subiculum. Reproduced from (Lavenex et al., 2011).

Lavenex and colleagues (2004) also published some preliminary observations on the distribution of non-phosphorylated, high-molecular-weight neurofilament immunostaining in the hippocampal formation of three-week-old, three-month-old and 9-17-year-old monkeys. As neurofilaments are cytoskeletal proteins necessary for the formation and maintenance of axons and dendrites (Carden, Trojanowski, Schlaepfer, & Lee, 1987; Lee & Cleveland, 1996), the expression of non-phosphorylated, high-molecular-weight neurofilament immunostaining is believed to reflect the maturation of certain neuronal populations. Although both the subiculum and the entorhinal cortex were heavily stained in adult monkeys, it was not the case in 3-month-old monkeys where only the subiculum really stood out (Figure 12). Moreover, their observations showed a possible earlier maturation of the entorhinal cortex superficial layers II and III (Figure 12 B, E and H), compared to deep layers V and VI. Those

observations were supported by preliminary data on neuronal soma size in the different layers of the intermediate subdivision (Ei) of the entorhinal cortex (Figure 13) (Lavenex & Banta Lavenex, 2013). They reported that neurons located in the deep layers were significantly smaller in 3-month-olds, as compared to 5-10-year-olds. In contrast, they found no difference between ages in the size of neurons located in the superficial layers, suggesting an earlier maturation of the superficial layers, the origin of projection to the hippocampus and dentate gyrus, as compared to deep layers, the target of returned projections from CA1 and the subiculum.

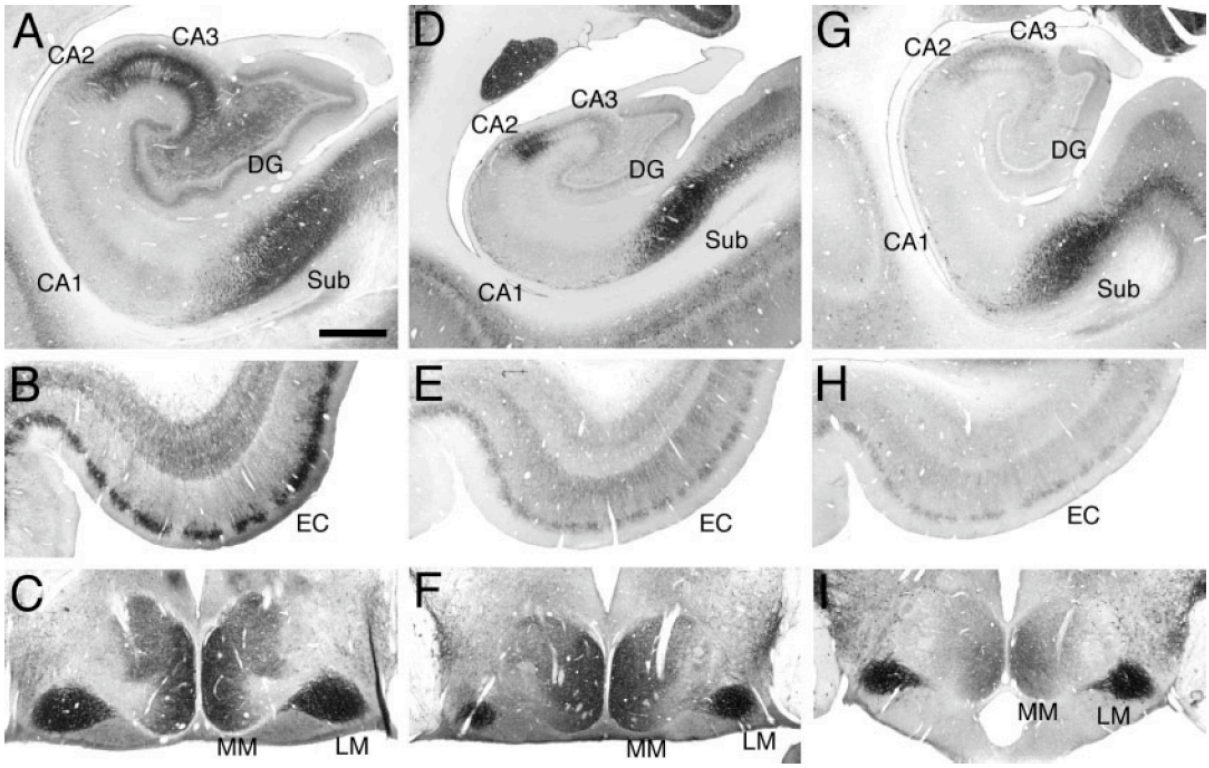

Figure 12: Distribution of high-molecular-weight neurofilament immunostaining in the hippocampal formation of adult (A-C), 3-month-old (D-F) and 3-week-old (G-I) rhesus monkeys. Reproduced from (Lavenex, Banta Lavenex, & Amaral, 2004).

Finally, Amaral and colleagues (2014) used anterograde tracers, including ^{3}H-amino acids, PHA-L (*Phaseolus vulgaris*-leucoagglutinin) and BDA (biotinylated dextran amine) to examine the projections from the entorhinal cortex to the dentate gyrus, hippocampus and subiculum of 2-week-old rhesus monkeys. Their analysis revealed that all the projections originating from the entorhinal cortex to the dentate gyrus, hippocampus, and subiculum were already established by 2 weeks of age in the macaque monkey. Moreover, they observed

that all the major features of the topographic and laminar organization of the adult monkey was already identifiable at 2 weeks of age (Amaral, Kondo, & Lavenex, 2014). In particular, they observed an innervation from labeled fibers in the outer two-thirds of the molecular layer of the dentate gyrus, in the full radial extent of stratum lacunosum-moleculare of the hippocampus, and through much of the molecular layer of the subiculum (Amaral et al., 2014).

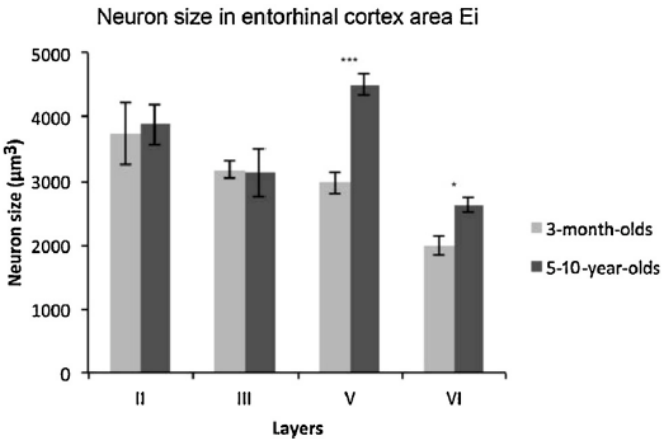

Figure 13: Estimation of neuronal soma size in the different layers of the intermediate entorhinal cortex (Ei) in 3-month-old and adults macaque monkeys. Reproduced from (Lavenex & Banta Lavenex, 2013).

In humans, although the relations between neuronal structures and mnemonic behaviors have reached an important level of understanding in the adult literature, it is far from being the case in developmental studies, where the neural bases of human memory development were not even considered until late 20th century (Bauer, 2004, 2008; Jabès & Nelson, 2015). In 1995, a model of memory development was proposed in attempt to provide a theoretical framework for explaining the neural bases of early memory development (Nelson, 1995). However, the paper was mostly based on inference, as at the time, data were very rare in the field. Twenty years later, thanks to the numerous of studies performed, we have a much better understanding of the ontogeny of memory (Jabès & Nelson, 2015; Lavenex & Banta Lavenex, 2013).

Grateron and colleagues (2003) described the presence of interneurons expressing calcium-binding proteins (parvalbumin, calbindin and calretinin) in the human entorhinal cortex from birth to 5 years of age. Calbindin-positive neurons are already present at birth, but principally in layers II and III, while they are also present in the deep layers by five years

of age. Large numbers of calretinin-immunoreactive neurons are also already present at birth all over the entorhinal cortex. In contrast, they did not observe any parvalbumin-positive neurons at birth, but only from five months of age. Their conclusion was that at birth, a pattern of calcium-binding proteins is already present, and that its topographic and laminar distributions corresponds largely to the adult pattern (Grateron et al., 2003). However, some differences suggest that there are some postnatal modifications that extend beyond five months of age and that the first postnatal year is a critical period in which most of the increase in interneurons takes place, probably impacting the intrinsic connectivity as well as their functional role in the regulation of the input and output of the entorhinal cortex (Grateron et al., 2003).

A tracer study by Hevner and Kinney (1996) indicated that reciprocal connections between the entorhinal cortex, the subiculum and the hippocampus were already established by 20 weeks of human gestation, in a similar way that adult non-human primates. In contrast, they found that the projections from the entorhinal cortex layer II neurons to the dentate gyrus was still very rudimentary by this antenatal age, suggesting a later maturation of those connections.

Altogether, studies on the development of the hippocampal formation and the entorhinal cortex, in human and nonhuman primates, have shed light on the morphological and neurochemical changes occurring in the hippocampal formation during postnatal development. They suggest that although the entorhinal projection to the hippocampus might be present very early in development, the feedback projections from the hippocampus to the entorhinal mature later. Moreover, the different developmental profiles of distinct hippocampal subregions suggest different temporal emergence of functional circuits. Quantitative data on the structural postnatal development of the monkey entorhinal cortex will provide, without a doubt, more clues about the development of distinct memory processing circuits inside the hippocampal formation and therefore will help to better understand the emergence of episodic memory.

1.3 Functional aspects

The entorhinal cortex has been the target of many recent functional studies to clarify its role in memory, and especially in spatial memory processing. In the first section, I will present a selection of the most important functional discoveries about the hippocampal formation and the entorhinal cortex in rodents. In the second section, I will explain the common "rostral versus caudal" functional distinction and why this strict dichotomic perspective has been recently questioned. The third section will then be dedicated to the very few functional studies in non-human primates. Finally, in the last section, I will describe a theoretical model explaining the results of behavioral studies on the emergence of memory in humans based on the structural development of the hippocampal formation in monkeys.

1.3.1 Functional studies in rodents

Numerous experimental studies have contributed to the current view that different hippocampal regions might serve computationally distinct but complementary roles during memory processing (Lavenex & Banta Lavenex, 2013). Here, I summarize some of the most convincing evidence regarding the specific functions of different hippocampal regions.

Dentate gyrus and pattern separation: Pattern separation consists in the process of transforming similar representations or memories into highly dissimilar, non-overlapping representations (Bakker, Kirwan, Miller, & Stark, 2008). Initial studies in rodents have suggested that this ability could be supported by the dentate gyrus, in cooperation with CA3 (Gilbert, Kesner, & Lee, 2001; Kesner, 2007; Rolls & Kesner, 2006). Indeed, Gilbert et al. (2001) tested the ability of rats with dentate gyrus lesions to choose between two identical objects and observed an impairment of spatial pattern separation in those animals. In humans, Bakker and colleagues (2008) used functional magnetic resonance imaging to measure brain activity during incidental memory encoding, and observed a strong bias toward pattern separation in, and limited to, the dentate gyrus and CA3.

CA3 and pattern completion: Pattern completion consists in the ability to retrieve complete memories on the basis of incomplete sets of cues. In rodents, studies showed that CA3 contributes partially to this ability (Leutgeb & Leutgeb, 2007). One of the most convincing evidence of the pattern completion function of CA3 was provided by Nakazawa and colleagues

(2002). They generated and analyzed behaviorally a mouse strain in which the N-methyl-D-asparate (NMDA) receptor gene was specifically and exclusively deleted in the CA3 pyramidal cells of adult mice. They found that mice without NMDA receptor function in CA3 normally acquired and retrieved spatial reference memory in the Morris water maze, but they were impaired in retrieving this memory in presence of an incomplete set of cues. These observations demonstrated the necessary implication of CA3 NMDA receptors in associative memory recall (Nakazawa et al., 2002). Since CA3 also receives direct inputs from entorhinal cortex layer II cells, it appears also important to understand the functional role and the development of entorhinal cortex layer II cells, and their contribution to the pattern completion process carried out by CA3.

CA1 and allocentric representation: A number of studies have implicated CA1 in the formation of basic allocentric representations of the environment, and more specifically, have shown that direct projections from the entorhinal cortex to CA1 are sufficient to form a basic allocentric representation. Mizumori and al. (1989) performed a reversible inactivation of the medial septal nucleus, which project majorly to the hippocampus. This septal inactivation reduced spontaneous firing of cells in CA3, and thus lead to a reversible suppression of CA3 output to CA1. Interestingly, they found that CA1 place cell coding were maintained despite the inactivation of CA3 cells (Mizumori, Barnes, & McNaughton, 1989), suggesting that CA3 projections were not necessary to the functional activity of CA1. Moreover, in order to determine whether direct entorhinal cortex projections to CA1 support spatial firing and spatial memory, Brun and colleagues (2002) produced selective, bilateral CA3 lesion by injections of ibotenic acid. CA1 was thus isolated from CA3 projections and had connections only with the entorhinal cortex. They observed that there was no impairment in the acquisition of an associative hippocampal-dependent spatial recognition task. CA1 place cell coding was maintained after the lesion, demonstrating that the direct projections from the entorhinal cortex to CA1 are sufficient for an associative spatial recognition task. In contrast, Brun et al. (2008) showed later that selective lesion of entorhinal cortex layer III, which sends direct projections to CA1, leads to an impairment in CA1 place cell coding. These results showed the fundamental role of the projections from entorhinal cortex layer III neurons to CA1 for place cell coding in CA1.

In conclusion, the few studies described above suggest that different hippocampal regions contribute differently, yet specifically, to the processing of spatial information.

Considering that the entorhinal cortex constitutes the main interface between the neocortex and these hippocampal regions, we can reasonably think that the emergence of these memory functions may depend on the parallel maturation of the superficial layers of the entorhinal cortex: layer II for the dentate gyrus and CA3, layer III for CA1 and subiculum.

If the hippocampus has been a major subject of research for a long time, it is not until recently that researchers have started investigating more precisely the functional role of the entorhinal cortex in the elaboration of spatial representations. Their results tend to show that the rat medial entorhinal cortex plays an essential role in spatial representation (McNaughton, Battaglia, Jensen, Moser, & Moser, 2006; Witter & Moser, 2006), via its contribution to the computational process known as path integration (Mittelstaedt & Mittelstaedt, 1980). Path integration is the result of a system that keeps tracks of relative spatial locations by integrating linear and angular motion while an individual moves about in the environment (McNaughton et al., 2006). An important advantage of this mechanism is that it can operate in the absence of specific landmarks, in contrast to other navigational strategies depending on particular external objects and features of the environment (Witter & Moser, 2006).

Path integration seems to be supported by a widespread brain network, including place cells found in the CA1 field of the hippocampus (Etienne & Jeffery, 2004), that fire according to a location in an open-field environment (O'Keefe & Dostrovsky, 1971), and head-direction cells, found in the presubiculum and several other areas, which encode information about the animal's directional heading, independent of the animal's on-going behavior (Taube, 1998). However, all these positional and directional signals are expressed in several different brain regions, leading researchers to suggest that one brain area might be involved in the integration of all these signals (Witter & Moser, 2006). Because the entorhinal cortex constitutes a major interface between the hippocampus and the other areas implicated in the formation of spatial representations, it stands to reason that the entorhinal cortex might play a fundamental role in this process. Indeed, recent studies confirmed that the elaboration of some types of spatial representations is supported by the dorsocaudal medial entorhinal cortex (dMEC) (Fyhn, Molden, Witter, Moser, & Moser, 2004; Hafting, Fyhn, Molden, Moser, & Moser, 2005). Fyhn et al. (2004) measured the spatial modulation of neural activity in the superficial layers of the medial entorhinal cortex projecting to the hippocampus and demonstrated that some cells of the entorhinal cortex have stable and discrete multipeaked

place fields predicting the rat's location as accurately as place cells in the hippocampus. Hafting et al. (2005) recorded spike activity in the dMEC while rats were running in large enclosures and determined that the firing patterns of dMEC neurons follow a map-like organization and described these cells as grid cells. The grid cells fire whenever the animal's position coincides with any vertex of a regular grid made of equilateral triangles spanning the surface of the environment, thus representing a directionally oriented, topographically organized neural map of the spatial environment (Hafting et al., 2005). The existence of grid cells in the entorhinal cortex suggests that this structure plays an essential role in the elaboration of some types of spatial representations. As a consequence, the medial portion of the entorhinal cortex has been identified as necessary for spatial memory processing and functionally distinct from the lateral portion. The common functionally segregation between those two areas as well as recent questioning about it will be reviewed in the next section.

1.3.2 Rostral vs caudal entorhinal cortex functions

As mentioned previously, the entorhinal cortex is commonly subdivided into two major areas, MEC and LEC, which correspond to the rostral and caudal portions of entorhinal cortex in monkeys. This functional and anatomical differentiation is supported by parallel patterns of projections from cortical regions to the entorhinal cortex. A first pathway, the parieto-medial-temporal pathway, reaches the parahippocampal cortex and appears to contribute to the processing of visual scenes, while a second pathway, the occipitotemporal-medial temporal pathway, leads to the perirhinal cortex and appears to be specialized for processing object-related information (Knierim, Neunuebel, & Deshmukh, 2014; Kravitz, Saleem, Baker, & Mishkin, 2011; Kravitz, Saleem, Baker, Ungerleider, & Mishkin, 2013). Additionally, a third pathway, occipitotemporal-medial temporal pathway, reaches the presubiculum and the parasubiculum, and seems to be involved in navigational signals (Kravitz et al., 2011). As the LEC (or rostral part of the entorhinal cortex in monkeys) receives its inputs mainly from the perirhinal cortex (although the segregation is clearer in rats than in monkeys) and the MEC (caudal part of the entorhinal cortex in monkeys) receives its inputs mainly from the postrhinal cortex (or parahippocampal cortex in monkeys), the main consensus has been to oppose those two pathways as the "what" versus "where" pathways (Knierim et al., 2014; Morrissey & Takehara-Nishiuchi, 2014). The LEC was then considered as providing information about

individual items and objects to the hippocampus, while the MEC was considered as relaying spatial information. Finally, the hippocampus has been considered as combining those pieces of information to elaborate flexible, conjunctive representations of “what happened where” (Knierim et al., 2014). The discovery of *grid cells,* described in the previous section, in the medial entorhinal cortex associated to various studies on the role of the lateral entorhinal cortex in object memory processing increased even further this simple functional distinction between the medial and lateral entorhinal cortex. The “what” versus “where” dualism was however questioned following some studies suggesting that both some spatial and non-spatial processing was supported by the LEC.

In a first study, Van Cauter and al. (2013) tested the ability of rats with LEC or MEC lesions to perform different tasks requiring spatial and nonspatial processing: the Morris water maze task, an object exploration task, a one-trial recognition task and a path integration task (see Figure 16 for a description of the tasks). Rats with MEC lesions were able to perform nonspatial object recognition, but they were impacted in the object exploration task and the one-trial recognition task when it required spatial information processing. In contrast, rats with LEC lesions were not impaired in the Morris water maze or the path integration task that require navigational abilities. However, in the object exploration task, LEC-lesioned rats were impaired in the recognition of both spatial and nonspatial changes (Van Cauter et al., 2013). These results suggest an implication of the LEC in both spatial and nonspatial information processing.

In another study, Hunsaker and colleagues (2013) tested the responses of LEC- or MEC-lesioned rats to item novelty, contextual novelty, or combined item and contextual novelty (see Figure 17 for a description of the task). Their results showed that LEC-lesioned rats were strongly impaired in the item recognition memory task and mildly impaired in the contextual recognition memory task, whereas MEC-lesioned rats were strongly impaired in the contextual recognition memory tasks and mildly impaired in the item recognition memory task (Hunsaker, Chen, Tran, & Kesner, 2013). These observations suggest, that although LEC is essential for item recognition memory, it also contributes to contextual recognition memory.

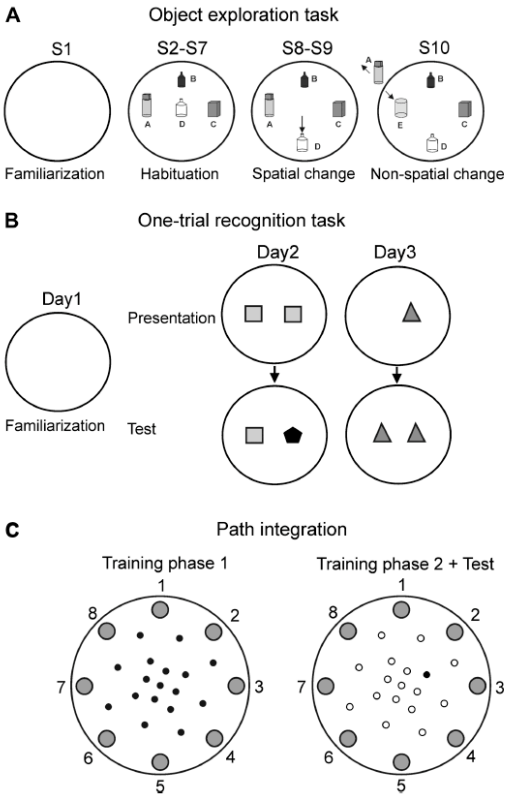

Figure 16:

(A) Object exploration task: The rat was placed in a circular grey open field that was empty in session S1; contained 4 objects at standard configuration at S2-S7; contained a different spatial configuration of the same objects at S8-S9; contained the replacement of one object with a novel object in the same spatial configuration.

(B) One-trial recognition task: After one day of familiarization, the rat was exposed, on day 2, to two identical copies of an object and, after a delay, to one of the copies and a novel object. On day 3, the rat was exposed to a single object and, after a delay, to two objects similar to the first one.

(C) Path integration task: The rat was placed in one of the eight starting places on a white circular elevated platform. In phase 1, 17 cups were baited, while in phase 2, only one cup was baited.

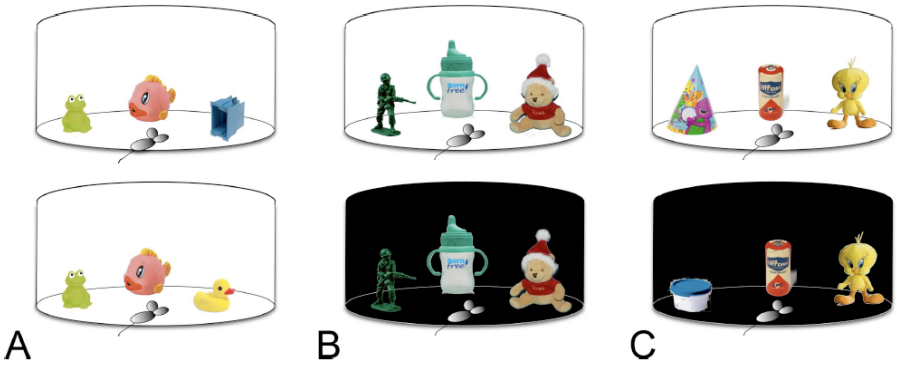

Figure 17: *(A) Item novelty detection:* the rat first explored an environment with three objects in a white context. Second, the rat was placed in the same environment where an object was replaced with a novel object. *(B)Contextual novelty detection:* the rat first explored an environment with three objects in a white context. Second, the rat was placed in a different black context with the same objects. *(C) Conjoint Item + contextual novelty detection:* the rat first explored an environment with three objects in a white context. Second, the rat was placed in a different black context, where an object was replaced with a novel object. Reproduced from (Hunsaker et al., 2013).

These experimental results implicating the lateral entorhinal cortex in some spatial processing led Knierim and colleagues (2014) to propose an alternative view of MEC and LEC functions. The MEC would be part of a global, holistic spatial map that would provide

information about where the organism is in its environment, where it is going and how to get there. The LEC would part of a system processing local cues to provide the content of an experience, including spatial information related to these objects (Knierim et al., 2014). The entorhinal cortex would therefore provide to the hippocampus a much more highly processed information than what was thought previously. The entorhinal cortex would be essential for establishing relational representations making the connections between spatial, non-spatial and contextual information (Morrissey & Takehara-Nishiuchi, 2014). This view is very much in line with the known neuroanatomical organization of the medial temporal lobe regions (Amaral and Lavenex, 2007), and more specifically the entorhinal cortex with its numerous associational connections that would be particularly suited for the integration of different types of information reaching these areas (Lavenex and Amaral, 2000; Chrobak and Amaral, 2007).

Some studies carried out in humans also suggest different functions of the rostral and caudal entorhinal portions. Reagh and Yassa (2014) used fMRI to measure the activity of the MEC and the LEC during object and spatial discrimination tasks. Consistent with previous functional studies in rodent, they found that LEC activity was selectively modulated by object interference, while MEC activity was selectively modulated by spatial interference (Reagh & Yassa, 2014). In another study, the same group of researchers used fMRI to measure the activity of the LEC, while participants were watching a television show episode (Montchal, Reagh, & Yassa, 2019). Still-frames appeared during the show and participants were asked to indicate on a timeline when the event in question happened (Montchal et al., 2019). Their results showed an increased activity in the LEC, suggesting that the temporal component of memory would be supported by the lateral entorhinal cortex.

The functional studies developed in this section indicate that different regions of the entorhinal cortex support different component of episodic memory. The MEC would be necessary for the spatial representation of an episode, while the LEC would be essential to process the content of an episode and its temporal aspects.

1.3.3 Functional studies in primates

The rat is definitely at the center of studies using animal models to understand the functional roles of the entorhinal cortex. However, some experimental studies on the

functions of the entorhinal cortex have been carried out in monkeys in the last decades. Here, I provide a description of the principal ones.

Suzuki et al. (1997) investigated the contribution of the entorhinal cortex in object or place memory tasks. In a first study involving object memory, the researchers recorded the response of entorhinal cells while the animals were performing two types of delayed match-to-sample tasks, a "standard" one and a "ABBA" one (Figure 14A). In the standard DMS, a sample stimulus was presented followed by nonmatching pictures and finally by a repetition of the sample stimulus (A…B…C…D…A) that the monkey had to identify. In the "ABBA" task, the setting was very similar, except that one of the nonmatching stimuli was repeated (A…B…B…C…A). This time, the monkey had to identify the correct stimulus and ignore the repetition of the nonmatching item (Suzuki, Miller, & Desimone, 1997). The results showed differences in the way entorhinal cortex neurons reacted to different stimuli. First, cells did not respond similarly to different objects, thus showing some object selectivity. Second, the entorhinal cells showed sample-selective activity in the delay intervals following the sample, suggesting the maintenance of a representation of the sample stimulus during the delay (Suzuki et al., 1997). Finally, when the stimuli matched, some cells increased their response, while some cells suppressed their response. This specific response occurred before the behavioral response of the animal, leading Suzuki and al. to suggest that these effects might contribute to the decision animal makes while performing the task.

In a second part of the study, Suzuki et al. (1997) used a delayed match-to-place task to investigate the implication of entorhinal cells in place memory (Figure 14B). In this task, a stimulus was presented sequentially at different locations on a screen with different backgrounds and the animal had to identify the repetition of the same location in the sequence. Their recordings indicated that entorhinal cells did not respond in the same way depending on the location of the cue on the screen (Suzuki et al., 1997). Moreover, they identified a population of cells that responded selectively to a location, independently of the background used. They also identified a population of cells that responded according to a particular background but were unresponsive for cue location on other background. These results suggested an active participation of the entorhinal cortex in object and spatial memory processing.

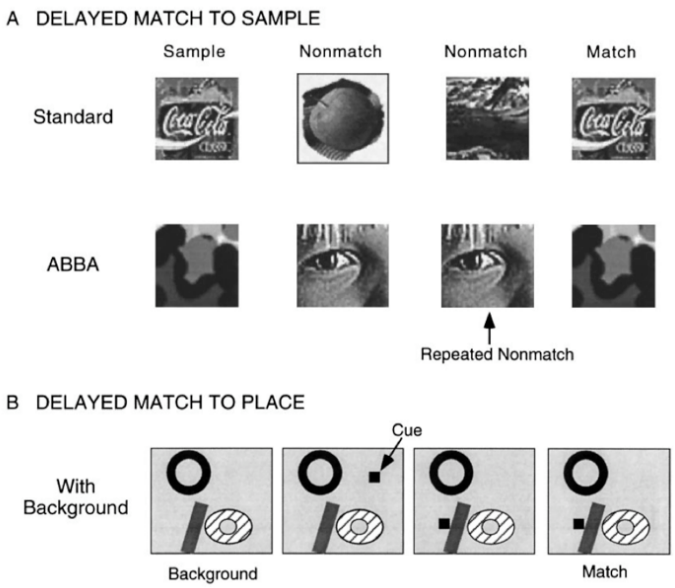

Figure 14: (A) Illustration of a standard and ABBA delayed match-to-sample tasks. (B) Illustration of a delayed match-to-place task. Reproduced from (Suzuki et al., 1997).

Buckmaster et al. (2004) studied the implication of the hippocampal system in relational representation et flexible memory, by producing selective ibotenic acid lesions of the entorhinal cortex in a group of monkeys. They compared the performance of control and lesioned monkeys in a succession of behavioral tasks. The first two standard memory tasks consisted of a delayed non-matching-to-sample (a sample presentation of stimuli followed by a recognition test) and a two-choice object discrimination (monkeys had to learn which stimulus in a pair was consistently associated with a reward) (C. A. Buckmaster, Eichenbaum, Amaral, Suzuki, & Rapp, 2004). On both tasks, monkeys with bilateral entorhinal cortex lesions were as efficient as controls in learning the association between stimulus and reward. However, lesioned monkeys were impaired in procedures testing relational information processing. In three tasks (paired associate task, transitive inference test, and spatial delayed recognition span), animals had to draw inferences or generalizations on the basis of a memory for the relationships between the items (C. A. Buckmaster et al., 2004). On all three tasks, lesioned monkeys were less performant than controls, suggesting that although recognition tasks are still possible without a properly functioning entorhinal cortex, more complex tasks involving relational representations requires the integrity of the entorhinal cortex (C. A. Buckmaster et al., 2004).

In a study published in 2017, Chareyron et al. quantified the number of cells expressing the protein c-fos (a marker of neuronal activity) in different regions of the medial temporal lobe, including all the subdivisions of the entorhinal cortex, to investigate the effect of neonatal hippocampal lesion on functional organization of the medial temporal lobe memory system (Chareyron, Banta Lavenex, Amaral, & Lavenex, 2017). In this study, they compared the number of c-fos positive cells between three groups of monkeys: a group of neonatally hippocampus-lesioned monkeys (L_E: Lesion Exploration monkeys) and a group of control monkeys (C_E: Control Exploration monkeys) that explored a novel environment immediately prior to their death, and a group of neonatally hippocampus-lesioned monkeys (L_C: Lesion Cage monkeys) that stayed in their cage before their death. Interestingly, they observed a difference in the number of c-fos-positive cells in the different subdivisions of the entorhinal cortex following the exploration of a novel environment between lesioned and control monkeys (Figure 15). In the most rostral subdivisions of the entorhinal cortex, Eo, Er and Elr, the number of c-fos positive cells did not differ in any layers between groups that explored a novel environment (L_E and C_E) and/or the group of monkeys that did not explore a new environment. As the novel environment monkeys explored contained no object or prominent proximal landmarks, those results are consistent with data suggesting that the rostral part of the entorhinal cortex would be particularly involved in object memory processing (Deshmukh & Knierim, 2011). In contrast, more c-fos-positive cells were found in the intermediate subdivision of the entorhinal cortex (Ei) in the two groups of monkeys, hippocampus-lesioned or not, that explored a novel environment (C_E and L_E) than in hippocampus-lesioned monkeys that stayed in their cage (L_C). This observation is consistent with the fact that Ei is connected to both the perirhinal and parahippocampal cortex and might therefore be implicated in both object and spatial memory processing. Finally, they did not find a difference of activity in the caudal subdivision of the entorhinal cortex (Ec) between hippocampal-lesioned monkeys that explored a novel environment (L_E) and hippocampal-lesioned monkeys that stayed in their cage (L_C), suggesting that the caudal part of the entorhinal cortex requires the integrity of the hippocampus in order to be fully functional.

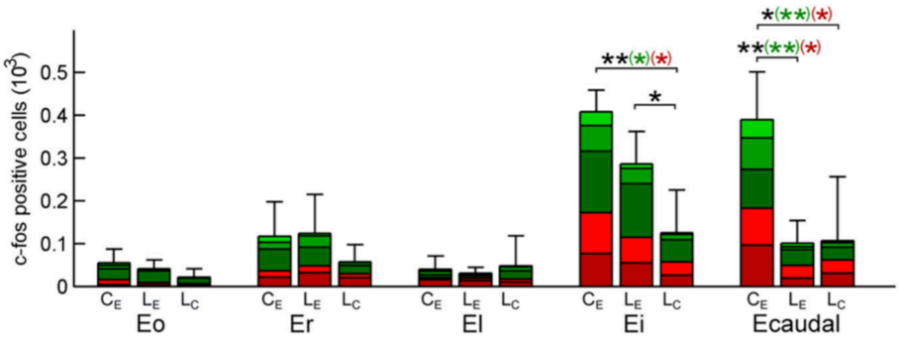

Figure 15: Number of c-fos positive cells in the entorhinal cortex of Control Exploration (C_E), Lesion Exploration (L_E) and Lesion Cage (L_C) monkeys (Chareyron et al., 2017).

All studies developed above provide more indications on the functions of the entorhinal cortex and in particular, demonstrate that the entorhinal cortex is involved in object and spatial memory processing. However, the development of memory in children is often investigated through the development of spatial capacities, as they do not require verbal skills. The studies investigating the emergence of spatial abilities in children will be developed in the next section.

1.3.4 The development of memory

In humans, significant changes in the capacity for episodic memory occur within the first seven years of life. Prior to about two years of age, children are unable to form or store episodic memories for recall later in life, a phenomenon known as infantile amnesia (Newcombe, Drummey, Fox, Lie, & Ottinger-Alberts, 2000; Newcombe, Lloyd, & Ratliff, 2007). The three-to-five years that follow this period are characterized by fewer episodic memories than would be predicted based on a simple forgetting function alone, a phenomenon referred to as childhood amnesia (Newcombe et al., 2000; Newcombe et al., 2007).

In very young children, the development of episodic memory is difficult to investigate because of the inability of children to talk (or at least to talk fluently). One way to investigate the emergence of episodic memory is thus through allocentric spatial memory, a fundamental component of episodic memory that is dependent on the integrity of the hippocampal formation. Allocentric spatial memory consists in viewpoint-independent representations of

the environment, in which spatial locations are coded in relation to different objects constituting the environment (O'Keef & Nadel, 1978). Following this approach, Ribordy and colleagues (2013) investigated the development of allocentric spatial memory in children from 18 months to 5 years of age using two versions of a hippocampus-dependent real-world spatial memory task.

In their first experiment, 18 white paper plates and inverted opaque plastic cups were symmetrically arranged in an inner hexagon composed of 6 locations and an outer hexagon composed of 12 locations (Figure 18). Children completed two different type of trials: Local Cue trials (LC) and Allocentric Spatial trials (AS). In LC trials, the cups under which the food was hidden were red, whereas all the other cups were white. In AS trials, the cups hiding the rewards were white and identical to the other cups. In these trials, in absence of visual cues, children had to rely on an allocentric spatial representation in order to find the cups hiding the rewards. All children from two years of age were able to discriminate the reward locations in the LC condition. In contrast, children younger than 3.5 years of age were not able to discriminate the reward locations in the AS condition but children older than 3.5 years of age could (Ribordy, Jabès, Banta Lavenex, & Lavenex, 2013).

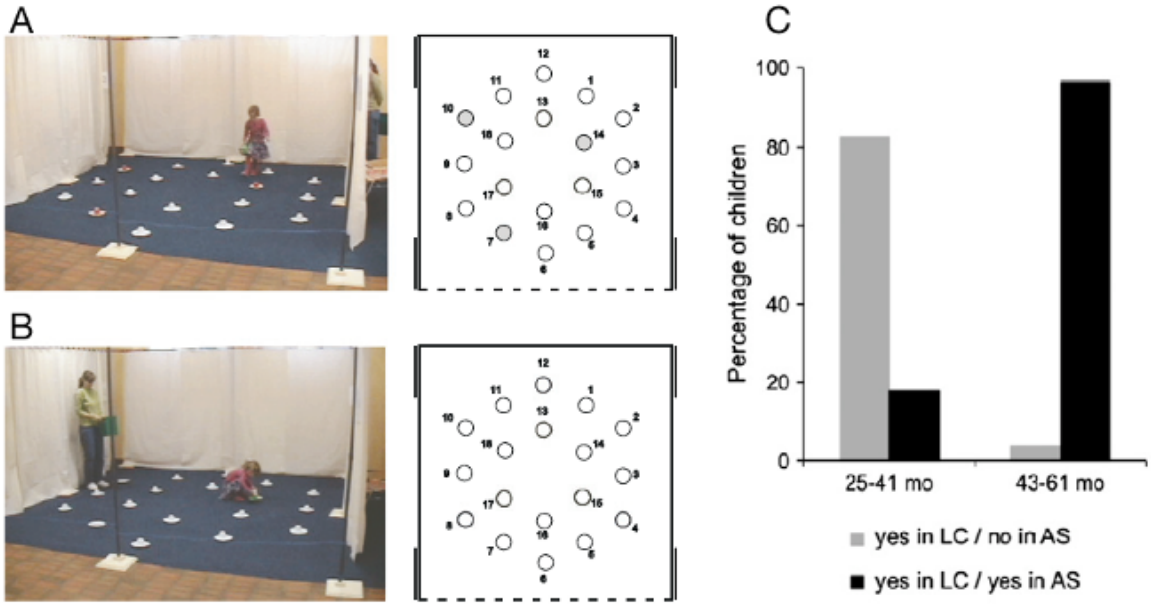

Figure 18: (A) Picture of a child completing a Local Cue trial (LC), in which the cups containing the hidden food are red. (B) Picture of a child completing an Allocentric Spatial trial (AS), in which all the cups are identical. (C) Performance of children from 25 to 61-month-old in the two different conditions. Reproduced from (Ribordy et al., 2013)

In their second experiment to further investigate the abilities of children under 3.5 years of age, Ribordy and al. used a similar design, except that only four paper plates and cups were symmetrically arranged in both LC and AS trials (Figure 19). Although the abilities of children varied greatly under 24 months of age, 84% of the children between 25 and 39 months of age were able to discriminate the reward location in the AS condition.

In sum, their results indicate that the ability to form a basic allocentric representation of the environment is present by 2 years of age (corresponding to the offset of infantile amnesia) and that, between 2 and 3.5 years, the children's ability to distinguish and remember closely related spatial locations improves (corresponding to the period of childhood amnesia) (Ribordy et al., 2013).

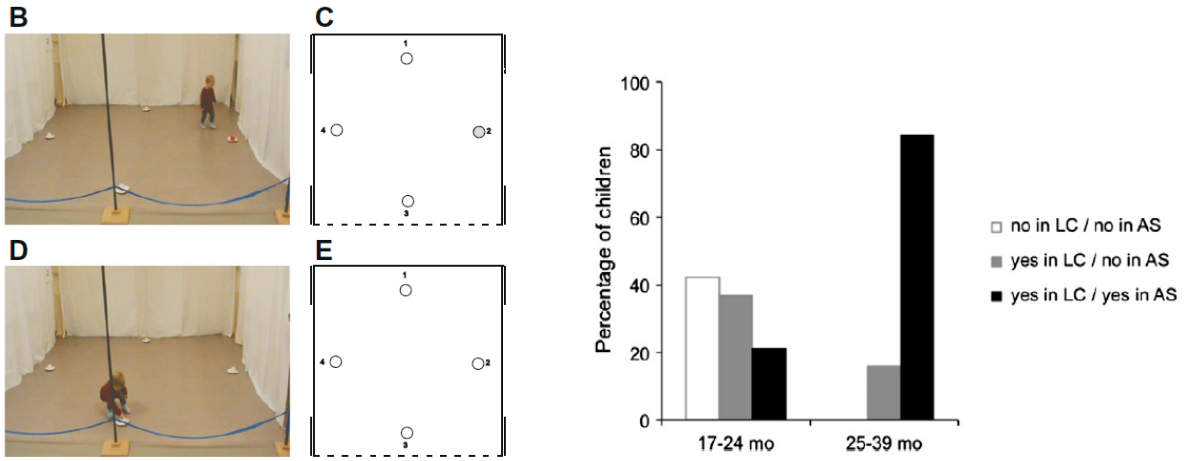

Figure 19: (A) Picture of a child completing a Local Cue trial (LC), in which the cup containing the hidden food is red. (B) Picture of a child completing an Allocentric Spatial trial (AS), in which all the cups are identical. (C) Performance of children from 17-to-39-month-old in the two different conditions. Reproduced from (Ribordy et al., 2013).

Until recently, the neurobiological basis for such early-life changes in episodic memory had remained highly speculative due to the lack of systematic, quantitative studies of postnatal brain development at the cellular or systems levels (Bauer, 2006; Lavenex, Banta Lavenex, & Amaral, 2007). As the hippocampal formation is the central component of a large neural network subserving memory processes, Lavenex and Banta Lavenex (2013) proposed a model suggesting how the differential maturation of distinct hippocampal circuits can be related to

behavioral findings in humans. As described in section 1.2.4.1, the CA1 field of the hippocampus exhibits an early maturation, reaching almost its adult size (Jabès et al., 2011) and demonstrating an adult-like pattern of gene expression (Favre et al., 2012b; Lavenex et al., 2011), at approximately six months of age in monkeys, which corresponds to approximately two years of age in humans (Lavenex & Banta Lavenex, 2013). This age corresponds precisely to the age at which a qualitative shift in the spatial capacities of children has been observed, with the emergence of the ability to learn, remember and use a basic allocentric spatial representation of the environment (Ribordy et al., 2013). In contrast, CA3 and the dentate gyrus were found to reach their mature size and adult-like patterns of gene expression later than CA1, after one year in monkeys, which corresponds to about 4 years of age in humans. This is the time at which we can observe gradual improvements in episodic memory capacities in humans. In conclusion, behavioral studies on the emergence of episodic memory are consistent with structural studies on the maturation of different regions and putative functional circuits of the hippocampal formation. However, all the hippocampal structures mentioned above receive projections from or send projections to the entorhinal cortex. A structural analysis of the monkey entorhinal postnatal development is therefore necessary in order to have a more complete developmental picture of the neuronal substrates underlying the emergence of hippocampus-dependent memory processes.

1.4 Experimental aim

This thesis is part of a larger research program aimed to characterize the structural postnatal development of the hippocampal formation in order to better understand the neurological substrates subserving the emergence of episodic memory. Quantitative data on the structural postnatal development of the monkey hippocampal formation have recently been published and provided the basis for a conceptual framework to explain the neurobiological basis of some memory processes. However, this theory is incomplete without similar quantitative data on the structural postnatal development of the monkey entorhinal cortex. In my thesis, I proposed to characterize the structural maturation of different layers and subdivisions of the monkey entorhinal cortex and to compare them with the morphological changes observed in other structures of the hippocampal formation.

2. Experimental results

My experimental results have been divided in two distinct publications:

- Article 1: “Stereological analysis of the rhesus monkey entorhinal cortex”

The first publication presents the first quantitative structural analysis of distinct layers of the seven subdivisions of the adult rhesus monkey entorhinal cortex.

- Article 2: “Postnatal development of the entorhinal cortex: a stereological study in macaque monkeys”

The second publication presents the first quantitative structural analysis of distinct layers of the seven subdivisions of the rhesus monkey entorhinal cortex at different postnatal ages, from birth to young adulthood.

Received: 29 March 2018 | Revised: 20 June 2018 | Accepted: 22 June 2018

DOI: 10.1002/cne.24496

WILEY JCN RESEARCH IN SYSTEMS NEUROSCIENCE THE JOURNAL OF COMPARATIVE NEUROLOGY

RESEARCH ARTICLE

Stereological analysis of the rhesus monkey entorhinal cortex

Olivia Piguet[1] | Loïc J. Chareyron[2] | Pamela Banta Lavenex[1] | David G. Amaral[3,4] | Pierre Lavenex[1,2]

[1]Laboratory of Brain and Cognitive Development, Institute of Psychology, University of Lausanne, 1015 Lausanne, Switzerland

[2]Laboratory of Brain and Cognitive Development, Department of Medicine, University of Fribourg, 1700 Fribourg, Switzerland

[3]Department of Psychiatry and Behavioral Sciences, MIND Institute, University of California, Davis, California

[4]California National Primate Research Center, University of California, Davis, California

Correspondence
Pierre Lavenex, Laboratory of Brain and Cognitive Development, Institute of Psychology, University of Lausanne, 1015 Lausanne, Switzerland.
Email: pierre.lavenex@unil.ch

Funding information
National Institutes of Health, Grant/Award Number: MH041479NS16980; Swiss National Science Foundation, Grant/Award Number: 310030_143956P00A-106701PP00P3-124536; California National Primate Research Center, Grant/Award Number: OD011107

Abstract

The entorhinal cortex is a prominent structure of the medial temporal lobe, which plays a pivotal role in the interaction between the neocortex and the hippocampal formation in support of declarative and spatial memory functions. We implemented design-based stereological techniques to provide estimates of neuron numbers, neuronal soma size, and volume of different layers and subdivisions of the entorhinal cortex in adult rhesus monkeys (*Macaca mulatta*; 5–9 years of age). These data corroborate the structural differences between different subdivisions of the entorhinal cortex, which were shown in previous connectional and cytoarchitectonic studies. In particular, differences in the number of neurons contributing to distinct afferent and efferent hippocampal pathways suggest not only that different types of information may be more or less segregated between caudal and rostral subdivisions, but also, and perhaps most importantly, that the nature of the interaction between the entorhinal cortex and the rest of the hippocampal formation may vary between different subdivisions. We compare our quantitative data in monkeys with previously published stereological data for the rat and human, in order to provide a perspective on the relative development and structural organization of the main subdivisions of the entorhinal cortex in two model organisms widely used to decipher the basic functional principles of the human medial temporal lobe memory system. Altogether, these data provide fundamental information on the number of functional units that comprise the entorhinal-hippocampal circuits and should be considered in order to build realistic models of the medial temporal lobe memory system.

KEYWORDS

hippocampal formation, neuron number, neurofilament, RRID:AB_2313581, RRID:AB_2314904

1 | INTRODUCTION

The entorhinal cortex is a prominent structure of the medial temporal lobe, which plays a pivotal role in the interaction between the neocortex and the hippocampal formation in support of declarative and spatial memory functions (Amaral, Insausti, & Cowan, 1987; Amaral & Lavenex, 2007; Chareyron, Banta Lavenex, Amaral, & Lavenex, 2017; Lavenex & Amaral, 2000; Witter, Doan, Jacobsen, Nilssen, & Ohara, 2017; Witter & Moser, 2006). The entorhinal cortex is the main entryway for much of the neocortical information reaching the hippocampal formation. It is also the main conduit for information processed by the hippocampus to be sent back to the neocortex. The entorhinal cortex, however, is far more than simply a relay station allowing information to be transferred between the hippocampus and the rest of the brain. Indeed, an important network of associational connections and intrinsic circuits between neurons located in different layers contribute to information processing carried out by the entorhinal cortex (Chrobak & Amaral, 2007; Lavenex & Amaral, 2000; Witter & Moser, 2006). Given its central role in memory function, the entorhinal cortex has been the focus of very intense investigation in animal models of human memory processes, in particular in rats and monkeys. However, although the general functional organization of the entorhinal cortex is conserved across species (Insausti, Herrero, & Witter, 1997; Witter et al., 2017), there are clear differences in the number, the relative development, and the structural characteristics of different subdivisions of the entorhinal cortex between rats,

monkeys, and humans (Amaral et al., 1987; Amaral & Lavenex, 2007; Insausti et al., 1997; Insausti, Tunon, Sobreviela, Insausti, & Gonzalo, 1995). It is therefore important to obtain reliable estimates of the fundamental neuroanatomical characteristics of the entorhinal cortex in these different species in order to be able to extrapolate the findings obtained in experimental studies in animals and create realistic models of the basic principles of human memory function (Witter & Moser, 2006).

1.1 | Subdivisions of the entorhinal cortex

Based on the organization of the afferent and efferent connections of the entorhinal cortex in the cynomolgus monkeys (*Macaca fascicularis*), together with the distribution of acetylcholinesterase histochemistry, heavy metal distribution and Golgi-impregnated preparations, Amaral et al. (1987) defined seven subdivisions in the monkey entorhinal cortex: Eo, the olfactory field of the entorhinal cortex; Er, the rostral division of the entorhinal cortex; El, the lateral division of the entorhinal cortex, which comprises the lateral rostral (Elr) and lateral caudal (Elc) subdivisions; Ei, the intermediate division of the entorhinal cortex; Ec, the caudal division of the entorhinal cortex; and Ecl, the caudal limiting division of the entorhinal cortex.

Based on the organization described in monkeys, Insausti et al. (1995) defined eight subdivisions in the human entorhinal cortex: Eo, the olfactory field; Er, the rostral field; Elr, the lateral rostral field; Emi, the medial intermediate field; Ei, the intermediate field; Elc, the lateral caudal field; Ec, the caudal field; and Ecl, the caudal limiting field. This parcellation of the human entorhinal cortex is thus largely consistent with the one originally described in monkeys. The different fields of the primate entorhinal cortex may be associated with specific functions, and susceptibility to pathology. Recent functional magnetic resonance imaging (fMRI) studies in humans have defined two major functional subregions, the anterolateral entorhinal cortex and the posteromedial entorhinal cortex (homologous to the rodent lateral entorhinal cortex [LEC] and medial entorhinal cortex [MEC], respectively; see below), based on their preferential connectivity with the perirhinal (PRC) and parahippocampal (PRH) cortices (Maass, Berron, Libby, Ranganath, & Duzel, 2015), or their global connectivity patterns (Schroder, Haak, Jimenez, Beckmann, & Doeller, 2015), which had been previously defined in rats and monkeys (Amaral & Lavenex, 2007; van Strien, Cappaert, & Witter, 2009). Based on the connectivity patterns established in monkeys (Insausti, Amaral, & Cowan, 1987; Suzuki & Amaral, 1994b) and the topological organization described in monkeys and humans (Amaral et al., 1987; Insausti et al., 1995), one may surmise that in humans LEC comprises the fields Eo, Er, Elr, Elc, and a portion of Ei, whereas MEC comprises a portion of Ei and the fields Emi, Ec, and Ecl.

Similarly, following the scheme developed in primates and the detailed analysis of the connectivity of this region, Insausti et al. (1997) described six subdivisions in the rat entorhinal cortex: the dorsal lateral entorhinal field (DLE), the dorsal intermediate field (DIE), the amygdalo-entorhinal transitional field (AE), the ventral intermediate entorhinal field (VIE), the medial entorhinal field (ME), and the caudal entorhinal field (CE). Despite the similarities in the overall organization of the hippocampal-cortical connectivity in rats and monkeys, this nomenclature is rarely used (Witter et al., 2017). Instead, most neuroanatomical and functional studies consider a simpler parcellation of the rat entorhinal cortex that includes the lateral entorhinal cortex (LEC), which comprises the fields DLE, DIE, AE, and VIE, and the medial entorhinal cortex (MEC), which comprises the fields ME and CE. Note that this simplified parcellation of the entorhinal cortex in rodent functional studies (Witter & Moser, 2006) contributed to the use of this simplified parcellation of the entorhinal cortex in human functional studies (Reagh et al., 2018) and some comparative neuroanatomical studies (Ding et al., 2017; Naumann et al., 2016).

1.2 | Different functional circuits

A simplified description of the connectivity of the entorhinal cortex, which is consistent across species, indicates that its superficial layers (II and III) represent the main entryways for much of the sensory information processed by the hippocampal formation, whereas its deep layers (V and VI) provide the main conduit through which processed information is sent back to the neocortex (Amaral & Lavenex, 2007; Witter et al., 2017).

In monkeys, the perirhinal and parahippocampal cortices provide about two-thirds of the cortical projections reaching the entorhinal cortex, but the projections from these two cortices are directed preferentially toward different subdivisions (Suzuki & Amaral, 1994a). The projections from the perirhinal cortex terminate predominantly in the rostral two-thirds of the entorhinal cortex, in particular areas Eo, Er, Elr, Elc, and Ei. The projections from the parahippocampal cortex, in contrast, terminate predominantly in the caudal two-thirds of the entorhinal cortex, particularly in areas Ei, Ec, and Ecl. Other cortical projections originate in the temporal lobes, in the frontal cortex, the insula, the cingulate, and retrosplenial cortices (Insausti et al., 1987). Consistent with the fact that the entorhinal cortex is not a homogeneous structure, the projections originating from these cortical regions each preferentially terminate in different subdivisions of the entorhinal cortex. Direct projections from the insula, the orbitofrontal cortex,and the anterior cingulate cortex are directed predominantly toward rostral areas Eo, Er, Elr, and Ei, whereas the projections from the retrosplenial cortex and the superior temporal gyrus are directed predominantly toward caudal areas Ei, Ec, and Ecl. Similarly, the projections originating from the amygdala, which are thought to contribute to the emotional regulation of memory, are directed toward the rostral subdivisions of the entorhinal cortex, including areas Eo, Er, Elr, and the rostral portions of areas Ei and Elc, with essentially no amygdala projections to the caudal areas, Ec and Ecl (Pitkänen, Kelly, & Amaral, 2002).

The entorhinal cortex projections to the dentate gyrus and the hippocampus also exhibit clear patterns of laminar and topographical organization, which suggests distinct functional circuits (Amaral, Kondo, & Lavenex, 2014; Witter & Amaral, 1991; Witter, Van Hoesen, & Amaral, 1989). Entorhinal cortex projections to the dentate gyrus, and the CA3 and CA2 fields of the hippocampus originate mainly from cells in layer II, whereas projections to CA1 and the subiculum originate mainly from cells in layer III. In monkeys, lateral portions of the entorhinal cortex project to caudal levels of the dentate gyrus and hippocampus, whereas medial portions of the entorhinal cortex project to rostral levels. In addition, the projections from the

entorhinal cortex to the dentate gyrus exhibit a different laminar distribution depending on the rostrocaudal location of the cells of origin. The rostral entorhinal cortex projects more heavily to the outer third of the molecular layer, whereas the caudal entorhinal cortex projects more heavily to the middle third of the molecular layer. Similarly, the projections from the entorhinal cortex to the hippocampus exhibit a different topographical distribution depending on the rostrocaudal location of the cells of origin. Projections from the rostral part of the entorhinal cortex terminate at the border of CA1 and the subiculum, whereas projections from the caudal part of the entorhinal cortex terminate in the portion of CA1 closer to CA2 and in the portion of the subiculum closer to the presubiculum.

The dentate gyrus and CA3 do not project back to the entorhinal cortex (Amaral & Lavenex, 2007). In contrast, CA1 and the subiculum project to the deep layers of the entorhinal cortex, following a topographical organization that largely reciprocates the entorhinal cortex projections to these regions (Amaral & Lavenex, 2007). In monkeys, the rostral entorhinal cortex receives projections originating from pyramidal cells located at the border of CA1 and the subiculum, whereas the caudal entorhinal cortex receives projections originating in the portion of CA1 closer to CA2 and the portion of the subiculum closer to the presubiculum. One final but important characteristic of the connectivity of the entorhinal cortex is the direct projections from the presubiculum to layer III of the caudal subdivisions of the entorhinal cortex, areas Ec and Ecl. Interestingly, this connection is also a defining feature of the rat MEC, which is particularly involved in spatial information processing (Knierim, Neunuebel, & Deshmukh, 2014; Witter & Moser, 2006).

1.3 | Aim of the current study

Despite all that is already known regarding the structural organization of the monkey entorhinal cortex, there is little quantitative information about its structural characteristics, including reliable estimates of the number of neurons and their features in the different layers of its different subdivisions. The aim of the current study was to provide these normative data for the rhesus monkey (*Macaca mulatta*) entorhinal cortex. We implemented modern, design-based stereological techniques to provide estimates of neuron numbers, neuronal soma size, and volume of different layers and subdivisions of adult macaque monkeys (5–9 years of age). We further compared our quantitative data with previously published stereological data for the rat and human entorhinal cortex, in order to provide a perspective on the relative development and structural organization of the main subdivisions of the entorhinal cortex in two model organisms widely used to decipher the basic functional principles of the medial temporal lobe memory system in humans.

2 | MATERIALS AND METHODS

2.1 | Experimental animals

Four rhesus monkeys, *Macaca mulatta* (two males: 5.3 and 9.4 years of age; two females: 7.7 and 9.3 years of age), were used for this study. Monkeys were born from multiparous mothers and raised at the California National Primate Research Center. They were maternally reared in 2,000 m^2 outdoor enclosures and lived in large social groups until they were killed. These monkeys were the same animals used in quantitative studies of the monkey hippocampal formation (Jabes, Banta Lavenex, Amaral, & Lavenex, 2010, 2011) and amygdala (Chareyron, Banta Lavenex, Amaral, & Lavenex, 2011; Chareyron, Banta Lavenex, Amaral, & Lavenex, 2012). All experimental procedures were approved by the Institutional Animal Care and Use Committee of the University of California, Davis.

2.2 | Histological processing

2.2.1 | Brain acquisition

Monkeys were deeply anesthetized with an intravenous injection of sodium pentobarbital (50 mg/kg i.v.; Fatal-Plus; Vortech Pharmaceuticals, Dearborn, MI) and perfused transcardially with 1% and then 4% paraformaldehyde in 0.1 M phosphate buffer (PB; pH 7.4) following protocols previously described (Lavenex, Banta Lavenex, Bennett, & Amaral, 2009). Serial coronal sections were cut with a freezing microtome in sets of seven sections, where the first six sections were 30-μm thick, and the seventh section was 60-μm thick (Microm HM 450, Microm International GmbH, Walldorf, Baden-Württemberg, Germany). The 60-μm sections were collected in 10% formaldehyde solution in 0.1 M PB (pH 7.4) and postfixed at 4 °C for 4 weeks prior to Nissl staining with thionin. All other series were collected in tissue collection solution (TCS) and kept at −70 °C until further processing.

2.2.2 | Nissl staining with thionin

The procedure for Nissl-stained sections followed our standard laboratory protocol described previously (Lavenex et al., 2009). Sections were taken out of the 10% formaldehyde solution, thoroughly washed 2 × 2 hr in 0.1 M PB, mounted on gelatin-coated slides from filtered 0.05 M PB (pH 7.4), and air-dried overnight at 37 °C. Sections were then defatted 2 × 2 hr in a mixture of chloroform/ethanol (1:1, vol.), and rinsed 2 × 2 min in 100% ethanol, 2 min in 95% ethanol and air-dried overnight at 37 °C. Sections were then rehydrated through a graded series of ethanol, 2 min in 95% ethanol, 2 min in 70% ethanol, 2 min in 50% ethanol, dipped in two separate baths of dH_2O, and stained 20 s in a 0.25% thionin (Fisher Scientific, Waltham, MA, cat# T-409) solution, dipped in two separate baths of dH_2O, 4 min in 50% ethanol, 4 min in 70% ethanol, 4 min in 95% ethanol + glacial acetic acid (1 drop per 100 mL of ethanol), 4 min in 95% ethanol, 2 × 4 min in 100% ethanol, 3 × 4 min in xylene, and coverslipped with the mounting medium DPX (BDH Laboratories, Poole, UK).

2.2.3 | SMI-32 immunohistochemistry

The immunohistochemical procedure for visualizing nonphosphorylated high-molecular-weight neurofilaments was carried out on free-floating sections using the monoclonal antibody SMI-32 (Sternberger Monoclonals, Lutherville, MD, cat# SMI-32, lot 16; RRID: AB_2314904), as previously described (Lavenex et al., 2009; Lavenex, Banta Lavenex, & Amaral, 2004). This antibody was raised in mouse against the nonphosphorylated 200 kDa heavy neurofilament. On conventional immunoblots, SMI-32 visualizes two bands (200 and

180 kDa) which merge into a single line on two-dimensional blots (Goldstein, Sternberger, & Sternberger, 1987; Sternberger & Sternberger, 1983). This antibody has been shown to react with nonphosphorylated high-molecular-weight neurofilaments of most mammalian species, including rats, cats, dogs, monkeys, and humans (de Haas Ratzliff & Soltesz, 2000; Hof & Morrison, 1995; Hornung & Riederer, 1999; Lavenex et al., 2004; Siegel et al., 1993), and may also show some limited cross-reactivity with nonphosphorylated medium-molecular-weight neurofilaments (Hornung & Riederer, 1999).

Sections that had been maintained in TCS at −70 °C were rinsed 3 × 10 min in 0.05 M Tris buffer (pH 7.4) with 1.5% NaCl, treated against endogenous peroxidase by immersion in 0.5% hydrogen peroxide solution in 0.05 M Tris/NaCl for 15 min and rinsed 6 × 5 min in Tris/NaCl buffer. Sections were then incubated for 4 hr in a blocking solution made up of 0.5% Triton X-100 (TX-100; Fisher Scientific, Waltham, MA; cat# BP151-500), and 10% normal horse serum (NHS; Biogenesis, Poole, UK; cat# 8270-1004) in 0.05 M Tris/NaCl buffer at room temperature. Sections were then incubated overnight with the primary antibody SMI-32 (1:2,000) in 0.3% TX-100 and 1% NHS in 0.05 M Tris/NaCl at 4 °C. Sections were then washed 3 × 10 min in 0.05 M Tris/NaCl buffer with 1% NHS, incubated with a secondary antibody, biotinylated horse antimouse IgG (1:227; Vector Laboratories, Burlingame, CA; cat# BA-2000; RRID:AB_2313581) in 0.3% TX-100 and 1% NHS in 0.05 M Tris/NaCl buffer, rinsed 3 × 10 min in 0.05 M Tris/NaCl buffer containing 1% NHS, incubated for 45 min in an avidin-biotin complex solution (Biostain ABC kit, Biomeda, Foster City, CA; cat# 11-001), washed 3 × 10 min in Tris/NaCl, incubated in secondary antibody solution for another 45 min, washed 3 × 10 min, incubated in avidin-biotin complex solution for 30 min, washed 3 × 10 min in Tris/NaCl, incubated for 30 min in a solution containing 0.05% diaminobenzidine (Sigma-Aldrich Chemicals, St. Louis, MO; cat# D9015-100MG), 0.04% H_2O_2 in 0.05 M Tris buffer, and washed 3 × 10 min. Sections were then mounted on gelatin-coated slides from filtered 0.05 M PB (pH 7.4) and air-dried overnight at 37 °C. Reaction product was then intensified with a silver nitrate–gold chloride method. Sections were defatted 2 × 2 hr in a chloroform/ethanol (1:1, vol.) solution, rehydrated through a graded series of ethanol, and air-dried overnight at 37 °C. Sections were then rinsed 10 min in running dH_2O, incubated for 40 min in a 1% silver nitrate ($AgNO_3$) solution at 56 °C, rinsed 10 min in dH_2O, incubated for 10 min in 0.2% gold chloride ($HAuCl_4 \cdot 3H_2O$) at room temperature with agitation, rinsed 10 min in dH_2O, stabilized in 5% sodium thiosulfate ($Na_2S_2O_3$) for 15 min with agitation, rinsed in running dH_2O for 10 min, dehydrated through a graded series of ethanol and xylene, and coverslipped with the mounting medium DPX.

2.3 | Stereological analyses

2.3.1 | Neuron number

The total number of neurons in the different layers (II, III, V, VI) of the seven subdivisions of the entorhinal cortex (Eo, Er, Ei, Elr, Elc, Ec, Ecl) was determined using the optical fractionator method on the Nissl-stained sections cut at 60 μm (West, Slomianka, & Gundersen, 1991). Neurons were counted when their nucleus came into focus within the counting frame, as it was moved through a known distance of the section thickness. We estimated neuron numbers using the following formula: $N = \sum Q \times 1/ssf \times 1/asf \times 1/tsf$ (ssf: section sampling fraction; asf: area sampling fraction; tsf: thickness sampling fraction). This design-based method allows an estimation of the number of neurons that is independent of volume estimates. About 43 sections per animal (240 μm apart) were used for the estimation of the total number of principal neurons in the different layers/subdivisions. We estimated neuron numbers in the left hemisphere for half of the animals and in the right hemisphere for the other half. No difference was observed between left and right hemisphere; reported estimates are unilateral values. We used a 100× Plan Fluor oil objective (N.A. 1.30) on a Nikon Eclipse 80i microscope (Nikon Instruments Inc., Melville, NY) linked to PC-based StereoInvestigator 9.0 (MBF Bioscience, Williston, VT). The sampling scheme was established to obtain individual estimates of neuron number with estimated coefficients of error around 0.11 (Table 1; $CE = sqrt(CE^2(\sum Q) + CE^2(t))$; $CE(\sum Q) = sum\ (Q_i) + ((3 \times (sum\ (Q_i \times Q_i) - sum\ (Q_i)) - (4 \times sum\ (Q_i \times Q_{i+1}) + (Q_i \times Q_{i+2}))/12$; $CE(t)$ = standard deviation (section thickness)/average (section thickness)). We identified neurons based on morphological criteria identifiable in Nissl preparations, as described in more details in previous publications (Chareyron et al., 2011; Fitting, Booze, Hasselrot, & Mactutus, 2008; Grady, Charleston, Maris, Witgen, & Lifshitz, 2003; Hamidi, Drevets, & Price, 2004; Morris, Jordan, & Breedlove, 2008; Palackal, Neuringer, & Sturman, 1993). Briefly, neurons are darkly stained and comprise a single large nucleolus. Astrocytes are relatively smaller in size and exhibit pale staining of the nucleus. Oligodendrocytes are smaller than astrocytes and contain round, darkly staining nuclei that are densely packed with chromatin. Microglia have the smallest nucleus, dark staining, and an irregular shape that is often rod-like, oval or bent.

2.3.2 | Volume estimates

We estimated the volume of the individual layers of the seven subdivisions of the monkey entorhinal cortex based on the outline tracings performed with Stereoinvestigator 9.0 for the estimation of neuron numbers. We used the section cutting thickness (60 μm) to determine the distance between sampled sections, which was then multiplied by the total surface area delineated for neuron counts to calculate the volume.

2.3.3 | Neuronal soma size

The volume of neuronal somas was measured on Nissl-stained preparations, using the nucleator probe of StereoInvestigator 9.0 (MBF Bioscience, Williston, VT). We measured an average of 291 neurons per layer per subdivision, sampled at every counting site during the optical fractionator analysis (Table 1). Briefly, the nucleator can be used to estimate the mean cross-sectional area and volume of cells. A point within the nucleus was selected randomly, and three rays at 120° angles were drawn in a random orientation to intersect the cell boundary. When the rays extended into proximal cell processes, the cell boundary was defined as the continuation of the adjacent cell boundary at the base of the process. The length of the intercept from the point to the cell boundary (l) is measured and the cell volume is obtained by $V = (4/3 \times 3.1416) \times l^3$. Essentially, this is the formula used to determine the volume of a sphere with a known radius. Note that the nucleator method provides accurate estimates of neuron size

TABLE 1 Parameters used for the stereological analysis of the monkey entorhinal cortex

Entorhinal area		Number of sections (range)	Distance between sections (μm)	Scan grid (μm)[a]	Counting frame (μm)	Disector height (μm)	Guard zones (μm)	Average section thickness (μm)[b]	Number of neurons counted (range)	Coefficients of error (CE)
Eo	II	18.25 (17–21)	240	130 × 130	40 × 40	5	2	12.07 (8.9–24.2)	393 (320–442)	0.13 (0.10–0.15)
	III	18.25 (17–21)	240	350 × 350	40 × 40	5	2	12.43 (9.9–17.0)	390 (320–446)	0.10 (0.09–0.12)
	V–VI	18.25 (17–21)	240	170 × 170	40 × 40	5	2	13.26 (10.4–17.1)	345 (286–409)	0.10 (0.09–0.11)
Er	II	15.00 (13–16)	240	150 × 150	40 × 40	5	2	12.49 (9.3–16.7)	357 (252–429)	0.11 (0.10–0.11)
	III	15.00 (13–16)	240	350 × 350	40 × 40	5	2	13.48 (10.0–17.3)	341 (274–401)	0.10 (0.09–0.11)
	V	15.00 (13–16)	240	150 × 150	40 × 40	5	2	13.75 (10.9–18.6)	287 (219–338)	0.10 (0.09–0.12)
	VI	15.00 (13–16)	240	250 × 250	40 × 40	5	2	13.92 (11–1-18.1)	298 (231–325)	0.10 (0.09–0.11)
Elr	II	15.25 (14–16)	240	140 × 140	40 × 40	5	2	13.75 (10.4–22.4)	276 (226–347)	0.12 (0.09–0.16)
	III	15.25 (14–16)	240	220 × 220	40 × 40	5	2	14.38 (11.4–22.1)	234 (210–254)	0.12 (0.10–0.14)
	V	15.25 (14–16)	240	120 × 120	40 × 40	5	2	14.76 (11.3–22.1)	274 (224–323)	0.11 (0.09–0.15)
	VI	15.25 (14–16)	240	170 × 170	40 × 40	5	2	14.51 (11.0–19.0)	314 (296–335)	0.10 (0.08–0.12)
Ei	II	13.25 (12–14)	240	300 × 300	40 × 40	5	2	13.32 (10.4–16.8)	231 (202–268)	0.10 (0.10–0.10)
	III	13.25 (12–14)	240	500 × 500	40 × 40	5	2	13.82 (10.4–17.3)	258 (199–292)	0.10 (0.08–0.11)
	V	13.25 (12–14)	240	300 × 300	40 × 40	5	2	14.09 (11.0–18.0)	251 (217–292)	0.09 (0.09–0.10)
	VI	13.25 (12–14)	240	450 × 450	40 × 40	5	2	14.32 (11.6–18.6)	226 (186–253)	0.09 (0.09–0.10)
Elc	II	11.50 (10–12)	240	130 × 130	40 × 40	5	2	14.43 (11.0–18.4)	313 (306–329)	0.11 (0.10–0.13)
	III	11.50 (10–12)	240	210 × 210	40 × 40	5	2	15.19 (11.9–18.1)	250 (200–307)	0.10 (0.09–0.10)
	V	11.50 (10–12)	240	140 × 140	40 × 40	5	2	15.12 (12.3–23.0)	235 (200–282)	0.10 (0.09–0.12)
	VI	11.50 (10–12)	240	170 × 170	40 × 40	5	2	14.98 (12.2–23.3)	292 (241–353)	0.11 (0.09–0.13)
Ec	II	11.75 (9–14)	240	200 × 200	40 × 40	5	2	14.30 (10.9–22.4)	296 (265–344)	0.12 (0.10–0.16)
	III	11.75 (9–14)	240	300 × 300	40 × 40	5	2	15.10 (11.4–27.4)	324 (272–356)	0.13 (0.10–0.18)
	V	11.75 (9–14)	240	200 × 200	40 × 40	5	2	15.14 (11.9–28.4)	291 (247–333)	0.12 (0.10–0.18)
	VI	11.75 (9–14)	240	300 × 300	40 × 40	5	2	15.19 (11.8–29.1)	271 (222–307)	0.13 (0.10–0.20)
Ecl	II	16.25 (13–19)	240	250 × 250	40 × 40	5	2	14.61 (10.4–26.2)	242 (220–266)	0.13 (0.10–0.17)
	III	16.25 (13–19)	240	320 × 320	40 × 40	5	2	15.59 (11.1–24.9)	264 (247–277)	0.12 (0.09–0.13)
	V	16.25 (13–19)	240	200 × 200	40 × 40	5	2	15.66 (11.4–23.5)	225 (206–242)	0.13 (0.12–0.15)
	VI	16.25 (13–19)	240	220 × 220	40 × 40	5	2	15.92 (10.9–22.7)	385 (330–433)	0.11 (0.08–0.13)

[a] Scan grid was placed in a random orientation.
[b] Section thickness was measured at every other counting site.

when isotropic-uniform-random sectioning of brain structures is employed (Gundersen, 1988). In our study all brains were cut in the coronal plane. Estimates of cell size might therefore be impacted by the nonrandom orientation of neurons in the different layers and subdivisions of the entorhinal cortex, which could lead to an overestimation or under-estimation of cell size in any given structure.

2.4 | Photomicrographic production

Low-magnification photomicrographs were taken with a Leica DFC420 digital camera on a Leica MZ9.5 stereomicroscope (Leica Microsystems GmbH, 35578 Wetzlar, Germany). High-magnification photomicrographs were taken with a Leica DFC490 digital camera Leica Microsystems GmbH, 35578 Wetzlar, Germany on a Nikon Eclipse 80i microscope (Nikon Instruments, Tokyo 108-6290, Japan). Artifacts located outside the sections were removed, and levels were adjusted in Adobe Photoshop CS4 V11.0.2 (Adobe Systems, San Jose, CA) to improve contrast and clarity.

3 | RESULTS

3.1 | Structural organization of the monkey entorhinal cortex

The nomenclature, topographical and cytoarchitectonic organization of the entorhinal cortex have been described previously for the cynomolgus monkey (*Macaca fascicularis*) (Amaral et al., 1987). The monkey entorhinal cortex comprises seven subdivisions: Eo, the olfactory field of the entorhinal cortex; Er, the rostral entorhinal cortex; El, the lateral entorhinal cortex, which comprises the lateral rostral (Elr) and lateral caudal (Elc) subdivisions; Ei, the intermediate division of the entorhinal cortex; Ec, the caudal division of the entorhinal cortex; and Ecl, the caudal limiting division of the entorhinal cortex. The cytoarchitectonic characteristics of the cynomolgus monkey entorhinal cortex are very similar to those that we observed in the rhesus monkey (*Macaca mulatta*) entorhinal cortex. However, subtle differences in the relative development of individual layers in certain subdivisions (see below), as observed in Nissl preparations, as well as the additional information provided by the immunohistochemical analysis of nonphosphorylated high-molecular-weight neurofilament distribution (SMI-32), prompted us to provide a thorough description of the cytoarchitectonic characteristics of the different subdivisions of the adult rhesus monkey entorhinal cortex (Figures 1 and 2).

3.2 | Overview of the laminar organization

Layer I, the outermost layer, corresponds to the molecular or superficial plexiform layer found in other cortical fields, and is relatively free of neurons. In SMI-32 preparations, the apical dendritic arborization of layer II neurons can be observed in the deeper half of the layer, with only occasional stained fibers visible in the superficial half of layer I. The remainder of layer I is at background level of staining.

Layer II is a narrow, cellular layer that varies considerably in appearance at different rostrocaudal levels. Its major cell type, generally described as "stellate," is in fact a type of modified pyramidal neuron. Neuron size varies across subdivisions, ranging from an average volume of about 1,200 μm^3 in Eo to 2,700 μm^3 in area Ec (see below for estimates in other subdivisions). In SMI-32 preparations, the cell bodies and the apical dendrites of layer II neurons are heavily stained. There are, however, two superimposed gradients in SMI-32 staining intensity that appear to correlate with gradients in cell size. First, staining intensity increases from rostral to caudal levels. Second, at rostral levels, labeling is higher laterally than medially. There is no obvious mediolateral gradient at caudal levels.

Layer III is the thickest of the entorhinal cell layers (Table 2; Figure 3). At rostral levels it has a patchy appearance, but it becomes increasingly more homogeneous and somewhat "columnar" at caudal levels. Neurons in the superficial portion of layer III are pyramidal neurons similar to layer II cells, whereas deeply located neurons are multipolar, round or fusiform neurons. In some subdivisions, layer III is quite sharply separated from layer II by a narrow, cell-free zone. In SMI-32 preparations, only a small proportion of layer III cells are labeled. At the most rostral levels, SMI-32-positive neurons are located in the deep portion of layer III, whereas at more caudal levels SMI-32-positive neurons are located in the superficial portion of layer III. In addition, there is a mediolateral gradient at rostral levels; medially SMI-32-positive cells are located deeper in layer III, whereas laterally SMI-32-positive neurons are located more superficially in layer III. This mediolateral gradient is not obvious at caudal levels, as all SMI-32-positive cells are located in the superficial portion of layer III.

Layer IV in the entorhinal cortex is usually referred to as the *lamina dissecans*. This is a cell-sparse zone that is rich in myelinated fibers especially at mid-rostrocaudal levels. In the rhesus monkey (*Macaca mulatta*), layer IV is generally more visible throughout most of the entorhinal cortex, as compared to the cynomolgus monkey (*Macaca fascicularis*). In SMI-32 preparations, layer IV appears largely unstained, except for the apical dendrites of neurons originating in layers V and VI.

Layer V has a stratified appearance over much of its extent in the cynomolgus monkey and can be divided in three laminae, Va, Vb, and Vc. This lamination is not as obvious in rhesus monkeys and it varies significantly at different rostrocaudal levels. Layers Va and Vb are often difficult to distinguish in Nissl preparations, and layer Vc, a cell sparse zone separating layer V from layer VI, appears more clearly only at mid rostrocaudal levels. In SMI-32 preparations, layer V also appears largely homogenous. The cell bodies of layer V neurons are only lightly stained, while their dendrites are moderately stained; the neuropil of layer V is moderately stained.

Layer VI is a striking, multi-laminated cellular layer. At some levels, as many as four distinct bands of cells can be distinguished in layer VI, and these bands often have a characteristically "coiled" appearance when seen in coronal Nissl-stained sections. In SMI-32 preparations, cell bodies of layer VI neurons are moderately stained, while their apical dendrites are darkly stained. The sublaminae of layer VI are therefore also clearly visible in SMI-32-preparations.

Deep to layer VI are scattered neurons in the subcortical white matter adjacent to the angular bundle. Their number and distribution do not appear sufficient to justify identifying them as a separate, seventh layer. These neurons have various morphologies in Nissl-stained preparations; some of these neurons as well as a number of individual fibers are SMI-32-positive.

3.3 | Detailed characteristics of individual subdivisions

Eo: Layer I is a rather thin layer in Eo. Layer II is either absent or very thin; this serves to distinguish the area and stands in marked contrast to the prominent cell islands typical of area Er. Where layer II is recognizable in Nissl preparations, its cells are distinctly smaller than those in Er (Table 2) and there is generally a cell-free zone beneath them that demarcates layer II from layer III. Layer III is formed by clusters of neurons that are characteristic of the rostral entorhinal cortex. However, the clusters are more densely aggregated than in Er so that, at low magnification, layer III has a more uniform appearance in Eo. The superficially located cells in layer III are more densely packed and thus appear more darkly stained than the deeper cells. There is no evident

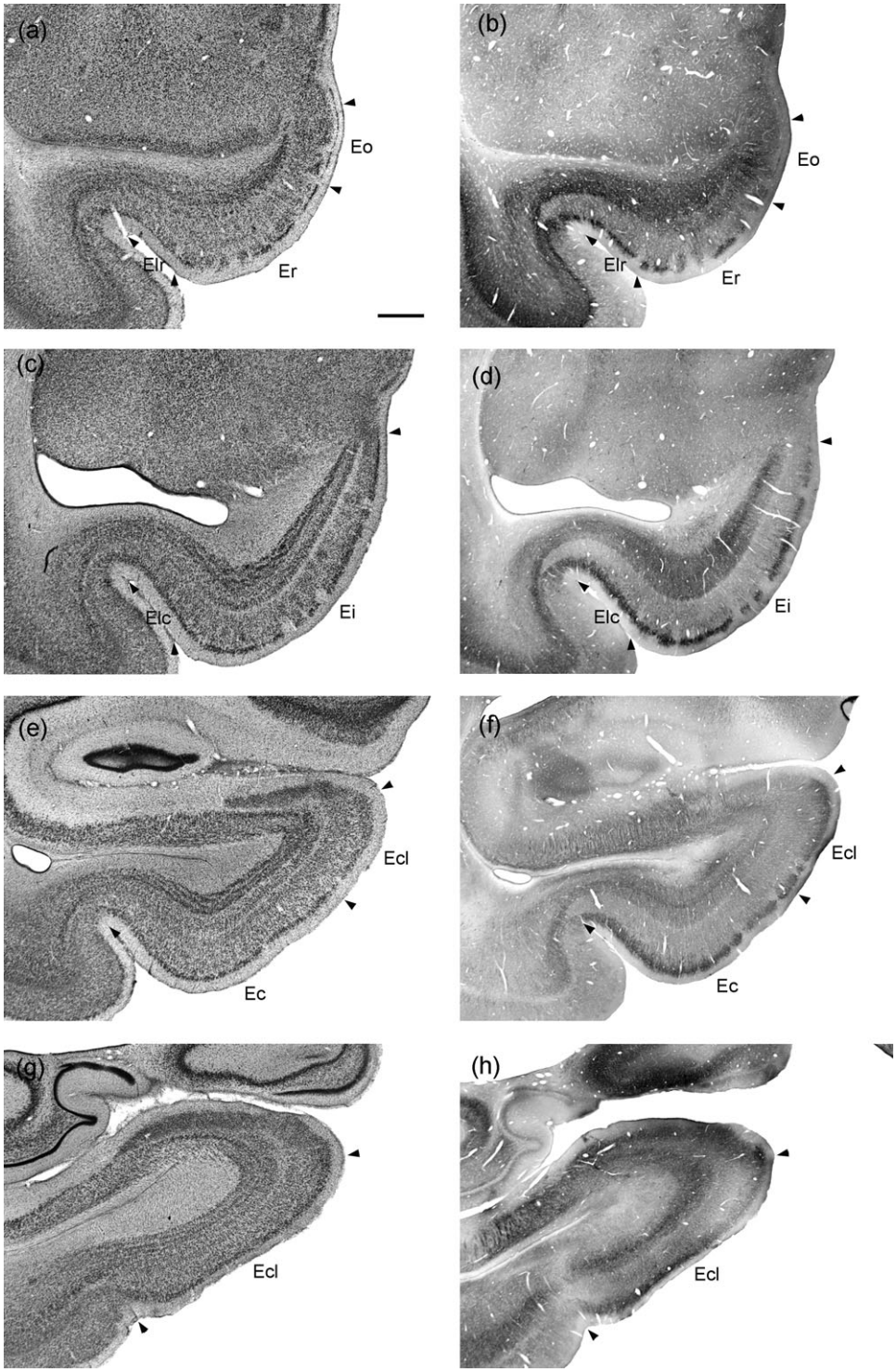

FIGURE 1 Low magnification photomicrographs of coronal sections through the adult rhesus monkey entorhinal cortex. (a), (c), (e), (g) Nissl-stained preparations, arranged from rostral (a) to caudal (g). (b), (d), (f), (h) SMI-32 immunohistochemistry preparations, arranged from rostral (b) to caudal (h). Eo = olfactory field; Er = rostral field; Elr = lateral rostral field; Elc = lateral caudal field; Ei = intermediate field; Ec = caudal field; and Ecl = caudal limiting field. Scale bar = 1 mm

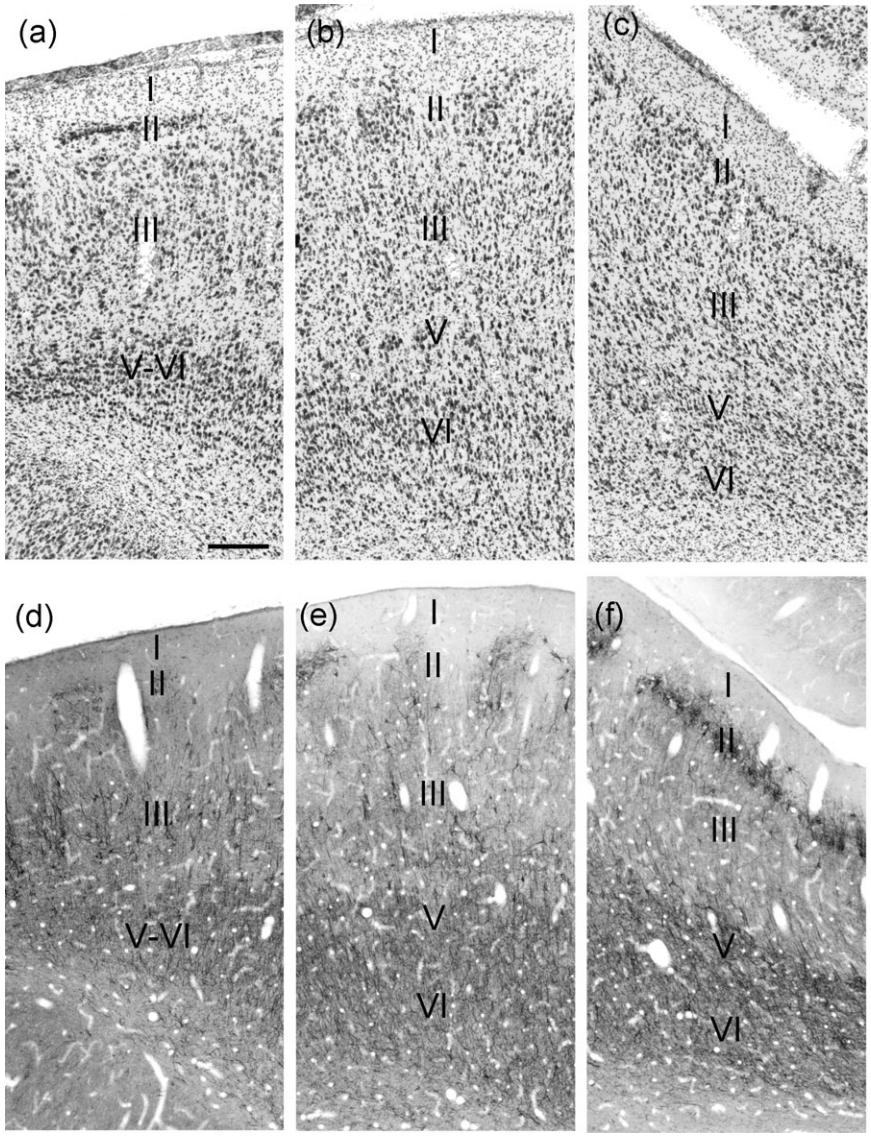

FIGURE 2 Continued on next page

layer IV in Eo. The deeper layers V and VI are poorly developed; at caudal levels and at the transition between Eo and Er, layer V appears like a cell-sparse layer, whereas layer VI contains densely packed, darkly stained neurons in Nissl preparations.

In SMI-32 preparations, Eo layer II cells are largely unstained. In layer III, a small number of neurons located in the deeper portion are strongly SMI-32-positive, while individual neurons located superficially are lightly labeled. Layer VI shows a large number of SMI-32-positive neurons; their cell bodies are moderately stained, while a relatively short portion of their dendrites appears heavily stained in coronal sections. A number of SMI-32-positive fibers, probably the dendrites of layer VI neurons, are also visible throughout layer III.

Er: Layer I is thicker in Er than in Eo. Layer II is made up of islands of multipolar cells that are separated by wide, relatively cell-sparse zones. These cell-sparse zones are continuous with similar zones in layer III, as are the cell islands. Layer III is composed of large, irregular patches of neurons that are separated by cell-sparse regions. The more superficial cells in the layer tend to be larger than those at deeper levels. No distinct layer IV is visible throughout most of this field. However, near its caudal boundary there are occasional cell-free patches between layers III and V that mark the beginning of the lamina dissecans. Layer V is well developed but its sublaminae are not easily distinguished. Layer V neurons are relatively large multipolar neurons, which contrast with the smaller, radially oriented layer VI neurons. Layer VI is as thick as at any caudal level of the entorhinal cortex, but it does not have the laminated appearance that is so characteristic of fields Ei and Ec.

In SMI-32 preparations, the cell bodies of layer II neurons are moderately to heavily stained. Their dendrites are strongly labeled but do not extend very far into layer I. SMI-32-positive neurons are found both in the superficial and deep portions of layer III. The cell bodies and dendrites are strongly labeled, whereas the neuropil stains only slightly above background level. SMI-32-positive neurons tend to be located more deeply in layer III at rostral and medial levels of Er, near the border with Eo; whereas they tend to be located more superficially at lateral and caudal levels, near the border with Elr and Ei, respectively. The cell bodies of layers V and VI neurons are moderately stained, whereas their dendrites are more darkly stained,

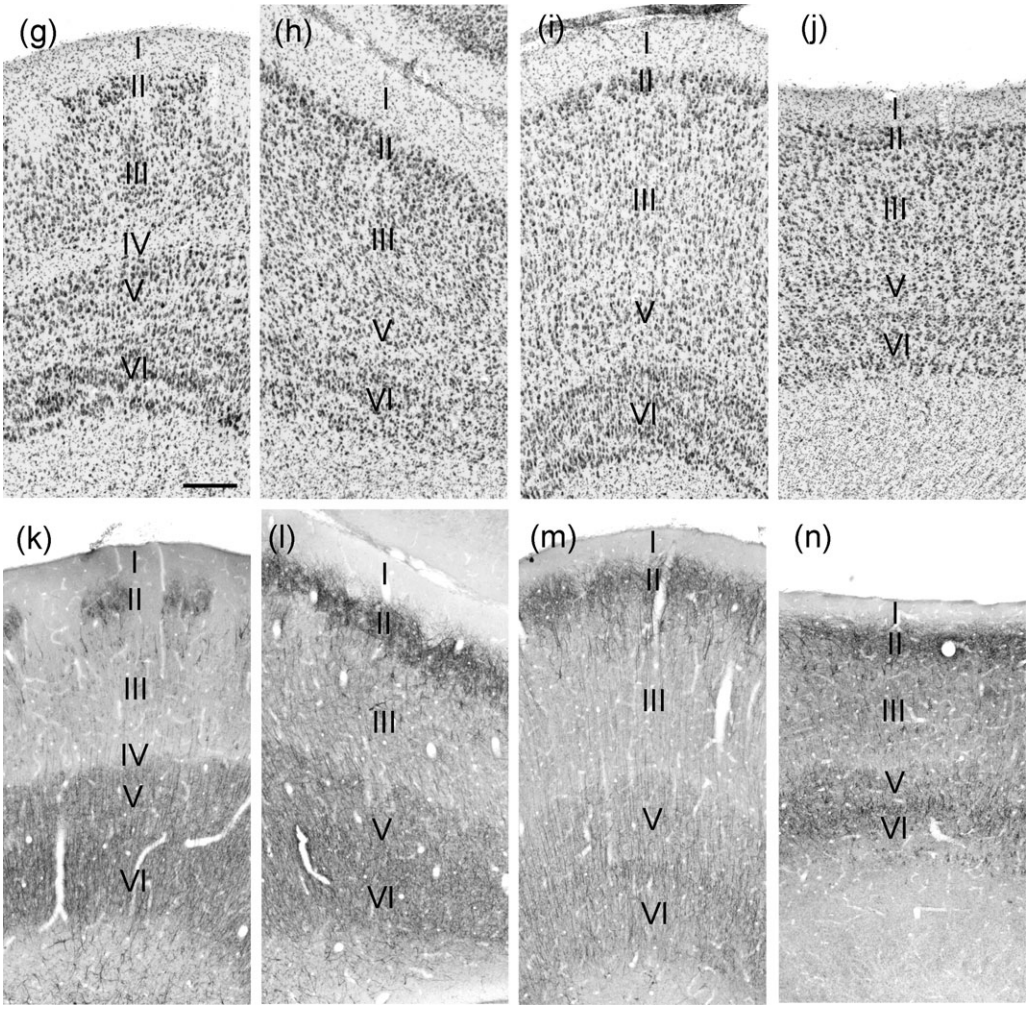

FIGURE 2 High magnification photomicrographs of coronal sections through the adult rhesus monkey entorhinal cortex. (a–c) and (g–j) Nissl-stained preparations. (d–f) and (k–n) SMI-32 immunohistochemistry preparations. (a) and (d) Eo = olfactory field; (b) and (e) Er = rostral field; (c) and (f) Elr = lateral rostral field. (g) and (k) Ei = intermediate field; (h) and (l) Elc = lateral caudal field; (i) and (m) Ec = caudal field; (j) and (n) Ecl = caudal limiting field. Scale bars in (a) and (g) = 250 μm

especially those of layer VI neurons. The neuropil of layers V and VI is moderately stained and stands in contrast with that of the very lightly stained layer III.

El (Elr and Elc): Layer I is generally thicker in Elr and Elc than in the more medial fields. This is likely due to the fact that El is located within the rhinal sulcus. Layer II is formed by large and relatively wide cell islands, so wide that they give the layer an almost continuous appearance, especially at caudal levels. In Elr, the cells of layer II merge with those of layer III, but in Elc, there is a narrow cell-free zone separating the two layers. Although the cells of layer III are still clustered, the layer as a whole has a more homogeneous appearance in Elr as compared to Er. The lamina dissecans is not evident in either Elr or Elc; in Elc the corresponding zone appears to be filled with a heterogeneous population of small cells. Layer V is rather narrow; there is a prominent band of darkly stained cells in layer V that appears continuous with layer V of area 35 in Nissl preparations. Layer VI is continuous with the same layer in Er or Ei, but tends to have a less laminated appearance in Elr and Elc, and thus resembles layer VI of area 35.

In SMI-32 preparations, the somas of layer II cells are strongly labeled, and their apical dendrites extend profusely in the deeper half of layer I. In contrast, layer III is largely unstained (except for a small population of superficially located neurons) and appears to extend into area 35. As in medially located areas Er and Ei, layer V neurons are moderately SMI-32-positive, whereas layer VI neurons are more darkly stained. SMI-32-positive dendrites of deep layer neurons are clearly visible and radially oriented in layer III. In contrast, there is no clear organization or orientation of SMI-32-positive processes within layers V and VI.

Ei: There is nothing distinctive about layer I. Layer II is formed by islands of multipolar cells; the mediolateral extent of the islands is highly variable, and some are quite wide. At rostral levels, the cells of layer II tend to merge with those of layer III, whereas at more caudal levels, a thin acellular band (typical of Ec) tends to separate layer II and layer III cells. Layer III is clearly bilaminate; the outer half of layer III has patches of multipolar and pyramidal cells, whereas the deep half of the layer has a more columnar appearance with multipolar and radially oriented fusiform neurons. Layer IV is present and clearly visible

TABLE 2 Volume, neuron number, and neuron soma size in the different layers of the seven subdivisions of the rhesus monkey entorhinal cortex

		Volume (mm^3)			Neuron number			Neuron soma size (μm^3)	
		Mean	*SD*	%	Mean	*SD*	%	Mean	*SD*
Eo	I	0.86	0.25	7.5	–	–		–	–
	II	0.98	0.17	8.4	40,137	7,108	10.0	1,216	66
	III	7.78	1.31	67.1	296,929	41,347	73.7	1,795	95
	V-VI	1.97	0.28	17.0	65,969	8,391	16.4	1,696	171
	Total	11.59	1.66	100.0	403,035	53,910	100.0	–	–
Er	I	1.50	0.39	9.2	–	–		–	–
	II	1.47	0.28	9.0	50,417	12,078	10.0	1,629	158
	III	8.24	1.26	50.9	281,868	48,238	55.7	1,850	99
	V	1.83	0.40	11.2	44,363	8,241	8.8	2,370	147
	VI	3.20	0.55	19.7	129,493	19,533	25.6	1,783	152
	Total	16.24	2.54	100.0	506,140	67,352	100.0	–	–
Ei	I	4.37	0.56	14.5	–	–	–	–	–
	II	3.56	0.25	11.8	138,243	16,063	12.9	2,637	171
	III	11.16	0.57	37.2	445,652	68,989	41.6	2,115	279
	IV	1.25	0.23	4.2	–	–	–	–	–
	V	3.92	0.50	13.0	159,237	20,188	14.9	2,492	238
	VI	5.82	0.99	19.3	328,132	46,213	30.6	1,755	160
	Total	30.08	1.99	100.0	1,071,264	40,889	100.0	–	–
Elr	I	1.08	0.08	15.0	–	–	–	–	–
	II	0.88	0.16	12.1	37,057	6,695	17.4	1.915	254
	III	2.42	0.17	33.4	81,430	8,653	38.2	1,906	316
	V	1.08	0.09	14.9	28,949	3,068	13.6	2,134	219
	VI	1.78	0.09	24.6	65,686	6,530	30.8	1,642	122
	Total	7.24	0.53	100.0	213,123	8,081	100.0	–	–
Elc	I	1.25	0.23	18.0	–	–	–	–	–
	II	0.89	0.07	13.0	38,090	593	17.4	2,280	283
	III	2.27	0.26	33.0	83,439	12,414	38.1	1,721	230
	V	0.96	0.14	13.9	34,604	3,957	15.8	2,089	181
	VI	1.52	0.19	22.0	62,761	7,761	28.7	1,518	87
	Total	6.89	0.70	100.0	218,894	22,439	100.0	–	–
Ec	I	2.75	0.58	15.3	–	–		–	–
	II	2.18	0.36	12.2	85,037	13,609	14.7	2,710	67
	III	6.61	1.44	36.7	220,281	29,678	38.0	1,945	218
	V	2.75	0.53	15.3	88,204	12,656	15.2	2,145	293
	VI	3.68	0.81	20.4	185,487	27,211	32.0	1,503	138
	Total	17.98	3.46	100.0	579,009	79,525	100.0	–	–
Ecl	I	3.13	0.28	18.6	–	–		–	–
	II	2.83	0.44	16.7	110,802	17,631	20.5	2,672	206
	III	6.19	1.03	36.6	211,414	26,276	39.1	2,150	139
	V	2.01	0.34	11.8	70,664	8,806	13.1	2,188	125
	VI	2.76	0.59	16.2	148,066	18,292	27.4	1,424	139
	Total	16.91	2.58	100.0	540,946	67,937	100.0	–	–
All subdivisions									
	I	14.94	1.81	14.0	–		–		
	II	12.79	1.55	12.0	499,784	64,505	14.1		
	III	44.66	4.17	41.8	1,621,012	102,823	45.9		
	IV	1.25	0.23	1.2	–	–	–		
	V	14.51	1.43	13.6	491,990	45,907	13.9		
	VI	18.76	2.77	17.5	919,625	105,028	26.0		
	Total	106.92	10.77	100.0	3,532,411	252,997	100.0		

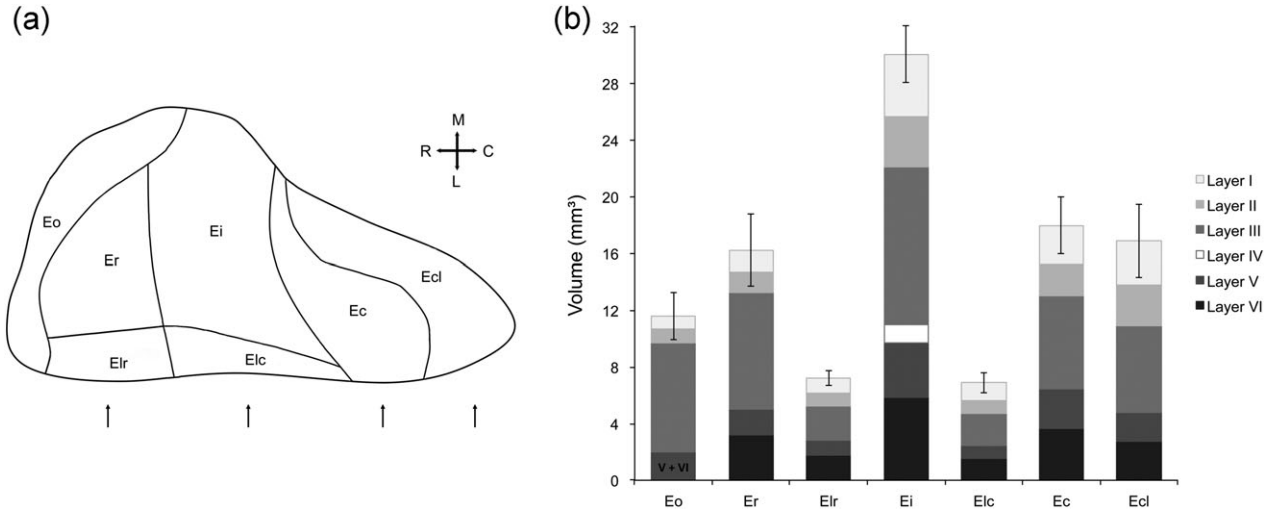

FIGURE 3 (a) Unfolded map of the rhesus monkey entorhinal cortex illustrating the relative position of its seven subdivisions. Black arrows indicate the approximate rostrocaudal locations of the coronal sections illustrated in Figures 1 and 2. (b) Volumes of the different layers of seven subdvisions of the adult rhesus monkey entorhinal cortex, measured on Nissl-stained sections cut at 60 μm on a freezing sliding microtome

throughout the entire subdivision. Layer V is well developed, but its lamination varies rostrocaudally and mediolaterally. At rostromedial levels, layer V cannot easily be distinguished from layer VI due to the lack of a clearly defined layer Vc. The cell-free layer Vc becomes increasingly more prominent at lateral and caudal levels. Layer VI is strongly laminated, especially at mid mediolateral and lateral levels, and the cell strands have a distinct "coiled" appearance. Packing density increases from lateral to medial, especially for neurons of the deepest portion of layer VI.

In SMI-32 preparations, cell bodies and apical dendrites of layer II neurons are heavily stained. In layer III, a number of large neurons located in the superficial half of the layer are heavily stained. The cell bodies are moderately to heavily stained and their basal and apical dendrites are heavily stained. There is also a large population of layer III neurons distributed throughout the layer, whose cell bodies and dendrites are only lightly stained. In addition, lightly to moderately labeled dendrites of deep layer neurons cross layer III, so that the neuropil of layer III appears moderately stained at low magnification. Layer IV is largely unstained, except for the dendrites from layer V and VI neurons, and rare SMI-32 labeled fibers running parallel to layer IV. The cell bodies and dendrites of layer V neurons are moderately stained, so that layer V stands in sharp contrast with the lightly stained neuropil of layers III and IV. The cell bodies of layer VI neurons are only slightly more heavily stained than those of layer V neurons, but the proximal dendrites of layer VI neurons appear clearly much thicker and more darkly stained than those of layer V neurons. This characteristic helps to distinguish layer V from layer VI in SMI-32 preparations. The white matter below layer VI is largely unstained, except for a small number of moderately stained neurons of various shapes. Short, heavily stained processes are also found throughout the white matter below layer VI.

Ec: Layer I is similar in thickness to that in Ei. Layer II is made up of much wider islands of cells and at caudal levels these islands are almost continuous. Beneath layer II, there is a thin acellular band separating it from layer III. Although still detectable, the lamination of layer III is not as obvious as in Ei, and decreases from rostral to caudal. There are no clear isolated patches of cells within layer III. Layer IV is no longer detectable except in the medial half of its more rostral portion. In contrast to the cynomolgus monkey, layer V does not appear clearly laminated in Ec of the rhesus monkey. Layer VI is well developed in Ec, as is observed in Ei; three to four distinct bands of cells are aligned parallel to one another.

In SMI-32 preparations, the cell bodies of layer II neurons are moderately stained and their dendrites are heavily stained. Cell density appears lower than in more rostral subdivisions of the entorhinal cortex and the dendritic arborization gives layer II a bushy appearance. A small number of darkly stained neurons are distributed in the superficial one-third of layer III; moderately stained neurons are found throughout the superficial half of layer III; the rest of the neuropil of layer III is moderately to lightly stained. The layer V neuropil is moderately stained, and contains a small number of moderately stained neurons with darkly stained dendrites, as well as the darkly stained dendrites of superficially located layer VI neurons. Few stained neurons are located in the deepest laminae of layer VI.

Ecl: There is nothing distinctive about layer I. Layer II is thicker in Ecl than in Ec, especially near its border with the parasubiculum. Layer II is more or less continuous and the acellular zone subjacent to it is not as prominent as in Ec. Layer III cells tend to be rounder and more darkly stained than in Ec. Layer IV is not discernible in Nissl preparations. The sublaminae of layer V are even less distinct than in Ec, and it is particularly difficult to see a clear layer Vc throughout much of the subdivision. Layer VI is less laminar than in Ec, perhaps because coronal sections through caudal portions of Ecl are cut obliquely.

In SMI-32 preparations, cell bodies of layer II neurons are moderately to heavily labeled and the highly stained dendrites of layer II neurons give this layer a bushy appearance as is observed in Ec. The darkly stained neurons observed in layer III are distributed throughout the superficial half of the layer. The density of moderately stained neurons with highly stained dendrites increases in layer V of Ecl, as compared to Ec. Layer V seems to be continuous with the darkly

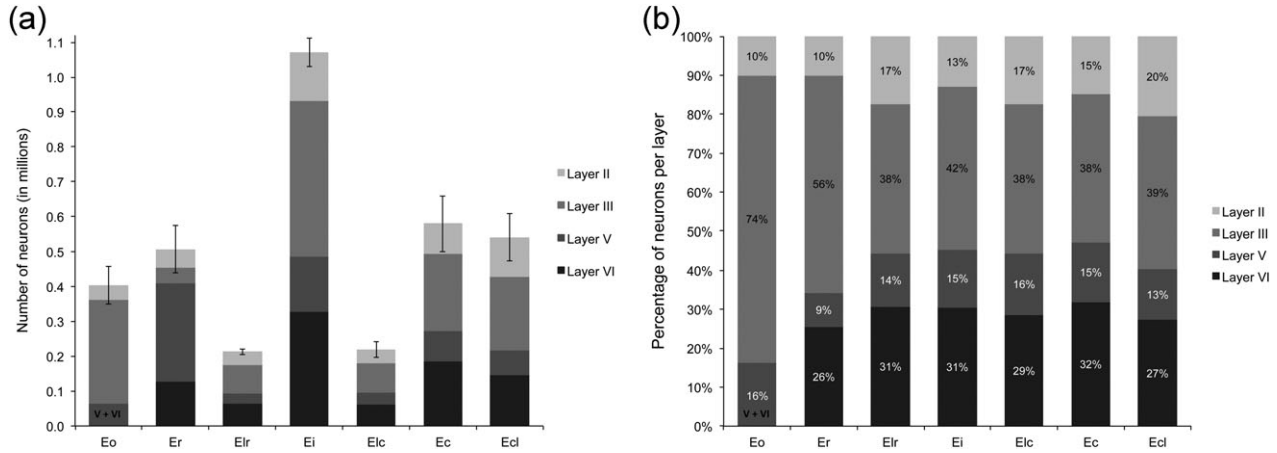

FIGURE 4 (a) Numbers of neurons in the different layers of the seven subdivisions of the rhesus monkey entorhinal cortex. (b) Percentage of neurons located in each layer, per subdivision. See also Table 2

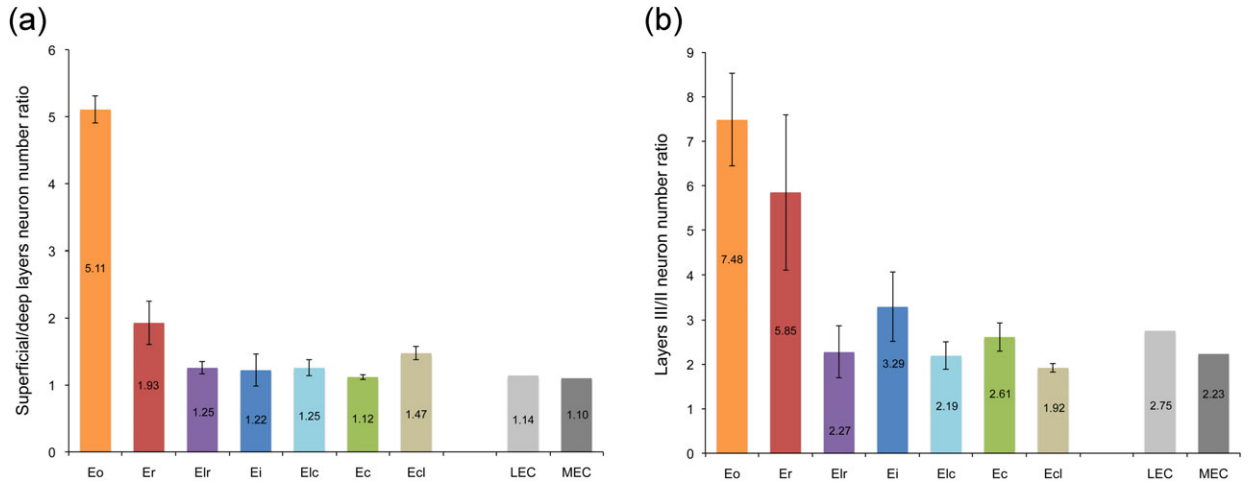

FIGURE 5 (a) Ratio of the number of neurons in the superficial layers (II and III) and the number of neurons in the deep layers (V and VI) in the seven subdivisions of the rhesus monkey entorhinal cortex. (b) Ratio of the number of neurons contained in layer III (projecting to CA1 and the subiculum) and the number of neurons contained in layer II (projecting to the dentate gyrus and CA3). Ratios in rat LEC and MEC calculated from the averages of the number of neurons reported in (Merrill, Chiba, & Tuszynski, 2001; Mulders, West, & Slomianka, 1997) for young adult rats

stained, deep layers of the parasubiculum and presubiculum. Layer VI contains a moderate density of moderately stained neurons with darkly stained dendrites.

3.4 | Stereological analyses

3.4.1 | Volumes of different layers and subdivisions

The volumes of the different layers of the seven subdivisions of the rhesus monkey entorhinal cortex are presented in Figure 3 and Table 2. Area Eo represents 11% of the entire volume of the entorhinal cortex, Er 15%, Elr 7%, Ei 28%, Elc 6%, Ec 17%, and Ecl 16%. Altogether, areas Eo, Er, and Elr constitute the rostral third of the volume of the entorhinal cortex; areas Ei + Elc constitute the intermediate third; and areas Ec and Ecl constitute the caudal third.

As one can observe on coronal sections, the relative volumetric development of individual layers varies between different subdivisions. Layer I of area Eo is very thin and represents only 7.5% of the volume of Eo. Layer I accounts for 9.2% of the volume of Er, but between 14.5% and 18.6% of the volume of all other subdivisions. Layer III represents the largest layer across the entorhinal cortex, but this is especially true in the most rostral subdivisions, Eo and Er, where the deep layers are significantly less developed. Layer III accounts for 67.1% of the volume of Eo, and 50.9% of the volume of Er, but between 33.0% and 37.2% of the volume of all other subdivisions. The relative volume of the deep layers, V and VI, is relatively stable across all the other subdivisions.

3.4.2 | Neuron numbers in different layers and subdivisions

The numbers of neurons in the different layers of the seven subdivisions of the rhesus monkey entorhinal cortex are presented in Figure 4 and Table 2. Consistent with the volumetric estimates, about 11% of all entorhinal neurons are located in area Eo, 14% in Er, 6% in Elr, 30% in Ei, 6% in Elc, 16% in Ec, and 15% in Elc. Neurons located in layer III, which contribute the direct entorhinal cortex projections to CA1 and the subiculum, represent almost half (46%) of all principal neurons found in the monkey entorhinal cortex. This percentage is significantly higher in the rostral areas Eo (74%) and Er (56%), but is

TABLE 3 Number of neurons in the different layers of the entorhinal cortex in rats and humans

	Layer II		Layer III		Layer V + VI		All layers	
	Mean	*SD*	Mean	*SD*	Mean	*SD*	Mean	*SD*
Rat MEC	**62,924**		**140,541**		**184,625**		**388,090**	
Mulders et al. (1997)	66,400	10,383	128,200	16,423	185,400	24,419	380,000	36,871
Merrill et al. (2001)	59,448	8,575	152,881	15,122	183,849	23,490	396,178	29,223
Rat LEC	**40,896**		**112,335**		**134,546**		**287,777**	
Mulders et al. (1997)	45,600	13,278	119,400	15,502	143,800	29,575	308,800	44,673
Merrill et al. (2001)	36,192	6,133	105,269	18,538	125,291	24,120	266,752	31,034
Rat EC	**103,820**		**252,875**		**319,170**		**675,865**	
Mulders et al. (1997)	112,000	22,327	247,600	22,843	329,200	53,844	688,800	76,594
Merrill et al. (2001)	95,640	10,543	258,150	23,294	309,140	33,668	663,000	46,000
Monkey EC	**499,784**	**64,505**	**1,621,012**	**102,823**	**1,411,615**	**145,832**	**3,532,411**	**252,997**
Human EC	**652,500**		**3,590,500**		**3,247,500**		**7,490,500**	
Gomez-Isla et al. (1996)	647,000	143,066	3,525,000	623,810	2,711,000	619,757	6,883,000	1,136,076
West and Slomianka (1998)	658,000	107,098	3,656,000	570,640	3,784,000	288,929	8,098,000	875,825

relatively stable and represents between 38% and 42% of the number of neurons in the remaining subdivisions. Neurons located in layer II, which contribute the entorhinal cortex projections to the dentate gyrus and CA3, represent only 10% of neurons in areas Eo and Er. This percentage varies between 13 and 21% in the other subdivisions.

In light of the variations in the number of neurons located in the different layers of the seven subdivisions of the rhesus monkey entorhinal cortex, it is interesting to consider the ratio between the number of neurons located in the superficial layers II and III, which originate the main feedforward projections toward the dentate gyrus and the hippocampus, and the number of neurons located in the deep layers V and VI, which represent the main recipient of the feedback projections originating in the hippocampus and the subiculum (Figure 5a). This ratio was greater in the rostral subdivisions (Eo and Er) than in all the other subdivisions ($F_{(6,18)}$ = 301.761, p < .001, η^2_p = .990). There were no differences between Ei, Elr, and Elc. Interestingly, the ratio in Ecl was lower than in Eo and Er, but overall higher than in the other subdivisions, in particular area Ec with which it is often associated.

Consistent with the poor development of the deep layers of area Eo, there are about five times more neurons in the superficial layers than in the deep layers in this subdivision. In area Er, there are about two times more neurons in the superficial layers than in the deep layers. This suggests that these rostral areas play a much larger role in relaying information to the dentate gyrus and the hippocampus than they do in receiving information that has been processed by the hippocampus. Despite some subtle variations between subdivisions, there are on average only about 25% more neurons in the superficial layers than in the deep layers in the other subdivisions of the entorhinal cortex. Interestingly, the ratios between the number of neurons in the superficial versus deep layers of the monkey entorhinal cortex are significantly higher than in the two main subdivisions of the rat entorhinal cortex (LEC-homologous to the primate rostral entorhinal cortex: 1.14; MEC-homologous to the primate caudal entorhinal cortex: 1.10; Table 3). These findings suggest differences in the degree of reciprocity of the connections between different subdivisions of the monkey entorhinal cortex and the rest of the hippocampal formation.

It is also interesting to consider the ratio between the number of neurons located in layer III, which originate the projections to CA1 and the subiculum, and the number of neurons located in layer II, which originate the projections to the dentate gyrus and CA3, in order to assess the relative importance of the direct and indirect projections to the hippocampus originating from different subdivisions of the entorhinal cortex (Figure 5b). This ratio was greater in the rostral subdivisions (Eo and Er) than in all the other subdivisions ($F_{(6,18)}$ = 29.042, p < .001, η^2_p = .906, Fisher Least Significant Difference, all p < .05). Note, moreover, that the difference between Er and Ei just failed to reach significance, whereas this ratio was higher in Ec than Ecl. In area Eo, there are about 7.5 times more neurons in layer III than in layer II. In area Er, there are about six times more neurons in layer III than in layer II. In area Ei, there are about three times more neurons in layer III than in layer II. Finally, there are between 2 and 2.5 times more neurons in layer III than in layer II in the remaining subdivisions of the rhesus monkey entorhinal cortex. These estimates reveal a clear rostrocaudal gradient, with a relatively greater development of layer III, as compared to layer II, in the rostral entorhinal cortex. Although less prominent, there is a similar pattern in the rat entorhinal cortex, with 2.75 times more neurons in layer III than in layer II in LEC, and only 2.23 times more neurons in layer III than in layer II in MEC.

3.4.3 | Neuronal soma size

In addition to the distinct patterns of connectivity described previously, and the differences in the relative number of neurons in the different layers of the seven subdivisions of the rhesus monkey entorhinal cortex shown here, we also found differences in the volume of neuronal somas between subdivisions (Table 2).

Layer II: The average soma volume of layer II neurons differed between subdivisions ($F_{(6,18)}$ = 43.751, p < .001, η^2_p = .936). Layer II neurons were smaller in area Eo than in all other subdivisions. Layer II neurons were also smaller in area Er than in more caudal subdivisions, but not area Elr (Eo < all other fields; Er < Ei, Elc, Ec, Ecl: all p < .05).

Layer III: Although the average soma volume of layer III neurons also differed between subdivisions ($F_{(6,18)}$ = 3.083, p = .030, η^2_p = .507), these differences were not as pronounced as for layer II neurons. Layer III neurons were smaller in Eo than in Ecl; they were larger in Ei than in Elc.

Layer V: The average soma volume of layer V neurons also differed between subdivisions ($F_{(6,18)}$ = 5.822, p = .002, η^2_p = .660). Layer V neurons were smaller in area Eo, as compared to all other areas, except for Ecl. Layer V neurons were larger in area Er than in areas Eo, Elr, Elc. Similarly, layer V neurons were larger in area Ei than in areas Eo and Ec.

Layer VI: The average volume of layer VI neurons also differed between subdivisions ($F_{(6,18)}$ = 4.256, p = .008, η^2_p = .587). Layer VI neurons were larger in Ei than in Elc, Ec, and Ecl. They were also larger in area Er than in area Elc. No other differences were statistically significant.

4 | DISCUSSION

4.1 | Comparison with previous studies in monkeys

The current study provides normative data on the volume, neuron number, and neuronal soma size in the different layers of the seven subdivisions of the adult rhesus monkey entorhinal cortex. To our knowledge, there are only two previous studies that provided partial analyses of neuron number and/or neuronal soma size in the rhesus monkey entorhinal cortex.

Gazzaley, Thakker, Hof, and Morrison (1997) reported a preserved number of entorhinal cortex layer II neurons in aged (24–29-year-old) macaque monkeys, as compared to young adult (7.5–12-year-old) and juvenile (1.2–2-year-old) monkeys. Gazzaley et al. subdivided the entorhinal cortex following the description by Van Hoesen and Pandya (1975). Their counts included the entire rostral and intermediate subdivisions, as well as the caudal subdivision that contained a visible lamina dissecans. As we have reported in our detailed description of the cytoarchitectonic organization of the rhesus monkey entorhinal cortex, the presence of a visible lamina dissecans by itself does not constitute a reliable criterion by which to delineate its different subdivisions. Moreover, in their study, Gazzaley and colleagues first cut the brains into 5–6-mm-thick blocks, prior to cutting coronal sections at 40 μm with a sliding microtome. This procedure necessarily leads to tissue loss with a resulting underestimation of total neuron numbers. Finally, the stereological parameters used to calculate neuron numbers, in particular the thickness of the processed sections and the height of the disector were not reported adequately, and detailed records of the study are no longer available (A. H. Gazzaley, J. H. Morrison and P. R. Hof, personal communication, May 31 and June 6, 2018). Given these uncertainties, it is difficult to compare the results in Gazzaley et al. (1997) with the current findings.

Merrill, Roberts, and Tuszynski (2000) also reported the conservation of neuron number and neuronal soma size in layers II, III, and V/VI in the intermediate division of the aged rhesus monkey entorhinal cortex. Their estimates correspond to about half the values we found for the intermediate division Ei in the current study. Inter-laboratory differences may be related to the calibration of the computer-aided analysis systems or other methodological differences that are difficult to identify (Altemus, Lavenex, Ishizuka, & Amaral, 2005). In their study, Merrill et al. cut the brains on a freezing microtome set at 40 μm and reported an average thickness of the Nissl-stained histological sections of about 21 μm. In our study, we cut the brains on a freezing microtome at 60 μm for the Nissl series, and measured an average thickness of Nissl-stained sections of 13.32 μm across all regions/layers. However, since the optical fractionator provides estimates of neuron numbers that are independent of volume measurements, and that the formula used to calculate neuron numbers includes the thickness sampling fraction, it is unclear how such differences in tissue processing may lead to differences in neuron numbers. We are confident regarding the measurement of the thickness of the sections used in the current study, since our computer-aided analysis system is equipped with a Focus Encoder providing 0.1 μm resolution measurements of the actual position of the microscope stage in the z axis, and does not rely on the predefined settings of the motorized stage. The average section thickness measured in the current study is similar to what we previously found during the completion of stereological studies of the rat and monkey amygdala, which have supported the reliability and generalizability of our normative data (Chareyron et al., 2011) and that were very close to those reported by other laboratories (Berdel, Morys, & Maciejewska, 1997; Carlo, Stefanacci, Semendeferi, & Stevens, 2010; Cooke, Stokas, & Woolley, 2007; Rubinow & Juraska, 2009). In our study, the disector height (5 μm) represented 37.5% of the averaged section thickness, the counting frame was 40 × 40 μm and we used different scan grids for individual layers (Table 1). In their study, Merrill and colleagues reported counting neurons in the middle 75% of total tissue thickness for each section, with the optical disector dimensions set at 50 μm^2 (which may have been 50 × 50 μm, M. Tuszynski, personal communication, June 1, 2018). However, there was no information about the scan grid size or the total number of neurons counted, which would enable us to recalculate the estimates of neuron numbers, and detailed records of the study are no longer available (D. A. Merrill and M. H. Tuszynski, personal communication, May 31 and June 1, 2018). Given these uncertainties, it is difficult to compare the results in Merrill et al. (2000) with the current findings.

4.2 | Interspecies comparisons

Previous comparisons of the structure of the entorhinal cortex in different species have emphasized either the conservation of the general functional organization of the entorhinal cortex across species (Insausti et al., 1997; Naumann et al., 2016; Witter et al., 2017), or the notable differences in the number, relative development and structural characteristics of different subdivisions of the entorhinal cortex between rats, monkeys, and humans (Amaral et al., 1987; Amaral & Lavenex, 2007; Insausti et al., 1995; Insausti et al., 1997). Here, we compare the number of neurons in the different layers of the rat, monkey, and human entorhinal cortex (Tables 3 and 4). As was the case for the comparison of our current findings with those of previous studies carried out in monkeys, it was difficult to find studies in rats and humans that used reliable, design-based stereological techniques

TABLE 4 Number of neurons in the different layers of the entorhinal cortex, in rats, monkeys and humans

	Rat[a]	Monkey[b]	Human[c]	M/R	H/R	H/M
II	103,820	499,784	652,500	4.81	6.28	1.31
III	252,875	1,621,012	3,590,500	6.41	14.20	2.21
V + VI	319,170	1,411,615	3,247,500	4.41	10.17	2.30
Total	675,865	3,532,411	7,490,500	5.23	11.08	2.12
(II + III)/(V + VI)	1.12	1.50	1.31			
III/II	2.44	3.24	5.50			

[a] Average data of studies reported in Table 3.
[b] Data from current study reported in Table 3.
[c] Average data of studies reported in Table 3.

combined with well-accepted delineations of layers and subdivisions of the entorhinal cortex. We considered two studies in rats, our current findings in monkeys, and two studies in humans, in order to compare the relative development and quantitative structural characteristics of the entorhinal cortex in different species.

4.2.1 | Rats

Mulders et al. (1997) estimated the number of neurons in the different layers of the lateral and medial entorhinal cortex of 30-day-old female Wistar rats. Merrill et al. (2001) estimated the number of neurons of the lateral and medial entorhinal cortex in 2-month-old female Fischer 344 rats (they also reported data on 21-month-old rats, which we did not include in Table 3). The results of these two studies, carried out in two independent laboratories, provide consistent estimates.

4.2.2 | Humans

Gomez-Isla et al. (1996) estimated the number of neurons in the entire entorhinal cortex of nondemented men and women between 60 and 89 years of age. Note that the definitions of the layers reported in their study differed from that used in other studies, so we adapted the presentation of their results to match the definitions used in the other studies. West and Slomianka (1998) estimated the number of neurons in the entire entorhinal cortex of 19–58-year-old men. The results of these two studies, carried out in two independent laboratories, provided consistent estimates of the number of neurons in layers II and III. In contrast, there was a relatively larger difference between studies in their estimates of the number of neurons in layers V and VI. Nevertheless, these estimates can be considered sufficiently reliable to perform interspecies comparisons of the relative number of neurons in different layers of the entorhinal cortex.

Since the previous studies in rats or humans did not report the number of neurons in the different subdivisions of the entorhinal cortex based on the nomenclature defined by Amaral and colleagues for monkeys (Amaral et al., 1987), Insausti and colleagues for humans (Insausti et al., 1995) and rats (Insausti et al., 1997), we limit our species comparisons to the number of neurons in the entire entorhinal cortex (Tables 3 and 4). We consider layer II neurons as the origin of the entorhinal cortex projections to the dentate gyrus and CA3; layer III neurons as the origin of the entorhinal cortex projections to CA1 and the subiculum; and layer V and VI neurons as the main layers of the entorhinal cortex receiving the hippocampal output projections originating in CA1 and the subiculum.

As compared to rats, the total number of neurons in the entorhinal cortex is about 5 times greater in monkeys, and 11 times greater in humans (and thus about 2 times greater in humans than in monkeys). In layer II, there are 4.8 times more neurons in monkeys than in rats, 6.3 times more neurons in humans than in rats, and 1.3 times more neurons in humans than in monkeys. In layer III, there are 6.4 times more neurons in monkeys than in rats, 14.2 times more neurons in humans than in rats, and 2.2 times more neurons in humans than in monkeys. In layer V and VI, there are 4.4 times more neurons in monkeys than in rats, 10.2 times more neurons in humans than in rats, and 2.3 times more neurons in humans than in monkeys. These findings suggest that the relative importance of the different inputs to the hippocampal formation (via entorhinal cortex layer II and layer III neurons, respectively) may vary between species. Specifically, the ratio between the number of neurons in layer III and the number of neurons in layer II is 2.4 in rats, 3.2 in monkeys, and 5.5 in humans. Thus, the direct entorhinal cortex projection to CA1 appears greater in primates than in rats, and appears further developed in humans as compared to monkeys. Interestingly, the ratio between the number of neurons in the superficial layers and the number of neurons in the deep layers appears greater in monkeys and humans than in rats (Table 4). This pattern may be related to the greater development of the neocortical areas projecting to the superficial layers of the entorhinal cortex in primates. This finding is similar to what we observed previously for different amygdala nuclei (Chareyron et al., 2011), and consistent with the theory that brain structures with major anatomical and functional links evolve together independently of evolutionary changes in other unrelated structures (Barton & Harvey, 2000).

In sum, our detailed analysis of neuron numbers and neuronal soma size in the different layers of distinct subdivisions of the monkey entorhinal cortex confirms that the entorhinal cortex is a very heterogeneous structure and that interspecies comparisons should take into account these important regional differences. Our data further suggest that, despite being consistent with functional studies in rodents and connectional studies in monkeys, a simple parcellation of the primate entorhinal cortex into two major functional subregions, homologous to the rodent LEC and MEC (Maass et al., 2015; Reagh et al., 2018; Schroder et al., 2015), may be too simplistic to capture the full complexity of information processing carried out by the human entorhinal cortex. The development of comprehensive high-resolution atlases of the human brain based on the microscopic evaluation of histological sections (Ding et al., 2017) may contribute to reach that goal. We will now focus on our findings in monkeys, in order to discuss the

possible functional implications of the relative development of the different layers in the different subdivisions of the primate entorhinal cortex.

4.3 | Different entorhinal-hipppocampal circuits

As was previously recognized from connectional studies and cytoarchitectural descriptions, the quantitative estimates of neuron numbers and descriptions of morphological characteristics reported here emphasize the heterogeneity of the entorhinal cortex, even within a single species.

4.3.1 | Area Eo

Although area Eo can be distinguished based on several cytoarchitectonic features, it was named based on the fact that in monkeys it is the only region of the entorhinal cortex that receives a direct input from the olfactory bulb. This input is unique in being unimodal and coming from a very early stage of olfactory sensory processing. It is thus interesting to consider that there are five times more neurons in the superficial layers than in the deep layers of Eo, and that there are about 7.5 times more neurons in layer III than in layer II. One can thus surmise that, in primates, the olfactory input from the olfactory bulb is mostly transmitted via direct projections from layer III neurons to the rostral portion of CA1 (Insausti, Marcos, Arroyo-Jimenez, Blaizot, & Martinez-Marcos, 2002). In turn, hippocampal output may have a rather limited influence on information processing taking place in area Eo.

4.3.2 | Areas Er and Elr

Area Er receives the majority of its cortical afferents from the perirhinal cortex, which projects mainly to the rostral two-thirds of the entorhinal cortex (areas Eo, Er, Elr, Elc, Ei) (Suzuki & Amaral, 1994b). Interestingly, the degree of reciprocity of the projections between the perirhinal cortex and the entorhinal cortex appears to vary depending on the region of the entorhinal cortex examined. Projections between the perirhinal cortex and the lateral portions of the entorhinal cortex (including area Elr) are more reciprocal than the projections with the medial portions of the entorhinal cortex. Projections from cells in layer III of the perirhinal cortex terminate most strongly in layers I, II and the superficial portion of layer III of the entorhinal cortex. Consistent with the fact that the projection from the entorhinal cortex to the perirhinal cortex originates mainly from cells situated in layer V (with only very few cells located in layers VI and III), the ratio between the number of neurons in the superficial layers and the number of neurons in the deep layers is higher for area Er than for area Elr. These findings are consistent with the observation that the connections between the perirhinal cortex and area Elr are more reciprocal than with area Er (an area sending relatively fewer feedback projections to the perirhinal cortex) (Suzuki & Amaral, 1994b).

4.3.3 | Area Ei and Elc

Area Ei is defined as the intermediate subdivision of the entorhinal cortex and shares some structural and functional characteristics with both the rostral and caudal subdivisions of the entorhinal cortex. Ei receives prominent projections from the perirhinal cortex, which reach the rostral two-thirds of the entorhinal cortex, and projections from the parahippocampal cortex, which reach the caudal two-thirds of the entorhinal cortex. Interestingly, the ratio between the number of neurons in the superficial layers and the number of neurons in the deep layers is lower in areas Ei and Elc than in rostral areas Er and Eo, and is similar to that found in area Elr and caudal areas Ec and Ecl. It thus seems consistent that highly reciprocal projections between the parahippocampal cortex and the entorhinal cortex are associated with a higher number of neurons in layer V in the subdivisions of the entorhinal cortex that originate the majority of these projections (Suzuki & Amaral, 1994b).

4.3.4 | Areas Ec and Ecl

Areas Ec and Ecl receive prominent projections from layer III neurons in the parahippocampal cortex, which terminate most strongly in layers I, II and III. In addition, areas Ec and Ecl are characterized by a direct projection from the presubiculum to layer III. Interestingly, this connection is also a defining feature of the rat MEC, which is particularly involved in spatial information processing (Knierim et al., 2014; Witter & Moser, 2006). The connections between these two areas and the parahippocampal cortex are highly reciprocal (Suzuki & Amaral, 1994b), which appears to be also reflected in the lower ratio between the number of neurons in the superficial layers and the number of neurons in the deep layers, as compared to the rostral subdivisions Er and Eo. However, this ratio was slightly higher in Ecl than in Ec, whereas the ratio between the number of neurons in layer III (projecting to CA1 and the subiculum) and the number of neurons in layer II (projecting to the dentate gyrus and CA3) was slightly higher in Ec than Ecl. Thus, although these two areas share some common connectional characteristics (Amaral & Lavenex, 2007; Suzuki & Amaral, 1994b) and functional properties (Chareyron et al., 2017), they nevertheless differ in the relative numbers of neurons contributing to different hippocampal circuits. Although areas Ec and Ecl represent approximately the same percentage of the volume of the entire entorhinal cortex, and contain about the same percentage of all the neurons in the entire entorhinal cortex, area Ec contains a proportionally larger number of neurons in layer II, which are known to contribute projections to the dentate gyrus and CA3. The functional consequences of such differences remain to be determined.

5 | CONCLUSION

This study provides normative data on the volume, neuron number and neuronal soma size in the different layers of the seven subdivisions of the rhesus monkey entorhinal cortex. These data corroborate the important structural differences between different subdivisions of the monkey entorhinal cortex. In particular, differences in the number of neurons contributing to distinct afferent and efferent hippocampal pathways suggest not only that different types of information may be more or less segregated between caudal and rostral subdivisions, but also, and perhaps most importantly, that the nature of the interaction between the entorhinal cortex and the rest of the hippocampal formation may vary between different subdivisions. Finally, these data provide fundamental information on the number of functional units that

comprise the entorhinal-hippocampal circuits and should be considered in order to build more realistic models of the human medial temporal lobe memory system.

ACKNOWLEDGMENTS

This work was supported by Swiss National Science Foundation Grants P00A-106701, PP00P3-124536, and 310030_143956; United States National Institutes of Health Grants MH041479 and NS16980; and California National Primate Research Center Grant OD011107.

ORCID

Olivia Piguet https://orcid.org/0000-0001-8398-0232
Loïc J. Chareyron https://orcid.org/0000-0003-2043-3711
Pamela Banta Lavenex https://orcid.org/0000-0001-8868-2912
David G. Amaral https://orcid.org/0000-0003-1525-8744
Pierre Lavenex http://orcid.org/0000-0002-9278-1312

REFERENCES

Altemus, K. L., Lavenex, P., Ishizuka, N., & Amaral, D. G. (2005). Morphological characteristics and electrophysiological properties of CA1 pyramidal neurons in macaque monkeys. *Neuroscience*, *136*(3), 741–756. https://doi.org/10.1016/j.neuroscience.2005.07.001

Amaral, D. G., Insausti, R., & Cowan, W. M. (1987). The entorhinal cortex of the monkey: I. Cytoarchitectonic organization. *The Journal of Comparative Neurology*, *264*(3), 326–355.

Amaral, D. G., Kondo, H., & Lavenex, P. (2014). An analysis of entorhinal cortex projections to the dentate gyrus, hippocampus, and subiculum of the neonatal macaque monkey. *The Journal of Comparative Neurology*, *522*(7), 1485–1505. https://doi.org/10.1002/cne.23469

Amaral, D. G., & Lavenex, P. (2007). Hippocampal neuroanatomy. In P. Andersen, R. G. M. Morris, D. G. Amaral, T. V. Bliss, & J. O'Keefe (Eds.), *The hippocampus book* (pp. 37–114). Oxford: Oxford University Press.

Barton, R. A., & Harvey, P. H. (2000). Mosaic evolution of brain structure in mammals. *Nature*, *405*(6790), 1055–1058. https://doi.org/10.1038/35016580

Berdel, B., Morys, J., & Maciejewska, B. (1997). Neuronal changes in the basolateral complex during development of the amygdala of the rat. *International Journal of Developmental Neuroscience*, *15*(6), 755–765.

Carlo, C. N., Stefanacci, L., Semendeferi, K., & Stevens, C. F. (2010). Comparative analyses of the neuron numbers and volumes of the amygdaloid complex in old and new world primates. *The Journal of Comparative Neurology*, *518*(8), 1176–1198. https://doi.org/10.1002/cne.22264

Chareyron, L. J., Banta Lavenex, P., Amaral, D. G., & Lavenex, P. (2011). Stereological analysis of the rat and monkey amygdala. *The Journal of Comparative Neurology*, *519*(16), 3218–3239. https://doi.org/10.1002/cne.22677

Chareyron, L. J., Lavenex, P. B., Amaral, D. G., & Lavenex, P. (2012). Postnatal development of the amygdala: A stereological study in macaque monkeys. *The Journal of Comparative Neurology*, *520*(9), 1965–1984. https://doi.org/10.1002/cne.23023

Chareyron, L. J., Lavenex, P. B., Amaral, D. G., & Lavenex, P. (2017). Functional organization of the medial temporal lobe memory system following neonatal hippocampal lesion in rhesus monkeys. *Brain Structure & Function*, *222*, 3899–3914. https://doi.org/10.1007/s00429-017-1441-z

Chrobak, J. J., & Amaral, D. G. (2007). Entorhinal cortex of the monkey: VII. Intrinsic connections. *The Journal of Comparative Neurology*, *500*(4), 612–633. https://doi.org/10.1002/cne.21200

Cooke, B. M., Stokas, M. R., & Woolley, C. S. (2007). Morphological sex differences and laterality in the prepubertal medial amygdala. *The Journal of Comparative Neurology*, *501*(6), 904–915. https://doi.org/10.1002/cne.21281

de Haas Ratzliff, A., & Soltesz, I. (2000). Differential expression of cytoskeletal proteins in the dendrites of parvalbumin-positive interneurons versus granule cells in the adult rat dentate gyrus. *Hippocampus*, *10*(2), 162–168.

Ding, S. L., Royall, J. J., Sunkin, S. M., Ng, L., Facer, B. A., Lesnar, P., … Lein, E. S. (2017). Comprehensive cellular-resolution atlas of the adult human brain. *The Journal of Comparative Neurology*, *525*(2), 407. https://doi.org/10.1002/cne.24130

Fitting, S., Booze, R. M., Hasselrot, U., & Mactutus, C. F. (2008). Differential long-term neurotoxicity of HIV-1 proteins in the rat hippocampal formation: A design-based stereological study. *Hippocampus*, *18*(2), 135–147. https://doi.org/10.1002/hipo.20376

Gazzaley, A. H., Thakker, M. M., Hof, P. R., & Morrison, J. H. (1997). Preserved number of entorhinal cortex layer II neurons in aged macaque monkeys. *Neurobiology of Aging*, *18*(5), 549–553.

Goldstein, M. E., Sternberger, L. A., & Sternberger, N. H. (1987). Varying degrees of phosphorylation determine microheterogeneity of the heavy neurofilament polypeptide (NF-H). *Journal of Neuroimmunology*, *14*, 135–148.

Gomez-Isla, T., Price, J. L., McKeel, D. W., Jr., Morris, J. C., Growdon, J. H., & Hyman, B. T. (1996). Profound loss of layer II entorhinal cortex neurons occurs in very mild Alzheimer's disease. *The Journal of Neuroscience*, *16*(14), 4491–4500.

Grady, M. S., Charleston, J. S., Maris, D., Witgen, B. M., & Lifshitz, J. (2003). Neuronal and glial cell number in the hippocampus after experimental traumatic brain injury: Analysis by stereological estimation. *Journal of Neurotrauma*, *20*(10), 929–941. https://doi.org/10.1089/089771503770195786

Gundersen, H. J. (1988). The nucleator. *Journal of Microscopy*, *151*(Pt 1), 3–21.

Hamidi, M., Drevets, W. C., & Price, J. L. (2004). Glial reduction in amygdala in major depressive disorder is due to oligodendrocytes. *Biological Psychiatry*, *55*(6), 563–569. https://doi.org/10.1016/j.biopsych.2003.11.006

Hof, P. R., & Morrison, J. H. (1995). Neurofilament protein defines regional patterns of cortical organization in the macaque monkey visual system: A quantitative immunohistochemical analysis. *The Journal of Comparative Neurology*, *352*(2), 161–186. https://doi.org/10.1002/cne.903520202

Hornung, J. P., & Riederer, B. M. (1999). Medium-sized neurofilament protein related to maturation of a subset of cortical neurons. *The Journal of Comparative Neurology*, *414*(3), 348–360. https://doi.org/10.1002/(SICI)1096-9861(19991122)414:3<348::AID-CNE5>3.0.CO;2-H

Insausti, R., Amaral, D. G., & Cowan, W. M. (1987). The entorhinal cortex of the monkey: II. Cortical afferents. *The Journal of Comparative Neurology*, *264*(3), 356–395.

Insausti, R., Herrero, M. T., & Witter, M. P. (1997). Entorhinal cortex of the rat: Cytoarchitectonic subdivisions and the origin and distribution of cortical efferents. *Hippocampus*, *7*(2), 146–183. https://doi.org/10.1002/(SICI)1098-1063(1997)7:2<146::AID-HIPO4>3.0.CO;2-L

Insausti, R., Marcos, P., Arroyo-Jimenez, M. M., Blaizot, X., & Martinez-Marcos, A. (2002). Comparative aspects of the olfactory portion of the entorhinal cortex and its projection to the hippocampus in rodents, nonhuman primates, and the human brain. *Brain Research Bulletin*, *57*(3–4), 557–560.

Insausti, R., Tunon, T., Sobreviela, T., Insausti, A. M., & Gonzalo, L. M. (1995). The human entorhinal cortex: A cytoarchitectonic analysis. *The Journal of Comparative Neurology*, *355*(2), 171–198. https://doi.org/10.1002/cne.903550203

Jabes, A., Lavenex, P. B., Amaral, D. G., & Lavenex, P. (2010). Quantitative analysis of postnatal neurogenesis and neuron number in the macaque monkey dentate gyrus. *The European Journal of Neuroscience*, *31*(2), 273–285. https://doi.org/10.1111/j.1460-9568.2009.07061.x

Jabes, A., Lavenex, P. B., Amaral, D. G., & Lavenex, P. (2011). Postnatal development of the hippocampal formation: A stereological study in macaque monkeys. *The Journal of Comparative Neurology*, *519*(6), 1051–1070. https://doi.org/10.1002/cne.22549

Knierim, J. J., Neunuebel, J. P., & Deshmukh, S. S. (2014). Functional correlates of the lateral and medial entorhinal cortex: Objects, path integration and local-global reference frames. *Philosophical Transactions of the Royal Society of London, Series B, Biological Sciences*, *369*(1635), 20130369. https://doi.org/10.1098/rstb.2013.0369

Lavenex, P., & Amaral, D. G. (2000). Hippocampal-neocortical interaction: A hierarchy of associativity. *Hippocampus*, *10*(4), 420–430. https://doi.org/10.1002/1098-1063(2000)10:4<420::AID-HIPO8>3.0.CO;2-5

Lavenex, P., Lavenex, P. B., & Amaral, D. G. (2004). Nonphosphorylated high-molecular-weight neurofilament expression suggests early maturation of the monkey subiculum. *Hippocampus*, *14*(7), 797–801. https://doi.org/10.1002/hipo.20028

Lavenex, P., Lavenex, P. B., Bennett, J. L., & Amaral, D. G. (2009). Postmortem changes in the neuroanatomical characteristics of the primate brain: Hippocampal formation. *The Journal of Comparative Neurology*, *512*(1), 27–51. https://doi.org/10.1002/cne.21906

Maass, A., Berron, D., Libby, L. A., Ranganath, C., & Duzel, E. (2015). Functional subregions of the human entorhinal cortex. *eLife*, *4*. https://doi.org/10.7554/eLife.06426

Merrill, D. A., Chiba, A. A., & Tuszynski, M. H. (2001). Conservation of neuronal number and size in the entorhinal cortex of behaviorally characterized aged rats. *The Journal of Comparative Neurology*, *438*(4), 445–456.

Merrill, D. A., Roberts, J. A., & Tuszynski, M. H. (2000). Conservation of neuron number and size in entorhinal cortex layers II, III, and V/VI of aged primates. *The Journal of Comparative Neurology*, *422*(3), 396–401.

Morris, J. A., Jordan, C. L., & Breedlove, S. M. (2008). Sexual dimorphism in neuronal number of the posterodorsal medial amygdala is independent of circulating androgens and regional volume in adult rats. *The Journal of Comparative Neurology*, *506*(5), 851–859. https://doi.org/10.1002/cne.21536

Mulders, W. H., West, M. J., & Slomianka, L. (1997). Neuron numbers in the presubiculum, parasubiculum, and entorhinal area of the rat. *The Journal of Comparative Neurology*, *385*(1), 83–94.

Naumann, R. K., Ray, S., Prokop, S., Las, L., Heppner, F. L., & Brecht, M. (2016). Conserved size and periodicity of pyramidal patches in layer 2 of medial/caudal entorhinal cortex. *The Journal of Comparative Neurology*, *524*(4), 783–806. https://doi.org/10.1002/cne.23865

Palackal, T., Neuringer, M., & Sturman, J. (1993). Laminar analysis of the number of neurons, astrocytes, oligodendrocytes and microglia in the visual cortex (area 17) of 6- and 12-month-old rhesus monkeys fed a human infant soy-protein formula with or without taurine supplementation from birth. *Developmental Neuroscience*, *15*(1), 54–67. https://doi.org/10.1159/000111317

Pitkänen, A., Kelly, J. L., & Amaral, D. G. (2002). Projections from the lateral, basal, and accessory basal nuclei of the amygdala to the entorhinal cortex in the macaque monkey. *Hippocampus*, *12*(2), 186–205.

Reagh, Z. M., Noche, J. A., Tustison, N. J., Delisle, D., Murray, E. A., & Yassa, M. A. (2018). Functional imbalance of anterolateral entorhinal cortex and hippocampal dentate/CA3 underlies age-related object pattern separation deficits. *Neuron*, *97*(5), 1187–1198 e1184. https://doi.org/10.1016/j.neuron.2018.01.039

Rubinow, M. J., & Juraska, J. M. (2009). Neuron and glia numbers in the basolateral nucleus of the amygdala from preweaning through old age in male and female rats: A stereological study. *The Journal of Comparative Neurology*, *512*(6), 717–725. https://doi.org/10.1002/cne.21924

Schroder, T. N., Haak, K. V., Jimenez, N. I. Z., Beckmann, C. F., & Doeller, C. F. (2015). Functional topography of the human entorhinal cortex. *eLife*, *4*. https://doi.org/10.7554/eLife.06738

Siegel, S. J., Ginsberg, S. D., Hof, P. R., Foote, S. L., Young, W. G., Kraemer, G. W., … Morrison, J. H. (1993). Effects of social deprivation in prepubescent rhesus monkeys: Immunohistochemical analysis of the neurofilament protein triplet in the hippocampal formation. *Brain Research*, *619*(1–2), 299–305 0006-8993(93)91624-2

Sternberger, L. A., & Sternberger, N. H. (1983). Monoclonal antibodies distinguish phosphorylated and nonphosphorylated forms of neurofilaments in situ. *Proceedings of the National Academy of Sciences of the United States of America*, *80*(19), 6126–6130.

Suzuki, W. A., & Amaral, D. G. (1994a). Perirhinal and parahippocampal cortices of the macaque monkey: Cortical afferents. *The Journal of Comparative Neurology*, *350*, 497–533.

Suzuki, W. A., & Amaral, D. G. (1994b). Topographic organization of the reciprocal connections between the monkey entorhinal cortex and the perirhinal and parahippocampal cortices. *Journal of Neuroscience*, *14*(3), 1856–1877.

Van Hoesen, G. W., & Pandya, D. N. (1975). Some connections of the entorhinal (area 28) and perirhinal (area 35) cortices of the rhesus monkey. I. Temporal lobe afferents. *Brain Research*, *95*(1), 1–24.

van Strien, N. M., Cappaert, N. L., & Witter, M. P. (2009). The anatomy of memory: An interactive overview of the parahippocampal-hippocampal network. *Nature Reviews Neuroscience*, *10*(4), 272–282. https://doi.org/10.1038/nrn2614

West, M. J., & Slomianka, L. (1998). Total number of neurons in the layers of the human entorhinal cortex. *Hippocampus*, *8*(1), 69–82 8: 426 corrigendum. https://doi.org/10.1002/(SICI)1098-1063(1998)8:1<69::AID-HIPO7>3.0.CO;2–2

West, M. J., Slomianka, L., & Gundersen, H. J. (1991). Unbiased stereological estimation of the total number of neurons in thesubdivisions of the rat hippocampus using the optical fractionator. *The Anatomical Record*, *231*(4), 482–497.

Witter, M. P., & Amaral, D. G. (1991). Entorhinal cortex of the monkey: V. Projections to the dentate gyrus, hippocampus, and subicular complex. *The Journal of Comparative Neurology*, *307*(3), 437–459.

Witter, M. P., Doan, T. P., Jacobsen, B., Nilssen, E. S., & Ohara, S. (2017). Architecture of the entorhinal cortex: A review of entorhinal anatomy in rodents with some comparative perspective. *Frontiers in Systems Neuroscience*, *11*. https://doi.org/10.3389/fnsys.2017.00046

Witter, M. P., & Moser, E. I. (2006). Spatial representation and the architecture of the entorhinal cortex. *Trends in Neurosciences*, *29*(12), 671–678. https://doi.org/10.1016/j.tins.2006.10.003

Witter, M. P., Van Hoesen, G. W., & Amaral, D. G. (1989). Topographical organization of the entorhinal projection to the dentate gyrus of the monkey. *Journal of Neuroscience*, *9*(1), 216–228.

How to cite this article: Piguet O, Chareyron LJ, Banta Lavenex P, Amaral DG, Lavenex P. Stereological analysis of the rhesus monkey entorhinal cortex. *J Comp Neurol*. 2018;526: 2115–2132. https://doi.org/10.1002/cne.24496

Received: 22 December 2019 | Revised: 26 February 2020 | Accepted: 28 February 2020

DOI: 10.1002/cne.24897

RESEARCH ARTICLE

JCN RESEARCH IN SYSTEMS NEUROSCIENCE THE JOURNAL OF COMPARATIVE NEUROLOGY WILEY

Postnatal development of the entorhinal cortex: A stereological study in macaque monkeys

Olivia Piguet[1] | Loïc J Chareyron[2] | Pamela Banta Lavenex[1,3] | David G Amaral[4,5] | Pierre Lavenex[1,2]

[1]Laboratory of Brain and Cognitive Development, Institute of Psychology, University of Lausanne, Lausanne

[2]Department of Medicine, University of Fribourg, Fribourg

[3]Faculty of Psychology, Swiss Distance University, Brig

[4]Department of Psychiatry and Behavioral Sciences, MIND Institute, University of California, Davis, California

[5]California National Primate Research Center, University of California, Davis, California

Correspondence
Pierre Lavenex, Laboratory of Brain and Cognitive Development, Institute of Psychology, University of Lausanne, 1015 Lausanne, Switzerland.
Email: pierre.lavenex@unil.ch

Funding information
California National Primate Research Center, Grant/Award Number: OD011107; National Institutes of Health, Grant/Award Numbers: MH041479, NS16980; Schweizerischer Nationalfonds zur Förderung der Wissenschaftlichen Forschung, Grant/Award Numbers: 310030_143956, P00A-106701, PP00P3-124536

Peer Review
The peer review history for this article is available at https://publons.com/publon/10.1002/cne.24897.

Abstract

The entorhinal cortex is the main gateway for interactions between the neocortex and the hippocampus. Distinct regions, layers, and cells of the hippocampal formation exhibit different profiles of structural and molecular maturation during postnatal development. Here, we provide estimates of neuron number, neuronal soma size, and volume of the different layers and subdivisions of the monkey entorhinal cortex (Eo, Er, Elr, Ei, Elc, Ec, Ecl) during postnatal development. We found different developmental changes in neuronal soma size and volume of distinct layers in different subdivisions, but no changes in neuron number. Layers I and II developed early in most subdivisions. Layer III exhibited early maturation in Ec and Ecl, a two-step/early maturation in Ei and a late maturation in Er. Layers V and VI exhibited an early maturation in Ec and Ecl, a two-step and early maturation in Ei, and a late maturation in Er. Neuronal soma size increased transiently at 6 months of age and decreased thereafter to reach adult size, except in Layer II of Ei, and Layers II and III of Ec and Ecl. These findings support the theory that different hippocampal circuits exhibit distinct developmental profiles, which may subserve the emergence of different hippocampus-dependent memory processes. We discuss how the early maturation of the caudal entorhinal cortex may contribute to path integration and basic allocentric spatial processing, whereas the late maturation of the rostral entorhinal cortex may contribute to the increased precision of allocentric spatial representations and the temporal integration of individual items into episodic memories.

KEYWORDS

allocentric spatial memory, episodic memory, hippocampal formation, infantile amnesia, RRID:SCR_000696, California National Primate Research Center Analytical and Resource Core, RRID:SCR_002526, Stereo Investigator, RRID:SCR_002865, SPSS, RRID:SCR_014199, Adobe Photoshop, *Macaca mulatta*, medial temporal lobe, object memory, path integration

1 | INTRODUCTION

The entorhinal cortex constitutes the main interface for bidirectional interactions between the neocortex and the hippocampal formation (i.e., which includes the dentate gyrus, hippocampus proper [CA3, CA2, CA1], subiculum, presubiculum, parasubiculum, and entorhinal cortex) in support of spatial and episodic memory functions (Amaral & Lavenex, 2007; Lavenex & Amaral, 2000; Witter, Doan, Jacobsen, Nilssen, & Ohara, 2017). Previous research has shown that distinct regions, layers and cells of the monkey hippocampal formation exhibit different profiles of structural and molecular changes during early postnatal development (Favre, Banta Lavenex, & Lavenex,

2012a, 2012b; Jabès, Banta Lavenex, Amaral, & Lavenex, 2010, 2011; Lavenex, Banta Lavenex, & Amaral, 2004, 2007; Lavenex, Banta Lavenex, & Favre, 2014). The protracted period of neuron addition and maturation in the dentate gyrus is accompanied by the late maturation of specific layers and structures in hippocampal regions that are located downstream from the dentate gyrus, in particular CA3. In contrast, distinct layers of hippocampal regions that receive direct projections from the entorhinal cortex, in particular CA1, exhibit a comparatively earlier maturation. The subiculum, presubiculum, parasubiculum, and CA2, which are highly interconnected with subcortical structures, mature even earlier. Together with studies of the development of human spatial memory (Ribordy, Jabès, Banta Lavenex, & Lavenex, 2013; Ribordy Lambert, Lavenex, & Banta Lavenex, 2015, 2016), these findings suggested that the differential maturation of distinct hippocampal circuits might underlie the emergence of different hippocampus-dependent memory processes (Lavenex & Banta Lavenex, 2013). This theory was based on the emerging principle that specific types of information processing are subserved by different neuronal circuits within the medial temporal lobe (Kesner, Lee, & Gilbert, 2004; Kesner & Rolls, 2015; Knierim & Neunuebel, 2016; Knierim, Neunuebel, & Deshmukh, 2014; Witter & Moser, 2006). To date, however, the developmental profiles of the different layers of the seven subdivisions of the monkey entorhinal cortex have yet to be determined, information that is critical to more fully understand the functional maturation of this memory system.

1.1 | Organization of the entorhinal cortex

The monkey entorhinal cortex comprises seven subdivisions (Amaral, Insausti, & Cowan, 1987; Piguet, Chareyron, Banta Lavenex, Amaral, & Lavenex, 2018): Eo, the olfactory subdivision; Er, the rostral subdivision; El, the lateral subdivision, which comprises the lateral rostral (Elr) and lateral caudal (Elc) subdivisions; Ei, the intermediate subdivision; Ec, the caudal subdivision; and Ecl, the caudal limiting subdivision. A simplified description of the connectivity of the entorhinal cortex indicates that its superficial Layers II and III represent the main entryways for much of the cortical information to be processed by the hippocampal formation, although the deep Layers V and VI also contribute minor projections to the dentate gyrus and the hippocampus (Witter, Van Hoesen, & Amaral, 1989). In contrast, its deep layers are the main recipients of projections from the CA1 region of the hippocampus and the subiculum, and provide the main conduit by which information is sent back to the neocortex. In monkeys, the perirhinal and parahippocampal cortices provide about two-thirds of the cortical projections reaching the entorhinal cortex, but these projections are preferentially directed toward different subdivisions (Suzuki & Amaral, 1994). The projections from the perirhinal cortex terminate predominantly in the rostral two-thirds of the entorhinal cortex, in particular Eo, Er, Elr, Ei, and Elc. The projections from the parahippocampal cortex, in contrast, terminate predominantly in the caudal two-thirds of the entorhinal cortex, in particular Ei, Ec, and Ecl. Other cortical projections to the entorhinal cortex originate in the temporal lobes, frontal cortex, insula, cingulate and retrosplenial cortices, and terminate preferentially in different subdivisions (Insausti & Amaral, 2008; Insausti, Amaral, & Cowan, 1987). Projections from the insula, the orbitofrontal cortex, and the anterior cingulate cortex are directed predominantly toward rostral areas Eo, Er, Elr, and the rostral part of Ei, whereas projections from the retrosplenial cortex and the superior temporal gyrus are directed predominantly toward caudal areas Ec and Ecl, and the caudal part of Ei. Projections from the amygdala are directed toward the rostral subdivisions of the entorhinal cortex, including Eo, Er, Elr, and the rostral parts of Ei and Elc, with essentially no amygdala projections to the caudal areas Ec and Ecl (Pitkänen, Kelly, & Amaral, 2002).

The entorhinal cortex projections to the dentate gyrus and the hippocampus also exhibit clear patterns of laminar and topographical organization, which suggest distinct functional circuits (Amaral, Kondo, & Lavenex, 2014; Witter et al., 1989; Witter & Amaral, 1991). Entorhinal cortex projections to the dentate gyrus, CA3, and CA2 originate mainly from Layer II neurons, and to a much lesser extent from Layer VI neurons. In contrast, projections to CA1 and the subiculum originate mainly from Layer III neurons, and to a much lesser extent from Layer V neurons. The dentate gyrus and CA3 do not project back to the entorhinal cortex (Amaral & Lavenex, 2007; Lavenex & Amaral, 2000). In contrast, CA1 and the subiculum project to the deep layers of the entorhinal cortex, following a topographical organization that reciprocates the entorhinal cortex projections to these regions (Amaral & Lavenex, 2007; Lavenex & Amaral, 2000). Another characteristic of the connectivity of the entorhinal cortex is the direct projection from the presubiculum to Layer III of the caudal entorhinal cortex areas Ec and Ecl. In contrast, projections from the parasubiculum terminate in Layer II in all subdivisions of the entorhinal cortex, although the projections to the rostral subdivisions may be less robust (Amaral & Lavenex, 2007). Interestingly, normative data on the volume, neuron number and neuronal soma size in the different layers of the seven subdivisions of the adult rhesus monkey entorhinal cortex (Piguet et al., 2018) corroborated the structural differences in connectivity and histochemical patterns previously described (Amaral et al., 1987). In addition, differences in the number of neurons contributing to distinct afferent and efferent hippocampal pathways suggest that the nature of the interactions between the entorhinal cortex and the rest of the hippocampal formation may vary between subdivisions (Piguet et al., 2018).

1.2 | Development of the entorhinal cortex

Although the entorhinal cortex has been the subject of numerous functional studies, particularly in rodents, there has been no systematic investigation of its postnatal structural development that includes its different layers and subdivisions in either rats, monkeys, or humans. In humans, the overall cytoarchitectonic organization of the entorhinal cortex is clearly identifiable at birth (Grateron et al., 2003). However, although the expression of several calcium-binding proteins is detected in the newborn entorhinal cortex, qualitative observations

suggested that some modifications occur postnatally. For example, calbindin-positive neurons are found almost exclusively in the superficial Layers II and III at 5 months of age, whereas calbindin-positive neurons are also found in Layers V and VI in adulthood. Similarly, no parvalbumin-positive neurons are detected at birth, but they are clearly visible and most abundant at lateral and caudal levels of the entorhinal cortex by 5 months of age.

In monkeys, qualitative observations of nonphosphorylated, high-molecular-weight neurofilament immunostaining revealed that the neurons located in Layers II and III of Ei mature earlier than those located in Layers V and VI (Lavenex et al., 2004, 2007). However, in the absence of systematic, quantitative information, it is difficult to extrapolate from these observations to other subdivisions of the primate entorhinal cortex that receive different cortical afferents. Nor is it possible to determine the exact ages at which morphological changes take place that may reflect the structural maturation of different neuronal populations. Such information is particularly relevant in order to determine whether putative functional circuits processing different types of sensory inputs mature simultaneously or at different times during early postnatal life.

1.3 | Aim of the study

This study aimed to provide normative data on the structural development of the seven subdivisions of the rhesus macaque monkey entorhinal cortex during early postnatal life. We implemented stereological techniques to provide estimates of neuron number, neuronal soma size, and volume of the different layers and subdivisions of the entorhinal cortex in male and female monkeys at 1 day, 6 months, 1 year, and 5–9 years of age. Consistent with previous findings in the hippocampal formation (Jabès et al., 2010, 2011), we found that different layers and subdivisions of the entorhinal cortex exhibit different profiles of structural development.

2 | MATERIALS AND METHODS

2.1 | Experimental animals

Sixteen rhesus monkeys, *Macaca mulatta*, four 1-day-olds (2 M, 2 F), four 6-month-olds (2 M, 2 F), four 1-year-olds (2 M, 2 F), and four adults (5.3, 9.4 [M], 7.7 and 9.3 [F] years of age) were used. Monkeys were born from multiparous mothers and raised at the California National Primate Research Center (CNPRC). They were maternally reared in 2,000-m^2 outdoor enclosures and lived in large social groups until they were killed. These animals were part of the same animals used in studies on the postnatal development of the hippocampal formation (Jabès et al., 2010, 2011) and amygdala (Chareyron, Banta Lavenex, Amaral, & Lavenex, 2011, 2012). All experimental procedures were approved by the Institutional Animal Care and Use Committee of the University of California, Davis, and were in accordance with the National Institutes of Health guidelines for the use of animals in research.

2.2 | Histological processing

2.2.1 | Brain acquisition

Monkeys were deeply anesthetized with an intravenous injection of sodium pentobarbital (50 mg/kg i.v.; FatalPlus; Vortech Pharmaceuticals, Dearborn, MI) and perfused transcardially with 1% and then 4% paraformaldehyde in 0.1 M phosphate buffer (PB; pH 7.4) following standard protocols (Lavenex, Banta Lavenex, Bennett, & Amaral, 2009). Coronal sections were cut with a freezing, sliding microtome in six series at 30-μm, and one series at 60-μm (Microm HM 450; Microm Int. GmbH, Walldorf, Germany). The 60-μm sections were collected in 10% formaldehyde solution in 0.1 M PB (pH 7.4) and post-fixed at 4°C for 4 weeks prior to Nissl staining with thionin. All other series were collected in tissue collection solution (TCS) and kept at −70°C until further processing.

2.2.2 | Nissl staining

The procedure for Nissl-stained sections followed standard protocols (Lavenex et al., 2009). Sections were removed from 10% formaldehyde solution, thoroughly washed for 2 × 2 hr in 0.1 M PB (pH 7.4), mounted on gelatin-coated slides from filtered 0.05 M phosphate buffer (pH 7.4), and air-dried overnight at 37°C. Sections were then defatted for 2 × 2 hr in a mixture of chloroform/ethanol (1:1, vol.) and rinsed for 2 × 2 min in 100% ethanol, 1× 2 min in 95% ethanol, and air-dried overnight at 37°C. Sections were then rehydrated through a graded series of ethanol, 2 min in 95% ethanol, 2 min in 70% ethanol, 2 min in 50% ethanol; dipped in two separate baths of dH_2O; and stained for 20 s in a 0.25% thionin solution (Fisher Scientific, Waltham, MA; catalog No. T-409), then dipped in two separate baths of dH_2O, 4 min in 50% ethanol, 4 min in 70% ethanol, 4 min in 95% ethanol + glacial acetic acid (1 drop per 100 ml of ethanol), 4 min in 95% ethanol, 2 × 4 min in 100% ethanol, 3 × 4 min in xylene; and coverslipped with DPX (BDH Laboratories, Poole, United Kingdom).

2.3 | Stereological analyses

2.3.1 | Structural organization of the monkey entorhinal cortex

The nomenclature, topographical, and cytoarchitectonic organization of the entorhinal cortex were initially described for the cynomolgus monkey (*Macaca fascicularis*; Amaral et al., 1987). The monkey entorhinal cortex comprises seven subdivisions (Figures 1 and 2). Although the cytoarchitectonic characteristics of the cynomolgus monkey and rhesus monkey (*Macaca mulatta*) entorhinal cortex are very similar, there are subtle species differences in the relative development of individual layers in certain subdivisions. We previously described the cytoarchitectonic characteristics of the adult rhesus monkey entorhinal cortex (Piguet et al., 2018). Here, we followed the same

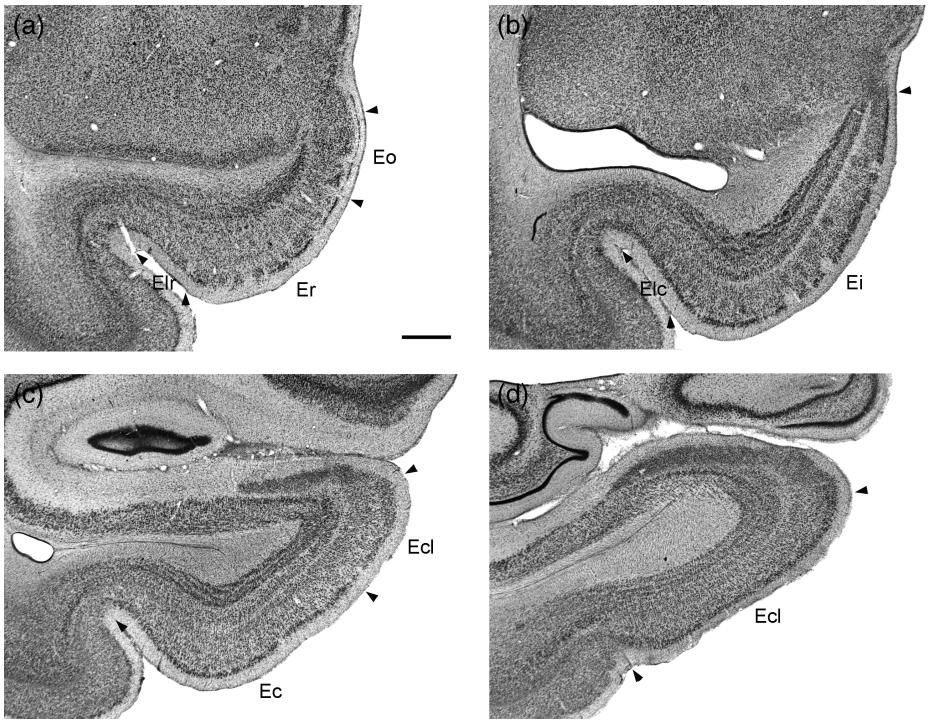

FIGURE 1 Low magnification photomicrographs of coronal sections through the adult rhesus monkey entorhinal cortex. Nissl-stained preparations, arranged from rostral (a) to caudal (d). Eo, olfactory subdivision; Er, rostral subdivision; Elr, lateral rostral subdivision; Elc, lateral caudal subdivision; Ei, intermediate subdivision; Ec, caudal subdivision; Ecl, caudal limiting subdivision. Scale bar = 1 mm

cytoarchitectonic criteria to perform a stereological analysis of the postnatal structural development of the entorhinal cortex.

2.3.2 | Neuron number

The total number of neurons in the different layers of the seven subdivisions of the monkey entorhinal cortex was determined using the optical fractionator method on 60-μm Nissl-stained sections (West, Slomianka, & Gundersen, 1991). For 1-day-old and adult monkeys, about 38 sections per animal (240 μm apart) were used, with the first section selected randomly within the first two sections of Eo. For 6-month-old and 1-year-old monkeys, about 17 sections per animal (480 μm apart) were used. We used a 100X Plan Fluor oil objective (N.A. 1.30) on a Nikon Eclipse 80i microscope (Nikon Instruments Inc, Melville, NY) linked to PC-based StereoInvestigator 9.0 (MicroBrightField, Williston, VT). See Piguet et al. (2018) for other parameters.

2.3.3 | Neuronal soma size

Neuronal soma size was determined using the nucleator method (Gundersen, 1988). We measured an average of 200 neurons per layer per subdivision, sampled at every counting site during the optical fractionator analysis. The nucleator can be used to estimate the mean volume of cells. A set of rays emanating from a randomly chosen point within the nucleus or nucleolus is drawn and oriented randomly. The length of the intercept from the point to the cell boundary (l) is measured, and the cell volume is obtained by $V = (4/3*3.1416)*l^3$.

2.3.4 | Volume of individual layers in distinct subdivisions

We estimated the volume of the individual layers of the seven subdivisions of the monkey entorhinal cortex based on the outline tracings performed for the estimation of neuron numbers. We used the section cutting thickness (60 μm) to determine the distance between sampled sections, which was then multiplied by the total surface area to calculate the volume of individual layers.

2.4 | Statistical analyses

We performed general linear model (GLM) analyses with age as a factor, and regions and layers as repeated measures, to compare the postnatal development of distinct entorhinal subdivisions or layers. We performed GLM analyses with age as a factor to analyze volume, neuronal soma size, and neuron number within individual layers of each subdivision. Degrees of freedom were adjusted following the Greenhouse–Geisser method, when the Mauchly's test of sphericity for repeated measures was significant. We report effect size with η^2_p (partial eta squared, as reported by SPSS 25.0, IBM statistics). We performed post hoc analyses with the Fisher-LSD test when the *F* ratio was significant, thus controlling for Type I error rate (Carmer & Swanson, 1973). Significance level was set at a two-tailed *p* value < .05 for GLM analyses and post hoc tests, unless specified otherwise for some comparisons between individual age groups (listed two-tailed *p* value < .10, which corresponds to a one-tailed *p* value < .05). All statistical analyses were performed on absolute values. Percentages of adult values are reported on figures and in

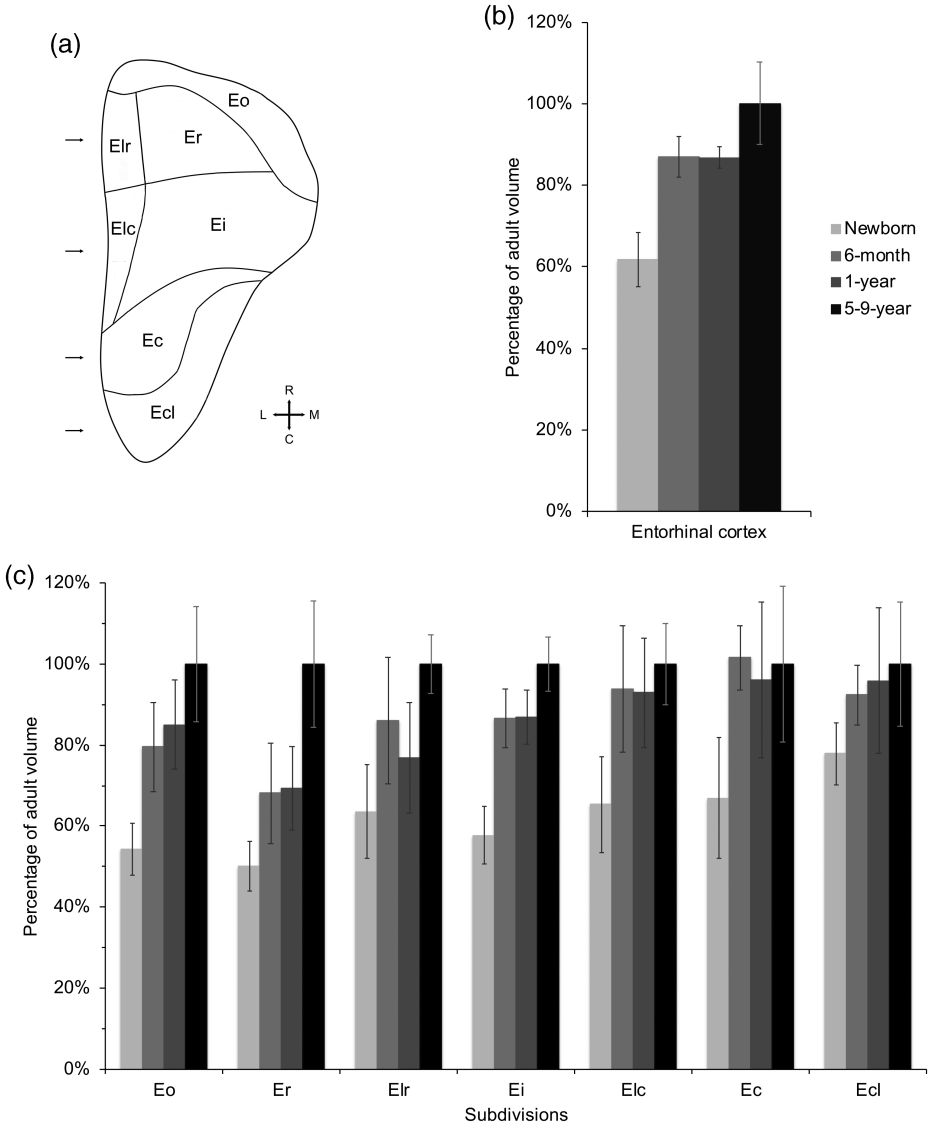

FIGURE 2 (a) Unfolded map of the rhesus monkey entorhinal cortex illustrating the relative position of its seven subdivisions. Black arrows indicate the approximate rostrocaudal locations of the coronal sections illustrated in Figure 1. (b) Percentage of the adult volume of the entire entorhinal cortex, at different ages during postnatal development. (c) Percentage of the adult volumes of the seven subdvisions of the entorhinal cortex, at different ages during postnatal development. See main text for details

the text to facilitate the comparisons of different developmental patterns.

No consistent sex differences were found for the measured parameters, so data from both sexes were combined for presentation. We also evaluated each structure in a systematic manner on the left or right side of the brain: we measured the left entorhinal cortex for one male and one female, and the right entorhinal cortex for one male and one female, in each age group. No lateralization was found for any of the measured parameters.

2.5 | Photomicrographic production

Photomicrographs were taken with a Leica DFC420 digital camera on a Leica MZ9.5 stereomicroscope (Leica Microsystems GmbH, Wetzlar, Germany). Artifacts located outside the sections were removed and levels were adjusted in Adobe Photoshop CS4 V11.0.2 (Adobe Systems, San Jose, CA) to improve contrast.

3 | RESULTS

3.1 | Volume

3.1.1 | Volume of different subdivisions

We first compared age-related changes in volume of the seven subdivisions of the monkey entorhinal cortex during early postnatal development (Figure 2; Tables 1 and 2). As expected, there were differences in the volume of the different subdivisions averaged across all ages ($F_{(6,72)}$ = 259.001, p < .001, η^2_p = .956; Elr (7% of entire entorhinal cortex volume) = Elc (7%) < Eo (10%) < Er (13%) < Ec (18%) = Ecl (17%) < Ei (28%)), as well as differences between age groups ($F_{(3,12)}$ = 23.016, p < .001, η^2_p = .852). In newborn monkeys, the volume of the entire entorhinal cortex was 62% of the adult volume (p < .001). It increased from birth to 6 months of age (p < .001), when it was 87% of the adult volume (6-month vs. 5–9-year, p = .016). It remained stable between 6 months and 1 year of age

TABLE 1 Average volume (mm^3 ± *SD*) of the different layers of the seven subdivisions of the rhesus monkey entorhinal cortex at four postnatal ages

		Newborn	6-month	1-year	5–9-year
Eo	I	0.88 ± 0.19	1.10 ± 0.06	1.08 ± 0.13	0.86 ± 0.25
	II	0.74 ± 0.13	0.96 ± 0.12	0.99 ± 0.16	0.98 ± 0.17
	III	3.68 ± 0.51	5.63 ± 0.94	6.33 ± 0.77	7.78 ± 1.31
	V–VI	0.98 ± 0.12	1.53 ± 0.22	1.45 ± 0.39	1.97 ± 0.28
	Eo total	**6.28 ± 0.74**	**9.22 ± 1.29**	**9.86 ± 1.28**	**11.59 ± 1.66**
Er	I	1,23 ± 0,28	1,52 ± 0,38	1,37 ± 0,26	1,50 ± 0,39
	II	0.87 ± 0.16	1.30 ± 0.27	1.28 ± 0.24	1.47 ± 0.28
	III	3.71 ± 0.44	5.01 ± 0.83	5.65 ± 0.92	8.24 ± 1.26
	V	0.82 ± 0.12	1.11 ± 0.22	1.04 ± 0.11	1.83 ± 0.40
	VI	1.50 ± 0.25	2.13 ± 0.42	1.89 ± 0.24	3.20 ± 0.55
	Er total	**8.13 ± 1.01**	**11.06 ± 2.01**	**11.24 ± 1.67**	**16.24 ± 2.54**
Elr	I	0.81 ± 0.14	1.08 ± 0.40	0.87 ± 0.20	1.08 ± 0.08
	II	0.52 ± 0.08	0.77 ± 0.13	0.68 ± 0.08	0.88 ± 0.16
	III	1.50 ± 0.27	1.96 ± 0.43	1.88 ± 0.31	2.42 ± 0.17
	V	0.63 ± 0.12	0.86 ± 0.05	0.74 ± 0.04	1.08 ± 0.09
	VI	1.14 ± 0.24	1.57 ± 0.23	1.39 ± 0.11	1.78 ± 0.09
	Elr total	**4.60 ± 0.84**	**6.23 ± 1.17**	**5.56 ± 0.60**	**7.24 ± 0.53**
Ei	I	2.88 ± 0.42	4.04 ± 0.53	3.79 ± 0.42	4.37 ± 0.56
	II	1.95 ± 0.22	3.31 ± 0.44	3.20 ± 0.36	3.56 ± 0.25
	III	7.11 ± 1.07	9.66 ± 0.86	10.17 ± 0.63	11.16 ± 0.57
	IV	0.52 ± 0.14	0.69 ± 0.09	0.74 ± 0.09	1.25 ± 0.23
	V	2.18 ± 0.27	3.30 ± 0.50	2.95 ± 0.30	3.92 ± 0.50
	VI	2.72 ± 0.29	5.05 ± 0.36	5.32 ± 0.83	5.82 ± 0.99
	Ei total	**17.35 ± 2.15**	**26.04 ± 2.18**	**26.17 ± 2.01**	**30.08 ± 1.99**
Elc	I	0.88 ± 0.16	1.20 ± 0.20	1.18 ± 0.03	1.25 ± 0.23
	II	0.45 ± 0.07	0.76 ± 0.14	0.75 ± 0.11	0.89 ± 0.07
	III	1.55 ± 0.32	1.81 ± 0.37	1.96 ± 0.39	2.27 ± 0.26
	V	0.62 ± 0.17	0.92 ± 0.21	0.85 ± 0.17	0.96 ± 0.14
	VI	1.00 ± 0.19	1.77 ± 0.27	1.66 ± 0.25	1.52 ± 0.19
	Elc total	**4.50 ± 0.82**	**6.47 ± 1.07**	**6.40 ± 0.94**	**6.89 ± 0.70**
Ec	I	2.01 ± 0.44	2.83 ± 0.43	2.66 ± 0.40	2.75 ± 0.58
	II	1.21 ± 0.20	2.13 ± 0.04	2.01 ± 0.46	2.18 ± 0.36
	III	4.89 ± 1.26	6.71 ± 0.46	6.44 ± 1.33	6.61 ± 1.44
	V	1.48 ± 0.33	2.51 ± 0.20	2.21 ± 0.71	2.75 ± 0.53
	VI	2.43 ± 0.55	4.09 ± 0.54	3.95 ± 0.88	3.68 ± 0.81
	Ec total	**12.03 ± 2.68**	**18.27 ± 1.43**	**17.26 ± 3.47**	**17.98 ± 3.46**
Ecl	I	2.71 ± 0.23	3.25 ± 0.45	3.13 ± 0.71	3.13 ± 0.28
	II	1.91 ± 0.22	2.53 ± 0.21	2.64 ± 0.41	2.83 ± 0.44
	III	5.24 ± 0.75	6.08 ± 0.39	6.47 ± 1.32	6.19 ± 1.03
	V	1.26 ± 0.07	1.49 ± 0.11	1.54 ± 0.32	2.01 ± 0.34
	VI	2.06 ± 0.26	2.27 ± 0.29	2.43 ± 0.42	2.76 ± 0.59
	Ecl total	**13.17 ± 1.29**	**15.62 ± 1.27**	**16.22 ± 3.03**	**16.91 ± 2.58**
Entire EC		**66.06 ± 7.07**	**92.90 ± 5.38**	**92.71 ± 2.77**	**106.92 ± 10.77**

(p = .971), at 87% of the adult volume. It differed between 1 year and 5–9 years of age (p = .015). However, we also found an interaction between subdivisions and age groups ($F_{(18,72)}$ = 4.047, p < .001, η^2_p = .503), which indicated different profiles of postnatal volumetric changes in the different subdivisions of the monkey entorhinal cortex (Figure 2c).

Based on analyses presented below, we defined several developmental profiles: (a) *Very early maturation*: newborn = 6-month = 1-year = 5–9-year.

TABLE 2 Results of the statistical analyses on the volume (mm^3 ± *SD*) of the different layers of the seven subdivisions of the rhesus monkey entorhinal cortex at four postnatal ages

		Profile	$F_{(3,12)}$	*p*	η^2_p	Post hoc comparisons
Eo	I	Very early	2.240	.136	.359	None significant
	II	Early	2.611	.100	.395	Newborn < 6-month — 1-year — 5–9-year
	III	Two-step	13.460	.000	.771	Newborn < 6-month — 1-year < 5–9-year
	V-VI	Two-step	9.159	.002	.696	Newborn < 6-month — 1-year < 5–9-year
	Eo total	**Two-step**	**11.825**	**.001**	**.747**	**Newborn < 6-month — 1-year < 5–9-year**
Er	I	Very early	0.677	.583	.145	None significant
	II	Early	4.365	.027	.522	Newborn < 6-month — 1-year — 5–9-year
	III	Two-step/late	17.476	.000	.814	Newborn < 6-month — 1-year < 5–9-year
	V	Late	12.753	.000	.761	Newborn — 6-month — 1-year < 5–9-year
	VI	Two-step/late	14.301	.000	.781	Newborn < 6-month — 1-year < 5–9-year
	Er total	**Two-step/late**	**12.635**	**.001**	**.760**	**Newborn < 6-month — 1-year < 5–9-year**
Elr	I	Very early	1.467	.273	.268	None significant
	II	Two-step	6.383	.008	.615	Newborn < 6-month — 1-year < 5–9-year
	III	Two-step	5.883	.010	.595	Newborn < 6-month — 1-year < 5–9-year
	V	Two-step	21.879	.000	.845	Newborn < 6-month — 1-year < 5–9-year
	VI	Two-step	8.918	.002	.690	Newborn < 6-month — 1-year < 5–9-year
	Elr total	**Two-step**	**7.226**	**.005**	**.644**	**Newborn < 6-month — 1-year < 5–9-year**
Ei	I	Early	6.920	.006	.634	Newborn < 6-month — 1-year — 5–9-year
	II	Early	19.265	.000	.828	Newborn < 6-month — 1-year — 5–9-year
	III	Two-step/early	18.384	.000	.821	Newborn < other ages; 6-month < 5–9-year
	IV	Late	18.088	.000	.819	Newborn — 6-month — 1-year < 5–9-years
	V	Two-step	12.702	.000	.761	Newborn < 6-month — 1-year < 5–9-year
	VI	Early	16.188	.000	.802	Newborn < 6-month — 1-year — 5–9-year
	Ei total	**Two-step/early**	**26.645**	**.000**	**.869**	**Newborn < 6-month — 1-year < 5–9-year**
Elc	I	Early	3.804	.040	.487	Newborn < 6-month — 1-year — 5–9-year
	II	Two-step/early	14.482	.000	.784	Newborn < 6-month — 1-year < 5–9-year
	III	Gradual	3.156	.064	.441	Newborn < 5–9-year
	V	Early	3.003	.073	.429	Newborn < 6-month — 1-year — 5–9-year
	VI	Early	8.871	.002	.689	Newborn < 6-month — 1-year — 5–9-year
	Elc total	**Early**	**5.686**	**.012**	**.587**	**Newborn < 6-month — 1-year — 5–9-year**
Ec	I	Early	2.562	.104	.390	Newborn < 6-month — 1-year — 5–9-year
	II	Early	8.498	.003	.680	Newborn < 6-month — 1-year — 5–9-year
	III	Early	2.065	.158	.341	Newborn < 6-month — 1-year — 5–9-year
	V	Early	5.193	.016	.565	Newborn < 6-month — 1-year — 5–9-year
	VI	Early	4.544	.024	.532	Newborn < 6-month — 1-year — 5–9-year
	Ec total	**Early**	**4.150**	**.031**	**.509**	**Newborn < 6-month — 1-year — 5–9-year**
Ecl	I	Very early	1.103	.386	.216	None significant
	II	Early	5.656	.012	.586	Newborn < 6-month — 1-year — 5–9-year
	III	Very early	1.275	.327	.242	None significant
	V	Early - late	6.641	.007	.624	Newborn — 6-month — 1-year < 5–9-year
	VI	Early - gradual	2.066	.158	341	Newborn < 5–9-year
	Ecl total	**Early**	**2.214**	**.139**	**.356**	**Newborn < 1-year — 5–9-year**
Entire EC		**Two-step/early**	**23.016**	**.000**	**.852**	**Newborn < 6-month — 1-year < 5–9-year**

(b) *Early maturation*: newborn < 6-month = 1-year = 5–9-year. We also considered the percentage of the adult volume at specific ages in order to further characterize this developmental profile, because a particular structure may be volumetrically more developed than another structure at birth but show later volumetric changes during postnatal development: *Early — Late*: newborn — 6-month — 1-year < 5–9-year; *Early — Gradual*: newborn < 5–9-year. (c) *Two-step maturation*: newborn < 6-month = 1-year < 5–9-year. This profile was further characterized as a *Two-step/early* profile when the volume at 6 months and 1 year of age was higher than 85% of the adult volume, and a *Two-step/late* profile when the volume at 6 months and 1 year of age was lower than 70% of the adult volume. (d) *Gradual maturation*: newborn < 6-month < 1-year < 5–9-year. (e) *Late maturation*: newborn = 6-month = 1-year < 5–9-year.

Eo exhibited a two-step maturation profile. It was 54% of the adult volume at birth ($p < .001$), and increased to 80% at 6 months of age (newborn vs. 6-month: $p = .007$). There was no difference in the volume of Eo between 6-month-old and 1-year-old monkeys (85%; $p = .495$), whereas it differed between 1-year-old and 5–9-year-old monkeys ($p = .081$).

Er exhibited a two-step/late maturation profile. It was 50% of the adult volume at birth ($p < .001$), and increased to 68% at 6 months of age (newborn vs. 6-month: $p = .049$). There was no difference in the volume of Er between 6-month-old and 1-year-old monkeys (69%; $p = .897$), whereas it differed between 1-year-old and 5–9-year-old monkeys ($p = .003$).

Elr exhibited a two-step maturation profile. It was 64% of the adult volume at birth ($p = .001$), and increased to 86% at 6 months of age (newborn vs. 6-month: $p = .016$). There was no difference in the volume of Elr between 6-month-old and 1-year-old monkeys (77%; $p = .276$), whereas it differed between 1-year-old and 5–9-year-old monkeys ($p = .014$).

Ei exhibited a two-step/early maturation profile. It was 58% of the adult volume at birth ($p < .001$), and increased to 87% at 6 months of age (newborn vs. 6-month: $p < .001$). There was no difference in the volume of Ei between 6-month-old and 1-year-old monkeys (87%; $p = .929$), whereas it differed between 1-year-old and 5–9-year-old monkeys ($p = .021$).

Elc exhibited an early maturation profile. It was 65% of the adult volume at birth ($p = .003$), and increased to 94% at 6 months of age (newborn vs. 6-month: $p = .009$). There was no difference in the volume of Elc between 6-month-old and 1-year-old monkeys (93%; $p = .916$), or between 1-year-old and 5–9-year-old monkeys ($p = .453$).

Ec exhibited an early maturation profile. It was 67% of the adult volume at birth ($p = .013$), and increased to 102% at 6 months of age (newborn vs. 6-month: $p = .010$). There was no difference in the volume of Ec between 6-month-old and 1-year-old monkeys (96%; $p = .631$), or between 1-year-old and 5–9-year-old monkeys ($p = .732$).

Ecl exhibited an early to very early maturation profile. It was 78% of the adult volume at birth ($p = .032$), and, although it increased to 92% at 6 months of age, the difference between newborn and 6-month-old monkeys was not statistically significant ($p = .139$). There was no difference in the volume of Ecl between 6-month-old and 1-year-old monkeys (96%; $p = .705$), or between 1-year-old and 5–9-year-old monkeys ($p = .663$).

In sum, the seven subdivisions of the monkey entorhinal cortex exhibited different profiles of volumetric changes during early postnatal life: Er exhibited a two-step/late maturation profile; Eo and Elr exhibited a two-step maturation profile; Ei exhibited a two-step/early maturation profile; Elc, Ec, and Ecl exhibited an early maturation profile.

3.1.2 | Volume of the distinct layers of different subdivisions

Following the characterization of different profiles of postnatal volumetric development of the different subdivisions of the monkey entorhinal cortex, we analyzed the profiles of postnatal volumetric development of distinct layers within each subdivision (Figure 3; Tables 1 and 2).

Global analysis

We first performed a global GLM analysis with repeated measures on the five layers (I, II, III, V, VI) that are common to six subdivisions (Er, Ei, Elr, Elc, Ec, Ecl), thus excluding all layers of Eo and Layer IV of Ei for this analysis. We found differences between age groups ($F_{(3,12)} = 22.296$, $p < .001$, $\eta^2_p = .848$), subdivisions ($F_{(5,60)} = 243.913$, $p < .001$, $\eta^2_p = .953$) and layers ($F_{(4,48)} = 959.934$, $p < .001$, $\eta^2_p = .988$), as well as significant interactions between age groups and subdivisions ($F_{(15,60)} = 3.928$, $p < .001$, $\eta^2_p = .495$), age groups and layers ($F_{(12,48)} = 7.791$, $p < .001$, $\eta^2_p = .661$), subdivisions and layers ($F_{(20,240)} = 146.224$, $p < .001$, $\eta^2_p = .924$), and age groups, subdivisions and layers ($F_{(60,240)} = 4.408$, $p < .001$, $\eta^2_p = .524$). This global analysis demonstrated that distinct layers of different subdivisions of the monkey entorhinal cortex exhibited different profiles of postnatal volumetric development. Based on these results, we performed two series of additional analyses. First, we compared the volumetric development of each layer across all subdivisions. Second, we compared the volumetric development of all layers within each subdivision. Although some information presented below is partly redundant, these two series of analyses are justified in order to provide comprehensive comparisons of the developmental profiles of individual layers both within and across individual subdivisions.

Analyses per layer across subdivisions

Layer I exhibited different postnatal volumetric maturation profiles in different subdivisions: age groups ($F_{(3,12)} = 4.611$, $p = .023$, $\eta^2_p = .535$; newborn < 6-month — 1-year — 5–9-year), subdivisions ($F_{(3.578,42.931)} = 234.792$, $p < .001$, $\eta^2_p = .951$), interaction ($F_{(10.733,42.931)} = 2.101$, $p = .042$, $\eta^2_p = .344$). There were no statistically significant overall differences between age groups in the volume of Layer I in Eo, Er, Elr, Ec, and Ecl. In contrast, there were differences between age groups in the volume of Layer I in Ei and Elc. Despite subtle differences between subdivisions, the postnatal volumetric

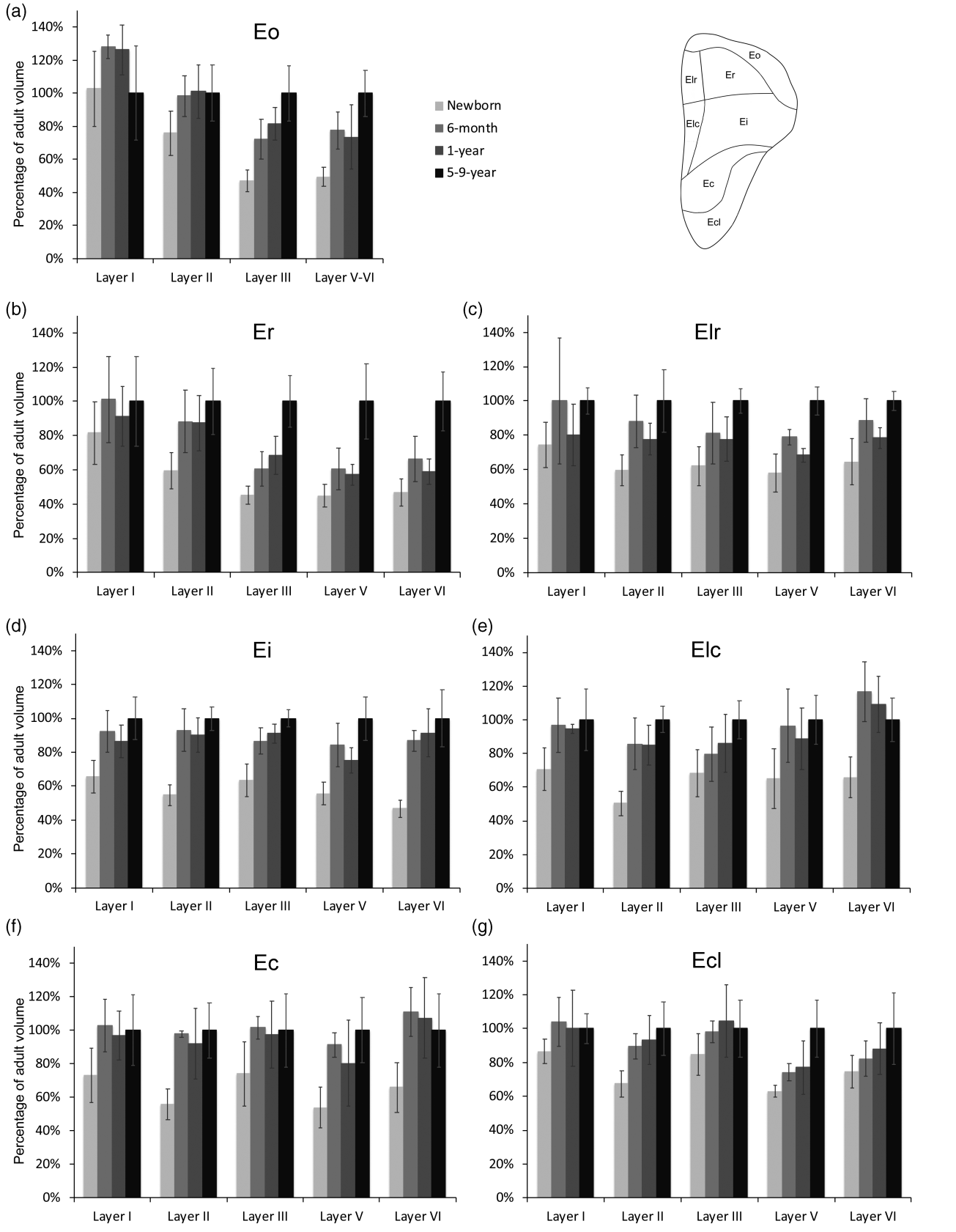

FIGURE 3 Percentage of the adult volume of the different layers of the seven subdivisions of the monkey entorhinal cortex, at different ages during postnatal development. (a) Area Eo; (b) area Er; (c) area Elr; (d) area Ei; (e) area Elc; (f) area Ec; (g) area Ecl. See main text for details

development of Layer I exhibited an early to very early maturation profile (>92% of adult volume at 6 months of age) in all subdivisions.

Layer II exhibited different postnatal volumetric maturation profiles in different subdivisions: age groups ($F_{(3,12)}$ = 19.183, p < .001, η^2_p = .827; newborn < 6-months — 1-year — 5–9-years), subdivisions ($F_{(2.988,35.856)}$ = 296.197, p < .001, η^2_p = .961), interaction ($F_{(8.964,35.856)}$ = 4.348, p = .001, η^2_p = .521). Despite the fact that in Eo the volume of Layer II was 76% of the adult volume in newborn monkeys (p = .041), the overall difference between age groups failed to reach statistical significance. In contrast, there were differences between age groups in the volume of Layer II in Er, Elr, Ei, Elc, Ec, and Ecl. Accordingly, and despite minor peculiarities in Elr (two-step profile) and Elc (two-step/early profile), the postnatal volumetric development of Layer II exhibited an early maturation profile in most subdivisions.

Layer III exhibited different postnatal volumetric maturation profiles in different subdivisions: age groups ($F_{(3,12)}$ = 19.966, p < .001, η^2_p = .833; newborn < 6-month — 1-year < 5–9-year), subdivisions ($F_{(6,72)}$ = 197.902, p < .001, η^2_p = .943), interaction ($F_{(18,72)}$ = 4.264, p < .001, η^2_p = .516). There were differences between age groups in the volume of Layer III in Eo, Er, Elr, and Ei. In both Elc and Ec, although the volume of Layer III was less than 75% of the adult volume in newborns, the overall difference between age groups failed to reach statistical significance. There were no differences between age groups in the volume of Layer III in Ecl. Accordingly, the postnatal volumetric development of Layer III exhibited a clear rostro-caudal gradient, with a two-step/late maturation profile in Er, a two-step maturation profile in Eo and Elr, a gradual maturation profile in Elc, a two-step/early maturation profile in Ei, and an early to very early maturation profile in Ec and Ecl.

Layer IV is only present in Ei. There were differences between age groups in the volume of Layer IV. It was 42% of the adult volume at birth, 55% at 6 months and 59% at 1 year of age; it was larger in adults compared to all other ages (all p < .001). Accordingly, Layer IV of Ei exhibited a late maturation profile.

Layer V exhibited different postnatal volumetric maturation profiles in different subdivisions: age groups ($F_{(3,12)}$ = 29.239, p < .001, η^2_p = .880; newborn < 6-month — 1-year < 5–9-year), subdivisions ($F_{(2.861,34.336)}$ = 130.764, p < .001, η^2_p = .916), interaction ($F_{(8.584,34.336)}$ = 2.495, p = .003, η^2_p = .384; note that we considered Layers V–VI of Eo as a Layer V in order to perform this analysis). There were differences between age groups in the volume of Layers V–VI in Eo. Similarly, there were differences between age groups in the volume of Layer V in Er, Elr, Ei, Ec, and Ecl. In Elc, although the volume of Layer V was only 65% of the adult volume in newborns (p = .018), the overall difference between age groups failed to reach statistical significance. Interestingly, the postnatal volumetric development of Layer V exhibited differences between subdivisions, but these differences did not follow a clear rostro-caudal gradient. Layer V exhibited a two-step maturation profile in Eo, Ei, and Elr, a late maturation profile in Er, and an early maturation profile in Elc and Ec. Interestingly, the volume of layer V was as developed in Ecl (63% of adult volume) as in Elc (65%) at birth, but it exhibited a more gradual/late maturation profile to reach adult volume in Ecl.

Layer VI exhibited different postnatal volumetric maturation profiles in different subdivisions: age groups ($F_{(3,12)}$ = 22.588, p < .001, η^2_p = .850; newborn < 6-month — 1-year < 5–9-year), subdivisions ($F_{(3.037,36.439)}$ = 137.275, p < .001, η^2_p = .920), interaction ($F_{(9.110,36.439)}$ = 5.051, p < .001, η^2_p = .558; note that we considered Layers V–VI of Eo as a Layer VI in order to perform this analysis). There were differences between age groups in the volume of Layer VI in Er, Elr, Ei, Elc, and Ec. In Ecl, the volume of Layer VI was 75% of the adult volume in newborn monkeys (p = .033), but the overall difference between age groups was not statistically significant. The postnatal volumetric development of layer VI exhibited a rostro-caudal gradient, with a two-step/late maturation profile in Er, a two-step maturation profile in Elr, an early maturation profile in Ei, Elc, and Ec. In Ecl, the volume of Layer VI was already 75% of the adult volume at birth, but it exhibited a gradual/late maturation profile thereafter, as was observed for Layer V.

Analyses per layer within subdivisions

Eo. The different layers of Eo exhibited different profiles of postnatal volumetric development (Figure 3a): age groups ($F_{(3,12)}$ = 11.825, p = .001, η^2_p = .747; newborn < 6-month — 1-year < 5–9-year), layers ($F_{(1.141,13.691)}$ = 472.975, p < .001, η^2_p = .975), interaction ($F_{(3.423,13.691)}$ = 13.118, p < .001, η^2_p = .766). There were no statistical differences between age groups in the volume of Layer I or II, even though the volume of Layer II was 76% of the adult volume in newborn monkeys (p = .041). In contrast, there were differences between age groups in the volume of Layers III and V–VI. Layers I and II exhibited an early maturation profile, whereas Layers III and V-VI exhibited a two-step maturation profile.

Er. The different layers of Er exhibited different profiles of postnatal volumetric development (Figure 3b): age groups ($F_{(3,12)}$ = 12.635, p = .001, η^2_p = .760; newborn < 6-month — 1-year < 5–9-year), layers ($F_{(1.342,16.110)}$ = 470.038, p < .001, η^2_p = .975), interaction ($F_{(4.027,16.110)}$ = 17.656, p < .001, η^2_p = .815). There was no difference between age groups in the volume of Layer I. In contrast, there were differences between age groups in the volume of Layers II, III, V, and VI. Nevertheless, Layers I and II exhibited an early maturation profile, whereas Layers III, V, and VI exhibited a two-step/late or late maturation profile.

Elr. The different layers of Elr exhibited different profiles of postnatal volumetric development (Figure 3c): age groups ($F_{(3,12)}$ = 7.366, p = .005, η^2_p = .648; newborn < 6-month — 1-year < 5–9-year), layers ($F_{(1.912,22.939)}$ = 233.323, p < .001, η^2_p = .951), interaction ($F_{(5.735,22.939)}$ = 2.682, p = .042, η^2_p = .401). There were no differences between age groups in the volume of Layer I, which exhibited an early maturation profile. In contrast, there were differences between age groups in Layers II, III, V, and VI, which all exhibited a two-step maturation profile.

Ei. The different layers of Ei exhibited different profiles of postnatal volumetric development (Figure 3d): age groups ($F_{(3,12)}$ = 26.645, p < .001, η^2_p = .869; newborn < 6-month — 1-year < 5–9-year), layers ($F_{(2.972,35.661)}$ = 742.411, p < .001, η^2_p = .984), interaction ($F_{(8.915,35.661)}$ = 6.968, p < .001, η^2_p = .635). There were differences

between age groups in all layers. Layers I, II, and VI exhibited an early maturation profile; Layer III exhibited a two-step/early maturation profile; Layer V exhibited a two-step maturation profile; and Layer IV exhibited a late maturation profile.

Elc. The different layers of Elc exhibited different profiles of postnatal volumetric development (Figure 3e): age groups ($F_{(3,12)}$ = 5.686, p = .012, η^2_p = .587; newborn < 6-month — 1-year — 5–9-year), layers ($F_{(4,48)}$ = 193.479, p < .001, η^2_p = .942), interaction ($F_{(12,48)}$ = 3.426, p = .001, η^2_p = .461). Layers I and VI exhibited an early maturation profile. Layer II exhibited a two-step/early maturation profile. The difference between age groups failed to reach statistical significance for the volume of Layers III and V, which exhibited a gradual and early maturation profile, respectively.

Ec. The different layers of Ec exhibited a similar profile of postnatal volumetric development (Figure 3f): age groups ($F_{(3,12)}$ = 4.151, p = .031, η^2_p = .509; newborn < 6-month — 1-year — 5–9-year), layers ($F_{(1.983,23.791)}$ = 236.598, p < .001, η^2_p = .952), interaction ($F_{(5.948,23.791)}$ = 1.138, p = .371, η^2_p = .222). Despite the fact that Layer I was 73% of the adult volume in newborn monkeys (p = .045), the overall difference between age groups was not statistically significant. There were differences between age groups in the volume of Layers II, V, and VI. The difference between age groups in the volume of Layer III did not reach statistical significance, although the maturation profile of Layer III was similar to that of the other layers. Thus, despite some peculiar results for Layers I and III, all layers of Ec exhibited an early maturation profile.

Ecl. Despite the lack of significant interaction between age groups and layers ($F_{(4.663,18.653)}$ = 1.296, p = .308, η^2_p = .245), different layers of Ecl exhibited different profiles of postnatal volumetric development (Figure 3g): age groups ($F_{(3,12)}$ = 2.214, p = .139, η^2_p = .356), layers ($F_{(1.554,18.653)}$ = 390.231, p < .001, η^2_p = .970). There was no difference between age groups in the volume of Layers I and III. There were differences between age groups in the volume of Layers II and V. Although there was no overall difference between age groups in the volume of Layer VI, it was 75% of the adult volume at birth and followed a gradual maturation profile. Thus, the superficial Layers I–III exhibited an early to very early maturation profile. Layer V was already quite large at birth but exhibited a late volumetric expansion to reach adult volume, which we defined as an early–late maturation profile.

3.2 | Neuron number

There were differences in the number of neurons between subdivisions across ages ($F_{(3.317,39.806)}$ = 231.294, p < .001, η^2_p = .951; Elr [6% of all entorhinal cortex neurons] = Elc [6%] < Eo [12%] < Er [12%] < Ec [17%] = Ecl [17%] < Ei [30%]; all p < .001), but no differences between age groups ($F_{(3,12)}$ = 0.799, p = .518, η^2_p = .166; newborn — 6-month — 1-year — 5–9-year), and no interaction between age groups and subdivisions ($F_{(9.952,39.806)}$ = 1.094, p = .390, η^2_p = .215; Table 3).

3.3 | Neuronal soma size

3.3.1 | Global analysis

We first performed a global GLM analysis with repeated measures on the four cellular layers (II, III, V, VI) that are common to six subdivisions (Er, Ei, Elr, Elc, Ec, Ecl), thus excluding area Eo that has only three cellular layers for this analysis. We found differences between age groups ($F_{(3,12)}$ = 17.283, p < .001, η^2_p = .812; newborn < 6-month — 1-year > 5–9-year), subdivisions ($F_{(5,60)}$ = 12.454, p < .001, η^2_p = .509), layers ($F_{(3,36)}$ = 91.197, p < .001, η^2_p = .884), as well as significant interactions between age groups and subdivisions ($F_{(15,60)}$ = 2.618, p = .004, η^2_p = .396), age groups and layers ($F_{(9,36)}$ = 12.559, p < .001, η^2_p = .758), subdivisions and layers ($F_{(15,180)}$ = 23.450 p < .001, η^2_p = .661), and age groups, subdivisions and layers ($F_{(45,180)}$ = 2.325, p < .001, η^2_p = .368). This global analysis demonstrated that the average neuronal soma size exhibited different profiles of postnatal changes in distinct layers of different subdivisions of the monkey entorhinal cortex. Based on these results, we performed two series of additional analyses. First, we compared age-related changes in neuronal soma size within each layer across the seven subdivisions. Second, we compared age-related changes in neuronal soma size across the different layers within each subdivision. Although some information presented below is partly redundant, these two series of analyses are justified in order to provide comprehensive comparisons of the developmental profiles of principal neurons in individual layers both within and across individual subdivisions (Figure 4; Tables 4 and 5).

3.3.2 | Analyses per layer across subdivisions

The developmental profiles of neuronal soma size differed from the developmental profiles of the volume of layers and subdivisions. Based on analyses presented below, we defined several maturation profiles for neuronal soma size: (a) *Late decrease*: newborn = 6-month = 1-year > 5–9-year; (b) *No change*: newborn = 6-month = 1-year = 5–9-year; (c) *Transient*: a transient increase at intermediate ages: newborn < 6-month/1-year > 5–9-year, no difference between newborn and 5–9-year; (d) *Transient increase*: a transient increase at intermediate ages, together with a net increase between birth and adulthood: newborn < 6-month/ 1-year > 5–9-year and newborn < 5–9 year; (e) *Early increase*: newborn < 6-month = 1-year = 5–9-year; (f) *Two-step increase*: newborn < 6-month = 1-year < 5–9-year.

Layer II. The soma size of Layer II neurons exhibited different postnatal developmental profiles in different subdivisions: age groups ($F_{(3,12)}$ = 16.802, p < .001, η^2_p = .808), subdivisions ($F_{(6,72)}$ = 85.734, p < .001, η^2_p = .877), interaction ($F_{(18,72)}$ = 2.440, p = .004, η^2_p = .379). The developmental profile of neuronal soma size exhibited a clear rostro-caudal gradient in Layer II, with a transient increase at 6 months and 1 year of age in Eo, Er, Elr, and Elc, which was followed by a decrease into adulthood; a two-step increase in Ei; and no significant changes in Ec and Ecl.

TABLE 3 Number of neurons in the different layers of the seven subdivisions of the rhesus monkey entorhinal cortex at four postnatal ages

		Newborn	6-month	1-year	5–9-year
Eo	II	56,998 ± 14,616	50,324 ± 11,012	43,573 ± 5,552	40,137 ± 7,108
	III	257,538 ± 53,436	232,567 ± 89,534	239,802 ± 27,701	296,929 ± 41,347
	V-VI	80,202 ± 18,971	91,625 ± 25,452	73,022 ± 13,160	65,969 ± 8,391
	Eo total	**394,738 ± 77,104**	**374,516 ± 121,978**	**356,397 ± 31,283**	**403,035 ± 53,910**
Er	II	49,249 ± 14,977	52,994 ± 15,035	45,477 ± 8,665	50,417 ± 12,078
	III	204,289 ± 55,036	184,467 ± 64,923	188,370 ± 53,426	281,868 ± 48,238
	V	38,259 ± 5,119	34,440 ± 12,002	28,994 ± 5,753	44,363 ± 8,241
	VI	106,700 ± 15,266	110,311 ± 23,743	80,800 ± 4,209	129,493 ± 19,533
	Er total	**398,497 ± 83,570**	**382,212 ± 112,320**	**343,640 ± 68,250**	**506,140 ± 67,352**
Elr	II	32,624 ± 10,586	38,208 ± 10,263	28,238 ± 4,328	37,057 ± 6,695
	III	76,867 ± 22,362	71,202 ± 26,083	67,970 ± 17,254	81,430 ± 8,653
	V	29,578 ± 7,710	30,873 ± 3,640	23,189 ± 4,720	28,949 ± 3,068
	VI	70,389 ± 15,478	67,671 ± 17,161	54,096 ± 5,807	65,686 ± 3,530
	Elr total	**209,458 ± 53,106**	**207,953 ± 54,114**	**173,493 ± 20,000**	**213,123 ± 8,081**
Ei	II	118,911 ± 19,579	130,430 ± 35,204	132,187 ± 33,624	138,243 ± 16,063
	III	388,879 ± 80,299	372,587 ± 51,551	374,793 ± 50,847	445,652 ± 68,989
	V	144,602 ± 25,470	148,560 ± 28,146	104,660 ± 16,160	159,237 ± 20,188
	VI	304,638 ± 52,134	365,010 ± 62,717	299,666 ± 73,535	328,132 ± 46,213
	Ei total	**957,030 ± 161,627**	**1,016,588 ± 130,008**	**911,307 ± 151,217**	**1,071,264 ± 40,889**
Elc	II	26,624 ± 6,395	33,693 ± 6,713	31,826 ± 5,448	38,090 ± 593
	III	70,589 ± 16,528	70,656 ± 18,621	67,518 ± 14,302	83,439 ± 12,414
	V	31,755 ± 7,888	36,877 ± 12,105	28,892 ± 6,343	34,604 ± 3,957
	VI	58,726 ± 9,809	85,161 ± 18,097	70,343 ± 16,279	62,761 ± 7,761
	Elc total	**187,693 ± 38,740**	**226,386 ± 55,094**	**198,579 ± 37,058**	**218,894 ± 22,439**
Ec	II	60,233 ± 21,859	71,250 ± 21,323	75,749 ± 20,533	85,037 ± 13,609
	III	222,020 ± 66,534	214,185 ± 33,337	205,258 ± 54,579	220,281 ± 29,678
	V	80,412 ± 19,808	92,638 ± 20,257	75,549 ± 17,689	88,204 ± 12,656
	VI	174,345 ± 50,666	224,050 ± 47,307	202,147 ± 71,812	185,487 ± 27,211
	Ec total	**537,009 ± 153,077**	**602,124 ± 119,346**	**558,703 ± 151,587**	**579,009 ± 79,525**
Ecl	II	100,238 ± 22,369	99,552 ± 14,937	93,000 ± 14,356	110,802 ± 17,631
	III	260,972 ± 44,181	222,921 ± 37,762	232,836 ± 42,565	211,414 ± 26,276
	V	73,980 ± 12,523	55,641 ± 2,095	56,303 ± 12,150	70,664 ± 8,806
	VI	173,389 ± 33,778	133,312 ± 25,297	145,144 ± 22,267	148,066 ± 18,292
	Ecl total	**608,579 ± 89,027**	**511,427 ± 74,813**	**527,283 ± 70,726**	**540,946 ± 67,937**
Entire EC		**3,293,005 ± 566,029**	**3,321,205 ± 533,323**	**3,069,402 ± 223,207**	**3,532,411 ± 252,997**

Layer III. The soma size of Layer III neurons exhibited different postnatal developmental profiles in different subdivisions: age groups ($F_{(3,12)}$ = 8.837, p = .002, η^2_p = .688), subdivisions ($F_{(3.589,43.068)}$ = 27.854, p < .001, η^2_p = .699), interaction ($F_{(10.767,43.068)}$ = 3.061, p = .004, η^2_p = .434). The developmental profile of neuronal soma size exhibited a clear rostro-caudal gradient in Layer III, with an increase between birth and 6 months of age in Eo, after which soma size remained stable; a transient increase between birth and 6 months of age in Er, Elr, and Ei, which was followed by a gradual decrease into adulthood; and a decrease after 6 months or 1 year of age in Elc, Ec, and Ecl.

Layer V. The soma size of Layer V neurons exhibited different postnatal developmental profiles in different subdivisions: age groups ($F_{(3,12)}$ = 21.891, p < .001, η^2_p = .846), subdivisions ($F_{(6,72)}$ = 25.555, p < .001, η^2_p = .680), interaction ($F_{(18,72)}$ = 2.598, p = .002, η^2_p = .394). The developmental profile of neuronal soma size exhibited a clear rostro-caudal gradient in Layer V. There was an increase between birth and 6 months of age in Eo, after which soma size remained stable; an increase between birth and 6 months of age in all other areas, which was followed by a gradual decrease to reach adult size. Neuronal soma size was smaller in newborn than in 5–9-year-old monkeys

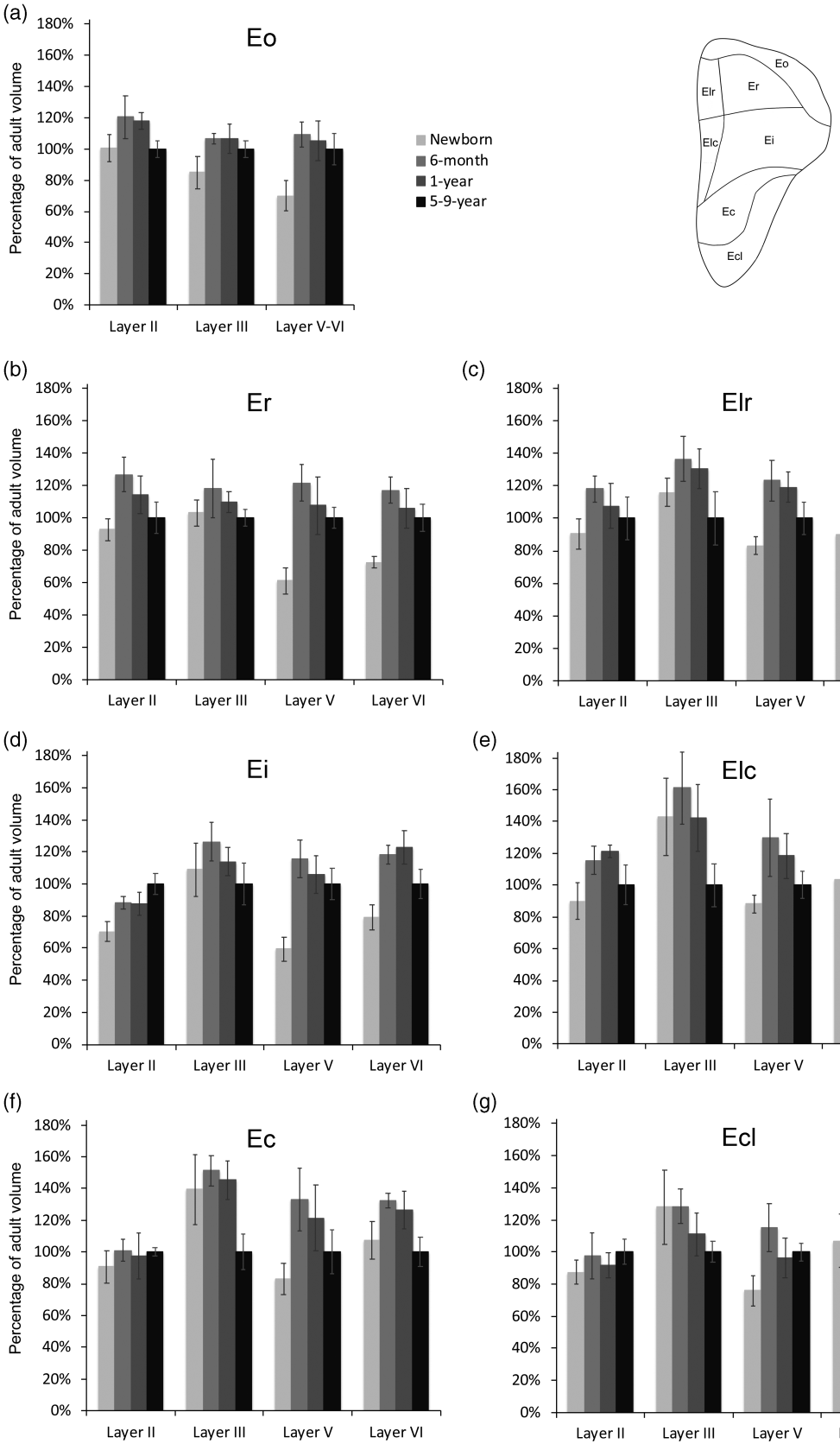

FIGURE 4 Percentage of the adult volume of neuronal soma size in the different layers of the seven subdivisions of the monkey entorhinal cortex, at different ages during postnatal development. (a) Area Eo; (b) area Er; (c) area Elr; (d) area Ei; (e) area Elc; (f) area Ec; and (g) area Ecl. See main text for details

TABLE 4 Neuronal soma size (μm^3 ± *SD*) in the different layers of the seven subdivisions of the rhesus monkey entorhinal cortex at four postnatal ages

		Newborn	6-month	1-year	5–9-year
Eo	II	1,222 ± 107	1,462 ± 169	1,437 ± 65	1,216 ± 66
	III	1,522 ± 183	1,907 ± 62	1,913 ± 171	1,795 ± 95
	V–VI	1,187 ± 168	1,853 ± 135	1,782 ± 213	1,696 ± 171
Er	II	1,509 ± 108	2,064 ± 172	1,858 ± 187	1,629 ± 158
	III	1,904 ± 148	2,187 ± 338	2,027 ± 117	1,850 ± 99
	V	1,444 ± 187	2,877 ± 269	2,552 ± 422	2,370 ± 147
	VI	1,290 ± 62	2,088 ± 149	1,884 ± 218	1,783 ± 152
Elr	II	1,733 ± 178	2,263 ± 152	2,061 ± 270	1,915 ± 254
	III	2,212 ± 166	2,601 ± 264	2,487 ± 234	1,906 ± 316
	V	1,772 ± 115	2,631 ± 266	2,545 ± 203	2,134 ± 219
	VI	1,481 ± 81	2,032 ± 328	1,948 ± 93	1,642 ± 122
Ei	II	1,856 ± 161	2,325 ± 101	2,310 ± 193	2,637 ± 171
	III	2,305 ± 351	2,673 ± 252	2,412 ± 187	2,115 ± 279
	V	1,480 ± 183	2,880 ± 293	2,634 ± 293	2,492 ± 238
	VI	1,385 ± 137	2,075 ± 100	2,151 ± 183	1,755 ± 160
Elc	II	2,049 ± 262	2,632 ± 203	2,765 ± 96	2,280 ± 283
	III	2,456 ± 417	2,773 ± 389	2,446 ± 359	1,721 ± 230
	V	1,844 ± 115	2,712 ± 509	2,473 ± 297	2,089 ± 181
	VI	1,571 ± 24	2,097 ± 219	1,859 ± 211	1,518 ± 87
Ec	II	2,459 ± 279	2,732 ± 187	2,642 ± 394	2,710 ± 67
	III	2,711 ± 428	2,943 ± 185	2,825 ± 240	1,945 ± 218
	V	1,786 ± 213	2,858 ± 422	2,600 ± 445	2,145 ± 293
	VI	1,616 ± 176	1,991 ± 65	1,901 ± 174	1,503 ± 138
Ecl	II	2,337 ± 204	2,602 ± 381	2,453 ± 214	2,672 ± 206
	III	2,754 ± 497	2,762 ± 235	2,386 ± 283	2,150 ± 139
	V	1,659 ± 206	2,522 ± 324	2,111 ± 269	2,188 ± 125
	VI	1,523 ± 236	1,788 ± 215	1,737 ± 132	1,424 ± 139

in Er, Elr, Ei, and Ecl, whereas it did not differ between newborn and 5–9-year-old monkeys in Elc and Ec.

Layer VI. The soma size of Layer VI neurons exhibited different postnatal developmental profiles in different subdivisions: age groups ($F_{(3,12)}$ = 21.881, p < .001, η^2_p = .845), subdivisions ($F_{(3.106,37.278)}$ = 5.779, p = .002, η^2_p = .325), interaction ($F_{(9.319,37.278)}$ = 3.644, p = .002, η^2_p = .477). The developmental profile of neuronal soma size exhibited a clear rostro-caudal gradient in Layer VI. There was an increase between birth and 6 months of age in Er, Elr, Ei, Elc, Ec, and Ecl, which was followed by a gradual decrease into adulthood. The soma size of Layer VI neurons was larger in 5–9-year-old than in newborn monkeys in Er and Ei, whereas it did not differ between newborn and 5–9-year-old monkeys in Elr, Elc, Ec, and Ecl.

3.3.3 | Analyses per layer within subdivisions

Eo. Neuronal soma size exhibited different postnatal developmental profiles in the different layers of Eo (Figure 4a): age groups ($F_{(3,12)}$ = 14.005, p < .001, η^2_p = .778), layers ($F_{(2,24)}$ = 59.478, p < .001, η^2_p = .832), interaction ($F_{(6,24)}$ = 3.807, p = .008, η^2_p = .488). In Layer II, there was a transient increase at 6 months and 1 year of age, and no difference between newborn and 5–9-year-old monkeys (p = .941). In Layers III and V–VI, there was an early increase between birth and 6 months of age, and no significant changes thereafter.

Er. Neuronal soma size exhibited different postnatal developmental profiles in the different layers of Er (Figure 4b): age groups ($F_{(3,12)}$ = 17.163, p < .001, η^2_p = .811), layers ($F_{(1.719,20.628)}$ = 47.191, p < .001, η^2_p = .797), interaction ($F_{(5.157,20.628)}$ = 9.162, p < .001, η^2_p = .696). Nevertheless, neurons in all layers exhibited a transient increase in soma size at 6 months of age, with a gradual decrease into adulthood. In Layer II, there was a large increase from birth to 6 months of age, followed by a gradual decrease toward 5–9-years of age when soma size was similar to that at birth. There were no statistically significant differences between age groups for Layer III neurons, even though neuronal soma size was larger in 6-month-old than in newborn (p = .069) and 5–9-year-old (p = .035) monkeys. In Layers V and VI, there was a large increase in neuronal soma size between

TABLE 5 Results of the statistical analyses on neuronal soma size ($\mu m^3 \pm SD$) in the different layers of the seven subdivisions of the rhesus monkey entorhinal cortex at four postnatal ages

		Profile	$F_{(3,12)}$	p	η^2_p	Post hoc comparisons
Eo	II	Transient	5.863	.011	.594	Newborn < 6-month — 1-year > 5–9-year
	III	Early increase	7.135	.005	.641	Newborn < 6-month — 1-year — 5–9-year
	V–VI	Early increase	12.066	.001	.751	Newborn < 6-month — 1-year — 5–9-year
Er	II	Transient	9.577	.002	.705	Newborn < 6-month > 1-year > 5–9-year
	III	Transient	2.233	.137	.358	Newborn < 6-month; 6-month > 5–9-year
	V	Transient increase	19.738	.000	.831	Newborn < other ages; 6-month > 5–9-year
	VI	Transient increase	19.007	.000	.826	Newborn < other ages; 6-month > 1-year — 5–9-year
Elr	II	Transient	4.194	.030	.512	Newborn < 6-month — 1-year; 6-month > 5–9-year
	III	Transient	6.105	.009	.604	Newborn < 6-month; 6-month — 1-year > 5–9-year
	V	Transient increase	14.565	.000	.785	Newborn < other ages; 6-month — 1-year > 5–9-year
	VI	Transient	7.747	.004	.659	Newborn < 6-month — 1-year > 5–9-year
Ei	II	Two-step increase	16.170	.000	.802	Newborn < 6-month — 1-year < 5–9-year
	III	Transient	2.900	.079	.420	Newborn < 6-month; 6-month > 5–9-year
	V	Transient increase	23.170	.000	.853	Newborn < other ages; 6-month > 5–9-year
	VI	Transient increase	22.242	.000	.848	Newborn < other ages; 6-month — 1-year > 5–9-year
Elc	II	Transient	8.603	.003	.683	Newborn < 6-month — 1-year > 5–9-year
	III	Late decrease	6.251	.008	.610	Newborn — 6-month — 1-year > 5–9-year
	V	Transient	6.118	.009	.605	Newborn < 6-month — 1-year; 6-month > 5–9-year
	VI	Transient	11.561	.001	.743	Newborn < 6-month — 1-year > 5–9-year
Ec	II	No change	0.900	.469	.184	None significant
	III	Late decrease	10.065	.001	.716	Newborn — 6-month — 1-year > 5–9-year
	V	Transient	7.153	.005	.641	Newborn < 6-month — 1-year > 5–9-year
	VI	Transient	10.069	.001	.716	Newborn < 6-month — 1-year > 5–9-year
Ecl	II	No change	1.317	.315	.248	Newborn < 5–9-year
	III	Gradual decrease	3.560	.047	.471	Newborn — 6-month > 5–9-year
	V	Transient increase	8.597	.003	.682	Newborn < other ages; 6-month > 5–9-year
	VI	Transient	3.451	.051	.463	Newborn < 6-month; 6-month — 1-year > 5–9-year

birth and 6 months of age ($p < .001$), followed by a gradual decrease leading to a smaller neuronal soma size in 5–9-year-old than in 6-month-old monkeys (both $p < .05$); soma size of Layers V and VI neurons was larger in 5–9-year-old than in newborn monkeys (both $p < .001$).

Elr. Neuronal soma size exhibited different postnatal developmental profiles in the different layers of Elr (Figure 4c): age groups ($F_{(3,12)]} = 10.933$, $p = .001$, $\eta^2_p = .732$), layers ($F_{(3,36)} = 39.981$, $p < .001$, $\eta^2_p = .769$), interaction ($F_{(9,36)} = 3.106$, $p = .007$, $\eta^2_p = .437$). Nevertheless, neurons in all layers exhibited a transient increase at 6 months of age, with a gradual decrease into adulthood. Neuronal soma size did not differ between newborn and 5–9-year-old monkeys in Layers II, III, and VI, but it was larger in 5–9-year-old than in newborn monkeys in Layer V ($p = .030$).

Ei. Neuronal soma size exhibited different postnatal developmental profiles in the different layers of Ei (Figure 4d): age groups ($F_{(3,12)} = 16.829$, $p < .001$, $\eta^2_p = .808$), layers ($F_{(3,36)} = 34.986$, $p < .001$, $\eta^2_p = .745$), interaction ($F_{(9,36)} = 10.908$, $p < .001$, $\eta^2_p = .732$). Layer II neurons exhibited a gradual increase from birth to 5–9 years of age. Layer III neurons exhibited a transient increase at 6 months of age, although the overall age difference failed to reach statistical significance. Layers V and VI neurons exhibited a transient increase from birth until at least 6 months of age, followed by a gradual decrease into adulthood; soma size of Layers V and VI neurons were larger in 5–9-year-old than in newborn monkeys (both $p < .005$).

Elc. Neuronal soma size exhibited different postnatal developmental profiles in the different layers of Elc (Figure 4e): age groups ($F_{(3,12)} = 8.123$, $p = .003$, $\eta^2_p = .670$), layers ($F_{(3,36)} = 41.674$, $p < .001$, $\eta^2_p = .776$), interaction ($F_{(9,36)} = 5.044$, $p < .001$, $\eta^2_p = .558$). Nevertheless, neurons from all layers exhibited a transient increase from birth until at least 6 months of age, followed by a gradual decrease into adulthood. Neuronal soma size did not differ between newborn and 5–9-year-old monkeys in Layers II, V, and VI. In contrast, neuronal soma size was smaller in 5–9-year-old monkeys than in younger monkeys in Layer III.

Ec. Neuronal soma size exhibited different postnatal developmental profiles in the different layers of Ec (Figure 4f): age groups ($F_{(3,12)}$ = 7.737, p = .004, η^2_p = .659), layers ($F_{(1.658,19.896)}$ = 54.463, p < .001, η^2_p = .819), interaction ($F_{(4.974,19.896)}$ = 5.691, p < .001, η^2_p = .587). Layer II neurons did not exhibit age-related changes in soma size. Layer III neurons exhibited a decrease between 1 year and 5–9 years of age, whereas neurons in Layers V and VI exhibited a transient increase until at least 6 months of age, followed by a gradual decrease into adulthood. Neuronal soma size did not differ between newborn and 5–9-year-old monkeys in Layers V and VI.

Ecl. Neuronal soma size exhibited different postnatal developmental profiles in the different layers of Ecl (Figure 4g): age groups ($F_{(3,12)}$ = 2.516, p = .108, η^2_p = .386), layers ($F_{(3,36)}$ = 82.145, p < .001, η^2_p = .873), interaction ($F_{(9,36)}$ = 6.419, p < .001, η^2_p = .616). Layer II neurons did not exhibit age-related changes in soma size. Layer III neurons exhibited a gradual decrease from 6 months to 5–9 years of age, whereas neurons in Layers V and VI exhibited a transient increase until at least 6 months of age, followed by a gradual decrease into adulthood. Neuronal soma size was larger in 5–9-year-old than in newborn monkeys in Layer V, whereas it did not differ between newborn and 5–9-year-old monkeys in Layer VI.

4 | DISCUSSION

Consistent with findings on the structural development of the hippocampal formation (Jabès et al., 2010, 2011), the different layers and neurons of the seven subdivisions of the monkey entorhinal cortex exhibit different postnatal developmental profiles. Importantly, the developmental profiles observed in the different layers and subdivisions of the entorhinal cortex parallel the developmental profiles observed in the hippocampal structures with which they are interconnected. Since the fundamental features of the laminar and topographical organization of the entorhinal cortex projections to the hippocampal formation are similar to those of adults by 2 weeks of age in rhesus monkeys (Amaral et al., 2014), the current findings may shed light on the differential structural maturation of putative functional circuits supporting the interactions between the entorhinal cortex and the rest of the hippocampal formation.

4.1 | Neuron number

As expected, we did not find age-related differences in neuron numbers in the postnatal monkey entorhinal cortex. Our estimates in monkeys from birth to 1 year of age were consistent with our previous results in adult monkeys (Piguet et al., 2018). Indeed, neurons destined for the entorhinal cortex are generated by mid gestation in monkeys, following an inside-out spatio-temporal gradient (Nowakowski & Rakic, 1981; Rakic & Nowakowski, 1981). Deeply located neurons are generated before superficially located neurons. The production of neurons located in the deep layers of the entorhinal cortex ends around E56, whereas neurons destined for the superficial layers are generated up until E70. Since, to our knowledge, there is no developmental study on the number of neurons in the entorhinal cortex in either rats, monkeys or humans, we refer the reader to our previous publication for a comparison of our current results with previous studies in adult individuals (Piguet et al., 2018).

4.2 | Neuronal soma size

The average neuronal soma size exhibited different profiles of postnatal changes in distinct layers of different subdivisions of the rhesus monkey entorhinal cortex. Nevertheless, neuronal soma size typically increased between birth and 6 months of age, except in the superficial Layers II and III of Ec and Ecl. Neuronal soma size then typically decreased from 6 months to 5–9 years of age, except in Layer II of Ei where it increased until 5–9 years of age, as well as in Layer II of Ec and Ecl where it remained stable from birth until 5–9 years of age. These findings are interesting in light of the overproduction of synapses observed in several cortical regions between birth and approximately 4 months of age in rhesus monkeys (Rakic, Bourgeois, Eckenhoff, Zecevic, & Goldman-Rakic, 1986), and between birth and 15 months of age in humans (Huttenlocher & Dabholkar, 1997). Synapse overproduction is followed by a systematic elimination of synapses until adulthood, when synaptic density is often close to that observed at birth in both monkeys and humans, although the proportion of different types of synapses found in neonate and adult individuals may vary (Huttenlocher & Dabholkar, 1997; Rakic et al., 1986). In monkeys, synapse overproduction was reported to be nearly simultaneous in the motor, somatosensory, prefrontal, and visual cortices, as well as a limbic area, which may have included the entorhinal cortex. However, a detailed evaluation of Figure 2 in Rakic et al. (1986) suggests that the exact ages at which synapse overproduction reaches its peak may vary slightly in different cortical areas in monkeys, as in humans. In the sample derived from the limbic area, the peak density of synapses per 100 μm^2 of neuropil occurred around 5 to 6 months of age. It stands to reason that increased synaptic density is accompanied by a corresponding increase in neuronal soma size (Beul & Hilgetag, 2019). This is essentially what we observed in most layers of most subdivisions of the entorhinal cortex between birth and 6 months of age. However, our data on neuronal soma size also suggest that following an initial increase the structural maturation of neurons follows different time courses in distinct layers of different subdivisions of the entorhinal cortex. Our findings in the monkey entorhinal cortex are thus consistent with a study in humans (Rabinowicz, Petetot, Khoury, & de Courten-Myers, 2009), which reported that changes in neuronal soma size from adolescence to young adulthood was also specific to, and may differ between, distinct layers in different cortical areas.

4.3 | Differential development of distinct subdivisions

We found various age-related differences in neuronal soma size in, and volume of, distinct layers in different subdivisions of the monkey

entorhinal cortex. As shown in the hippocampus, postnatal changes in the volume of individual layers or structures are correlated with functional changes revealed by genome-wide patterns of gene expression (Favre et al., 2012a, 2012b; Jabès et al., 2010, 2011; Lavenex et al., 2004, 2007; Lavenex et al., 2014). In the entorhinal cortex, we found postnatal changes in neuronal soma size that often included a transient increase at 6 months of age. Although soma size is not sufficient by itself to reflect the functional maturation of neurons, changes in neuronal soma size together with volumetric changes of individual layers may provide information on the structural development of putative functional circuits to which these neurons contribute. We now review our main findings for each subdivision of the entorhinal cortex, and consider the changes in volume of each layer with the changes in neuronal soma size (Figure 5).

4.3.1 | Eo

Eo is the only subdivision of the entorhinal cortex that receives a direct unimodal input from the olfactory bulb (Insausti et al., 1987). In addition, Eo has limited interconnections with other subdivisions of the entorhinal cortex and projects to the rostral portion of the hippocampus and dentate gyrus (Witter & Amaral, 1991). Kesner (2013) reported that in rats, the ventral dentate gyrus, which corresponds to the rostral dentate gyrus in primates, contributes to odor pattern separation. We have shown in monkeys that there are 4–5 times more neurons in the superficial layers than in the deep layers of Eo, and that there are about 5–7 times more neurons in Layer III than in Layer II. Accordingly, since the targets of the projection of Layer II neurons, the dentate gyrus granule cells, exhibit a rather late maturation extending beyond 1 year of age in monkeys (Jabès et al., 2010, 2011), the direct projection from Layer III neurons to CA1 may contribute to the encoding of odors as contextual information in early hippocampus-dependent memories. With the late maturation of the granule cells pattern separation for odor information might become more specific and help disambiguate closely related odors enabling the encoding of more distinct memories. Within the hippocampus, we also observed a two-step maturational process, with CA1 maturing before CA3 (Favre et al., 2012a; Jabès et al., 2010, 2011; Lavenex, Sugden, Davis, Gregg, & Lavenex, 2011). Accordingly, whereas neuronal somas reached adult-like size by 6 months of age in Layers III and V–VI, the volumes of Layers III and V–VI increased between birth and 6 months of age and again after 1 year of age. In contrast, whereas the volume of Layer II did not change with age, the soma size of Layer II neurons decreased after 1 year of age to become adult-like. Altogether, these results suggest that the two-step maturation of intra-hippocampal circuits may contribute to the two-step maturation of Eo, via feedback projections from CA1 and the subiculum, and via intrinsic deep-to-superficial projections within the entorhinal cortex (Chrobak & Amaral, 2007). Eo also receives some more minor projections from the basal, accessory basal, and paralaminar nuclei of the amygdala, which are restricted to Layers III and V–VI. The protracted maturation of the amygdala, which we reported previously (Chareyron et al., 2012), may thus also contribute to the structural changes observed in Eo.

4.3.2 | Er

Er receives the majority of its cortical afferents from Layer III neurons of the perirhinal cortex, which terminate most strongly in Layers I, II, and the superficial portion of Layer III. Although Er sends relatively

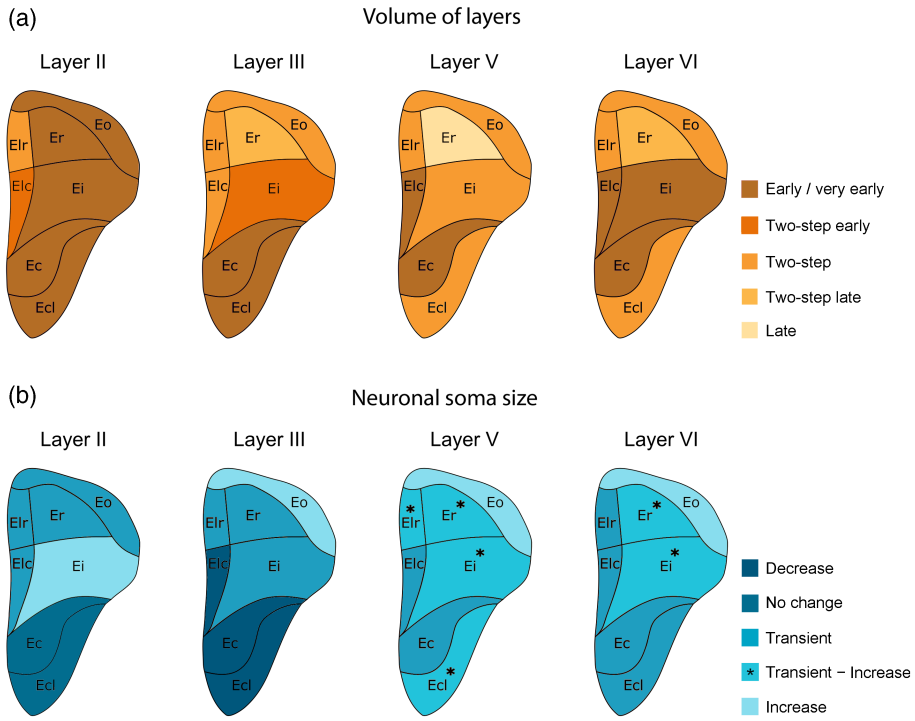

FIGURE 5 Summary of the different profiles of postnatal development in the seven subdivisions of the monkey entorhinal cortex. (a) Volume of distinct layers. (b) Neuronal soma size in distinct layers. See main text for details [Color figure can be viewed at wileyonlinelibrary.com]

fewer feedback projections to the perirhinal cortex (as compared to Elr and more caudal subdivisions) (Suzuki & Amaral, 1994), these projections originate mainly from cells located in Layer V, which is also the recipient of hippocampal projections. Er receives the heaviest input from the lateral and basal nuclei of the amygdala, with fibers and terminals located in all layers, but most heavily in Layers III, V, and VI (Pitkänen et al., 2002). Er also receives projections from the parvicellular division of the accessory basal nucleus. In monkeys, the lateral, basal, and accessory basal nuclei exhibit a large increase in volume between birth and 3 months of age, followed by a slower growth continuing beyond 1 year of age (Chareyron et al., 2012). In contrast, the paralaminar nucleus contains a large pool of immature neurons that gradually develop into mature neurons, leading to a late increase in volume of this nucleus. Although it is difficult to draw strict parallels between the postnatal development of the hippocampal formation (Jabès et al., 2010, 2011) and that of the amygdala (Chareyron et al., 2012), the interconnections with both structures likely influence the structural maturation of Er. Altogether, our data indicate that the layers of Er that receive major cortical inputs from the perirhinal cortex mature first, and that the maturation of Layer III may also be influenced by the maturation of the amygdala projections and the feedback projections from the hippocampus reaching Layer V. In contrast to what was observed in the caudal portion of the entorhinal cortex, the deep layers of Er are rather late developing and may therefore be particularly dependent on the conjunctive maturation of amygdala and hippocampal projections.

4.3.3 | Elr

The development of Elr is very similar to that of Er, not surprisingly since both areas exhibit similar connectivity with the perirhinal cortex, the hippocampal formation and the amygdala, with the exception of fewer projections from the paralaminar nucleus in Elr (Pitkänen et al., 2002). In addition, Elr is more highly interconnected with the caudal hippocampus, whereas Er is more highly interconnected with the mid portion of the hippocampus (Chrobak & Amaral, 2007; Witter & Amaral, 1991). Nevertheless, such differences do not appear to be reflected in major differences in the structural development of the distinct layers and neurons in these two subdivisions. Altogether, our data indicate that the layers of Elr that receive major cortical inputs from the perirhinal cortex mature first, and that the maturation of Layer III may also be influenced by both the maturation of the amygdala projections and the feedback projections from the hippocampus reaching Layer V. In contrast to what was observed in the caudal entorhinal cortex, the deep layers of Elr are developing later, perhaps in relation to the conjunctive maturation of amygdala and hippocampal projections.

4.3.4 | Ei

Ei shares some structural and functional characteristics with both the rostral and caudal subdivisions of the entorhinal cortex. Ei receives prominent projections from Layer III neurons of the perirhinal and parahippocampal cortices, which terminate most heavily in Layers I–III. In contrast to Ec and Ecl, Ei does not receive any projections from the presubiculum. In addition, the rostral half of Ei receives projections from the lateral nucleus of the amygdala, with the densest labeling in Layer III (Pitkänen et al., 2002). Very light projections from the parvicellular divisions of the basal and accessory basal nuclei also reach the rostral half of Ei. It is therefore not surprising that Ei exhibited a developmental profile that was intermediate between those observed in more rostral subdivisions, in particular Er, and those observed in more caudal subdivisions, in particular Ec. Layers I and II exhibited an early maturation, consistent with an early maturation of the cortical inputs reaching the entorhinal cortex. In contrast to Eo, Er, and Elr, but in accordance with Elc and Ec, Ei exhibited an early volumetric maturation of Layer I and VI and a transient increase of neuronal soma size in Layer VI. Interestingly, these layers and regions are reciprocally connected with the retrosplenial cortex (Insausti et al., 1987; Insausti & Amaral, 2008; Kobayashi & Amaral, 2003, 2007). In turn, the retrosplenial cortex is interconnected with the presubiculum and the parasubiculum (Kobayashi & Amaral, 2003, 2007), which both exhibit a very early maturational profile (Jabès et al., 2010, 2011; Lavenex et al., 2004, 2007). Accordingly, the complex patterns of postnatal development of Ei likely reflect the complexity of its interconnections with various brain regions involved in distinct functional networks.

4.3.5 | Elc

Elc receives projections from Layer III neurons of the perirhinal cortex, the rostral parahippocampal cortex, anterior cingulate cortex, and the superior temporal gyrus, which terminate most strongly in Layers I and III (Insausti & Amaral, 2008). Elc also receives prominent projections from the prefrontal cortex, which terminate in Layer VI. Overall, Elc exhibited an early volumetric maturation profile. And, despite subtle differences between layers, all of its layers appeared to exhibit an early maturation profile. Neurons in all layers of Elc exhibited a transient increase in soma size from birth until at least 6 months of age, followed by a gradual decrease into adulthood. The developmental profile of Elc was thus somewhat intermediate between those of Elr and Ec, and distinct from the adjacent medially situated Ei.

4.3.6 | Ec

Ec receives prominent projections from Layer III neurons of the parahippocampal cortex, which terminate most strongly in Layers I–III (Suzuki & Amaral, 1994). In addition, Ec is characterized by a direct projection from the presubiculum to Layer III. The connections between the entorhinal cortex and the parahippocampal cortex are highly reciprocal. Feedback projections originate mainly from Layer V neurons in Ec, with fewer Layer VI neurons and occasional Layer III neurons. Layers V and VI of Ec exhibited an early maturation.

Accordingly, our current findings suggest that some putative functional circuits within Ec and with some interconnected brain regions including the presubiculum and the parahippocampal cortex may mature early. Since both the presubiculum and the parahippocampal cortex are interconnected with the retrosplenial cortex (Kobayashi & Amaral, 2003, 2007), it would be interesting to determine whether these two cortical areas exhibit developmental profiles corresponding to those observed in Ec and the presubiculum (Jabès et al., 2011).

4.3.7 | Ecl

Similar to Ec, Ecl receives prominent projections from Layer III neurons of the parahippocampal cortex, which terminate most strongly in Layers I–III, as well as a direct projection from the presubiculum to Layer III (Suzuki & Amaral, 1994). Accordingly, the maturation profile of Layers I–III was similar in Ec and Ecl. In contrast, Layers V and VI of Ecl exhibited a delayed maturation profile as compared to Layers V and VI of Ec. Thus, although Ec and Ecl share some common connectional characteristics and functional properties, they differ not only in the relative numbers of superficial neurons contributing to different hippocampal circuits (Piguet et al., 2018), but also in the maturation profile of their deep Layers V and VI, which receive feedback projections from CA1 and the subiculum, as well as projections from several cortical areas (Insausti et al., 1987; Insausti & Amaral, 2008).

4.4 | Differential development of individual layers

Although the postnatal development of distinct layers differed between subdivisions, overall the superficial layers developed earlier than the deep layers. This was particularly the case in the rostral portion of the entorhinal cortex, suggesting that the postnatal maturation of the deep layers may be more highly dependent on the feedback projections from CA1 and the subiculum in the rostral entorhinal cortex. In contrast, the maturation of the deep layers of the caudal portion of the entorhinal cortex may be associated to the maturation of functional circuits including projections from the presubiculum and its interconnections with the retrosplenial cortex, also via the parahippocampal cortex. Here, we compare the postnatal development of individual layers between subdivisions.

4.4.1 | Layer I

Layer I receives cortical afferents and contains the dendrites of entorhinal cortex neurons. Despite subtle differences between subdivisions, the volumetric development of Layer I exhibited an early or very early maturation profile. The vast majority of cortical afferent projections to the entorhinal cortex terminate in Layers I–III (Insausti & Amaral, 2008). In addition, the intrinsic connections of the entorhinal cortex terminate predominantly in Layers III and I (Chrobak & Amaral, 2007), which contain the dendrites of many neurons from Layers II, III, and V (Buckmaster, Alonso, Canfield, & Amaral, 2004). Consequently, it is difficult to draw clear inferences regarding the maturation of specific circuits based on the postnatal developmental profile of Layer I. However, since Layer I is one of the main termination layers of cortical afferents, sensory inputs reaching Layer I may contribute to its volumetric maturation by 6 months of age in all subdivisions.

4.4.2 | Layer II

Layer II receives cortical afferents and the majority of its principal neurons project to the dentate gyrus, CA3, and CA2 (Ohara et al., 2019; Witter et al., 2017). Despite some peculiar differences in Elr and Elc, the postnatal volumetric development of Layer II exhibited an early maturation profile. In contrast, the postnatal developmental profile of neuronal soma size exhibited a clear rostro-caudal gradient, with a transient increase at 6 months and 1 year of age in Eo, Er, Elr, and Elc, a two-step increase from birth to adulthood in Ei, and no significant changes in Ec and Ecl. Since Layer II is one of the main termination layers of cortical afferents, it is tempting to consider that sensory inputs reaching Layer II contribute to the volumetric maturation of this layer, and that this maturation is relatively complete by 6 months of age in all subdivisions. Although different cortical afferents terminate in different subdivisions of the entorhinal cortex, they do not seem to have a differential impact on the postnatal volumetric development of Layer II. However, in addition to the neocortical projections reaching Layer II, Layer II is also the recipient of direct projection from the parasubiculum, which exhibits a very early maturation profile (Jabès et al., 2011). We may thus conclude that both sets of inputs may contribute to this early maturation.

In contrast, postnatal changes in neuronal soma size suggest that the maturation of the principal circuits involving Layer II neurons, namely the projections to the dentate gyrus, CA3, and CA2, varies between subdivisions. Indeed, Layer II comprises several cell types including, but not limited to, stellate and pyramidal cells (Amaral & Lavenex, 2007; Buckmaster et al., 2004). Quantitative data on the proportion of these different cell types in the rodent medial entorhinal cortex revealed that the majority of these neurons are stellate cells (rat: 81% (Schwartz & Coleman, 1981); rat: 67%, mouse: 74% (Gatome, Slomianka, Lipp, & Amrein, 2010)). In rats, principal cells in Layer II come in two chemical types: reelin and calbindin expressing cells (Ohara et al., 2019). Reelin-positive stellate cells are the exclusive origin of the entorhinal cortex projections to the dentate gyrus, CA2, and CA3. Calbindin-positive pyramidal neurons provide excitatory input to the reelin-positive stellate cells both directly and indirectly (Witter et al., 2017). We did not consider the cytoarchitectonic criteria defined in Nissl-stained sections for rodents to be sufficiently reliable to define distinct neuronal phenotypes that would be consistent across different subdivisions of the monkey entorhinal cortex. Nevertheless, the maturation of both Layer II stellate and pyramidal cells together likely contributes to the increased influence of the trisynaptic pathway, as compared to the direct projection from Layer III neurons to CA1, during early postnatal development.

The transient increase in neuronal soma size in Eo, Er, Elr, and Elc is consistent with the initial overproduction of synapses around 6 months of age, followed by their selective elimination (Rakic et al., 1986). In contrast, neuronal soma size remained stable between birth and adulthood in Ec and Ecl, suggesting that the initial synapse overproduction and subsequent elimination may occur prior to birth in these areas. Finally, neuronal soma size exhibited a two-step increase between birth and adulthood in Ei, revealing that its Layer II neurons did not follow the same developmental pattern observed in other subdivisions. The patterns of amygdala projections within different subdivisions of the entorhinal may explain these differences. Indeed, amygdala projections terminate predominantly in Layer II in Ei, whereas amygdala projections terminate in Layers III and V in Eo and Er, and there are no amygdala projections to Ec and Ecl.

The dentate gyrus, one of the main targets of entorhinal cortex Layer II neuron projections, exhibits a protracted period of neuron addition that is accompanied by a late maturation of its granule cell population, which continues beyond the first postnatal year in monkeys (Jabès et al., 2010, 2011). Our results in the rostral entorhinal cortex are consistent with the results in the dentate gyrus. In contrast, our results in the caudal entorhinal cortex suggest an early maturation of Layer II neurons. Interestingly, the projections from the caudal entorhinal cortex terminate predominantly in the middle third of the molecular layer of the dentate gyrus and in the outer portion of stratum lacunosum-moleculare of CA3 and CA2, whereas the projections from the rostral entorhinal cortex terminate predominantly in the outer third of the molecular layer and the inner portion of stratum lacunosum-moleculare of CA3 and CA2 (Amaral et al., 2014; Witter & Amaral, 1991). Accordingly, the projections from Ec and Ecl may have an earlier and stronger influence on information processing in the developing dentate gyrus, CA3, and CA2 than the projections from the other subdivisions of the entorhinal cortex, which mature later and terminate more distally on the dendrites of the dentate granule cells and the pyramidal neurons of CA3 and CA2.

4.4.3 | Layer III

Layer III neurons receive cortical afferents and project to CA1 and the subiculum. The postnatal volumetric development of Layer III exhibited a clear rostro-caudal gradient, with a two-step/late maturation profile in Er, a two-step maturation profile in Eo and Elr, a gradual maturation profile in Elc, a two-step/early maturation profile in Ei, and an early maturation profile in Ec and Ecl. Similarly, the postnatal developmental profile of neuronal soma size exhibited a clear rostro-caudal gradient in Layer III, with an increase between birth and 6 months of age in Eo, after which soma size remained stable; an increase between birth and 6 months of age, followed by a gradual decrease of soma size into adulthood in Er, Elr, and Ei; and a decrease in soma size after 6 months of age in Elc, Ec, and Ecl.

Similar to Layers I and II, Layer III is the recipient of various cortical projections, which are preferentially directed toward different subdivisions. Projections from the perirhinal cortex terminate predominantly in Eo, Er, Elr, Elc, and the rostral part of Ei. Projections from the parahippocampal cortex, in contrast, terminate predominantly in Ec and Ecl, and the caudal part of Ei. Projections from the insula, the orbitofrontal cortex, and the anterior cingulate cortex are directed predominantly toward Eo, Er, Elr, and Ei, whereas projections from the retrosplenial cortex and the superior temporal gyrus are directed predominantly toward Ei, Ec, and Ecl. Projections from the amygdala are directed toward Eo, Er, Elr, and the rostral portions of Ei and Elc, with essentially no amygdala projections to Ec and Ecl (Pitkänen et al., 2002). In contrast to what was observed in Layer II, the postnatal development of Layer III suggests that the structural development of different subdivisions of the entorhinal cortex, which may be involved in the processing of different types of information, exhibit different maturation profiles. The caudal entorhinal cortex matures relatively early, whereas the rostral entorhinal cortex matures relatively late.

The main targets of entorhinal cortex Layer III neurons projections, CA1 and the subiculum, exhibit a relatively early maturation already by 6 months of age (Jabès et al., 2011; Lavenex et al., 2004; Lavenex et al., 2011). In particular, stratum lacunosum-moleculare of CA1, which is the target of the direct entorhinal cortex projection, exhibits an earlier maturation than the other layers of CA1. Similarly, the molecular layer of the subiculum, which receives direct projections from the entorhinal cortex matures earlier than the rest of the subiculum. Interestingly, the direct connections between the entorhinal cortex and CA1 and the subiculum are largely reciprocal. The relative segregation of these reciprocal connections suggests that the maturation of separate hippocampal circuits may be related to the type of information being processed and thus may exhibit differential patterns along the transverse axis of the hippocampus during postnatal development. In addition, in Ec and Ecl, we found that neuronal soma size was larger at birth, 6 months, and 1 year of age, as compared to 5–9 years of age. Interestingly, Layer III of Ec and Ecl is the recipient of direct projections from the presubiculum, which exhibits a similar developmental pattern (Jabès et al., 2011).

4.4.4 | Layer V

Layer V neurons receive feedback projections from the hippocampus and subiculum. The postnatal volumetric development of Layer V exhibited differences between subdivisions, but these differences did not appear to follow a clear rostro-caudal gradient. Eo, Ei, and Elr exhibited a two-step maturation profile, Er exhibited a late maturation profile, Elc and Ec exhibited an early maturation profile, and Ecl exhibited an early-late maturation profile. In contrast, the postnatal developmental profile of neuronal soma size exhibited a clear rostro-caudal gradient in Layer V. There was an increase in soma size of Layers V–VI neurons between birth and 6 months of age in Eo, after which soma size remained stable; and an increase in neuronal soma size between birth and 6 months of age, followed by a gradual decrease thereafter in all other subdivisions. Neuronal soma size was smaller in newborn than in 5–9-year-old monkeys in Er, Elr, Ei, and Ecl, whereas it did not differ between newborn and 5–9-year-old monkeys in Elc and Ec.

Layer V is the main recipient of hippocampal output via feedback projections from CA1 and the subiculum, which are topologically in register with the projections of Layer III neurons to the hippocampus and subiculum. However, Layer V neurons are also the recipients of different cortical afferents in different subdivisions of the entorhinal cortex, which may further influence their structural development. Specifically, Layer V neurons in Er and Elr receive some projections from the orbitofrontal cortex, whereas Layer V neurons in Ei, Ec, and Ecl receive some projections from the parahippocampal and retrosplenial cortices. Furthermore, as was shown in the rodent medial entorhinal cortex (which corresponds to the caudal entorhinal cortex areas Ec and Ecl in primates), Layer V neurons may receive direct inputs from the presubiculum and parasubiculum onto their apical dendrites in Layers III and II (respectively; Canto, Koganezawa, Beed, Moser, & Witter, 2012), as well as a direct input from entorhinal cortex Layer II stellate cells that contribute the main projection to the dentate gyrus, CA3, and CA2 (Surmeli et al., 2015). Accordingly, different sets of cortical projections may have a differential impact on the structural maturation of Layer V neurons in different subdivisions of the entorhinal cortex. It would be interesting to obtain similar information on the structural development of the cortical areas projecting to Layer V, principally the orbitofrontal, parahippocampal, and retrosplenial cortices, to determine whether these areas exhibit similar developmental profiles.

4.4.5 | Layer VI

It is also interesting to consider the postnatal structural development of Layer VI in light of the different sets of cortical inputs reaching different subdivisions of the entorhinal cortex (Insausti & Amaral, 2008). In Er and Elr, Layer VI is the recipient of direct projections from the insula, as well as the orbitofrontal and medial prefrontal cortices. In Ei and Ec, Layer VI is the recipient of direct projections from the retrosplenial cortex, as well as the orbitofrontal and medial prefrontal cortices. In Elc, Layer VI is the recipient of direct projections from the orbitofrontal and medial prefrontal cortices. In Ecl, Layer VI is the recipient of direct projections from the orbitofrontal and retrosplenial cortices. In rats, Layer VI neurons of the medial entorhinal cortex also receive direct projections from the presubiculum and the parasubiculum (Canto et al., 2012). Based on these patterns of connectivity, the early maturation of Layer VI in Ec and Ecl may be linked to functional circuits involving the presubiculum, parasubiculum, and the retrosplenial cortex. In contrast, the additional influence of the structural development of functional circuits involving cortical regions in the frontal lobe may be more difficult to link to the specific patterns observed in Layer VI of the entorhinal cortex.

4.5 | Functional implications

We previously proposed that the differential maturation of distinct hippocampal circuits contributes to the emergence of different hippocampus-dependent memory processes (Lavenex & Banta Lavenex, 2013). Here, we have shown that different layers and subdivisions of the monkey entorhinal cortex exhibit different profiles of structural development, thus further suggesting that different networks processing different types of information mature at different times during early postnatal life. Most interestingly, the developmental profiles observed in the different layers and subdivisions of the entorhinal cortex parallel the developmental profiles observed in the hippocampal structures with which they are directly interconnected (Jabès et al., 2010, 2011). Now, we discuss the types of learning and memory processes that may be subserved by these networks, mainly based on electrophysiological and behavioral studies in rodents, and consider the potential implications of our findings for the emergence and development of spatial and episodic memory in humans.

4.5.1 | Path integration

Consistent with our earlier model linking the early development of the subiculum, presubiculum, and parasubiculum with the early emergence of path integration (Lavenex & Banta Lavenex, 2013), we found that Ec and Ecl exhibited an early structural development. As described above, Ec and Ecl are interconnected with a functional network including the subiculum, presubiculum, parasubiculum, retrosplenial, and parahippocampal cortices. These brain regions contain several cell types that contribute to spatial information processing, including place cells, head direction cells, grid cells, and boundary cells (Taube, 2007). During development, head-direction cells in the presubiculum and parasubiculum are the first to exhibit adult-like activity patterns (Langston et al., 2010). Hippocampal place cells evolve more gradually, whereas entorhinal cortex grid cells exhibit the slowest development. Interestingly, most cells in Layer III of the medial entorhinal cortex exhibit directional preferences at a very young age, as is the case in adult individuals (Langston et al., 2010). Altogether, these cells may support path integration, which can be defined as a computational process by which an organism continually monitors its own movement (Taube, 2007), or an internal computation that transforms a sense of motion into a sense of location (Savelli & Knierim, 2019). The inputs necessary for such a computation are essentially derived from self-motion cues produced by locomotion (Cullen & Taube, 2017). However, path integration is an imprecise mechanism, and errors will accumulate over time in absence of an external reference. Accordingly, the head direction signal must be periodically updated or recalibrated with respect to environmental landmarks. Importantly, visual calibration does not depend on visual information derived from the postrhinal cortex (Peck & Taube, 2017), which corresponds to the parahippocampal cortex in primates and is thought to be implicated in processing visual scene information (Epstein, 2008). Instead, the visual information necessary to maintain the calibration of the head direction system is derived from direct projections from the visual cortex to the presubiculum, which then exerts top-down control at the level of the lateral mammillary nuclei (Yoder, Peck, & Taube, 2015). Accordingly, path integration may enable

rodents and primates to successfully update their position and navigate in their environment before either visual scene information dependent on the parahippocampal cortex, or a basic allocentric spatial representations dependent on the functional maturation of CA1, become available. We therefore propose that the functional maturation of this discrete network including the subiculum, presubiculum, parasubiculum, and the caudal entorhinal cortex may underlie the emergence of path integration abilities in children between 6 and 12 months of age (Acredolo, 1978; Bremner, Knowles, & Andreasen, 1994; Rieser & Heiman, 1982).

4.5.2 | Basic allocentric spatial processing

Consistent with our earlier model linking the maturation of CA1 with the emergence of basic allocentric spatial processing and the offset of infantile amnesia (Lavenex & Banta Lavenex, 2013), Ec and Ecl exhibited an early structural development, between birth and 6 months of age, which is similar to what we observed in CA1 at the structural and molecular levels (Favre et al., 2012a; Jabès et al., 2011; Lavenex et al., 2011). Similarly, Ei exhibited a first volumetric increase between birth and 6 months of age, followed by a second increase after 1 year of age. In contrast, Er exhibited a late volumetric increase after 1 year of age, which was largely due to the development of its Layers III, V, and VI. Research in rodents demonstrated that CA1 place cell activity and a basic allocentric representation of the environment can be subserved by the direct monosynaptic pathway from the entorhinal cortex to CA1 (Brun et al., 2002). We therefore propose that the maturation of the reciprocal connections between the caudal entorhinal cortex and CA1 may underlie the emergence of allocentric spatial processing, which is reliably observed in children at 2 years of age (Newcombe, Huttenlocher, Bullock Drummey, & Wiley, 1998; Ribordy et al., 2013; Ribordy Lambert et al., 2015).

The bi-directional interaction between the hippocampus and the caudal entorhinal cortex may be critical to support this capacity. Grid cells found in the rat medial entorhinal cortex require an excitatory input from the hippocampus in order to maintain their normal firing pattern (Bonnevie et al., 2013). In the absence of hippocampal signal, grid cells become head direction cells likely driven by direct inputs from the presubiculum. Similarly, we have shown in monkeys that normal activation of the caudal entorhinal cortex (Ec and Ecl) during spatial exploration is dependent on the integrity of the hippocampus (Chareyron, Banta Lavenex, Amaral, & Lavenex, 2017). These two studies, using different methodologies in different species, suggest that the caudal entorhinal cortex (i.e., medial entorhinal cortex in rodents) may not be fully functional in the absence of functional hippocampal circuits. Accordingly, we propose that the functional maturation of CA1 may contribute to the functional maturation of the caudal entorhinal cortex in support of basic allocentric spatial processing (i.e., beyond its ability to support path integration via its interconnections with the subiculum, presubiculum, and parasubiculum). Such functional maturation includes the ability to integrate visual scene information provided by the parahippocampal cortex, which may enable the construction of low-resolution, allocentric spatial representations of the environment.

4.5.3 | Increased spatial memory precision and content

Consistent with our earlier model linking the protracted development of the dentate gyrus and CA3 with the age-related improvements in pattern separation which subserve high-resolution allocentric spatial representations (Lavenex & Banta Lavenex, 2013), we found that Er exhibited a late structural development after 1 year of age. The rostral entorhinal cortex (Er and the rostral part of Ei) receives significant projections from the amygdala and the perirhinal cortex (Pitkänen et al., 2002; Suzuki & Amaral, 1994). Accordingly, these two areas may be involved in the integration of emotional information, as well as the processing of local features related to individual items and objects, respectively. As proposed by Knierim et al. (2014), the lateral entorhinal cortex in rats, which corresponds to the rostral entorhinal cortex in primates, may be particularly involved in the processing of individual items and locations based on a local frame of reference, and provide the hippocampus with information about the content of an experience (Nilssen, Doan, Nigro, Ohara, & Witter, 2019). Similarly, Suzuki, Miller, and Desimone (1997) reported the activity of egocentric space-sensitive neurons in both the rostral and caudal entorhinal cortex recorded while monkeys were performing a delayed-matching-to-place task presented on a computer screen placed in front of them. Accordingly, rats with lesions of the lateral entorhinal cortex are impaired in their ability to learn a local spatial framework defined by an arrangement of small objects placed on the testing apparatus (Kuruvilla & Ainge, 2017).

In sum, the rostral entorhinal cortex may further contribute to the integration of spatial information about individual objects into a global representation of the environment. The rostral entorhinal cortex may thus contribute to increasing the precision of the spatial representation of the environment by integrating information about object locations, as well as provide the hippocampus with information about the content of an experience (Knierim et al., 2014). The late maturation of the rostral entorhinal cortex suggests that the increase in the content and precision of spatial and episodic memories develops progressively after the emergence of the ability to form a basic allocentric spatial representation, which is dependent on the maturation of the caudal entorhinal cortex (Lavenex & Banta Lavenex, 2013; Ribordy et al., 2013; Ribordy Lambert et al., 2015, 2016).

4.5.4 | Episodic memory

We previously proposed that the immaturity of the dentate gyrus may underlie the phenomenon of childhood amnesia, and that the gradual maturation of the trisynaptic hippocampal pathway subserves the gradual improvement, from 2 to 7 years of age, in our ability to create

autobiographical memories that can be recalled later in life (Lavenex & Banta Lavenex, 2013; Ribordy Lambert et al., 2015, 2016). Several mechanisms have been proposed to explain how hippocampal networks may represent moments in temporally organized experiences (Eichenbaum, 2017), but there was no clear indication regarding a specific contribution of the entorhinal cortex to the representation of time in support of episodic memory. However, a recent study by Tsao et al. (2018) reported that neurons in the rat lateral entorhinal cortex may provide a temporal signal that encodes time across multiple scales from seconds to hours, and may thus reflect the temporal structure of ongoing experience across different contexts. Accordingly, one may consider that the primate rostral entorhinal cortex may contribute to the definition of the temporal component of episodic memory. Together with the protracted maturation of the trisynaptic pathway, which is critical for rapid, single-trial contextual learning in support of the encoding of episodic memories, the late maturation of Er may contribute to the late improvement in our ability to create spatio-temporally distinct autobiographical memories.

4.6 | Conclusion

Consistent with our findings on the structural development of the hippocampal formation (Jabès et al., 2010, 2011), the different layers of the seven subdivisions of the monkey entorhinal cortex exhibit different postnatal developmental profiles. Most interestingly, the developmental profiles observed in the different layers and subdivisions of the entorhinal cortex parallel the developmental profiles observed in the hippocampal structures with which they are interconnected. Since the fundamental features of the laminar and topographical distributions of the entorhinal cortex projections to the hippocampal formation are largely similar to those of adults by 2 weeks of age in rhesus monkeys (Amaral et al., 2014), the current findings shed light on the differential structural maturation of putative functional circuits supporting the interactions between the entorhinal cortex and the rest of the hippocampal formation. The early maturation of the caudal entorhinal cortex may contribute to path integration and basic allocentric spatial processing, whereas the late maturation of the rostral entorhinal cortex may contribute to the increased precision of allocentric spatial representations and the temporal integration of individual items into episodic memories. Altogether, these results support the theory that the differential maturation of distinct hippocampal circuits contributes to the emergence of different hippocampus-dependent memory processes.

ACKNOWLEDGMENTS

This work was supported by Swiss National Science Foundation Grants P00A-106701, PP00P3-124536, and 310030_143956; US National Institutes of Health Grants MH041479 and NS16980; and California National Primate Research Center Grant OD011107.

DATA AVAILABILITY STATEMENT

The data that support the findings of this study are available from the corresponding author upon reasonable request.

ORCID

Olivia Piguet https://orcid.org/0000-0001-8398-0232
Loïc J Chareyron https://orcid.org/0000-0003-2043-3711
Pamela Banta Lavenex https://orcid.org/0000-0001-8868-2912
David G Amaral https://orcid.org/0000-0003-1525-8744
Pierre Lavenex https://orcid.org/0000-0002-9278-1312

REFERENCES

Acredolo, L. P. (1978). Development of spatial orientation in infancy. *Developmental Psychology*, *14*(3), 224–234.

Amaral, D. G., Insausti, R., & Cowan, W. M. (1987). The entorhinal cortex of the monkey: I. Cytoarchitectonic organization. *The Journal of Comparative Neurology*, *264*(3), 326–355.

Amaral, D. G., Kondo, H., & Lavenex, P. (2014). An analysis of entorhinal cortex projections to the dentate gyrus, hippocampus, and subiculum of the neonatal macaque monkey. *The Journal of Comparative Neurology*, *522*(7), 1485–1505. https://doi.org/10.1002/cne.23469

Amaral, D. G., & Lavenex, P. (2007). Hippocampal neuroanatomy. In P. Andersen, R. G. M. Morris, D. G. Amaral, T. V. Bliss, & J. O'Keefe (Eds.), *The hippocampus book* (pp. 37–114). Oxford: Oxford University Press.

Beul, S. F., & Hilgetag, C. C. (2019). Neuron density fundamentally relates to architecture and connectivity of the primate cerebral cortex. *NeuroImage*, *189*, 777–792. https://doi.org/10.1016/j.neuroimage.2019.01.010

Bonnevie, T., Dunn, B., Fyhn, M., Hafting, T., Derdikman, D., Kubie, J. L., … Moser, M. B. (2013). Grid cells require excitatory drive from the hippocampus. *Nature Neuroscience*, *16*(3), 309–317. https://doi.org/10.1038/nn.3311

Bremner, J. G., Knowles, L., & Andreasen, G. (1994). Processes underlying young children's spatial orientation during movement. *Journal of Experimental Child Psychology*, *57*(3), 355–376.

Brun, V. H., Otnass, M. K., Molden, S., Steffenach, H. A., Witter, M. P., Moser, M. B., & Moser, E. I. (2002). Place cells and place recognition maintained by direct entorhinal-hippocampal circuitry. *Science*, *296*(5576), 2243–2246.

Buckmaster, P. S., Alonso, A., Canfield, D. R., & Amaral, D. G. (2004). Dendritic morphology, local circuitry, and intrinsic electrophysiology of principal neurons in the entorhinal cortex of macaque monkeys. *The Journal of Comparative Neurology*, *470*(3), 317–329. https://doi.org/10.1002/cne.20014

Canto, C. B., Koganezawa, N., Beed, P., Moser, E. I., & Witter, M. P. (2012). All layers of medial entorhinal cortex receive presubicular and parasubicular inputs. *Journal of Neuroscience*, *32*(49), 17620–17631. https://doi.org/10.1523/Jneurosci.3526-12.2012

Carmer, S. G., & Swanson, M. R. (1973). Evaluation of 10 pairwise multiple comparison procedures by Monte-Carlo methods. *Journal of the American Statistical Association*, *68*(341), 66–74. https://doi.org/10.2307/2284140

Chareyron, L. J., Banta Lavenex, P., Amaral, D. G., & Lavenex, P. (2011). Stereological analysis of the rat and monkey amygdala. *The Journal of Comparative Neurology*, *519*(16), 3218–3239. https://doi.org/10.1002/cne.22677

Chareyron, L. J., Banta Lavenex, P., Amaral, D. G., & Lavenex, P. (2012). Postnatal development of the amygdala: A stereological study in macaque monkeys. *The Journal of Comparative Neurology*, *520*(9), 1965–1984. https://doi.org/10.1002/cne.23023

Chareyron, L. J., Banta Lavenex, P., Amaral, D. G., & Lavenex, P. (2017). Functional organization of the medial temporal lobe memory system following neonatal hippocampal lesion in rhesus monkeys. *Brain Structure & Function*, *222*(9), 3899–3914. https://doi.org/10.1007/s00429-017-1441-z

Chrobak, J. J., & Amaral, D. G. (2007). Entorhinal cortex of the monkey: VII. Intrinsic connections. *The Journal of Comparative Neurology*, *500*(4), 612–633. https://doi.org/10.1002/cne.21200

Cullen, K. E., & Taube, J. S. (2017). Our sense of direction: Progress, controversies and challenges. *Nature Neuroscience*, *20*(11), 1465–1473. https://doi.org/10.1038/nn.4658

Eichenbaum, H. (2017). On the integration of space, time, and memory. *Neuron*, *95*(5), 1007–1018. https://doi.org/10.1016/j.neuron.2017.06.036

Epstein, R. A. (2008). Parahippocampal and retrosplenial contributions to human spatial navigation. *Trends in Cognitive Sciences*, *12*(10), 388–396. https://doi.org/10.1016/j.tics.2008.07.004

Favre, G., Banta Lavenex, P., & Lavenex, P. (2012a). Developmental regulation of expression of schizophrenia susceptibility genes in the primate hippocampal formation. *Translational Psychiatry*, *2*, e173. https://doi.org/10.1038/tp.2012.105

Favre, G., Banta Lavenex, P., & Lavenex, P. (2012b). miRNA regulation of gene expression: A predictive bioinformatics analysis in the postnatally developing monkey hippocampus. *PLoS One*, *7*(8), e43435. https://doi.org/10.1371/journal.pone.0043435

Gatome, C. W., Slomianka, L., Lipp, H. P., & Amrein, I. (2010). Number estimates of neuronal phenotypes in layer II of the medial entorhinal cortex of rat and mouse. *Neuroscience*, *170*(1), 156–165. https://doi.org/10.1016/j.neuroscience.2010.06.048

Grateron, L., Cebada-Sanchez, S., Marcos, P., Mohedano-Moriano, A., Insausti, A. M., Munoz, M., … Insausti, R. (2003). Postnatal development of calcium-binding proteins immunoreactivity (parvalbumin, calbindin, calretinin) in the human entorhinal cortex. *Journal of Chemical Neuroanatomy*, *26*(4), 311–316.

Gundersen, H. J. (1988). The nucleator. *Journal of Microscopy*, *151*(Pt 1), 3–21.

Huttenlocher, P. R., & Dabholkar, A. S. (1997). Regional differences in synaptogenesis in human cerebral cortex. *The Journal of Comparative Neurology*, *387*(2), 167–178. https://doi.org/10.1002/(sici)1096-9861(19971020)387:2<167::aid-cne1>3.0.co;2-z

Insausti, R., & Amaral, D. G. (2008). Entorhinal cortex of the monkey: IV. Topographical and laminar organization of cortical afferents. *The Journal of Comparative Neurology*, *509*(6), 608–641. https://doi.org/10.1002/cne.21753

Insausti, R., Amaral, D. G., & Cowan, W. M. (1987). The entorhinal cortex of the monkey: II. Cortical afferents. *The Journal of Comparative Neurology*, *264*(3), 356–395.

Jabès, A., Banta Lavenex, P., Amaral, D. G., & Lavenex, P. (2010). Quantitative analysis of postnatal neurogenesis and neuron number in the macaque monkey dentate gyrus. *The European Journal of Neuroscience*, *31*(2), 273–285. https://doi.org/10.1111/j.1460-9568.2009.07061.x

Jabès, A., Banta Lavenex, P., Amaral, D. G., & Lavenex, P. (2011). Postnatal development of the hippocampal formation: A stereological study in macaque monkeys. *The Journal of Comparative Neurology*, *519*(6), 1051–1070. https://doi.org/10.1002/cne.22549

Kesner, R. P. (2013). An analysis of the dentate gyrus function. *Behavioural Brain Research*, *254*, 1–7. https://doi.org/10.1016/j.bbr.2013.01.012

Kesner, R. P., Lee, I., & Gilbert, P. (2004). A behavioral assessment of hippocampal function based on a subregional analysis. *Reviews in the Neurosciences*, *15*(5), 333–351.

Kesner, R. P., & Rolls, E. T. (2015). A computational theory of hippocampal function, and tests of the theory: New developments. *Neuroscience and Biobehavioral Reviews*, *48*, 92–147. https://doi.org/10.1016/j.neubiorev.2014.11.009

Knierim, J. J., & Neunuebel, J. P. (2016). Tracking the flow of hippocampal computation: Pattern separation, pattern completion, and attractor dynamics. *Neurobiology of Learning and Memory*, *129*, 38–49. https://doi.org/10.1016/j.nlm.2015.10.008

Knierim, J. J., Neunuebel, J. P., & Deshmukh, S. S. (2014). Functional correlates of the lateral and medial entorhinal cortex: Objects, path integration and local-global reference frames. *Philosophical Transactions of the Royal Society of London. Series B, Biological Sciences*, *369*(1635), 20130369. https://doi.org/10.1098/rstb.2013.0369

Kobayashi, Y., & Amaral, D. G. (2003). Macaque monkey retrosplenial cortex: II. Cortical afferents. *The Journal of Comparative Neurology*, *466*(1), 48–79. https://doi.org/10.1002/cne.10883

Kobayashi, Y., & Amaral, D. G. (2007). Macaque monkey retrosplenial cortex: III. Cortical efferents. *The Journal of Comparative Neurology*, *502*(5), 810–833. https://doi.org/10.1002/cne.21346

Kuruvilla, M. V., & Ainge, J. A. (2017). Lateral entorhinal cortex lesions impair local spatial frameworks. *Frontiers in Systems Neuroscience*, *11*, 1-12. https://doi.org/10.3389/fnsys.2017.00030

Langston, R. F., Ainge, J. A., Couey, J. J., Canto, C. B., Bjerknes, T. L., Witter, M. P., … Moser, M. B. (2010). Development of the spatial representation system in the rat. *Science*, *328*(5985), 1576–1580.

Lavenex, P., & Amaral, D. G. (2000). Hippocampal-neocortical interaction: A hierarchy of associativity. *Hippocampus*, *10*(4), 420–430. https://doi.org/10.1002/1098-1063(2000)10:4<420::AID-HIPO8>3.0.CO;2-5

Lavenex, P., & Banta Lavenex, P. (2013). Building hippocampal circuits to learn and remember: Insights into the development of human memory. *Behavioural Brain Research*, *254*, 8–21. https://doi.org/10.1016/j.bbr.2013.02.007

Lavenex, P., Banta Lavenex, P., & Amaral, D. G. (2004). Non-phosphorylated high-molecular-weight neurofilament expression suggests early maturation of the monkey subiculum. *Hippocampus*, *14*(7), 797–801. https://doi.org/10.1002/hipo.20028

Lavenex, P., Banta Lavenex, P., & Amaral, D. G. (2007). Postnatal development of the primate hippocampal formation. *Developmental Neuroscience*, *29*(1–2), 179–192. https://doi.org/10.1159/000096222

Lavenex, P., Banta Lavenex, P., Bennett, J. L., & Amaral, D. G. (2009). Postmortem changes in the neuroanatomical characteristics of the primate brain: Hippocampal formation. *The Journal of Comparative Neurology*, *512*(1), 27–51. https://doi.org/10.1002/cne.21906

Lavenex, P., Banta Lavenex, P., & Favre, G. (2014). What animals can teach clinicians about the hippocampus. *Frontiers of Neurology and Neuroscience*, *34*, 36–50. https://doi.org/10.1159/000356418

Lavenex, P., Sugden, S. G., Davis, R. R., Gregg, J. P., & Lavenex, P. B. (2011). Developmental regulation of gene expression and astrocytic processes may explain selective hippocampal vulnerability. *Hippocampus*, *21*(2), 142–149. https://doi.org/10.1002/hipo.20730

Newcombe, N. S., Huttenlocher, J., Bullock Drummey, A., & Wiley, J. G. (1998). The development of spatial location coding: Place learning and dead reckoning in the second and third years. *Cognitive Development*, *13*, 185–200.

Nilssen, E. S., Doan, T. P., Nigro, M. J., Ohara, S., & Witter, M. P. (2019). Neurons and networks in the entorhinal cortex: A reappraisal of the lateral and medial entorhinal subdivisions mediating parallel cortical pathways. *Hippocampus*, *29*, 1238–1254. https://doi.org/10.1002/hipo.23145

Nowakowski, R. S., & Rakic, P. (1981). The site of origin and route and rate of migration of neurons to the hippocampal region of the rhesus monkey. *The Journal of Comparative Neurology*, *196*(1), 129–154.

Ohara, S., Gianatti, M., Itou, K., Berndtsson, C. H., Doan, T. P., Kitanishi, T., … Witter, M. P. (2019). Entorhinal layer II calbindin-expressing neurons originate widespread telencephalic and intrinsic projections. *Frontiers in Systems Neuroscience*, *13*, 54. https://doi.org/10.3389/fnsys.2019.00054

Peck, J. R., & Taube, J. S. (2017). The postrhinal cortex is not necessary for landmark control in rat head direction cells. *Hippocampus*, *27*(2), 156–168. https://doi.org/10.1002/hipo.22680

Piguet, O., Chareyron, L. J., Banta Lavenex, P., Amaral, D. G., & Lavenex, P. (2018). Stereological analysis of the rhesus monkey entorhinal cortex. *The Journal of Comparative Neurology*, *526*(13), 2115–2132. https://doi.org/10.1002/cne.24496

Pitkänen, A., Kelly, J. L., & Amaral, D. G. (2002). Projections from the lateral, basal, and accessory basal nuclei of the amygdala to the entorhinal cortex in the macaque monkey. *Hippocampus*, *12*(2), 186–205.

Rabinowicz, T., Petetot, J. M., Khoury, J. C., & de Courten-Myers, G. M. (2009). Neocortical maturation during adolescence: change in neuronal soma dimension. *Brain and Cognition*, *69*(2), 328–336. https://doi.org/10.1016/j.bandc.2008.08.005

Rakic, P., Bourgeois, J. P., Eckenhoff, M. F., Zecevic, N., & Goldman-Rakic, P. S. (1986). Concurrent overproduction of synapses in diverse regions of the primate cerebral cortex. *Science*, *232*(4747), 232–235. https://doi.org/10.1126/science.3952506

Rakic, P., & Nowakowski, R. S. (1981). The time of origin of neurons in the hippocampal region of the rhesus monkey. *Journal of Comparative Neurology*, *196*(1), 99–128.

Ribordy, F., Jabès, A., Banta Lavenex, P., & Lavenex, P. (2013). Development of allocentric spatial memory abilities in children from 18 months to 5 years of age. *Cognitive Psychology*, *66*(1), 1–29. https://doi.org/10.1016/j.cogpsych.2012.08.001

Ribordy Lambert, F., Lavenex, P., & Banta Lavenex, P. (2015). Improvement of allocentric spatial memory resolution in children from 2 to 4 years of age. *International Journal of Behavioral Development*, *39*(4), 318–331. https://doi.org/10.1177/0165025415584808

Ribordy Lambert, F., Lavenex, P., & Banta Lavenex, P. (2016). The "when" and the "where" of single-trial allocentric spatial memory performance in young children: Insights into the development of episodic memory. *Developmental Psychobiology*, *59*(2), 185–196.

Rieser, J. J., & Heiman, M. L. (1982). Spatial self-reference systems and shortest-route behavior in toddlers. *Child Development*, *53*, 524–533.

Savelli, F., & Knierim, J. J. (2019). Origin and role of path integration in the cognitive representations of the hippocampus: Computational insights into open questions. *Journal of Experimental Biology*, *222*(Pt Suppl. 1), 1-13. https://doi.org/10.1242/jeb.188912

Schwartz, S. P., & Coleman, P. D. (1981). Neurons of origin of the perforant path. *Experimental Neurology*, *74*(1), 305–312. https://doi.org/10.1016/0014-4886(81)90169-2

Surmeli, G., Marcu, D. C., McClure, C., Garden, D. L. F., Pastoll, H., & Nolan, M. F. (2015). Molecularly defined circuitry reveals input-output segregation in deep layers of the medial entorhinal cortex. *Neuron*, *88*(5), 1040–1053. https://doi.org/10.1016/j.neuron.2015.10.041

Suzuki, W. A., & Amaral, D. G. (1994). Topographic organization of the reciprocal connections between the monkey entorhinal cortex and the perirhinal and parahippocampal cortices. *Journal of Neuroscience*, *14*(3), 1856–1877.

Suzuki, W. A., Miller, E. K., & Desimone, R. (1997). Object and place memory in the macaque entorhinal cortex. *Journal of Neurophysiology*, *78*(2), 1062–1081 Retrieved from < Go to ISI>://A1997XT27300041.

Taube, J. S. (2007). The head direction signal: Origins and sensory-motor integration. *Annual Review of Neuroscience*, *30*, 181–207. https://doi.org/10.1146/annurev.neuro.29.051605.112854

Tsao, A., Sugar, J., Lu, L., Wang, C., Knierim, J. J., Moser, M. B., & Moser, E. I. (2018). Integrating time from experience in the lateral entorhinal cortex. *Nature*, *561*(7721), 57. https://doi.org/10.1038/s41586-018-0459-6

West, M. J., Slomianka, L., & Gundersen, H. J. (1991). Unbiased stereological estimation of the total number of neurons in thesubdivisions of the rat hippocampus using the optical fractionator. *The Anatomical Record*, *231*(4), 482–497.

Witter, M. P., & Amaral, D. G. (1991). Entorhinal cortex of the monkey: V. projections to the dentate gyrus, hippocampus, and subicular complex. *The Journal of Comparative Neurology*, *307*(3), 437–459.

Witter, M. P., Doan, T. P., Jacobsen, B., Nilssen, E. S., & Ohara, S. (2017). Architecture of the entorhinal cortex: A review of entorhinal anatomy in rodents with some comparative perspective. *Frontiers in Systems Neuroscience*, *11*, 1-12. https://doi.org/10.3389/fnsys.2017.00046

Witter, M. P., & Moser, E. I. (2006). Spatial representation and the architecture of the entorhinal cortex. *Trends in Neurosciences*, *29*(12), 671–678. https://doi.org/10.1016/j.tins.2006.10.003

Witter, M. P., Van Hoesen, G. W., & Amaral, D. G. (1989). Topographical organization of the entorhinal projection to the dentate gyrus of the monkey. *The Journal of Neuroscience*, *9*(1), 216–228.

Yoder, R. M., Peck, J. R., & Taube, J. S. (2015). Visual landmark information gains control of the head direction signal at the lateral mammillary nuclei. *Journal of Neuroscience*, *35*(4), 1354–1367. https://doi.org/10.1523/Jneurosci.1418-14.2015

How to cite this article: Piguet O, J Chareyron L, Banta Lavenex P, G Amaral D, Lavenex P. Postnatal development of the entorhinal cortex: A stereological study in macaque monkeys. *J Comp Neurol*. 2020;528:2308–2332. https://doi.org/10.1002/cne.24897

3. Discussion and perspective

My thesis work is part of a larger project investigating the postnatal development of the medial temporal lobe with the optic of better understanding the neurological substrates underlying the development of declarative memory in general and episodic memory in particular. Following previous publications on the structural postnatal development of the hippocampal formation (Jabès et al., 2010, 2011), this study represents the first comprehensive quantitative analysis of the monkey entorhinal cortex.

In this chapter, I will first summarize the main published results of my research. I will then explain how having a precise view of the structural organization of the monkey entorhinal cortex brings an important perspective to the field of memory. In a third part, will then compare my results to the functional development of different spatial cells in the rat. The fourth section will be dedicated to highlighting the differential development of parallel pathways participating in the emergence of episodic memory. Finally, I will expose general theories on the emergence and development of episodic memory in humans.

3.1 Summary of my results

My study was divided in two chapters published independently: a first article focusing on the structural organization of the entorhinal cortex of adult rhesus monkeys; a second article describing the postnatal structural development of the monkey entorhinal cortex. Here, I summarize my major findings.

3.1.1 Different entorhinal-hippocampal circuits

In general, the number of neurons and average neuronal soma size differed between layers and subdivisions. Most importantly, the percentage of neurons located in distinct layers differed between entorhinal subdivisions, following a rostrocaudal gradient and a deep-to-superficial gradient.

The percentage of layer III neurons (relative to neurons included in all layers), which project to CA1 and the subiculum, was higher in rostral areas Eo and Er, compared to other subdivisions. In contrast, the percentage of layer II neurons, which project to the dentate gyrus and CA3, was lower in rostral areas Eo and Er than in all the other. Consistently, the ratio

between the number of neurons located in superficial layer III and in superficial layer II revealed a clear rostrocaudal gradient, layer III exhibiting a relatively greater development in the rostral entorhinal cortex, as compared to layer II. Additionally, the ratio between the number of neurons in the superficial layers II and III, which are the origins of projections to the hippocampus, and the number of neurons in the deep layers V and VI, which are the targets of feedback projections from the hippocampus, also revealed a rostrocaudal gradient, as it was greater in rostral areas Eo and Er compared to all other subdivisions. However, it was interesting to observe that this ratio was higher in Ecl (although it was still lower than in Eo and Er) than in the intermediate (Ei) and caudal (Ec, Ecl) subdivisions. These findings suggest that different subdivisions of the entorhinal cortex do not have the same degree of reciprocity in their connectivity with the rest of the hippocampal formation.

3.1.2 Different profiles of development of distinct entorhinal subdivisions and layers

Although there was no age-related difference in the number of neurons, our quantitative measurements of volumes and neuronal soma sizes in the different layers and subdivisions of the monkey entorhinal cortex revealed different developmental profiles:

- The volumetric measurement as well as neuronal soma size indicated a differential development of the superficial and deep layers. Our results suggest a relative early volumetric development of the superficial layers II and III, which provide the major inputs to the hippocampus, as compared to the deep layers V and VI, which receive the major outputs from the hippocampus.
- The differential development of layers has to be appreciated with regard to the differential development of the seven subdivisions of the entorhinal cortex. Indeed, my results revealed different development profiles and suggest in general a relative earlier maturation of the caudal entorhinal cortex, as compared to the rostral entorhinal cortex. Additionally, the intermediate region of the entorhinal cortex, Ei exhibited an intermediate pattern of development as it shared characteristics with both the rostral and caudal portions of the entorhinal cortex.
- An interesting finding was the observation of larger neuronal soma size at birth than in adulthood in layers III of the caudal subdivisions. As layer III of the caudal entorhinal

cortex is the recipient of presubiculum projections, my results suggest an early maturation of the presubiculum-entorhinal circuit.

- Finally, neurons in all layers and subdivisions, at the exception of layers II and III in Ei, Ec and Ecl, exhibited a transient increase at 6 months of age, followed by a gradual decrease until adulthood.

My analyses thus revealed that distinct layers and subdivisions of the monkey entorhinal cortex exhibit different maturation profiles. These results are consistent with previous analyses of the postnatal structural development of the monkey hippocampal formation (Jabès et al., 2010, 2011), and suggest a differential maturation of entorhinal-hippocampal circuits which may subserve the emergence of specific memory processes. In the next sections, I will integrate my results to what is known at the functional level in animals and humans, in order to transpose this knowledge to the development of episodic memory in humans.

3.2 The entorhinal cortex: an heterogenous structure

Although some studies investigated the number of neurons in the monkey entorhinal cortex, it was always limited to some layers or subdivisions (Gazzaley, Thakker, Hof, & Morrison, 1997; Merrill, Roberts, & Tuszynski, 2000) . My first article published as a part of this thesis provided the first comprehensive structural analysis of the seven subdivisions and layers of the monkey entorhinal cortex. In this section, I will review why investigating the seven subdivisions and the layers of the monkey entorhinal cortex is particularly relevant with respect to possible species differences in structure and functions.

The entorhinal cortex has been extensively investigated in the last decades, especially for its role in declarative memory and spatial representations (Knierim et al., 2014; Morrissey & Takehara-Nishiuchi, 2014; Witter & Moser, 2006). The vast majority of functional studies about the entorhinal cortex are performed on rats for ethical and practical reasons. In these studies, the entorhinal cortex is classically divided into only two main areas the medial entorhinal cortex (MEC), which corresponds to caudal subdivisions of the monkey entorhinal cortex, and the lateral entorhinal cortex (LEC), which corresponds to rostral subdivisions of the monkey entorhinal cortex (Amaral & Lavenex, 2007). This dichotomic distinction has the

major advantage to make the entorhinal cortex comparable between species as in many mammalian species, rostrocaudal and mediolateral portions of the entorhinal cortex can be identified (Insausti, 1993). However, one should be careful when it comes to extrapolate some results acquired in one species to another species, because, as my results suggest, this dichotomy is likely too reductive.

As described in section 1.2.3, although the hippocampal formation has generally similar organization in rats and monkeys (Amaral & Lavenex, 2007; Insausti, 1993), we can observe three major differences between the two species : (1) a substantial increase of number of cells in primates (Piguet et al., 2018; West et al., 1991), (2) stronger connection of the associational areas with the entorhinal cortex in primates (Amaral & Lavenex, 2007), and (3) a more extensive rostrocaudal extent of intrinsic connections in rats than in monkeys (Chrobak & Amaral, 2007; Dolorfo & Amaral, 1998a). It is therefore reasonable to think that the LEC-MEC distinction generally used in functional studies would be limited when it comes to monkeys.

The results detailed in my first article revealed different number of neurons and neuronal soma size in the layers of distinct subdivisions of the monkey entorhinal cortex (Piguet et al., 2018). This observation by itself suggests that the entorhinal cortex of the monkey is a very heterogenous structure. However, more striking differences appear when we compare the different layers and entorhinal subdivisions in rats and monkeys: Ei, Ec and Ecl for example. If we consider the caudal entorhinal as MEC in rats, those three regions are not considered individually anymore. Yet, they express important structural differences. Two different ratios of neuron number have been calculated in each subdivision: (1) number of neurons in layers II and III / number of neurons in layers V and VI, and (2) number of neurons in layer III / number of neurons in layer II. As superficial layers project to the hippocampus and deep layers receive projection from the hippocampus, the first ratio gives us an indication of the degree of reciprocity between the entorhinal cortex and the hippocampus. The second ratio indicates the proportion of projections to CA1 and the subiculum versus projections to CA3 and the dentate gyrus (different structures of the hippocampal formation that contribute to different functions). If we compare Ec and Ecl, the ratio of the number of neurons in superficial/deep layers was higher in Ecl than in Ec, whereas the ratio of neuron number in layer III/II was higher in Ec than in Ecl. This suggests that those two subdivisions do not participate in the same manner to entorhinal-hippocampal circuits. Moreover, Ei, a subdivision that does not appear in the dichotomy LEC/MEC, is another example of structural differences between monkeys

and rats. A particularity of Ei is that it shares proprieties with both the rostral and caudal entorhinal portions. This is not surprising, considering that rostrocaudal extent of intrinsic connections is about two third of the structure in monkeys (Chrobak & Amaral, 2007; Dolorfo & Amaral, 1998a).

Finally, the ratios between the number of layer III and layer II neurons, or between superficial and deep layers differ between rats and monkeys, thus suggesting that the pattern of connections between the entorhinal cortex and the hippocampus might differ importantly between different species. The greater ratio between the number of neurons in layer III and II in monkeys, indicates that the projections from the entorhinal cortex to CA1 might be more important in monkeys than in rats. Similarly, the greater ratio between the number of neurons in superficial and deep layers might reflect the stronger connections of the monkey entorhinal cortex with neocortical associational areas, as compared to rats.

To conclude, an important contribution of my quantitative results on the structural organization of the adult monkey entorhinal cortex is to highlight the heterogeneity between layers in the seven subdivisions of the monkey entorhinal cortex. It indicates that the entorhinal cortex is a complex structure and that a dichotomic distinction between LEC and MEC might be too reductive to fully understand the nature of the interactions between the entorhinal cortex and the rest of the hippocampal formation. One should thus take this distinction into account when extrapolating functional results obtained in rats to monkeys or, even further, to humans.

3.3 A link between structural and functional studies

A common way to investigate the development of episodic memory is through one of its principal components: spatial memory. Many different types of cells participating in the elaboration of spatial representations have been identified in the rat hippocampal formation. Three main types of spatial cells will be the subject of this section: place cells, head directions cells, and grid cells.

Before reviewing the development of spatial cells in rats, it is important to clarify two points. First, although my data do not directly reveal functional maturation, it is reasonable to think that the differential structural development of distinct layers and subdivisions of the monkey entorhinal cortex reflect somehow the differential functional maturation of

hippocampal circuits. Therefore, reviewing the electrophysiological studies on the development of the rat spatial representation system and putting it in parallel with the structural data acquired in monkeys could give clues about the emergence and development of spatial and episodic memory in humans.

Second, and most importantly, it is necessary to clearly expose the existing gap between the heterogeneity of the monkey entorhinal cortex as it has been demonstrated in the last section and the reductive segregation of the rat entorhinal cortex into two general areas, LEC and MEC, in functional studies. However, this difference should not prevent us from using the available functional data in rats and putting them in parallel with my data acquired in monkeys. Although further investigations would be needed to clarify the transposition from one species to another, I state here that assembling those knowledges is sufficient to build a better understanding of the emergence of hippocampus-dependent memory processes.

Functional studies on the development of spatial networks in rats showed that head directions cells, place cells and grid cells emerge and mature at different times (Tan, Wills, & Cacucci, 2017).

Head direction cells. The first type of functional cells to emerge in rats are *head direction cells*. To remember, head direction cells have been recorded in the presubiculum, the medial entorhinal cortex and several other areas, and encode information about the animal's directional heading, independent of the animal's on-going behavior (Taube, 1998). Although functional and behavioral studies investigating head direction cells are mainly performed in rodents, head direction cells have been found in monkeys (Robertson, Rolls, Georges-Francois, & Panzeri, 1999) as well as in humans (Shine, Valdes-Herrera, Hegarty, & Wolbers, 2016). Different recording studies demonstrated that, in the rat, head direction cells are already present and show adult-like proprieties at P16, when the rat leaves the nest for the first time, in the MEC, the presubiculum and the parasubiculum (Langston et al., 2010; Wills, Cacucci, Burgess, & O'Keefe, 2010). Moreover, although their number and properties are fewer than at P16, head direction cells have already been recorded at P11 and P12 in the rat presubiculum, the anteriodorsal thalamic nucleus (Tan, Bassett, O'Keefe, Cacucci, & Wills, 2015) and the MEC (Bjerknes, Langston, Kruge, Moser, & Moser, 2015). These observations are particularly interesting as the rat has no visual input at this time. The fact that a signal from head direction cells is observable in rats before other spatial cell types or, even more,

before visual or spatial experience, suggests that the organization of head direction network might occur independently of other spatial cell types (Tan et al., 2017). However, if head direction cells are primely influenced by self-motion, external features as visual landmarks are necessary to their calibration (Munn & Giocomo, 2020). Visual landmarks information are transmitted from the visual cortex to the presubiculum (Yoder, Clark, & Taube, 2011), which in turn reaches the medial entorhinal cortex, preferentially in superficial layer III (Canto, Koganezawa, Beed, Moser, & Witter, 2012).

The early emergence of head direction cells suggest that the other types of spatial cells are not necessary for the emergence of head direction signal. Consistently, a lesion of the hippocampus does not affect head direction signals (Golob & Taube, 1999). Therefore, it stands to reason that the source of head direction signal is generated outside of the hippocampal formation (Tan et al., 2017). The vestibular system has been identified as a key structure to detect self-motion and is necessary for the maintenance of head direction signal (Cullen & Taube, 2017; Golob & Taube, 1999; Tan et al., 2017; Yoder & Taube, 2014). From the vestibular system, the vestibular information is sent to the entorhinal cortex through the anterior thalamocortical pathway, which comprises the anterior dorsal thalamus, the retrosplenial cortex, the presubiculum and finally the medial entorhinal cortex (Cullen & Taube, 2017; Yoder & Taube, 2014). An early functional development of the vestibular system could be involved in the head direction cells first development even before the eye-opening of the rat. Another theory concerning the early development of head directions cells implicates the olfactory system and tactile system as those two systems are functional even earlier (Tan et al., 2017). However, one should remember that the olfactory connections are very different between rats and monkeys. Indeed, the olfactory bulb projects to the entire entorhinal cortex in rats, as it is restricted to the olfactory subdivision Eo in monkeys (Amaral & Lavenex, 2007; Insausti et al., 2002). This hypothesis is therefore difficult to generalize.

Functional studies about the maturation of head direction cells are consistent with the quantitative data obtained in this work. Most of head direction cells are located in the presubiculum which projects intensively to layer III in the caudal portion of the monkey entorhinal cortex. Compared to all other layers and subregions of the entorhinal cortex, my results showed a very early development of the caudal entorhinal subdivisions Ec and Ecl, in particular of layer III neurons who exhibited a larger soma size at birth compared to adulthood. Moreover, those results are consistent with previous observations of a larger neuronal soma

size in the presubiculum at birth as compared to adulthood, in contrast to what is observed in all other regions of the hippocampal formation (Jabès et al., 2011). Together with functional developmental studies these data support the idea of a very early maturation of the head direction cells network.

Place cells. The second spatial related cells that were recorded in rat pups are *place cells.* Place cells are found extensively in the CA1 field of the hippocampus, and fire according to a unique location in an open-field environment (O'Keefe & Dostrovsky, 1971). As head direction cells, place cells have been recorded before spatial exploration at P16 in rats (Langston et al., 2010; Wills et al., 2010). However, they have a much more gradual development than head direction cells and, in preweaning rats, they are fewer and immature in comparison to the cells found in adult rats (Martin & Berthoz, 2002; Scott, Richard, Holmes, & Lenck-Santini, 2011). Finally, as it will be described below, the stability and accuracy of place cells coding improve at the same time as the maturation of grid cells (Tan et al., 2017).

As described in section 1.2.2, CA1 field of the hippocampus receives extensive projections from layer III neurons of the entorhinal cortex. My volumetric and neuronal soma sizes measurements in layer III exhibited a clear rostro-caudal gradient with a relatively earlier development of the caudal portion of the entorhinal cortex. Consistently, previous analysis revealed an early maturation of CA1, and in particular of the stratum lacunosum-moleculare that receives direct projections from the entorhinal cortex layer III neurons, at about 6 months of age in monkeys. The relatively early development of both layer III of the entorhinal cortex and CA1 is consistent with the idea of an early functional development of place cells.

Grid cells. The last type of spatial cells to emerge postnatally are *grid cells*. To recall, grid cells have been recorded in the medial entorhinal cortex and fire whenever the animal's position coincides with any vertex of a regular grid made of equilateral triangles spanning the surface of the environment, thus representing a directionally oriented, topographically organized neural map of the spatial environment (Hafting et al., 2005). The age at which grid cells are first detected in rats is subject to discussion, as two studies found slightly different results (Bjerknes, Moser, & Moser, 2014; Langston et al., 2010). However, adult-like firing has been first reported at P20 (Wills et al., 2010).

The discovery of grid cells raised two questions: 1) Are grid cells functional in absence of place cells, and 2) would a path integration be possible without the integrity of the hippocampus, and thus without the place cells (McNaughton et al., 2006; Tan et al., 2017)? Recording of grid cells in the MEC of rats following hippocampal lesions revealed that in the absence of feedback from the hippocampus, grid cells do not show a grid pattern anymore, but behave as head direction cells (Bonnevie et al., 2013). This observation is consistent with an earlier functional maturation of place cells compared to grid cells in the postnatal development of the rat (Wills et al., 2010). Moreover, functional studies in monkeys demonstrated that the integrity of the hippocampus is necessary for the normal functioning of the caudal entorhinal cortex (Ec and Ecl) during spatial exploration (Chareyron et al., 2017). Altogether, these findings suggest that the development of place cells in the hippocampus is necessary for the maturation of grid cells in the entorhinal cortex. Accordingly, it is reasonable to think that the relative early development of layer III, which project to CA1 parallel the relative early maturation of place cells in the first part, and in turn, the relatively later development of deep layers in the caudal entorhinal, which receive feedback from the hippocampus, would allow the maturation of grid cells in a second part. In turn, the emergence of grid cells activity contributes to the stabilization of place cells representations, especially in the absence of clear landmarks (Vegard Heimly Brun et al., 2008; Hales et al., 2014; Muessig, Hauser, Wills, & Cacucci, 2015). Finally, head direction cells that develop earlier, might be necessary to the emergence and stability of grid cells (Winter, Clark, & Taube, 2015). Altogether, these findings suggest a later maturation of grid cells, which would require the functional maturation of other spatial cells types.

In conclusion, my results on the structural development of the monkey entorhinal cortex are consistent with functional data acquired on rats. Although, as exposed in section 3.2, it is necessary to be careful when it comes to transferring data acquired in rats to monkeys, the parallel between structural studies in monkeys and functional studies in rats reveals a possible similarity in the development of spatial memory in the two species.

3.4 Different pathways emerge at different times

Our results revealed various age-related structural differences in distinct layers and subdivisions of the monkey entorhinal cortex, which parallel the developmental profiles of hippocampal structures with which they are directly interconnected (Jabès et al., 2010, 2011). Although those structural changes do not directly reflect a functional maturation, they attest of different developmental profiles of entorhinal subregions that participate in different functional circuits. These findings suggest a differential functional maturation of distinct "hippocampal-based" memory circuits. In the previous section, I exposed how our structural observations support what was previously demonstrated in functional developmental studies. I would like now to explain how structural, functional and behavioral studies can be put together in order to build a general vision of episodic memory development in humans.

As previously mentioned, three parallel systems of projections from cortical regions to the entorhinal have been identified. A first pathway reaches the entorhinal cortex via the parahippocampal cortex and appears to contribute to the processing of visual scenes. A second pathway reaches the entorhinal cortex via the perirhinal cortex and appears to be specialized for processing object-related information (Knierim et al., 2014; Kravitz et al., 2011; Kravitz et al., 2013). Finally, a third pathway reaches the entorhinal cortex via the presubiculum and seems to be involved in navigational signals. Interestingly, my data support a differential temporal development of those three pathways: a very early development of the presubiculum-entorhinal pathway, followed by an early development of parahippocampal-caudal entorhinal pathway, and finally, a relatively later development of the perirhinal-rostral entorhinal cortex pathway.

3.4.1 The presubiculum - entorhinal cortex pathway: a first navigational system supported by head direction cells

One of the most striking results I found was the very early development of layer III in the caudal subdivisions of the entorhinal cortex. Neurons exhibited a larger neuronal soma size at birth than any other age. The fact that the developmental profile of these neurons differs from the neurons in all the other entorhinal regions indicates a specific development of this region. As stated previously, this observation is consistent with earlier observation in the presubiculum, which projects extensively to the caudal entorhinal layer III (Jabès et al., 2011).

The combination of those two structural studies and functional developmental studies about the early functional emergence of head direction cells, developed in section 3.3, suggests that the presubiculum-caudal entorhinal pathway, although not necessarily fully mature, might be one of the earliest pathways to be functionally operative in the hippocampal formation memory circuits.

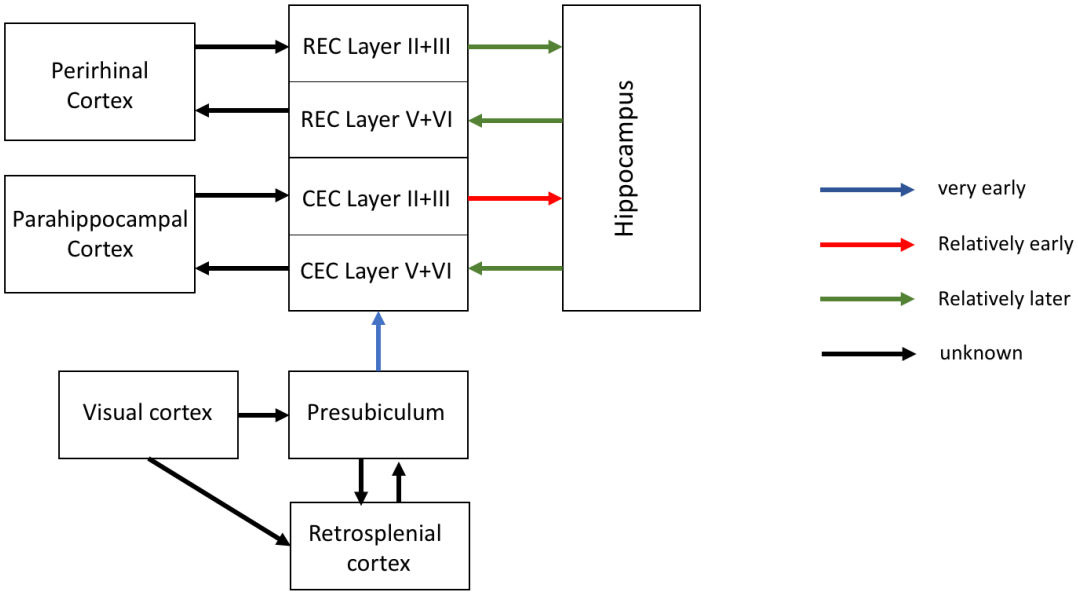

Figure 20: Differential development of distinct functional circuits implicated in the emergence of episodic memory.

As explained in the previous section, head direction cells are extensively present in the structures constituting the anterior thalamocortical pathway, which comprises the anterior dorsal thalamus, the retrosplenial cortex, the presubiculum and finally the medial entorhinal cortex (Cullen & Taube, 2017; Yoder & Taube, 2014), and appears to be the earliest type of spatial cell to develop functionally (Langston et al., 2010). This early maturation may be linked to the direction signal generated by the vestibular system (Tan et al., 2017). Interestingly, in humans, there is evidence that the vestibular system is already functional in newborn, although it continues to mature during the first year (Nandi & Luxon, 2008; Ornitz, Atwell, Walter, Hartmann, & Kaplan, 1979). The very early emergence of head direction signal initiated by the vestibular system could then be a source of early path integration abilities in very young children.

3.4.2 Parahippocampal cortex - caudal entorhinal cortex - hippocampus pathway: a first allocentric spatial representation

My results suggest a relatively early structural development of the caudal entorhinal cortex, especially the subdivisions Ec and Ecl, as compared to the rostral entorhinal cortex. The parahippocampal-caudal entorhinal-hippocampal pathway have been identified as a key pathway in spatial processing, notably because of the numerous spatial related cells discovered in these regions and described in section 3.3. More than just a spatial representation of the environment, Knierim et al. (2014) proposed that the caudal portion of the entorhinal cortex would be part of a global, holistic spatial map that would provide information about where the organism is in its environment, where it is going and how to get there. In other words, it would provide the hippocampus with the spatial context of an experience (Knierim et al., 2014).

The early structural development of Ec and Ecl observed in this work is consistent with what was previously observed in CA1 (Jabès et al., 2011). As other evidence suggests, the projections from entorhinal cortex layer III neurons to CA1 may be sufficient to support place cells activity (V. H. Brun et al., 2002). The early development of those two structures could therefore allow the emergence of low-resolution, allocentric spatial representations of the environment. Accordingly, behavioral data acquired in children demonstrated that the ability to form a basic allocentric representation of the environment is already present by 2 years of age (Ribordy et al., 2013), which corresponds approximately to six months of age in monkeys.

3.4.3 Perirhinal cortex - rostral entorhinal - hippocampal pathway: the emergence of episodic memory

My analysis of neuronal soma sizes and volumes suggests a relatively later development of the rostral subdivisions of the entorhinal cortex, especially Er. As seen in the previous section, while the parahippocampal cortex - caudal entorhinal cortex pathway is considered as responsible for spatial processing, the rostral entorhinal cortex is classically viewed as responsible for object memory processing (Bussey, Saksida, & Murray, 2005; Deshmukh & Knierim, 2011; Norman & Eacott, 2005).

If the role of the medial entorhinal cortex has been the subject of major focus in the last decade, the role of the lateral entorhinal cortex in the formation of episodic memory

remains less clear. Consistent with the findings that lesions of the perirhinal cortex impair non-contextual object tasks (Norman & Eacott, 2005), LEC has been first identified as processing nonspatial information (Hargreaves, Rao, Lee, & Knierim, 2005). Therefore, episodic memory would be the result of the integration by the hippocampus of two different sources of processed information: the perirhinal cortex and the LEC (or rostral entorhinal cortex) forming representations of distinct items (e.g., people, objects, events), and the parahippocampal cortex and the MEC (or caudal entorhinal cortex) providing information about the context (Eichenbaum, Yonelinas, & Ranganath, 2007). Recent experiments (developed in section 1.3.3), however, demonstrated that, although limited, some spatial information is also processed by the LEC, suggesting that the LEC does not only process individual items and objects, but also local features related to them (Hunsaker et al., 2013; Van Cauter et al., 2013). The rostral portion of the entorhinal cortex would then process information about individual items and locations based on a local frame of reference, and provide the hippocampus with information about the content of an experience (Knierim et al., 2014).

In addition to processing the content component of episodic memory, recent experiments suggest that the LEC would also be involved in the temporal representation of memory processing. The unstable responses of LEC cells to objects across time (Deshmukh & Knierim, 2011; Hargreaves et al., 2005) led Tsao et al. (2018) to investigate the potential role of LEC in representation of time. Electrophysiological recordings performed in similar behavioral tasks across repeated trials revealed a reduction of the encoding of temporal flow across trials, but an improvement of encoding time relative to the start of trials, demonstrating a unique temporal signal in the LEC that can encode time across multiple scales from seconds to hours and across different environmental contexts (Tsao et al., 2018). This experiment thus provides promising evidence that the LEC could be implicated in generating the time representation necessary to generate episodic memory. Consistently, a recent study in humans by Montchal et al. (2019) suggests the implication of the LEC in the temporal component of memory (see section 1.3.3 for more details of the research).

The late maturation of the rostral entorhinal cortex is consistent with the protracted development of the dentate gyrus, necessary for pattern separation, and CA3 (Jabès et al., 2011). The combined maturation of the two structures, as well as the late functional emergence of grid cells (Langston et al., 2010), could explain the emergence of high-resolution allocentric spatial representations (Lavenex & Banta Lavenex, 2013). Accordingly, behavioral

studies demonstrated that children's ability to distinguish and remember closely related spatial locations improves between 2 and 3.5 years of age (Ribordy et al., 2013).

Finally, our results of a late structural development of Er also suggest a later maturation of the projections from the amygdala to Er (Pitkänen et al., 2002; Suzuki & Amaral, 1994). The maturation of the rostral entorhinal cortex could therefore allow the integration of emotional information, an important contextual cue for encoding episodic memory information (Allen, Kaut, & Lord, 2008).

3.5 The emergence of episodic memory

As defined in the first section of this work (section 1.1), episodic memory can be described as the memory of our personal life experience, the ability to remember an "episode" of our life, and comprised three fundamental components: "what", "where" and "when" (Nyberg et al., 1996; Tulving, 2002). Episodic memory therefore does not simply refer to an event that happened in the past, but it is somehow reconstructed via the integration of its spatial and temporal components. Therefore, it stands to reason that the emergence of episodic memory is dependent on the hippocampus ability to receive and combine processed information about items, space and time in order to build a souvenir.

The structural development of the monkey entorhinal cortex presented in my work combined with previous structural studies about the hippocampal formation and functional studies performed with rats, suggest that the spatial component of the episodic memory is the first to emerge, although it is at the beginning immature. Indeed, the relative early development of the caudal entorhinal cortex, the presubiculum, and CA1 suggests that an organism may first develop the ability to form a global representation of the environment. In a second time, the development of the rostral portion of the entorhinal cortex, combined with the maturation of the dentate gyrus would allow the representation, discrimination and integration of individuals objects in this global frame, and thus would bring the "*item*" component of the episodic memory. Moreover, the development of the rostral entorhinal cortex could also possibly bring the time component to the equation. The hippocampus would thus be able to combine "what", "where", and, "when" in order to form a souvenir.

Another perspective of the development of memory involving pattern completion and pattern separation has been proposed by Keresztes et al. (2018). As a reminder, pattern completion is the ability to retrieve complete memories on the basis of incomplete sets of cues and is dependent on CA3 (Nakazawa et al., 2002; Yassa & Stark, 2011). Pattern separation consists in the process of transforming similar representations or memories into highly dissimilar, non-overlapping representations (Bakker et al., 2008) and is dependent on the dentate gyrus (Kesner, 2007; Rolls & Kesner, 2006). Accordingly, the maturation of hippocampal processing would follow a schema from generalization to specificity. The generalization would first be supported by the early emergence of pattern completion, as specialization would develop in a second time following the later emergence of pattern separation. According to Keresztes et al. (2018), the initial emergence of pattern completion would be developmentally advantageous as the generalization would facilitate initial learning through the extraction of commonalities across experiences (Keresztes, Ngo, Lindenberger, Werkle-Bergner, & Newcombe, 2018). Then, there would be a shift to specificity, with the emergence of pattern separation, only after accumulation of sufficient world knowledge, to encode, consolidate, and retrieve details (Keresztes et al., 2018).

The hypothesis of the early emergence of pattern completion is consistent with the early development of the CA3 distal portion (Jabès et al., 2011), which receives direct entorhinal projections from layer II neurons. As a reminder, neuronal somas in layer II of the caudal entorhinal subdivisions did not exhibit differences from birth to adulthood, suggesting a very early maturation. Moreover, the concept of generalization is coherent with the relatively early development of the caudal entorhinal cortex suggested by my results, which might functionally support the early emergence of low-resolution, allocentric spatial representations and therefore allow a first global perspective of the context. The later emergence of specialization associated with pattern separation is also consistent with structural developmental data indicating the protracted developmental period of the dentate gyrus which would support pattern separation (Jabès et al., 2010). Additionally, the relatively later development of the rostral entorhinal cortex observed in my research is furthermore coherent with this hypothesis, as it would provide the content, details, of an experience. The increase of precision would enable to distinguish one episode from another and thus to build a specific souvenir. Accordingly, the generalization would be the early ability to have a global

spatial representation of a situation, supported by the functional maturation of the caudal part of the entorhinal cortex, and the specificity would be the later ability to distinguish the content of a situation, supported by the functional maturation of the rostral entorhinal cortex.

3.6 Conclusion

The structural analyses presented in my thesis work represent the first comprehensive quantitative data about the development of the primate entorhinal cortex. Consistent with previous analyses of the rest of the monkey hippocampal formation (Jabès et al., 2010, 2011), my results indicate that the different layers of the seven subdivisions of the monkey entorhinal cortex exhibit different postnatal developmental profiles. The relatively early development of the caudal entorhinal cortex suggests a very early emergence of path integration, followed by an early representation of allocentric representation. The later development of the rostral entorhinal cortex suggests a later development of item and temporal representations that contribute to the formation of episodic memory.

4 Reference

Allen, P. A., Kaut, K. P., & Lord, R. R. (2008). Chapter 1.8 Emotion and episodic memory. In E. Dere, A. Easton, L. Nadel, & J. P. Huston (Eds.), *Handbook of Behavioral Neuroscience* (Vol. 18, pp. 115-132): Elsevier.

Amaral, D. G., Insausti, R., & Cowan, W. M. (1987). The entorhinal cortex of the monkey: I. Cytoarchitectonic organization. *J Comp Neurol, 264*(3), 326-355. doi:10.1002/cne.902640305

Amaral, D. G., Kondo, H., & Lavenex, P. (2014). An analysis of entorhinal cortex projections to the dentate gyrus, hippocampus, and subiculum of the neonatal macaque monkey. *J Comp Neurol, 522*(7), 1485-1505. doi:10.1002/cne.23469

Amaral, D. G., & Lavenex, P. (2007). Hippocampal neuroanatomy. In P. Anderson, R. G. M. Morris, D. G. Amaral, & T. V. Bliss (Eds.), *The hippocampus book* (pp. 37-114). Oxford: Oxford University Press.

Bakker, A., Kirwan, C. B., Miller, M., & Stark, C. E. (2008). Pattern separation in the human hippocampal CA3 and dentate gyrus. *Science, 319*(5870), 1640-1642. doi:10.1126/science.1152882

Bartsch, T., & Butler, C. (2013). Transient amnesic syndromes. *Nat Rev Neurol, 9*(2), 86-97. doi:10.1038/nrneurol.2012.264

Bauer, P. J. (2004). Getting explicit memory off the ground: Steps toward construction of a neuro-developmental account of changes in the first two years of life. *Developmental Review, 24*(4), 347-373. doi:https://doi.org/10.1016/j.dr.2004.08.003

Bauer, P. J. (2006). Constructing a past in infancy: a neuro-developmental account. *Trends Cogn Sci, 10*(4), 175-181. doi:10.1016/j.tics.2006.02.009

Bauer, P. J. (2008). Toward a neuro-developmental account of the development of declarative memory. *Dev Psychobiol, 50*(1), 19-31. doi:10.1002/dev.20265

Bird, C. M., & Burgess, N. (2008). The hippocampus and memory: insights from spatial processing. *Nat Rev Neurosci, 9*(3), 182-194. doi:10.1038/nrn2335

Bjerknes, T. L., Langston, R. F., Kruge, I. U., Moser, E. I., & Moser, M. B. (2015). Coherence among head direction cells before eye opening in rat pups. *Curr Biol, 25*(1), 103-108. doi:10.1016/j.cub.2014.11.009

Bjerknes, T. L., Moser, E. I., & Moser, M. B. (2014). Representation of geometric borders in the developing rat. *Neuron, 82*(1), 71-78. doi:10.1016/j.neuron.2014.02.014

Boccara, C. N., Kjonigsen, L. J., Hammer, I. M., Bjaalie, J. G., Leergaard, T. B., & Witter, M. P. (2015). A three-plane architectonic atlas of the rat hippocampal region. *Hippocampus, 25*(7), 838-857. doi:10.1002/hipo.22407

Bonnevie, T., Dunn, B., Fyhn, M., Hafting, T., Derdikman, D., Kubie, J. L., . . . Moser, M. B. (2013). Grid cells require excitatory drive from the hippocampus. *Nat Neurosci, 16*(3), 309-317. doi:10.1038/nn.3311

Brodmann, K. (1909). *Vergleichende Lokalisationslehre der Grosshirnrinde in ihren Prinzipien dargestellt auf Grund des Zellenbaues*. Leipzig.

Brun, V. H., Leutgeb, S., Wu, H.-Q., Schwarcz, R., Witter, M. P., Moser, E. I., & Moser, M.-B. (2008). Impaired Spatial Representation in CA1 after Lesion of Direct Input from Entorhinal Cortex. *Neuron, 57*(2), 290-302. doi:https://doi.org/10.1016/j.neuron.2007.11.034

Brun, V. H., Otnæss, M. K., Molden, S., Steffenach, H.-A., Witter, M. P., Moser, M.-B., & Moser, E. I. (2002). Place Cells and Place Recognition Maintained by Direct Entorhinal-Hippocampal Circuitry. *Science, 296*(5576), 2243-2246. doi:10.1126/science.1071089

Buckmaster, C. A., Eichenbaum, H., Amaral, D. G., Suzuki, W. A., & Rapp, P. R. (2004). Entorhinal cortex lesions disrupt the relational organization of memory in monkeys. *J Neurosci, 24*(44), 9811-9825. doi:10.1523/JNEUROSCI.1532-04.2004

Buckmaster, P. S., Alonso, A., Canfield, D. R., & Amaral, D. G. (2004). Dendritic morphology, local circuitry, and intrinsic electrophysiology of principal neurons in the entorhinal cortex of macaque monkeys. *J Comp Neurol, 470*(3), 317-329. doi:10.1002/cne.20014

Bussey, T. J., Saksida, L. M., & Murray, E. A. (2005). The perceptual-mnemonic/feature conjunction model of perirhinal cortex function. *Q J Exp Psychol B, 58*(3-4), 269-282. doi:10.1080/02724990544000004

Canto, C. B., Koganezawa, N., Beed, P., Moser, E. I., & Witter, M. P. (2012). All layers of medial entorhinal cortex receive presubicular and parasubicular inputs. *J Neurosci, 32*(49), 17620-17631. doi:10.1523/JNEUROSCI.3526-12.2012

Carden, M. J., Trojanowski, J. Q., Schlaepfer, W. W., & Lee, V. M. (1987). Two-stage expression of neurofilament polypeptides during rat neurogenesis with early establishment of adult phosphorylation patterns. *J Neurosci, 7*(11), 3489-3504. Retrieved from https://www.ncbi.nlm.nih.gov/pubmed/3119790

Chareyron, L. J., Banta Lavenex, P., Amaral, D. G., & Lavenex, P. (2017). Functional organization of the medial temporal lobe memory system following neonatal hippocampal lesion in rhesus monkeys. *Brain Struct Funct, 222*(9), 3899-3914. doi:10.1007/s00429-017-1441-z

Chrobak, J. J., & Amaral, D. G. (2007). Entorhinal cortex of the monkey: VII. intrinsic connections. *J Comp Neurol, 500*(4), 612-633. doi:10.1002/cne.21200

Cullen, K. E., & Taube, J. S. (2017). Our sense of direction: progress, controversies and challenges. *Nat Neurosci, 20*(11), 1465-1473. doi:10.1038/nn.4658

Deshmukh, S. S., & Knierim, J. J. (2011). Representation of non-spatial and spatial information in the lateral entorhinal cortex. *Front Behav Neurosci, 5*, 69. doi:10.3389/fnbeh.2011.00069

Dolorfo, C. L., & Amaral, D. G. (1998a). Entorhinal cortex of the rat: organization of intrinsic connections. *J Comp Neurol, 398*(1), 49-82. Retrieved from https://www.ncbi.nlm.nih.gov/pubmed/9703027

Dolorfo, C. L., & Amaral, D. G. (1998b). Entorhinal cortex of the rat: topographic organization of the cells of origin of the perforant path projection to the dentate gyrus. *J Comp Neurol, 398*(1), 25-48. Retrieved from https://www.ncbi.nlm.nih.gov/pubmed/9703026

Eichenbaum, H., Yonelinas, A. P., & Ranganath, C. (2007). The medial temporal lobe and recognition memory. *Annu Rev Neurosci, 30*, 123-152. doi:10.1146/annurev.neuro.30.051606.094328

Etienne, A. S., & Jeffery, K. J. (2004). Path integration in mammals. *Hippocampus, 14*(2), 180-192. doi:10.1002/hipo.10173

Favre, G., Banta Lavenex, P., & Lavenex, P. (2012a). Developmental regulation of expression of schizophrenia susceptibility genes in the primate hippocampal formation. *Transl Psychiatry, 2*, e173. doi:10.1038/tp.2012.105

Favre, G., Banta Lavenex, P., & Lavenex, P. (2012b). miRNA regulation of gene expression: a predictive bioinformatics analysis in the postnatally developing monkey hippocampus. *PLoS One, 7*(8), e43435. doi:10.1371/journal.pone.0043435

Fyhn, M., Molden, S., Witter, M. P., Moser, E. I., & Moser, M. B. (2004). Spatial representation in the entorhinal cortex. *Science, 305*(5688), 1258-1264. doi:10.1126/science.1099901

Gatome, C. W., Slomianka, L., Mwangi, D. K., Lipp, H. P., & Amrein, I. (2010). The entorhinal cortex of the Megachiroptera: a comparative study of Wahlberg's epauletted fruit bat and the straw-coloured fruit bat. *Brain Struct Funct, 214*(4), 375-393. doi:10.1007/s00429-010-0239-z

Gazzaley, A. H., Thakker, M. M., Hof, P. R., & Morrison, J. H. (1997). Preserved number of entorhinal cortex layer II neurons in aged macaque monkeys. *Neurobiol Aging, 18*(5), 549-553. doi:10.1016/s0197-4580(97)00112-7

Gilbert, P. E., Kesner, R. P., & Lee, I. (2001). Dissociating hippocampal subregions: A double dissociation between dentate gyrus and CA1. *Hippocampus, 11*(6), 626-636. doi:https://doi.org/10.1002/hipo.1077

Golob, E. J., & Taube, J. S. (1999). Head direction cells in rats with hippocampal or overlying neocortical lesions: evidence for impaired angular path integration. *J Neurosci, 19*(16), 7198-7211. Retrieved from https://www.ncbi.nlm.nih.gov/pubmed/10436073

Grateron, L., Cebada-Sanchez, S., Marcos, P., Mohedano-Moriano, A., Insausti, A. M., Munoz, M., . . . Insausti, R. (2003). Postnatal development of calcium-binding proteins immunoreactivity (parvalbumin, calbindin, calretinin) in the human entorhinal cortex. *J Chem Neuroanat, 26*(4), 311-316. doi:10.1016/j.jchemneu.2003.09.005

Hafting, T., Fyhn, M., Molden, S., Moser, M. B., & Moser, E. I. (2005). Microstructure of a spatial map in the entorhinal cortex. *Nature, 436*(7052), 801-806. doi:10.1038/nature03721

Hales, J. B., Schlesiger, M. I., Leutgeb, J. K., Squire, L. R., Leutgeb, S., & Clark, R. E. (2014). Medial entorhinal cortex lesions only partially disrupt hippocampal place cells and hippocampus-dependent place memory. *Cell Rep, 9*(3), 893-901. doi:10.1016/j.celrep.2014.10.009

Hargreaves, E. L., Rao, G., Lee, I., & Knierim, J. J. (2005). Major dissociation between medial and lateral entorhinal input to dorsal hippocampus. *Science, 308*(5729), 1792-1794. doi:10.1126/science.1110449

Hevner, R. F., & Kinney, H. C. (1996). Reciprocal entorhinal-hippocampal connections established by human fetal midgestation. *J Comp Neurol, 372*(3), 384-394. doi:10.1002/(SICI)1096-9861(19960826)372:3<384::AID-CNE4>3.0.CO;2-Z

Hunsaker, M. R., Chen, V., Tran, G. T., & Kesner, R. P. (2013). The medial and lateral entorhinal cortex both contribute to contextual and item recognition memory: a test of the binding of items and context model. *Hippocampus, 23*(5), 380-391. doi:10.1002/hipo.22097

Insausti, R. (1993). Comparative anatomy of the entorhinal cortex and hippocampus in mammals. *Hippocampus, 3 Spec No*, 19-26. Retrieved from https://www.ncbi.nlm.nih.gov/pubmed/8287096

Insausti, R., & Amaral, D. G. (2008). Entorhinal cortex of the monkey: IV. Topographical and laminar organization of cortical afferents. *J Comp Neurol, 509*(6), 608-641. doi:10.1002/cne.21753

Insausti, R., Amaral, D. G., & Cowan, W. M. (1987a). The entorhinal cortex of the monkey: II. Cortical afferents. *J Comp Neurol, 264*(3), 356-395. doi:10.1002/cne.902640306

Insausti, R., Amaral, D. G., & Cowan, W. M. (1987b). The entorhinal cortex of the monkey: III. Subcortical afferents. *J Comp Neurol, 264*(3), 396-408. doi:10.1002/cne.902640307

Insausti, R., Herrero, M. T., & Witter, M. P. (1997). Entorhinal cortex of the rat: cytoarchitectonic subdivisions and the origin and distribution of cortical efferents. *Hippocampus, 7*(2), 146-183. doi:10.1002/(SICI)1098-1063(1997)7:2<146::AID-HIPO4>3.0.CO;2-L

Insausti, R., Marcos, P., Arroyo-Jimenez, M. M., Blaizot, X., & Martinez-Marcos, A. (2002). Comparative aspects of the olfactory portion of the entorhinal cortex and its projection to the hippocampus in rodents, nonhuman primates, and the human brain. *Brain Res Bull, 57*(3-4), 557-560. doi:10.1016/s0361-9230(01)00684-0

Insausti, R., Munoz-Lopez, M., Insausti, A. M., & Artacho-Perula, E. (2017). The Human Periallocortex: Layer Pattern in Presubiculum, Parasubiculum and Entorhinal Cortex. A Review. *Front Neuroanat, 11*, 84. doi:10.3389/fnana.2017.00084

Insausti, R., Tunon, T., Sobreviela, T., Insausti, A. M., & Gonzalo, L. M. (1995). The human entorhinal cortex: a cytoarchitectonic analysis. *J Comp Neurol, 355*(2), 171-198. doi:10.1002/cne.903550203

Jabès, A., Lavenex, P. B., Amaral, D. G., & Lavenex, P. (2010). Quantitative analysis of postnatal neurogenesis and neuron number in the macaque monkey dentate gyrus. *Eur J Neurosci, 31*(2), 273-285. doi:10.1111/j.1460-9568.2009.07061.x

Jabès, A., Lavenex, P. B., Amaral, D. G., & Lavenex, P. (2011). Postnatal development of the hippocampal formation: a stereological study in macaque monkeys. *J Comp Neurol, 519*(6), 1051-1070. doi:10.1002/cne.22549

Jabès, A., & Nelson, C. A. (2015). 20 years after "The ontogeny of human memory: A cognitive neuroscience perspective," where are we? *International Journal of Behavioral Development, 39*(4), 293-303. doi:10.1177/0165025415575766

Keresztes, A., Ngo, C. T., Lindenberger, U., Werkle-Bergner, M., & Newcombe, N. S. (2018). Hippocampal Maturation Drives Memory from Generalization to Specificity. *Trends Cogn Sci, 22*(8), 676-686. doi:10.1016/j.tics.2018.05.004

Kesner, R. P. (2007). A behavioral analysis of dentate gyrus function. *Prog Brain Res, 163*, 567-576. doi:10.1016/S0079-6123(07)63030-1

Knierim, J. J., Neunuebel, J. P., & Deshmukh, S. S. (2014). Functional correlates of the lateral and medial entorhinal cortex: objects, path integration and local-global reference frames. *Philos Trans R Soc Lond B Biol Sci, 369*(1635), 20130369. doi:10.1098/rstb.2013.0369

Kobayashi, Y., & Amaral, D. G. (2007). Macaque monkey retrosplenial cortex: III. Cortical efferents. *J Comp Neurol, 502*(5), 810-833. doi:10.1002/cne.21346

Kondo, H., Lavenex, P., & Amaral, D. G. (2008). Intrinsic connections of the macaque monkey hippocampal formation: I. Dentate gyrus. *J Comp Neurol, 511*(4), 497-520. doi:10.1002/cne.21825

Kondo, H., Lavenex, P., & Amaral, D. G. (2009). Intrinsic connections of the macaque monkey hippocampal formation: II. CA3 connections. *J Comp Neurol, 515*(3), 349-377. doi:10.1002/cne.22056

Kravitz, D. J., Saleem, K. S., Baker, C. I., & Mishkin, M. (2011). A new neural framework for visuospatial processing. *Nat Rev Neurosci, 12*(4), 217-230. doi:10.1038/nrn3008

Kravitz, D. J., Saleem, K. S., Baker, C. I., Ungerleider, L. G., & Mishkin, M. (2013). The ventral visual pathway: an expanded neural framework for the processing of object quality. *Trends Cogn Sci, 17*(1), 26-49. doi:10.1016/j.tics.2012.10.011

Langston, R. F., Ainge, J. A., Couey, J. J., Canto, C. B., Bjerknes, T. L., Witter, M. P., . . . Moser, M. B. (2010). Development of the spatial representation system in the rat. *Science, 328*(5985), 1576-1580. doi:10.1126/science.1188210

Lavenex, P., & Amaral, D. G. (2000). Hippocampal-neocortical interaction: a hierarchy of associativity. *Hippocampus, 10*(4), 420-430. doi:10.1002/1098-1063(2000)10:4<420::AID-HIPO8>3.0.CO;2-5

Lavenex, P., & Banta Lavenex, P. (2013). Building hippocampal circuits to learn and remember: insights into the development of human memory. *Behav Brain Res, 254*, 8-21. doi:10.1016/j.bbr.2013.02.007

Lavenex, P., Banta Lavenex, P., & Amaral, D. G. (2004). Nonphosphorylated high-molecular-weight neurofilament expression suggests early maturation of the monkey subiculum. *Hippocampus, 14*(7), 797-801. doi:10.1002/hipo.20028

Lavenex, P., Banta Lavenex, P., & Amaral, D. G. (2007). Postnatal development of the primate hippocampal formation. *Dev Neurosci, 29*(1-2), 179-192. doi:10.1159/000096222

Lavenex, P., Banta Lavenex, P., & Favre, G. (2014). What animals can teach clinicians about the hippocampus. *Front Neurol Neurosci, 34*, 36-50. doi:10.1159/000356418

Lavenex, P., Sugden, S. G., Davis, R. R., Gregg, J. P., & Lavenex, P. B. (2011). Developmental regulation of gene expression and astrocytic processes may explain selective hippocampal vulnerability. *Hippocampus, 21*(2), 142-149. doi:10.1002/hipo.20730

Lavenex, P., Suzuki, W. A., & Amaral, D. G. (2002). Perirhinal and parahippocampal cortices of the macaque monkey: projections to the neocortex. *J Comp Neurol, 447*(4), 394-420. doi:10.1002/cne.10243

Lee, M. K., & Cleveland, D. W. (1996). Neuronal intermediate filaments. *Annu Rev Neurosci, 19*, 187-217. doi:10.1146/annurev.ne.19.030196.001155

Leutgeb, S., & Leutgeb, J. K. (2007). Pattern separation, pattern completion, and new neuronal codes within a continuous CA3 map. *Learn Mem, 14*(11), 745-757. doi:10.1101/lm.703907

Lorente de Nó, R. (1933). Studies on the structure of the cerebral cortex. I. The area entorhinalis. *J Psychol Neurol, 45*, 381-438.

Lorente de Nó, R. (1934). Studies on the structure of the cerebral cortex. II. Continuation of the study of the ammonic system. *J Psychol Neurol, 46*, 113-177.

Martin, P. D., & Berthoz, A. (2002). Development of spatial firing in the hippocampus of young rats. *Hippocampus, 12*(4), 465-480. doi:10.1002/hipo.10021

McNaughton, B. L., Battaglia, F. P., Jensen, O., Moser, E. I., & Moser, M. B. (2006). Path integration and the neural basis of the 'cognitive map'. *Nat Rev Neurosci, 7*(8), 663-678. doi:10.1038/nrn1932

Merrill, D. A., Roberts, J. A., & Tuszynski, M. H. (2000). Conservation of neuron number and size in entorhinal cortex layers II, III, and V/VI of aged primates. *J Comp Neurol, 422*(3), 396-401. doi:10.1002/1096-9861(20000703)422:3<396::aid-cne6>3.0.co;2-r

Milner, B., Squire, L. R., & Kandel, E. R. (1998). Cognitive neuroscience and the study of memory. *Neuron, 20*(3), 445-468. doi:10.1016/s0896-6273(00)80987-3

Mittelstaedt, M. L., & Mittelstaedt, H. (1980). Homing by path integration in a mammal. *Naturwissenschaften, 67*(11), 566-567. doi:10.1007/BF00450672

Mizumori, S. J., Barnes, C. A., & McNaughton, B. L. (1989). Reversible inactivation of the medial septum: selective effects on the spontaneous unit activity of different hippocampal cell types. *Brain Res, 500*(1-2), 99-106. doi:10.1016/0006-8993(89)90303-x

Montchal, M. E., Reagh, Z. M., & Yassa, M. A. (2019). Precise temporal memories are supported by the lateral entorhinal cortex in humans. *Nat Neurosci, 22*(2), 284-288. doi:10.1038/s41593-018-0303-1

Morris, R. (2007). Theories of hippocampal function. In P. Anderson, R. G. M. Morris, D. G. Amaral, & T. V. Bliss (Eds.), *The hippocampus book*. Oxford: Oxford University Press.

Morrissey, M. D., & Takehara-Nishiuchi, K. (2014). Diversity of mnemonic function within the entorhinal cortex: a meta-analysis of rodent behavioral studies. *Neurobiol Learn Mem, 115*, 95-107. doi:10.1016/j.nlm.2014.08.006

Muessig, L., Hauser, J., Wills, T. J., & Cacucci, F. (2015). A Developmental Switch in Place Cell Accuracy Coincides with Grid Cell Maturation. *Neuron, 86*(5), 1167-1173. doi:10.1016/j.neuron.2015.05.011

Munn, R. G., & Giocomo, L. M. (2020). Multiple head direction signals within entorhinal cortex: origin and function. *Curr Opin Neurobiol, 64*, 32-40. doi:10.1016/j.conb.2020.01.015

Munoz, M., & Insausti, R. (2005). Cortical efferents of the entorhinal cortex and the adjacent parahippocampal region in the monkey (Macaca fascicularis). *Eur J Neurosci, 22*(6), 1368-1388. doi:10.1111/j.1460-9568.2005.04299.x

Nakazawa, K., Quirk, M. C., Chitwood, R. A., Watanabe, M., Yeckel, M. F., Sun, L. D., . . . Tonegawa, S. (2002). Requirement for hippocampal CA3 NMDA receptors in associative memory recall. *Science, 297*(5579), 211-218. doi:10.1126/science.1071795

Nandi, R., & Luxon, L. M. (2008). Development and assessment of the vestibular system. *Int J Audiol, 47*(9), 566-577. doi:10.1080/14992020802324540

Nelson, C. A. (1995). The Ontogeny of Human Memory: A Cognitive Neuroscience Perspective. *Developmental Psychology, 31*(5), 723-738.

Newcombe, N. S., Drummey, A. B., Fox, N. A., Lie, E., & Ottinger-Alberts, W. (2000). Remembering Early Childhood:How Much, How, and Why (or Why Not). *Current Directions in Psychological Science, 9*(2), 55-58. doi:10.1111/1467-8721.00060

Newcombe, N. S., Lloyd, M. E., & Ratliff, K. R. (2007). Development of episodic and autobiographical memory: a cognitive neuroscience perspective. *Adv Child Dev Behav, 35*, 37-85. doi:10.1016/b978-0-12-009735-7.50007-4

Norman, G., & Eacott, M. J. (2005). Dissociable effects of lesions to the perirhinal cortex and the postrhinal cortex on memory for context and objects in rats. *Behav Neurosci, 119*(2), 557-566. doi:10.1037/0735-7044.119.2.557

Nyberg, L., McIntosh, A. R., Cabeza, R., Habib, R., Houle, S., & Tulving, E. (1996). General and specific brain regions involved in encoding and retrieval of events: what, where, and when. *Proc Natl Acad Sci U S A, 93*(20), 11280-11285. doi:10.1073/pnas.93.20.11280

O'Keefe, J., & Dostrovsky, J. (1971). The hippocampus as a spatial map. Preliminary evidence from unit activity in the freely-moving rat. *Brain Res, 34*(1), 171-175. doi:10.1016/0006-8993(71)90358-1

O'Keef, J., & Nadel, L. (1978). *The hippocampus as a cognitive map*. Oxford: Clarendon Press.

Ornitz, E. M., Atwell, C. W., Walter, D. O., Hartmann, E. E., & Kaplan, A. R. (1979). The maturation of vestibular nystagmus in infancy and childhood. *Acta Otolaryngol, 88*(3-4), 244-256. doi:10.3109/00016487909137166

Piguet, O., Chareyron, L. J., Banta Lavenex, P., Amaral, D. G., & Lavenex, P. (2018). Stereological analysis of the rhesus monkey entorhinal cortex. *J Comp Neurol, 526*(13), 2115-2132. doi:10.1002/cne.24496

Pitkanen, A., Pikkarainen, M., Nurminen, N., & Ylinen, A. (2000). Reciprocal connections between the amygdala and the hippocampal formation, perirhinal cortex, and

postrhinal cortex in rat. A review. *Ann N Y Acad Sci, 911*, 369-391. doi:10.1111/j.1749-6632.2000.tb06738.x

Ramón Y Cajal, S. (1901-1902). Estudios sobre la corteza cerebral humana. *Trab. Inst. Cajal Invest. Biol, 1*, 1-227.

Ramón Y Cajal, S. (1909). *Histologie du système neurveux de l'homme et des vertébrés*. Paris: A. Maloine.

Reagh, Z. M., & Yassa, M. A. (2014). Object and spatial mnemonic interference differentially engage lateral and medial entorhinal cortex in humans. *Proc Natl Acad Sci U S A, 111*(40), E4264-4273. doi:10.1073/pnas.1411250111

Ribordy, F., Jabès, A., Banta Lavenex, P., & Lavenex, P. (2013). Development of allocentric spatial memory abilities in children from 18 months to 5 years of age. *Cogn Psychol, 66*(1), 1-29. doi:10.1016/j.cogpsych.2012.08.001

Robertson, R. G., Rolls, E. T., Georges-Francois, P., & Panzeri, S. (1999). Head direction cells in the primate pre-subiculum. *Hippocampus, 9*(3), 206-219. doi:10.1002/(SICI)1098-1063(1999)9:3<206::AID-HIPO2>3.0.CO;2-H

Rolls, E. T., & Kesner, R. P. (2006). A computational theory of hippocampal function, and empirical tests of the theory. *Prog Neurobiol, 79*(1), 1-48. doi:10.1016/j.pneurobio.2006.04.005

Scott, R. C., Richard, G. R., Holmes, G. L., & Lenck-Santini, P. P. (2011). Maturational dynamics of hippocampal place cells in immature rats. *Hippocampus, 21*(4), 347-353. doi:10.1002/hipo.20789

Scoville, W. B. (1954). The limbic lobe in man. *J Neurosurg, 11*(1), 64-66. doi:10.3171/jns.1954.11.1.0064

Scoville, W. B., & Milner, B. (1957). Loss of recent memory after bilateral hippocampal lesions. *J Neurol Neurosurg Psychiatry, 20*(1), 11-21. doi:10.1136/jnnp.20.1.11

Shine, J. P., Valdes-Herrera, J. P., Hegarty, M., & Wolbers, T. (2016). The Human Retrosplenial Cortex and Thalamus Code Head Direction in a Global Reference Frame. *J Neurosci, 36*(24), 6371-6381. doi:10.1523/JNEUROSCI.1268-15.2016

Squire, L. R. (1992). Memory and the hippocampus: a synthesis from findings with rats, monkeys, and humans. *Psychol Rev, 99*(2), 195-231. doi:10.1037/0033-295x.99.2.195

Suzuki, W. A., & Amaral, D. G. (1994a). Perirhinal and parahippocampal cortices of the macaque monkey: cortical afferents. *J Comp Neurol, 350*(4), 497-533. doi:10.1002/cne.903500402

Suzuki, W. A., & Amaral, D. G. (1994b). Topographic organization of the reciprocal connections between the monkey entorhinal cortex and the perirhinal and parahippocampal cortices. *J Neurosci, 14*(3 Pt 2), 1856-1877. Retrieved from https://www.ncbi.nlm.nih.gov/pubmed/8126576

Suzuki, W. A., Miller, E. K., & Desimone, R. (1997). Object and place memory in the macaque entorhinal cortex. *J Neurophysiol, 78*(2), 1062-1081. doi:10.1152/jn.1997.78.2.1062

Tan, H. M., Bassett, J. P., O'Keefe, J., Cacucci, F., & Wills, T. J. (2015). The development of the head direction system before eye opening in the rat. *Curr Biol, 25*(4), 479-483. doi:10.1016/j.cub.2014.12.030

Tan, H. M., Wills, T. J., & Cacucci, F. (2017). The development of spatial and memory circuits in the rat. *Wiley Interdiscip Rev Cogn Sci, 8*(3). doi:10.1002/wcs.1424

Taube, J. S. (1998). Head direction cells and the neurophysiological basis for a sense of direction. *Prog Neurobiol, 55*(3), 225-256. doi:10.1016/s0301-0082(98)00004-5

Tsao, A., Sugar, J., Lu, L., Wang, C., Knierim, J. J., Moser, M. B., & Moser, E. I. (2018). Integrating time from experience in the lateral entorhinal cortex. *Nature, 561*(7721), 57-62. doi:10.1038/s41586-018-0459-6

Tulving, E. (2002). Episodic memory: from mind to brain. *Annu Rev Psychol, 53*, 1-25. doi:10.1146/annurev.psych.53.100901.135114

Van Cauter, T., Camon, J., Alvernhe, A., Elduayen, C., Sargolini, F., & Save, E. (2013). Distinct roles of medial and lateral entorhinal cortex in spatial cognition. *Cereb Cortex, 23*(2), 451-459. doi:10.1093/cercor/bhs033

van Groen, T. (2001). Entorhinal cortex of the mouse: cytoarchitectonical organization. *Hippocampus, 11*(4), 397-407. doi:10.1002/hipo.1054

West, M. J., & Slomianka, L. (1998). Total number of neurons in the layers of the human entorhinal cortex. *Hippocampus, 8*(1), 69-82. doi:10.1002/(SICI)1098-1063(1998)8:1<69::AID-HIPO7>3.0.CO;2-2

West, M. J., Slomianka, L., & Gundersen, H. J. (1991). Unbiased stereological estimation of the total number of neurons in thesubdivisions of the rat hippocampus using the optical fractionator. *Anat Rec, 231*(4), 482-497. doi:10.1002/ar.1092310411

Wills, T. J., Cacucci, F., Burgess, N., & O'Keefe, J. (2010). Development of the hippocampal cognitive map in preweanling rats. *Science, 328*(5985), 1573-1576. doi:10.1126/science.1188224

Winter, S. S., Clark, B. J., & Taube, J. S. (2015). Spatial navigation. Disruption of the head direction cell network impairs the parahippocampal grid cell signal. *Science, 347*(6224), 870-874. doi:10.1126/science.1259591

Witter, M. P. (2007). The perforant path: projections from the entorhinal cortex to the dentate gyrus. *Prog Brain Res, 163*, 43-61. doi:10.1016/S0079-6123(07)63003-9

Witter, M. P., & Amaral, D. G. (1991). Entorhinal cortex of the monkey: V. Projections to the dentate gyrus, hippocampus, and subicular complex. *J Comp Neurol, 307*(3), 437-459. doi:10.1002/cne.903070308

Witter, M. P., & Amaral, D. G. (2021). The entorhinal cortex of the monkey: VI. Organization of projections from the hippocampus, subiculum, presubiculum, and parasubiculum. *J Comp Neurol, 529*(4), 828-852. doi:10.1002/cne.24983

Witter, M. P., & Moser, E. I. (2006). Spatial representation and the architecture of the entorhinal cortex. *Trends Neurosci, 29*(12), 671-678. doi:10.1016/j.tins.2006.10.003

Witter, M. P., Van Hoesen, G. W., & Amaral, D. G. (1989). Topographical organization of the entorhinal projection to the dentate gyrus of the monkey. *J Neurosci, 9*(1), 216-228. Retrieved from https://www.ncbi.nlm.nih.gov/pubmed/2913203

Yassa, M. A., & Stark, C. E. (2011). Pattern separation in the hippocampus. *Trends Neurosci, 34*(10), 515-525. doi:10.1016/j.tins.2011.06.006

Yoder, R. M., Clark, B. J., & Taube, J. S. (2011). Origins of landmark encoding in the brain. *Trends Neurosci, 34*(11), 561-571. doi:10.1016/j.tins.2011.08.004

Yoder, R. M., & Taube, J. S. (2014). The vestibular contribution to the head direction signal and navigation. *Front Integr Neurosci, 8*, 32. doi:10.3389/fnint.2014.00032